

M 9821326 1
BN 9821326 1



A COMPUTER MODEL FOR HEAT
EXCHANGE PROCESSES IN MOBILE
AIR-CONDITIONING SYSTEMS

MAHMOUD A. ABU-MADI

A thesis submitted in partial fulfilment of
the requirements of the University of
Brighton for the degree of Doctor of
Philosophy

March 1998

University of Brighton in collaboration
with ACR Heat Transfer Ltd

ABSTRACT

The last few years have seen a rapid growth in the number of cars equipped with air-conditioning systems. The space available to fit the system is limited and the under bonnet environment is hostile. Moreover, the depletion of the stratospheric ozone has led to legislation on the phasing out of the chlorofluorocarbons (CFCs) and hydrochlorofluorocarbons (HCFCs). These substances are used as refrigerants in most refrigeration, heat pump and air-conditioning systems in service today. The aim of this research project was to study existing air-conditioning systems used in automotive applications to develop a model that simulates the components of these systems. This provides a better understanding of the effect of using different refrigerants in the system and its performance. Experimental studies of the performance of the different heat exchanger geometries used provided inputs to the model developed. Automotive air-conditioning condensers and evaporators simulation models were developed and used to compare the performance of these heat exchangers using CFC and HCFC refrigerants and the non-ozone depleting replacements. Thermodynamic properties of the new refrigerants were derived from the equation of state. The evaporator was simulated taking into consideration the mass transfer associated with the heat transfer in humid conditions. Two types of compact heat exchangers were modelled, round tube with plane fin and plate tube with corrugated fin. These cover most automotive, domestic and industrial applications. The basic performance data of various geometries were determined experimentally. An existing thermal wind tunnel was re-instrumented and modified to improve accuracy at the low air velocities was used in this study. A new data logger linked to a personal computer was used with newly written software to collect and analyse the test data. The results for all geometries tested were correlated and presented in non-dimensional form. The test data were used to determine the effect of various geometrical parameters on the performance for an optimisation of condenser and evaporator designs. The model developed is being used by industrial collaborators for the design of heat exchangers in automotive air-conditioning systems.

LIST OF CONTENTS

ABSTRACT	b
LIST OF CONTENTS	c
LIST OF TABLES	g
LIST OF FIGURES	h
ACKNOWLEDGEMENT	k
DECLARATION	l
NOMENCLATURE	m
1. Introduction	
1.1 Automotive vapour compression systems	1
1.2 Environmental considerations	4
1.3 Heat exchanger performance and geometry effects	6
1.4 Objectives	7
1.5 Aim	8
1.6 Thesis structure	8
2. Literature survey	
2.1 Introduction	9
2.2 Refrigerant-side heat transfer coefficient and pressure drop	10
2.2.1 Two-phase evaporation heat transfer coefficient	10
2.2.2 Two-phase condensation heat transfer coefficient	15
2.2.3 Single-phase heat transfer coefficient	17
2.2.4 Refrigerant-side pressure drop	18
2.3 External surface performance and geometry effects	21
2.3.1 Heat transfer and pressure drop correlations	21
2.3.2 Effect of fin thickness and number of rows	24
2.4 Effect of refrigerant properties	26
2.5 Air-conditioning modelling and automotive application	27

2.6	Summary	29
3.	Thermal wind tunnel	
3.1	Introduction	31
3.2	Thermal wind tunnel	31
3.3	Air-side flow and measurement	33
3.4	Water-side flow and measurement	36
3.5	Data acquisition hardware and software	36
3.6	Experimental procedure	39
3.7	Geometries considered	40
3.7.1	Round tube and plate fin heat exchangers	40
3.7.2	Flat tube and corrugated fin heat exchangers	45
4.	Condenser model	
4.1	Introduction	47
4.2	Configurations	47
4.3	Heat transfer theory	51
4.3.1	Refrigerant-side heat transfer coefficient	53
4.3.2	Air-side heat transfer coefficient	54
4.3.3	Air-side pressure drop	55
4.3.4	Refrigerant pressure drops	55
4.4	Condenser simulation	60
4.4.1	Round tube condensers with single-pass flow	60
4.4.1.1	Assumptions	62
4.4.1.2	Model description	62
4.4.1.3	Calculation process	63
4.4.2	Parallel flow condensers with single and multi-pass flow	66
4.4.2.1	Assumptions	66
4.4.2.2	Model description	67
4.4.2.3	Calculation process	68

5. Evaporator model

5.1	Introduction	70
5.2	Configuration	71
5.3	Heat transfer calculations	71
5.3.1	Refrigerant-side heat transfer coefficient	74
5.3.2	Air-side heat transfer coefficient and pressure drop	77
5.3.3	Refrigerant-side pressure drop	78
5.4	Round tube evaporator simulation model	79
5.4.1	Model description	81
5.4.2	Calculation procedure	82

6. External heat transfer coefficient and geometry description

6.1	Introduction	84
6.2	Analysis	84
6.2.1	Colburn factor	84
6.2.2	Friction factor	86
6.2.3	Reynolds number	87
6.3	Geometrical parameters (R_1 ... R_8).....	87
6.3.1	Round tube and plate fin heat exchangers	87
6.3.2	Flat tube and corrugated fin, parallel flow, heat exchangers	92
6.4	Software and data analysis	96

7. Model validation

7.1	Introduction	97
7.2	Evaporator model validation	97
7.3	Condenser model validation	102

8. Effect of refrigerant properties

8.1	Introduction	106
8.2	Comparison between R12 and R134a performance	106

BRITISH THESIS SERVICE

DX204113

Page Count \neq 260

Awarding Body : The University of Brighton

Thesis By : ABU - MADI Mahmoud A.

Thesis Title : A COMPUTER MODEL FOR HEAT EXCHANGE ...

We have assigned this thesis the number given at the top of this sheet.

**THE BRITISH LIBRARY
DOCUMENT SUPPLY CENTRE**

8.2.1	Effect of refrigerant properties on the performance of round tube condenser	107
8.2.2	Effect of refrigerant properties on the performance of a parallel flow condenser.	111
8.2.3	Effect of refrigerant properties on evaporator performance	113
8.3	Comparison between R22 and R407C performance	118
8.3.1	Effect of refrigerant properties on condenser performance	118
8.3.2	Effect of refrigerant properties on evaporator performance	120
8.4	Summary	122

9. Geometry effects and performance correlating

9.1	Introduction	124
9.2	Effect geometry	124
9.2.1	Effect of fin type	125
9.2.2	Effect of fin spacing	126
9.2.3	Effect of fin thickness	130
9.3	Colburn and friction factors correlation for round tube heat exchangers	136
9.3.1	Colburn and friction factors for heat exchangers with 4-rows	139
9.3.2	Correlation for the effect of the number of tube rows	141
9.4	Correlations for the Colburn and friction factor for flat tube heat exchange	143
9.5	Error analysis	143
9.6	Summary	146

10. Conclusion and further work

10.1	Conclusion	148
10.2	Further work	149

11. Appendices

A	Refrigerant properties
B	Program listing
C	References
D	List of publications

LIST OF TABLES

2.1	Constants in equation (2.55) for different void fraction correlations	20
3.1	Geometry of group 1 samples (with flat fin)	43
3.2	Geometry of group 2 samples (with corrugated fin)	44
3.3	Geometry of group 3 sample	46
4.1	Return bend (180°) loss coefficients	58
4.2	Headers loss coefficients	59
5.1	Fluid dependent parameters, Kandlikar (1991)	77
7.1	Evaporator geometry used in Hilton air-conditioning unit	98
7.2	Test operating conditions used in Hilton air-conditioning unit	98
7.3	Heat exchanger geometries and operating conditions from El-Mahdy and Biggs (1978)	100
7.4	Parallel flow condenser geometry	102
7.5	Round tube condenser geometry	104
8.1	Condenser operating conditions and geometry	107
8.2	Parallel flow condenser operating conditions and geometry	112
8.3	Evaporator operating conditions and geometry	114
9.1	Indices for four row heat exchangers	140
9.2	Limits of 4-row heat exchangers correlations	140
9.3	Constants and indices for effect of number of rows	142
9.4	Limits of number of rows effect correlation	142
9.5	Instrument errors	145
9.6	Uncertainties caused by the different measured parameters for sample “2147” ..	146

LIST OF FIGURES

1.1	Sketch of automotive air-conditioning system	1
1.2	Vapour compression system components	2
1.3	Pressure-specific enthalpy diagram for vapour compression cycle	3
3.1	Schematic diagram of the wind tunnel	32
3.2	Air velocity fluctuation after modification	34
3.3	Low air pressure drop transducer calibration	35
3.4	Wind tunnel software main menu	38
3.5	Cold test output screen	38
3.6	Hot test output screen	38
3.7	Round tube and plate fin configurations	41
3.8	Fins with modified edges	42
3.9	Flat tube heat exchanger	45
3.10	Picture of corrugated fin used with flat tube heat exchangers	46
4.1	Parallel flow condenser configurations	48
4.2	Round tube and plate fin heat exchanger configurations	49
4.3	Simple configurations for round tube and plate fins heat exchangers	50
4.4	Hexagonal fin array	52
4.5	Return bend	58
4.6	Condenser model input screen	61
4.7	Schematic diagram of the condenser model	63
4.8	Calculation procedure for the condenser model	65
5.1	Psychometric chart	72
5.2	Evaporator model input screen	81
5.3	Schematic diagram of evaporator model	82
5.4	Calculation procedure for the evaporator model	83

6.1	Round tube with flat and corrugated fins	88
6.2	Tube diameter at mean distance	89
6.3	One cell of round tube heat exchanger	91
6.4	Plate tube and corrugated fins, parallel flow, heat exchangers	93
6.5	Multi channels flat tube	93
7.1	Comparison of the evaporator model prediction and Hilton air-conditioning unit	99
7.2	Percentage difference for 4-row heat exchanger results	101
7.3	Percentage difference for 8-row heat exchanger results	101
7.4	Difference between experiment and prediction for heat transfer rate for parallel flow condenser	103
7.5	Round tube condenser model validation	105
8.1	Comparison of refrigerant performance in round tube condenser with R12 and R134a	108
8.2	Comparison of refrigerant mass velocity in round tube condenser with R12 and R134a	109
8.3	Comparison of refrigerant pressure drop in round tube condenser with R12 and R134a	109
8.4	Comparison of refrigerant mass velocity per unit duty in round tube condenser with R12 and R134a	110
8.5	Comparison of refrigerant pressure drop per unit duty in round tube condenser with R12 and R134a	111
8.6	Comparison of refrigerant mass velocity per unit duty in parallel flow condenser with R12 and R134a	112
8.7	Comparison of refrigerant pressure drop per unit duty in parallel flow condenser with R12 and R134a	113
8.8	Comparison of refrigerant performance in evaporator with R12 and R134a	115
8.9	Comparison of refrigerant mass velocity in evaporator with R12 and R134a	115
8.10	Comparison of refrigerant pressure drop in evaporator with R12 and R134a	116

8.11	Comparison of refrigerant mass velocity per unit duty in evaporator with R12 and R134a	117
8.12	Comparison of refrigerant pressure drop per unit duty in evaporator with R12 and R134a	118
8.13	Comparison of refrigerant mass velocity per unit duty in condenser with R22 and R407C	119
8.14	Comparison of refrigerant pressure drop per unit duty in condenser with R22 and R407C	120
8.15	Comparison of refrigerant mass velocity per unit duty in evaporator with R22 and R407C	121
8.16	Comparison of refrigerant pressure drop per unit duty in evaporator with R22 and R407C	122
9.1	Fin surface type effect	127
9.2	Fin edge effect, samples of group (2) with 2-row	128
9.3	Fin edge effect, samples of group (2) with 4-row	129
9.4	Fin spacing effect, samples of group (1) with 1-row	131
9.5	Fin spacing effect, samples of group (1) with 2-row	132
9.6	Fin spacing effect, samples of group (1) with 4-row	133
9.7	Fin spacing effect, samples of group (2) with 2-row	134
9.8	Fin spacing effect, samples of group (2) with 4-row	135
9.9	Fin thickness effect, samples of group (1)	137
9.10	Fin thickness effect, samples of group (2)	138
9.11	Validation of flat fin correlation	141
9.12	Colburn and friction factors for flat tube heat exchange	144

ACKNOWLEDGEMENT

All praise and thanks are due to Allah the Almighty who sent his book as the best of speeches, which established science as an absolute proof, his mercy and compassion have allowed me to be at the stage that I am.

I would like to thank my family for giving me all the courage and support I needed in my study.

I would like to thank my supervisors Prof R A Johns and Prof M R Heikal for their invaluable support and encouragement.

I would like to thank the collaborating companies, ACR Heat Transfer Ltd for their generous contribution which included a number of heat exchanger samples; Denso Marsten for providing a number of samples and condenser test data and Calsonic Ltd for their generous contribution of condenser test data.

And finally I would also like to thank the technicians, who helped me throughout my experimental work.

DECLARATION

I hereby certify that this thesis is my own work except where otherwise indicated. I have identified my sources of information, and, in particular have put in quotation marks any passages have been quoted word-for-word and identified their origins.

Signed:



Date: 19 May 98

NOMENCLATURE

A	area
Al	constant in the void fraction equation
b	laplace constant
Bo	boiling number
c_1, c_2	coefficients in El-Mahdy's equation
C	capacity rate ratio
C_{max}	maximum fluid capacity
C_{min}	minimum fluid capacity
C_p	specific heat capacity at constant pressure
Co	convection number
d	diameter
D	depth
$D_{ch,1}$	depth of channel near the edges, corrugated fin and flat tube geometry
$D_{ch,2}$	depth of middle channel, corrugated fin and flat tube geometry
E	enhancement factor
E_p	variable in Klomenko's correlation
f	friction factor
F	enhancement factor
F_2	parameter in Traviss's correlation
Fr	Froude number
F_{fl}	fluid dependent parameter
F_{tt}	parameter in Traviss's correlation
FP	parameter in McQuiston's equation
g	gravity
\dot{G}	mass velocity
h	air side heat transfer coefficient
H	height

i_{fg}	specific enthalpy of vaporisation
j	Colburn factor
JP	parameter in McQuiston's equation
k	thermal conductivity
K_c	contraction loss coefficient
K_e	expansion loss coefficient
l	fin length from root to centre
L	length
Le	Lewis number
m	fin effectiveness parameter
\dot{m}	mass flow rate
N	the number of
Ntu	Number of transfer units
Nu	Nusselt number
N_{cb}	convective boiling number
p	pressure
Pe_*	modified Peclet number
Pr	Prandtl number
q	heat flux
Q	heat transfer rate or duty
Ql	constant in the void fraction equation
r	radius
r^*	hydraulic radius in McQuiston's equation
R_n	geometrical parameter
Re	Reynolds number
Re_*	modified Reynolds number
Rl	constant in the void fraction equation
S	spacing
Sl	constant in the void fraction equation
St	Stanton number

T	temperature
u	velocity
U_{all}	overall heat transfer coefficient
v	specific volume
V	volt
wp	wetted perimeter
x	vapour quality
X	Lockhart-Martinelli parameter
Y	variable in Shah's correlation

Subscripts

a	air
b	bend
bo	boiling
bs	bubble suppression
c	cross sectional
C	critical
cb	convective boiling
ch	channel
co	forced convection
col	collar
db	dry bulb
eq	equivalent
f	fin
ff	face
fr	friction
h	hydraulic
i	in, inlet
l	liquid
m	mean

<i>mix</i>	mixture
<i>mom</i>	momentum
<i>nb</i>	nucleate boiling
<i>o</i>	out
<i>p</i>	primary
<i>s</i>	secondary
<i>t</i>	tube
<i>t / r</i>	tube per row
<i>tp</i>	two-phase
\overline{tp}	average two-phase
<i>tt</i>	turbulent
<i>r</i>	row
<i>re</i>	reduction
<i>ref</i>	refrigerant
<i>v</i>	vapour
<i>w</i>	water

Symbols

α	void fraction
β	two-phase flow factor
θ	liquid/vapour gradient ratio
ψ	two-phase multiplier in Shah's correlation
μ	viscosity
ϵ	Effectiveness
Δ	difference
ϕ_v	two-phase frictional multiplier
δ	thickness
η_a	total surface temperature effectiveness
η_f	fins temperature effectiveness

λ	local pressure losses coefficient
ω	moist content
σ	surface tension
ρ	density

CHAPTER 1

Introduction

1.1 Automotive vapour compression systems

The use of automotive air-conditioning systems is increasing rapidly. The system typically uses a belt driven compressor mounted on the engine block, flexible hoses to connect the compressor to a condenser located in front of the radiator, an evaporator inside the passenger compartment, and an expansion valve or orifice tube to control refrigerant flow. A typical automotive air-conditioning system is shown schematically in figure (1.1).

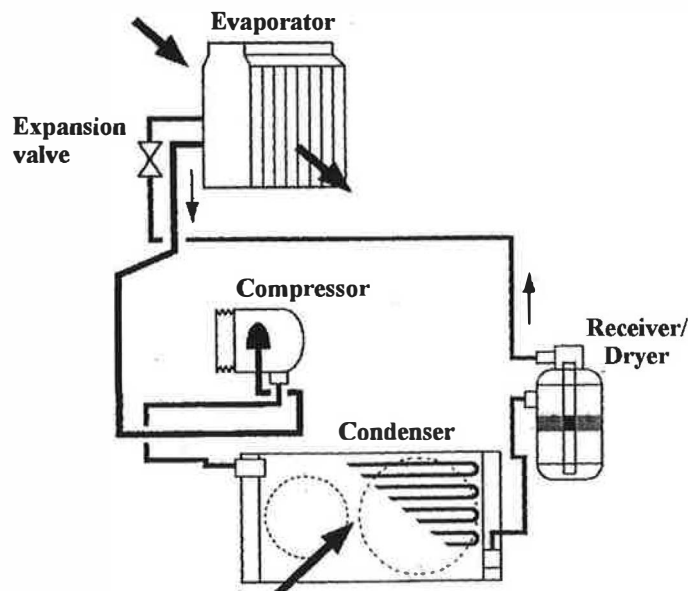


Figure (1.1) Sketch of automotive air-conditioning system

Figure (1.2) shows a schematic diagram of the vapour compression unit used in automotive air-conditioning systems. A number of other features must be considered when modelling a system accurately. The cooling capacity is determined both by the

need to “pull down” the inside temperature quickly and also by the need to provide adequate cooling in the hot idle type of condition experienced in stop and go rush hour traffic in a hot, humid climate.

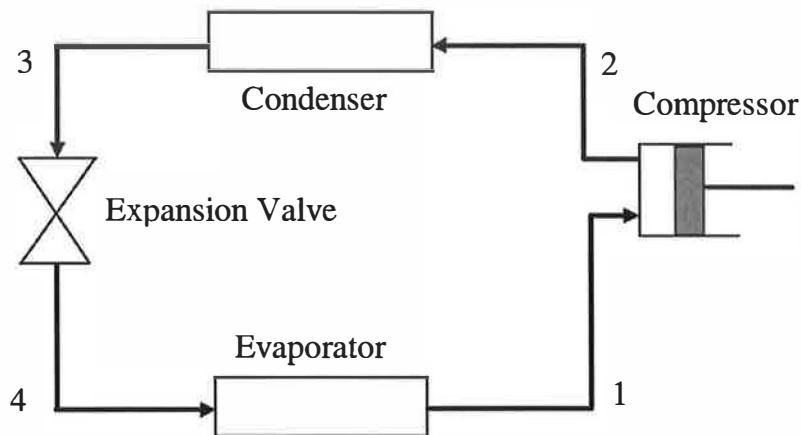


Figure (1.2) Vapour compression system components

In tropical and temperate summer climates the air-conditioning system is required not only to transfer heat from the air renewed and re-circulated in the vehicle but also to reduce the relative humidity to a level in the comfort zone. The system operates between two pressure levels, high pressure or condensing pressure, and low pressure or evaporating pressure. In steady-state operation, the system seeks an operating condition which achieves both a mass flow and pressure balance between the flow control device and the compressor, and an energy balance on the heat transfer to the evaporator, work transfer to the compressor, and heat transfer from the condenser.

The compressor utilises a work transfer from the engine to compress the refrigerant vapour from low pressure to high pressure. The pressure difference is maintained by the compressor. The expansion valve controls the mass flow rate to ensure that the refrigerant leaves the evaporator as a superheated vapour. Any liquid entering the compressor would have a detrimental effect on the mechanical components of the compressor. Figure (1.3) shows the thermodynamic cycle on the pressure-specific enthalpy diagram.

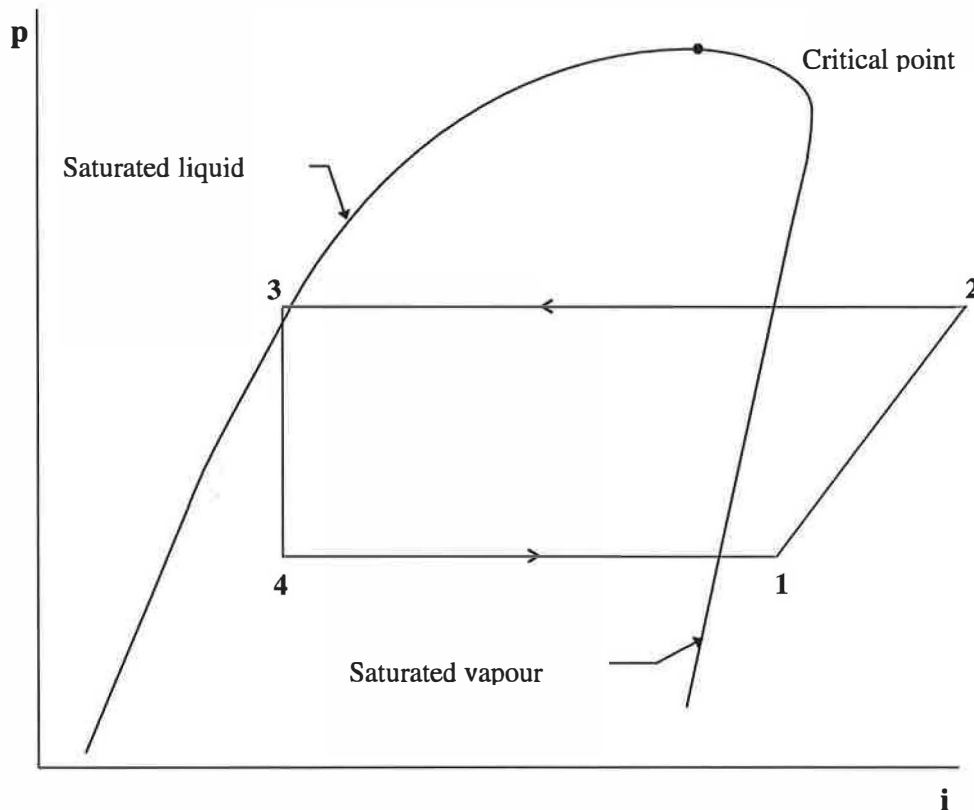


Figure (1.3) Pressure-specific enthalpy diagram for vapour compression cycle

Each component has a specific function and may be studied independently of the remaining components provided that sufficient thermodynamic parameters are known. The design for each component may be optimised. The selection and design of each component can be matched to limitations, such as energy consumption, space, weight, cost, etc. Separate models can be built for each component. This study focuses on heat exchangers which can be used individually or as a part of a simulation of the whole system. In particular the focus is on automotive air-conditioning systems where space for installation of evaporators and condensers is severely restricted and “under bonnet” conditions are hostile. Furthermore, the weight of each component is an important issue in the car design. Accurate sizing of the heat exchangers is, therefore, very important. Ambient temperatures are usually high. Further, relatively long hose runs make the system particularly sensitive to pressure losses. It is, therefore, important that designers of heat exchangers for automotive use have modelling techniques available to predict the performance of

condensers and evaporators with different refrigerants, including the newly introduced non-ozone depleting ones.

1.2 Environmental considerations

The working fluids available to refrigeration engineers in the late 19th century were far from ideal. They were restricted to using fluids that were readily available at that time. Early vapour compression refrigeration systems made use of ethyl ether, carbon dioxide, ammonia or sulphur dioxide. However, none of these fluids is ideally suited to safe refrigeration use. Ethyl ether is explosive, ammonia is toxic and inflammable, sulphur dioxide is toxic and the critical pressure for carbon dioxide is high. Other refrigerants such as methyl chloride, dichloroethylene and isobutane were introduced in the early 1900s. The latter two were for use in centrifugal compressors. Sulphur dioxide and methyl chloride dominated the small unit market until development of the chlorofluorocarbon refrigerants by Frigidaire in the late 1920s. These were low in toxicity, non-flammable in the working range, exhibited good chemical stability and were miscible with lubricating oils. Dichlorodifluoromethane (R12) dominated the market for small positive displacement compressors, particularly hermetically sealed units. Large installations continued to use the early refrigerants, carbon dioxide and ammonia. Where toxicity was a concern, such as in the food industry, secondary fluid circuits with brine were often used. The chemical and transport properties of CFCs also provided manufacturers with economic propelling fluids for use in aerosols, blowing agents for synthetic foams and solvents. Some 85% of the R12 produced was used in aerosols and foams only to be released eventually into the atmosphere.

Research in the 1970s showed that CFCs have a life of many decades when released into the atmosphere. CFCs do not break down in the lower atmosphere and are transported to the stratosphere. The action of ultraviolet radiation from the sun breaks down the CFCs in the stratosphere releasing chlorine which acts as a catalyst in the destruction of stratospheric ozone. Depletion of stratospheric ozone increases the levels of ultraviolet radiation reaching the surface of the earth and this may

damage crops and lead to skin cancers in humans and animals. During the 1980s a number of countries recognised the environmental consequences of the depletion of stratospheric ozone and took independent action to reduce the production of CFCs. The Vienna Convention for the Protection of the Ozone Layer was signed in 1985 by the member countries of the European Community and 21 others. The Montreal Protocol to control the production and consumption of CFCs and halons was approved in 1987. Under this convention production and consumption of CFCs was frozen at 1986 levels from 1989. The Montreal Protocol was amended in 1990, and much stricter controls were agreed for the phasing out of CFCs. By 1998 the production and consumption of CFCs was to be reduced to 50% of the 1986 level. The environmental impact of the hydrochlorofluorocarbons (HCFCs), which include chlorodifluoromethane (R22), was also recognised. HCFCs contain a hydrogen atom and break up more easily in the lower atmosphere with the result that smaller quantities of chlorine reach the stratosphere. HCFCs are known as transitional substances and their phase out was scheduled for between 2020 and 2040. However, the European Community Regulations adopted in 1994, brought forward the complete phasing out of CFCs to 1995 and HCFCs to 2015.

The principal alternative refrigerant to dichlorodifluoromethane (R12) is 1,1,1,2-tetrafluoroethane designated by ASHRAE as R134a. This is a hydrofluorocarbon (HFC) which has no chlorine atoms and contains hydrogen atoms within the molecule. HFCs have a shorter life than that of CFCs when discharged into the atmosphere and do not deplete stratospheric ozone. HFCs are considered to be long term alternatives to CFCs. R134a has thermodynamic and transport properties similar to those of R12. Although HCFCs such as chlorodifluoromethane (R22) will continue to be manufactured for 10 years, legislation exists in Europe to freeze consumption at the 1995 level and to phase consumption out between 2004 and 2015. There is no single HFC with thermodynamic and transport characteristics similar to those of R22. HFC near azeotropic blends (R407A, R407B and R407C) of difluoromethane (R32), pentafluoroethane (R125) and R 134a have been developed as alternatives for R22. These are non-flammable and have comparable operating pressures.

Further, global warming concerns are providing a stimulus to develop more efficient systems to reduce electricity consumption and thereby reduce emissions of carbon dioxide(CO₂) from power stations. Many of the alternative refrigerants being introduced are actually blends of two or more separate fluids that do not stay uniformly mixed throughout the complete refrigeration cycle. During use the blends, called zeotropes, tend to separate into the individual components as they pass through the refrigeration cycle. Unlike CFCs and HCFCs these zeotropes evaporate and condense over a range of temperatures at a constant pressure.

At present there is little experimental data giving detailed information on the performance of the new refrigerants in condensers and evaporators, particularly in the presence of the new lubricating oils. Manufacturers of refrigeration and air-conditioning heat exchangers have little definitive data on which to base their designs and tend to err on the side of caution with designs that are larger than necessary. Also, there is little information about retrofitting systems designed to use CFCs with the new refrigerants.

1.3 Heat exchanger performance and geometry effects

Traditional round tube and plate fin heat exchangers are widely used in applications where pressure drops for the internal fluid flow is a critical design factor, notably in automotive applications for engine cooling and air-conditioning. The heat transfer and pressure loss correlations used on the internal tube surfaces provide adequate accuracy. Since the air-side thermal resistance is significantly higher than that of the tube internal wall, small errors in predicting the air-side heat transfer performance lead to significant errors in predicting the overall thermal performance of heat exchangers. The accuracy of a heat exchanger model may, therefore, be judged by the ability to predict the air-side heat transfers and pressure losses accurately.

Many experimental studies (see chapter 2) have been carried out on this type of compact heat exchanger to improve the understanding of heat transfer performance and pressure losses over a wide range of “air on” velocities. Correlations have been

developed to predict the Colburn factor, j , and friction factor, f , from experimental results for the wide range of fin and tube geometries used in these applications.

The published correlations, are restricted to flat finned heat exchangers and to a limited number of geometrical configurations. None report any plate fin with modified surfaces such as corrugated and sine wave. Limited data has been found in the literature for the external heat transfer coefficient and pressure losses for the types of modified fins used by air-conditioning manufacturers. Furthermore, a little conflicting data has been found in the literature on the effect of the fin and tube geometries on the performance, such as the effect of fin thickness. The need of accurate experimental data, therefore, covering the types of modified fins has been recognised and forms part of this study.

1.4 Objectives

The objectives of this research are:

1. To analyse existing correlations for heat transfer coefficients and friction factors for current refrigerants inside round tubes.
2. To develop correlations for thermodynamic and transport properties for the new non-ozone depleting refrigerants.
3. To develop an empirical model to simulate the performance of condensers and evaporators used in automotive air-conditioning systems.
4. To validate the models against existing manufacturers' data and experimental data from the literature for current refrigerants.
5. To enable industrial collaborators to use the condenser and the evaporator models for designing and sizing heat exchangers using different refrigerants including the non-ozone depleting refrigerants.
6. To evaluate the effect of the new refrigerant thermodynamic and transport properties on vapour compression systems and to produce a comparison of results for retrofitting the new non-ozone depleting refrigerants in existing systems.
7. To investigate the effect of fin and tube geometries on the performance of the compact heat exchangers used in automotive air-conditioning systems.

8. To determine the external heat transfer coefficients and pressure drops for heat exchangers geometries.
9. To derive correlations from experimental tests for heat transfer performance and pressure losses.

1.5 Aim

The aim of this research programme was to develop an empirical model of the performance of the heat exchangers used in automotive air-conditioning systems using the new non-ozone depleting refrigerants for use by designers of new systems and for users considering retrofitting existing systems with these new refrigerants.

1.6 Thesis structure

The thesis main body is divided into eight chapters. Past work concerning automotive air-conditioning systems, refrigerant heat transfer and pressure drop, round tube and plate fin performance is reviewed in a literature survey in chapter 2. Chapter 3 describes the thermal wind tunnel used for testing the heat exchanger geometries, the measurements, the results, and the geometries considered. The condenser and the evaporator models are described in chapters 4 and 5 respectively. The configurations used, the heat transfer and pressure drop theory and the analysis procedure are also reported. Chapter 6 describes the analysis of the wind tunnel results to determine Colburn factor, friction factor and Reynolds number. The derivation of various geometrical parameters are also discussed. Validation of the condenser and evaporator models developed against experimental data are shown in chapter 7. The effect of refrigerant properties on the thermal performance and pressure losses are discussed in chapter 8. Chapter 9 contains the wind tunnel test results. Chapter 10 draws conclusion from the findings of this investigations and recommends the areas to which further work should be directed.

CHAPTER 2

Literature survey

2.1 Introduction

This chapter contains a review of the most important publications on refrigerant heat transfer, pressure drop and the external performance of compact heat exchangers and simulation models for air-conditioning systems. A number of studies covering the refrigerant heat transfer and pressure drop are found in the literature. Correlations to predict the heat transfer and pressure drop during the various regions of flow were found. The most important studies were listed in this survey to allow the use of suitable and accurate correlations to predict the refrigerant performance. The second area of concern deals with the external performance of compact heat exchangers. Compact heat exchangers are widely used in many industrial, residential, and commercial applications including automotive air-conditioning. Many investigators have studied, experimentally, the performance of compact heat exchangers. Attempts have been made to correlate the heat transfer coefficients and pressure drops to non-dimensional numbers to take the effect of the heat exchanger geometries into account. However, many of the resulting correlations produce large errors (up to 50%) when compared with the data of other investigators. Furthermore, many of the heat exchanger geometries used were not included in these studies. Finally, the last area of this survey reviews the simulation models for air-conditioning systems. There are a number of simulation models to predict the performance of heat pumps and refrigeration systems. However, few were found in the literature presumably due to commercial confidentiality. Use of these models contributes to the optimisation of the heat exchanger design, reducing costs and reducing energy consumption. The accuracy of these models depends mainly on the accuracy of the external performance data. However, very little information is given about the external performance data used in the existing models. Further, the phase out of the ozone depletion refrigerant used in air-conditioning systems and replacing them with non-ozone depletion refrigerants has been paid very little attention.

2.2 Refrigerant-side heat transfer coefficient and pressure drop

2.2.1 Two-phase evaporation heat transfer coefficient

A large number of correlations to predict the two-phase evaporating heat transfer coefficient is available in the literature. Some of the correlations were developed by investigators using one set of experimental data, and some were developed on the basis of a large number of data sets involving a number of fluids over a wide range of parameters. These latter correlations are more valuable since they represent a larger data base and cover a much broader range of operating conditions. This makes them suitable for use with evaporator design models. One of the early correlations was developed by Chen (1966) on the basis of six different data sources. It offered a relatively simple additive form of nucleate boiling and convective terms. Many later experimental studies, such as those of Anderson (1966), Chaddock and Noerager (1966), Jallouk (1974), and Mohr and Runge (1977), have indicated that this correlation tends to over predict the effect of nucleation resulting in large deviations from the measured values. Further, refinement in Chen's correlation was directed at the prediction of the nucleate boiling component with other pool boiling correlations; while the Cooper (1984) correlation was used by Gungor and Winterton (1986). Efforts were also directed at correlating the enhancement factor and the suppression factor in the Chen correlation to a number of operating and system variables, e.g., Ross (1985) and Bennett and Chen (1980).

Shah (1976) proposed a correlation in a graphic form using the boiling number, Bo , and the convection number, Co . Shah also proposed the replacement of the Martinelli parameter X_{tt} with the convection number Co , since the viscosity ratio was found to have no significant influence. A total of 800 data points was used to develop the correlation. In a later paper, Shah (1982) presented a set of equations to fit the graphical chart published earlier. Shah's correlation was compared to data from 19 different experimental studies and showed a mean deviation of 14%. The correlation which can be used for evaporation inside vertical and horizontal tubes

and annuli represents the two-phase evaporating heat transfer coefficient as a function of the liquid heat transfer coefficient as;

$$\Psi = \frac{h_{tp}}{h_l} \quad (2.1)$$

Where Ψ is calculated as the largest of Ψ_{nb} , Ψ_{bs} or Ψ_{cb} ;

$$\Psi_{cb} = \frac{1.8}{Y^{0.8}} \quad (2.2)$$

$$\Psi_{nb} = 230Bo^{0.5} \quad \text{For } Y > 1, Bo > 0.3E-4 \quad (2.3)$$

$$\Psi_{nb} = 1 + 46Bo^{0.5} \quad Y > 1, Bo < 0.3E-4 \quad (2.4)$$

$$\Psi_{bs} = FBo^{0.5} \exp(2.74Y^{-0.1}) \quad 1 \geq Y > 0.1 \quad (2.5)$$

$$\Psi_{bs} = FBo^{0.5} \exp(2.47Y^{-0.15}) \quad 0.1 \geq Y \quad (2.6)$$

Where F is taken as;

$$F = 14.7 \quad \text{For } Bo \geq 11E-4 \quad (2.7)$$

$$F = 15.43 \quad Bo < 11E-4 \quad (2.8)$$

And the variable Y is defined as;

$$Y = Co \quad \text{For vertical tube} \quad (2.9)$$

$$Y = Co \quad \text{horizontal tube with } F\eta \geq 0.04 \quad (2.10)$$

$$Y = 0.38F\eta^{-0.3}Co \quad \text{horizontal tube with } F\eta \leq 0.04 \quad (2.11)$$

Kandlikar and Thakur (1982) proposed an additive correlation with nucleate boiling and convective contributions. The same data sets used by Shah (1976) were employed in the development of their correlation. The mean deviation with the data was 13.7%. The model was further refined by Kandlikar (1983) to include the effects of different fluids through a fluid dependent parameter F_{fl} introduced in the

nucleate boiling term. Kandlikar reported a considerable improvement over Shah's correlation with all the data.

Khanpara et al. (1986) compared experimental data for R113 in a plane tube with published correlations in the literature and found the best agreement to be given by Kandlikar (1983) although no R113 data was used in the development of Kandlikar correlation. The correlation proposed by Gungor and Winterton (1986) is a modification of the Chen correlation and was developed using over 4300 data points for seven different fluids tested by 28 investigators. The data used include evaporation in vertical and horizontal tubes and annuli. The enhancement factor F is replaced by E which is dependent on the boiling number Bo and the Martinelli parameter X_{tt} . The suppression factor S is correlated as a function of X_{tt} and liquid Reynolds number Re_l . The mean deviation for the suggested correlation was 21.4% for saturated boiling and 25.0% for sub-cooled boiling.

Klimenko (1988) proposed a flow boiling correlation in vertical and horizontal channels with a fully wetted perimeter. The correlation was based on experimental data for nine different fluids in the range of vapour quality from 0.017 to 1.00 and pressure from 0.61 to 30.4 bar. Klimenko suggested that the heat transfer rate during evaporation depends on the tube wall thermal conductivity. The two-phase condensation heat transfer coefficient in vertical and horizontal channels with fully wetted perimeter with liquid is calculated as,

$$Nu_{tp} = Nu_{bo} \quad \text{For } N_{cb} < 16000 \quad (2.12)$$

$$Nu_{tp} = Nu_{co} \quad N_{cb} > 16000 \quad (2.13)$$

where Nu_{bo} is calculated as;

$$Nu_{bo} = 0.0074 Pe_*^{0.6} E_p^{0.5} Pr_l^{-1/3} \left(\frac{k_t}{k_l} \right)^{0.15} \quad (2.14)$$

$$E_p = \frac{P}{\sqrt{\sigma g (\rho_l - \rho_v)}} \quad (2.15)$$

The modified Peclet number Pe_* is calculated from,

$$Pe_* = \frac{qb}{i_{fg}\rho_v\mu_l} \quad (2.16)$$

and Nu_{co} is calculated as;

$$Nu_{co} = 0.087Re_{mix}^{0.6}Pr_l^{1/6}\left(\frac{\rho_v}{\rho_l}\right)^{0.2}\left(\frac{k_t}{k_l}\right)^{0.09} \quad (2.17)$$

where the Reynolds number of the two-phase mixture Re_{mix} is calculated as;

$$Re_{mix} = \frac{u_{mix}b}{\mu_l} \quad (2.18)$$

$$u_{mix} = \left(\frac{\dot{G}}{\rho_l}\right)\left(1 + x\left(\frac{\rho_l}{\rho_v} - 1\right)\right) \quad (2.19)$$

$$b = \sqrt{\frac{\sigma}{g(\rho_l - \rho_v)}} \quad (2.20)$$

The convective boiling number N_{cb} is calculated as,

$$N_{cb} = Bo_*\left(\frac{\rho_v}{\rho_l}\right)^{1/3} = \frac{Re_{mix}}{Re_*}\left(\frac{\rho_l}{\rho_v}\right)^{2/3} \quad (2.21)$$

The modified Reynolds number Re_* is calculated from,

$$Re_* = \frac{qb}{i_{fg}\rho_v\mu_l} \quad (2.22)$$

and the modified boiling number Bo_* is calculated from,

$$Bo_* = \left(\frac{i_{fg}\dot{G}}{q}\right)\left(1 + x\left(\frac{\rho_l}{\rho_v} - 1\right)\right) \quad (2.23)$$

As reported by Kandlikar (1990), in the nucleate boiling region, no flow effects are included, while in the convective boiling region, the two-phase heat transfer coefficient is assumed to be independent of the tube diameter.

The additive model for the convective and nucleate boiling components originally suggested by Bergles and Rohsenow (1964) for sub-cooled and low quality regions was employed in the Kandlikar (1990) formula for flow boiling in smooth tubes. The correlation by Kandlikar was developed from over 5000 data points for 10 different fluids for two-phase flow boiling inside horizontal and vertical tubes with diameters between 4 mm and 32 mm and quality change from 0.001 to 0.987. The

two-phase local evaporating heat transfer coefficients inside smooth tubes are calculated from the single-phase liquid heat transfer coefficients modified for nucleate and convective boiling. Kandlikar recommended the use of the following set of equations.

For nucleate boiling.

$$h_{tp,nb} = 0.6683Co^{-0.2}(1-x)^{0.8}h_l + 1058Bo^{0.7}(1-x)^{0.8}F_{fl}h_l \quad (2.24)$$

and for convective boiling.

$$h_{tp,cb} = 1.136Co^{-0.9}(1-x)^{0.8}h_l + 667.2Bo^{0.7}(1-x)^{0.8}F_{fl}h_l \quad (2.25)$$

Correlations (2.24) and (2.25) are valid for vertical tubes and for horizontal tubes with Froude number, $Fr_l > 0.04$. However, for horizontal tubes with Froude number, $Fr_l \leq 0.04$ the correlations becomes;

For nucleate boiling.

$$h_{tp,nb} = 0.6683Co^{-0.2}(1-x)^{0.8}(25Fr_l)^{0.3}h_l + 1058Bo^{0.7}(1-x)^{0.8}F_{fl}h_l \quad (2.26)$$

and for convective boiling.

$$h_{tp,cb} = 1.136Co^{-0.9}(1-x)^{0.8}(25Fr_l)^{0.3}h_l + 667.2Bo^{0.7}(1-x)^{0.8}F_{fl}h_l \quad (2.27)$$

The Froude number is calculated with all of the refrigerant flow considered as liquid from;

$$Fr_l = \frac{\dot{G}^2}{\rho_l g d} \quad (2.28)$$

The non-dimensional boiling number, Bo , and the convection number, Co , proposed by Shah (1976) are defined as;

$$Bo = \frac{q}{\dot{G}i_{fg}} \quad (2.29)$$

$$Co = \left(\frac{1-x}{x} \right)^{0.8} \left(\frac{\rho_g}{\rho_l} \right)^{0.5} \quad (2.30)$$

Further work was done to include augmented tubes and compact evaporators, Kandlikar (1991), by adding two separate factors to the correlations developed

earlier. The correlation developed by Kandlikar (1990) has a mean deviation of 18.8% comparing to 25.8% for Shah correlation (1982) and 24% for Gungor and Winterton correlation (1987) compared to the same sets of data used by Kandlikar (1990). More investigators are listed in Kandlikar (1990) and Webb and Gupte (1992).

2.2.2 Two-phase condensation heat transfer coefficient

General correlations for two-phase condensation heat transfer coefficient have been suggested by many investigators. Akers and Rosson (1960) derived one of the early correlation to predict the heat transfer coefficient during condensation. They obtained over 300 data points during condensation of two fluids, R12 and Methanol, inside a horizontal tube. The heat transfer was presented in terms of Nusselt number as;

$$Nu = 13.8Pr^{1/3} \left(\frac{i_{fg}}{C_p \Delta T} \right)^{1/6} Re_v^{0.2} \quad \text{For } 1000 \leq Re_v \leq 20000 \quad (2.31)$$

$$Nu = 0.1Pr^{1/3} \left(\frac{i_{fg}}{C_p \Delta T} \right)^{1/6} Re_v^{2/3} \quad 20000 \leq Re_v \leq 100000 \quad (2.32)$$

The above equations are valid for liquid Reynolds number $Re_l < 5000$. For $Re_l > 5000$ and $Re_v > 20000$, they recommended the use of the following correlation;

$$Nu = 0.026Pr^{1/3} (Re_v + Re_l)^{0.8} \quad (2.33)$$

where

$$Re_l = \frac{d_i \dot{G}L}{\mu_l} \quad (2.34)$$

Cavallini and Zecchin (1974) developed a correlation to calculate the heat transfer coefficient during condensation. The correlation was developed specifically for the halocarbons R11, R12, R21, R22, R113 and R114.

$$h_{tp} = 0.05Re_{eq}^{0.8} Pr_l^{0.33} \left(\frac{k_l}{d_i} \right) \quad (2.35)$$

Where the equivalent Reynolds number, Re_{eq} , is defined as;

$$Re_{eq} = Re_l + Re_v \left(\frac{\mu_v}{\mu_l} \right) \left(\frac{\rho_l}{\rho_v} \right)^{0.5} \quad (2.36)$$

The correlation was based on 460 data points and valid for liquid Reynolds number, Re_l , between 7000 and 53000 and liquid to vapour viscosity ratio, (μ_l / μ_v) , from 11:1 to 314:1.

Traviss et al. (1972) developed a correlation from 160 data points for R12 and R22 to calculate the heat transfer coefficient during condensation. The correlation was developed assuming $Pr_l > 3$.

$$Nu = F_{tt} \left(\frac{Pr_l Re_l^{0.9}}{F_2} \right) \quad (2.37)$$

The above equation is valid for $5 < F_{tt} < 15$, where F_{tt} is calculated from;

$$F_{tt} = 0.015(X_{tt}^{-1} + 2.85X_{tt}^{-0.467}) \quad (2.38)$$

The parameter F_2 can be determined from the following equations;

$$F_2 = 0.707 Pr_l Re_l^{0.5} \quad \text{For } Re_l < 50 \quad (2.39)$$

$$F_2 = 5Pr_l + 5Ln(1 + Pr_l(0.09636Re_l^{0.585} - 1)) \quad 50 < Re_l < 1125 \quad (2.40)$$

$$F_2 = 5Pr_l + 5Ln(1 + 5Pr_l) + 2.5Ln(0.00313Re_l^{0.812}) \quad Re_l > 1125 \quad (2.41)$$

Shah (1979) developed a non-dimensional correlation from experimental data, 474 data points, for a wide range of fluids. The correlation developed can be used to calculate two-phase condensation heat transfer coefficients in vertical, horizontal and inclined tubes of diameters ranging from 7 mm to 40 mm.

$$h_{tp} = h_l \left((1-x)^{0.8} + \frac{3.8x^{0.76}(1-x)^{0.04}}{pre^{0.38}} \right) \quad (2.42)$$

Where the pressure reduction, pre , is defined by;

$$pre = \frac{p}{p_c} \quad (2.43)$$

The two-phase heat transfer coefficient is expressed as a function of the liquid heat transfer coefficient, reduced pressure and refrigerant vapour quality for a wide range

of tube diameters and operating conditions. The liquid heat transfer coefficient should be calculated from an equation suitable for the tube and flow conditions as suggested by Shah (1979). The limits of the original correlation published in (1979) were extended to a reduced pressure, p_{re} , up to 0.82 in a later paper, Shah (1981), with a total number of 777 data points used from 10 different fluids.

Tandon et al. (1995) studied the two-phase condensing heat transfer coefficient for R12 and R22. The experimental results were correlated based on the previously published correlation by Akers and Rosson (1960).

2.2.3 Single-phase heat transfer coefficient

The generalised correlation suggested by Dittus-Boelter, McAdams (1954), has been widely used to calculate the single-phase heat transfer coefficient for fully developed turbulent flow in smooth tubes:

$$Nu = 0.023 Re^{0.8} Pr^n \quad (2.44)$$

Where n is 0.3 when the fluid is being cooled and 0.4 when being heated.

Petukhov (1970) has developed a more complicated correlation for fully developed turbulent flow in smooth tubes. This accounts for the Prandtl number effect for different fluids more accurately:

$$h_l = \frac{Re_l Pr_l \left(\frac{f}{2}\right) d}{\left(1.07 + 12.7(Pr_l^{2/3} - 1)\left(\frac{f}{2}\right)^{1/2}\right) k_l} \quad (2.45)$$

For lower Reynolds number, the Gnielinski (1976) correlation can be used to calculate the single-phase heat transfer coefficient in smooth tube:

$$h_l = \frac{(Re_l - 1000) Pr_l \left(\frac{f}{2}\right) d}{\left(1 + 12.7(Pr_l^{2/3} - 1)\left(\frac{f}{2}\right)^{1/2}\right) k_l} \quad (2.46)$$

Where the friction factor, f , in both correlations is given by:

$$f = (1.58 \ln(Re_l) - 3.28)^{-2} \quad (2.47)$$

2.2.4 Refrigerant-side pressure drop

Total pressure drop for a heat exchanger is the sum of frictional pressure drop, momentum change pressure drop, local fitting pressure drops and gravitational pressure drop. The gravitational component, however, is negligible for automotive applications. The frictional component is mainly caused by the tube roughness, while the momentum component is caused by the change of the properties and the flow velocity. The local pressure drops are caused by the local pressure losses due to the change in the cross sectional area, flow direction, etc.. The frictional pressure drop and momentum change pressure drop should be calculated for each flow region separately.

The frictional single-phase pressure drop calculation is well established in the literature and can be calculated accurately from Darcy-Weisbach equation, ASHRAE (1993), as follow;

$$\Delta p_{fr} = \frac{f \dot{G}^2 v_i L}{2d_h} \quad (2.48)$$

The friction factor calculations are well established for the single-phase region inside tubes with both laminar and turbulent flow. For fully developed laminar-viscous flow in a pipe, the friction factor f is evaluated as follows

$$f = \frac{64}{Re} \quad \text{For } Re \leq 1187 \quad (2.49)$$

With turbulent flow, friction losses depend not only on the flow conditions as characterised by Reynolds number, but also on the nature of the tube wall surface.

With smooth tube walls, the friction factor can be calculated as;

$$f = \frac{0.3164}{Re^{0.25}} \quad \text{For } 1187 \leq Re \leq 100,000 \quad (2.50)$$

$$f = 0.0032 + \frac{0.221}{Re^{0.237}} \quad 100,000 < Re < 3,000,000 \quad (2.51)$$

The momentum change pressure drop is caused by the change in properties of the fluid between inlet and outlet and can be estimated from the general equation relating the mass flow and specific volume as;

$$\Delta p_{mom} = \dot{G}^2 (v_o - v_i) \quad (2.52)$$

In the two-phase region, two models were used by a number of investigators to evaluate frictional and momentum change pressure drops; the homogeneous model, which assumes equal vapour and liquid velocities, and the heterogeneous model (or separate flow model) in which the velocities for liquid and vapour.

The frictional pressure drop for two-phase flow can be determined using a two-phase frictional multiplier and the single-phase friction factor. The momentum change pressure drop can be determined using the void fraction, the ratio of gas flow area to total flow area.

Several equations for the determination of the frictional and momentum change pressure drops have been developed based on both models, homogeneous and heterogeneous. One of the main and early heterogeneous models was developed by Lockhart and Martinelli (1949) for isothermal two-phase flow. Their experimental data were collected for tube diameters from 1.49 mm to 25.83 mm and for mixtures of air and other fluids including benzene, kerosene and water. Their correlation calculates the two-phase frictional pressure drop per unit length as follow;

$$\left(\frac{\Delta p}{\Delta L} \right)_{tp} = \phi_v^2 \left(\frac{\Delta p}{\Delta L} \right)_v \quad (2.53)$$

Where the two-phase frictional multiplier, ϕ_v , is given in a graphical form as a function of X . The parameter suggested by Lockhart and Martinelli, X , depends on the type of flow of each phase, laminar or turbulent and is defined as a function of the liquid pressure gradient and the vapour pressure gradient.

$$X = \sqrt{\frac{\left(\frac{\Delta p}{\Delta L}\right)_l}{\left(\frac{\Delta p}{\Delta L}\right)_v}} \quad (2.54)$$

Equations were given by Lockhart and Martinelli (1949) to calculate the parameter, X , for different flow patterns. Many later investigators modified the above correlation based on additional experimental data and approximated the graphical results into correlations, ASHRAE (1993).

The momentum change pressure drop, based on the heterogeneous model is given by Sur and Azer (1991) as;

$$\left(\frac{dp}{dL}\right)_{mom} = 2\dot{G}^2 \left(\frac{(1-x)}{\rho_l(1-\alpha)} - \frac{x}{\rho_v\alpha} \right) \frac{dx}{dL} + \dot{G}^2 \left(\frac{x^2}{\rho_v\alpha^2} - \frac{(1-x)^2}{\rho_l(1-\alpha)^2} \right) \frac{dx}{dL} \frac{d\alpha}{dL} \quad (2.55)$$

The void fraction, α , can be calculated from a generalised equation suggested by Butterworth (1975). The suggested equation can be used for homogeneous and heterogeneous models.

$$\alpha = \frac{1}{1 + AI \left(\frac{(1-x)}{x} \right)^{QI} \left(\frac{\rho_V}{\rho_l} \right)^{RI} \left(\frac{\mu_l}{\mu_V} \right)^{SI}} \quad (2.56)$$

Where the factors AI , QI , RI , SI are given for the homogeneous and the heterogeneous models in table (2.1).

Model	AI	QI	RI	SI
Homogeneous	1	1	1	0
Heterogeneous	0.28	0.64	0.36	0.07

Table (2.1) Constants in equation (2.56) for different void fraction correlations

Based on the homogeneous model, Pierre (1964) developed one of the early correlation for two-phase evaporating pressure drop for R12 and R22.

$$\Delta p_{tp, fr} = \left(f_m + \frac{(x_o - x_i)d_h}{x_m L} \right) \frac{\dot{G}_l v_m L}{d_h} \quad (2.57)$$

where the friction factor, f_m , is calculated as;

$$f_m = 0.0185 \left(\frac{Bo}{Re} \right)^{0.25} \quad (2.58)$$

The momentum change pressure drop assuming the homogeneous model is given by Souza et al. (1993) as follow;

$$\Delta p_{mom} = \left[\frac{\dot{G}^2 x^2}{\alpha \rho_v} + \frac{\dot{G}^2 (1-x)^2}{(1-\alpha) \rho_l} \right]_{out} - \left[\frac{\dot{G}^2 x^2}{\alpha \rho_v} + \frac{\dot{G}^2 (1-x)^2}{(1-\alpha) \rho_l} \right]_{in} \quad (2.59)$$

The homogeneous model provides a simple method for computing the acceleration component of pressure drop. However, its accuracy to predict frictional pressure drop at high vapour quality is low, Muller-Steinhagen and Heck (1986). Jung and Radermacher (1989c) found that the refrigerant pressure drop was best described using the heterogeneous model.

2.3 External surface performance and geometry effects

2.3.1 Heat transfer and pressure drop correlations

Many experimental studies have been carried out on compact heat exchangers to improve the understanding of heat transfer performance and pressure losses over a wide range of air on velocities. Correlations have been developed to predict the Colburn factor j and friction factor f from experimental results for the wide range of fin and tube geometries used in many applications.

McQuiston (1978b) developed a correlation to determine j and f factors for round tube and plate fin heat exchangers with staggered rows from the air-side Reynolds number based on the tube outside diameter. Geometrical effects were included as the ratio of the total air-side area to the tube outside area. The equation was derived from practical tests on heat exchangers with 4 rows of tubes.

$$j_{N_r=4} = 0.0014 + 0.2618JP \quad (2.60)$$

$$JP = \left(\frac{A_a}{A_p} \right)^{-0.15} Re_{d_o}^{-0.4} \quad (2.61)$$

$$f = 0.004904 + 1.382FP^2 \quad (2.62)$$

$$FP = Re_{d_o}^{-0.25} \left(\frac{r_o}{r^*} \right)^{0.25} \left(\frac{(S_t - 2r_o)S_f}{4(1 - S_f\delta_f)} \right)^{-0.4} \left(\frac{S_t}{2r^*} - 1 \right)^{-0.5} \quad (2.63)$$

where

$$\frac{r^*}{r_o} = \frac{\frac{A_a}{A_p}}{(S_t - 2r)S_f + 1} \quad (2.64)$$

while the j factor formula correlates 90% of the data within $\pm 10\%$, the friction factor correlation had a lower accuracy of $\pm 35\%$.

El-Mahdy and Biggs (1979) used previously published data for heat exchangers with round tubes and staggered tube arrangements and circular or continuous flat fins to develop a correlation for the calculation of the j factor from Reynolds number, based on the hydraulic diameter.

$$j = c_1 Re_{d_h}^{c_2} \quad (2.65)$$

The geometric effects were included as ratios of fin thickness to fin length, hydraulic diameter to fin thickness and fin spacing to fin thickness.

$$c_1 = 0.159 \left(\frac{\delta_f}{H_f} \right)^{0.141} \left(\frac{d_h}{\delta_f} \right)^{0.065} \quad (2.66)$$

$$c_2 = -0.323 \left(\frac{\delta_f}{H_f} \right)^{0.049} \left(\frac{S_f}{\delta_f} \right)^{0.077} \quad (2.67)$$

where the fin height, H_f , is calculated as;

$$H_f = 0.5(D_f - d_o) \quad (2.68)$$

Equation (2.65) was validated by testing a geometry which has not been included in the data bank but within the equation limits. An agreement of 3 to 5% was found between the experiment and prediction.

Gray and Webb (1986) collected published data on samples of 4-row heat exchangers with continuous flat fins and round tubes in a staggered arrangement to develop a correlation of j factor and Reynolds number based on the tube diameter. Geometrical effects were included as the ratios of tube spacing to row spacing and fin spacing to tube outside diameter. A multiplier was used to account for the effect of the number of tube rows. The effect of the number of tube rows above 5 was found to be small. The j factor is calculated as;

$$j_{N_r=4} = 0.14 Re_{d_o}^{-0.328} \left(\frac{S_t}{S_r} \right)^{-0.502} \left(\frac{S_f - \delta_f}{d_o} \right)^{0.0312} \quad (2.69)$$

Gray and Webb also derived a correlation for f factor based on the superposition of friction over the tubes and that on the fins. Reynolds number was based on the tube outside diameter. Geometric effects were included as the ratio of tube spacing to tube diameter. The tubes friction factor was calculated in this correlation from the work of Zukankas (1972). The fin-side friction factor is correlated as;

$$f_f = 0.508 Re_{d_o}^{-0.521} \left(\frac{S_t}{d_o} \right)^{1.318} \quad (2.70)$$

and the friction factor for the finned tube heat exchanger is obtained as;

$$f = f_f \frac{A_f}{A_a} + f_t \left(1 - \frac{A_f}{A_a} \right) \left(1 - \frac{\delta_f}{S_f} \right) \quad (2.71)$$

Two to three data points for each sample were used to correlate the j and f factors. The coefficient of determination for the j factor equation was 96.0% with 89% of the data correlated within 10%. The row effect equation correlated the data within +8 to -4%. The friction factor equation correlated 95% of the data within $\pm 13\%$.

Wang et al. (1996) studied the performance of 15 samples of plate fin heat exchangers with different geometrical parameters, including the number of tube rows, fin spacing and fin thickness in an open circuit wind tunnel. The results were presented in the form of j and f factors against Reynolds number based on the tube collar diameter. The results for 2, 4 and 6 tube rows were correlated using a multiple linear regression technique in a partial range of the experimental data ($800 < Re <$

7500) based on the previously published correlation by Briggs and Young (1963). Although Wang et al suggested a negligible effect of the fin thickness on the thermal performance and pressure drop, the proposed correlations for j and f factors contained the number of tube rows and the ratios of the fin thickness and fin pitch to the tube collar diameter as follow;

$$j = 0.394 Re_{d_{col}}^{-0.392} \left(\frac{\delta_f}{d_{col}} \right)^{-0.0449} \left(\frac{S_f}{d_{col}} \right)^{-0.212} N_r^{-0.0897} \quad (2.72)$$

$$f = 1.0394 Re_{d_{col}}^{-0.418} \left(\frac{\delta_f}{d_{col}} \right)^{-0.104} \left(\frac{S_f}{d_{col}} \right)^{-0.197} N_r^{-0.0935} \quad (2.73)$$

Ninety seven percent of the experimental data of j factor were correlated within $\pm 10\%$ while 88% of the f factor data were correlated within $\pm 10\%$.

Most of the general correlations and studies found in the literature are described above. However, many other studies, directed to investigate and correlate the performance of round tube and plate fins heat exchangers for a limited number of geometries, can be found in Yu (1992).

2.3.2 Effect of fin thickness and number of rows

The effect of varying the number of tube rows on the performance was studied by Rich (1975). He tested six heat exchangers with the number of rows varied from 1 to 6 with all the other parameters kept the same. Rich reported a “crossover phenomena” for j factor when Reynolds number is increased. Rich suggested that the fin spacing to tube diameter ratio affected the crossover point. This occurred at a row space based Reynolds number of $Re=10000$. Rich, however only tested one geometry. This effect was explained as the result of vortices affecting the local temperature distribution. The effect of the number of tube rows on j factor was correlated by McQuiston (1978b) through the use of the experimental data of Rich (1975).

$$\frac{j_{N_r}}{j_{N_r=4}} = \frac{1 - 1280 N_r Re_{S_r}^{-1.2}}{1 - 5120 Re_{S_r}^{-1.2}} \quad (2.74)$$

Gray and Webb (1986) suggested that the number of tube rows had a negligible effect on the heat transfer coefficient for heat exchangers with more than four rows. However, for heat exchangers with 1 to 4 rows, the performance was found to decrease with increasing the number of rows at low Reynolds numbers. A crossover of j factor occurred at Reynolds number of 8000, based on the tube outside diameter, for a higher Reynolds numbers, as suggested by Rich (1975).

$$\frac{j_{N_r}}{j_{N_r=4}} = 0.991 \left(2.24 Re_{d_o}^{-0.092} \left(\frac{N_r}{4} \right)^{-0.031} \right)^{0.607(4-N_r)} \quad (2.75)$$

Gray and Webb (1986) used the data of Rich (1975) with some adjustment as the original data was believed to have poor accuracy at low Reynolds numbers.

Heat exchanger samples with 2, 4 and 6 tube rows were tested by Wang et al. (1996) as described above. They reported an increase in the j factor with a reduced number of rows at low Reynolds numbers. However, this effect diminishes as the Reynolds number, based on the tube collar diameter, increases over 2000.

Nir (1991) used published data as well as his own to correlate the heat transfer and friction factor for individually finned tubes with staggered arrangements. Most of the experimental data, 33 for heat transfer and 72 for friction factor, were correlated within $\pm 10\%$. However, the proposed correlation for j factor over predicted Kays and London data by 50%.

McQuiston and Tree (1971) showed an increase in f and j factors, by up to 70 and 34% respectively, with increased fin spacing from 1.776 mm to 3.175 mm. The samples tested were aluminium round tubes with plate fins. Rich (1973) found that the fin friction and j factors were independent of the fin pitch when the Reynolds number was based on row spacing.

El-Mahdy and Biggs (1979) reported the effect of fin thickness on j factor through the equation described above, equation (2.65). A strong relationship was found between the j factor and the ratio of the fin thickness to the fin height, δ_f / H_f . The increase in the j factor when the ratio, δ_f / H_f , increased was due to the fin thickness which effects the fin efficiency and heat transfer coefficient.

Although Wang et al. (1996) suggested a negligible effect of the fin thickness on the thermal performance and pressure drop, the proposed correlations for j and f factors contained the number of tube rows and the ratios of the fin thickness and fin pitch to the tube collar diameter. Wang et al. (1996) reported that the fin spacing had no effect on the heat transfer.

2.4 Effect of refrigerant properties

The effect of refrigerant properties on the heat transfer coefficients and pressure losses during different flow phases has been studied by many investigators. Jung et al. (1989a), (1989b), Jung et al. (1993a) and (1993b) studied the heat transfer coefficient and pressure drops during evaporation for pure and refrigerant mixtures experimentally. Eckels and Pate (1990) compared the heat transfer coefficient for R12 with R134a as calculated from an existing correlation available in the literature for single-phase and two-phase flow. In a later publication, Eckels and Pate (1991) studied the evaporation and condensation heat transfer coefficients in round tube for the refrigerants R12 and R134a experimentally. They reported higher heat transfer coefficients during evaporation and condensation with R134a for the same mass velocity.

Carpenter (1992) studied the retrofitting of R134a for an industrial refrigeration unit designed for R12. The results showed an overall improvement of the duty and a reduction of compressor power when R134a was used in place of R12 with the coefficient of performance increasing by 12%.

Struss et al. (1990) compared the performance of R12 and R134a experimentally in an automotive air-conditioning system. The comparison was carried out considering two types of condensers, parallel flow and serpentine. A higher pressure ratio across the compressor and a higher head pressure were found for R134a, while the passenger compartment temperatures were in the same range for both refrigerants. The same results were found by El-Bourini et al. (1990) and (1991). They concluded that the head pressure could be reduced with R134a by increasing the condenser performance.

2.5 Air-conditioning modelling and automotive application

The importance of a simulation model for estimating heat exchanger performance had been realised by many investigators. Hiller and Glicksman (1976) developed one of the early simulation models for heat pumps using the refrigerant R22. The condenser model was developed for staggered round tubes using the Effectiveness-Ntu method. The effect of condensation on the evaporator surfaces was included using a modified version of the effective surface temperature approach. They used Kays and London data, with some modifications, to determine the external heat transfer and the pressure drop factor. Two heat exchanger configurations can be simulated using the model, a single-pass and multi-pass with the single-phase regions, superheat and sub-cooled ahead of the two-phase region. The condenser model predictions were within 5% when compared with experiment. However, nothing was mentioned about the evaporator model accuracy.

Based on the previously developed simulation model of Hiller and Glicksman (1976), Dabiri (1982) developed a steady state simulation model for air-to-air heat pumps. The main use of the model was to produce and compare performance data for different types of heat pumps.

A series of reports were published by the Oak Ridge National Laboratory, Ellison and Creswick (1978), Raymond et al. (1981), Fischer and Rice (1983). The initial simulation model was based on the early work of Hiller and Glicksman (1976).

However, modifications were made by Fischer and Rice (1983) to improve the accuracy of pressure drop calculations on both the air-side and the refrigerant-side. The new version allowed the use of more refrigerants in the simulation such as R12, and R502. However, the air-side heat transfer coefficient still had not been calculated accurately. The louvered fin and wavy fin heat transfer coefficients were calculated from a correlation for smooth fins with a constant correction factor. Yet, the model was validated against experimental tests for wavy fin condensers and evaporators.

Domanski and Didion (1983) considered a tube-by-tube analysis to model condensers and evaporators in their heat pump simulation model. The performance calculations were based on the Effectiveness-Ntu method. The two-phase condensation and evaporation heat transfer coefficients were calculated from a correlation suggested for R12 and R22. The correlation of Briggs and Young (1962) was used to derive the external heat transfer coefficient.

O'Neill and Crawford (1989) and Kempfak and Crawford (1992) modelled one condenser configuration with round tube and plate fins with refrigerant R134a under steady state conditions. The geometry modelled was tested experimentally under two operating conditions and showed an overall agreement between 2% and 20% for heat transfer and pressure drop respectively. However, a good agreement between experiment and prediction was expected since the overall heat transfer coefficient was derived from the experimental test using the least-squares analysis. Further, the model accuracy was not examined beyond the test data, and predicting accurate results outside this range is very doubtful.

One of the early automotive air-conditioning simulation models to predict the performance under steady state conditions, using the refrigerant R134a, was developed by Kyle et al. (1993). The model was based on the residential heat pump model developed at the Oak Ridge National Laboratory as described by Ellison and Creswick (1978). The condenser model can only model heat exchangers with round

tubes and smooth fins, while the evaporator model can only simulate heat exchangers with plate tubes and corrugated fin.

Castro et al. (1993) developed a condenser and evaporator simulation model based on the Effectiveness-Ntu relation. The model was valid for round tube and plate fin condensers and evaporators and for flat tube and corrugated fin condensers. The equivalent Reynolds number suggested by Klimenko (1988) was used to consider the two-phase evaporation heat transfer coefficient. The generic equation by Shah (1979) was implemented to calculate the heat transfer coefficient during two-phase condensation. However, nothing was mentioned about the refrigerant pressure drops.

Mignot and Henon (1995) developed a simulation model for automotive parallel flow condensers. The model considers a cell by cell technique to simulate the three different flow regions found in condensers, superheat, two-phase flow and subcooled liquid. The local two-phase heat transfer coefficient and pressure loss were calculated using Shah and Martinelli equations respectively. Although the heat transfer rates were computed accurately within 5%, the refrigerant pressure drop was around 20% of the test values.

2.6 Summary

Air-conditioning heat exchanger designers may use some of the design software available commercially to predict performance, size or to optimise the design to reduce the cost. The phase out of the CFC (R12) and the HCFC (R22) and replacing them with the HFC (R134a) and (R407C) respectively forced designers to consider these alternative refrigerants in their designs. However, the new replacements need more attention to study their behaviour experimentally and theoretically. It was decided, therefore, to develop a heat exchanger simulation model which could be used to design and size air-conditioning and refrigeration condensers and evaporators. The accuracy of this model was to be judged by the accuracy of the thermal and air pressure losses predictions, which depend strongly on the external performance data. Since the air-side thermal resistance is significantly larger than

that for the tube wall and the internal fluid thermal resistance, any small change in the external heat transfer coefficient results in a large change in the overall heat transfer coefficient. Therefore, the air-side performance expressed as j and f factors is required to be presented in an accurate and easy to use form.

All earlier simulation models required extensive inputs and are limited. Further, most models could only calculate the performance of a heat exchanger from operating conditions fixed by the whole system. The ability to input the operating conditions would enable the optimisation of the components and the system.

CHAPTER 3

Thermal wind tunnel

3.1 Introduction

This chapter describes the hardware, software and the experimental procedures employed for testing the heat exchangers. An existing thermal wind tunnel, used in previous research projects, Achaichia (1987) and Yu (1992), was used to determine external heat transfer coefficients and pressure loss data for the surfaces under steady state conditions. The existing facilities were upgraded for this programme of experimental work.

3.2 Thermal wind tunnel

The thermal performance of the various test surfaces was measured with hot water circulated through a heat exchanger sample and ambient air drawn over the external finned area. Pressure drops were measured in isothermal tests without hot water circulation to eliminate inertia terms and changes in air transport properties. Figure (3.1) shows a schematic diagram for the wind tunnel used. It is an open circuit design divided into three main sections, a contraction, test section and plenum chamber.

a. Contraction. The contraction converges from an opening of 377 x 377 mm to 152 x 152 mm cross section with an angle of 8° over a length of 800 mm. The area contraction ratio of 6.2 is within the range suggested by Pankhurst (1952). Ideally the contraction should produce a uniform velocity distribution at the working section. A honeycomb was fitted at the entrance to reduce turbulence and guide the air as it enters the tunnel.

b. Test section. The test section has constant cross section of 152 mm x 152 mm and is divided into two parts, a fixed part and a removable section. The

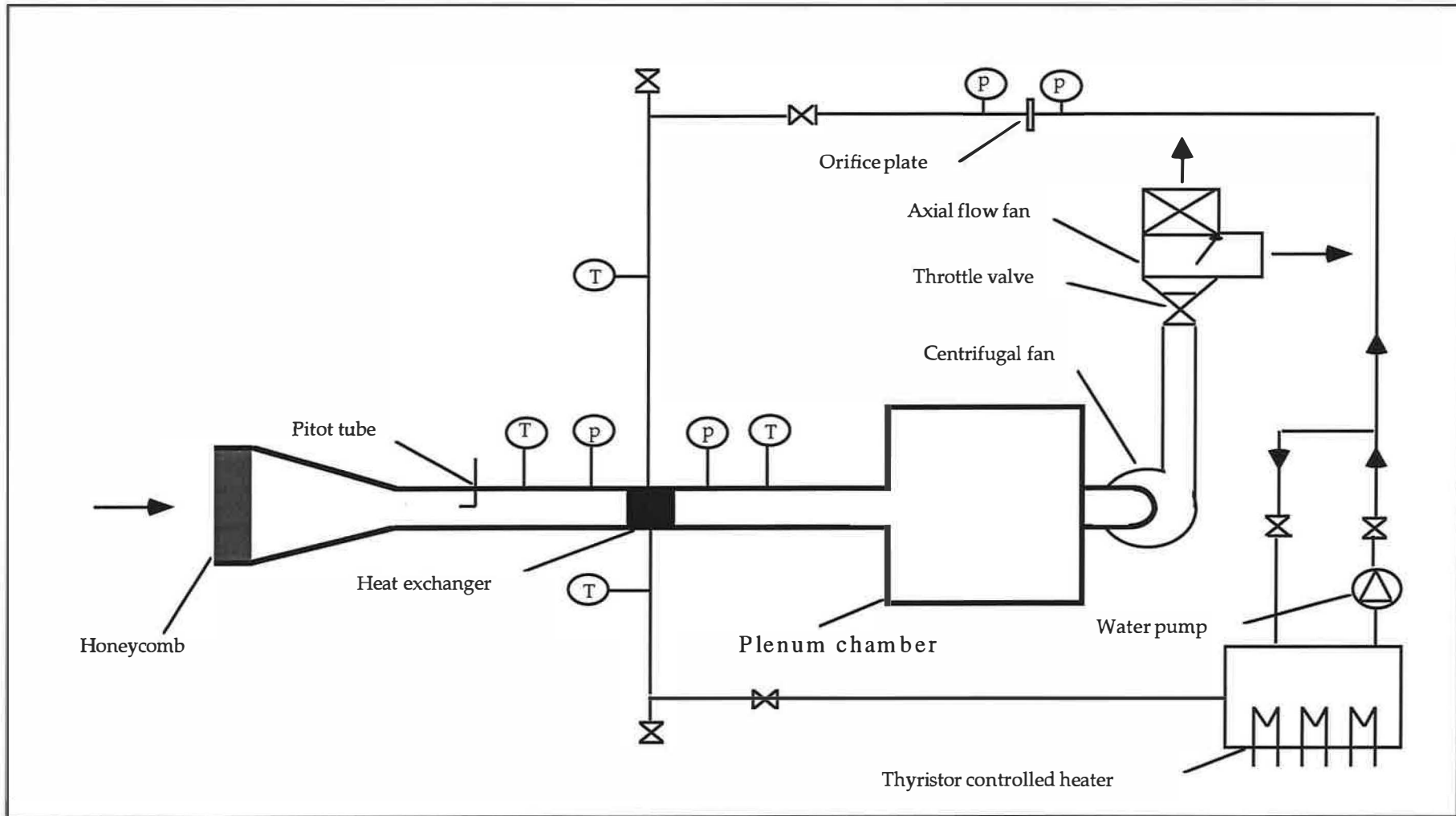


Figure (3.1) Schematic diagram of the wind tunnel

latter section facilitated the mounting of samples with various depths. The original working section was replaced with a newly constructed one identical to that described by Achaichia (1987). The new test section made of plywood was varnished to provide protection against any water leaks. All measurements on the air-side were made in this section.

c. The plenum chamber. The diffuser in the original design was replaced by plenum chamber to reduce air flow fluctuations at low velocities as recommended by Yu (1992). Two layers of fine mesh were placed inside the chamber to enhance the damping effect.

3.3 Air-side flow and measurement

In the original design of the thermal wind tunnel, the air flow was generated using a centrifugal fan for high velocities and an axial flow fan for low velocities. The air flow was restricted by blocking off part of the air duct with a throttle valve. The centrifugal flow fan expelled the hot air to the outside of the laboratory while the axial flow fan discharged it into the laboratory. The latter generated an increase in the air temperature inside the laboratory and created unstable operating conditions. A set of pulleys was fitted between the three phase motor and the centrifugal fan to reduce the fan speed by 50%. This enabled the use of the centrifugal fan at intermediate speeds, between those for the axial fan and those for the centrifugal fan at full speed. This modification reduced the air flow fluctuations to within $\pm 1\%$ and variations in the ambient temperature within the laboratory. Figure (3.2) shows the face velocity fluctuation after modification.

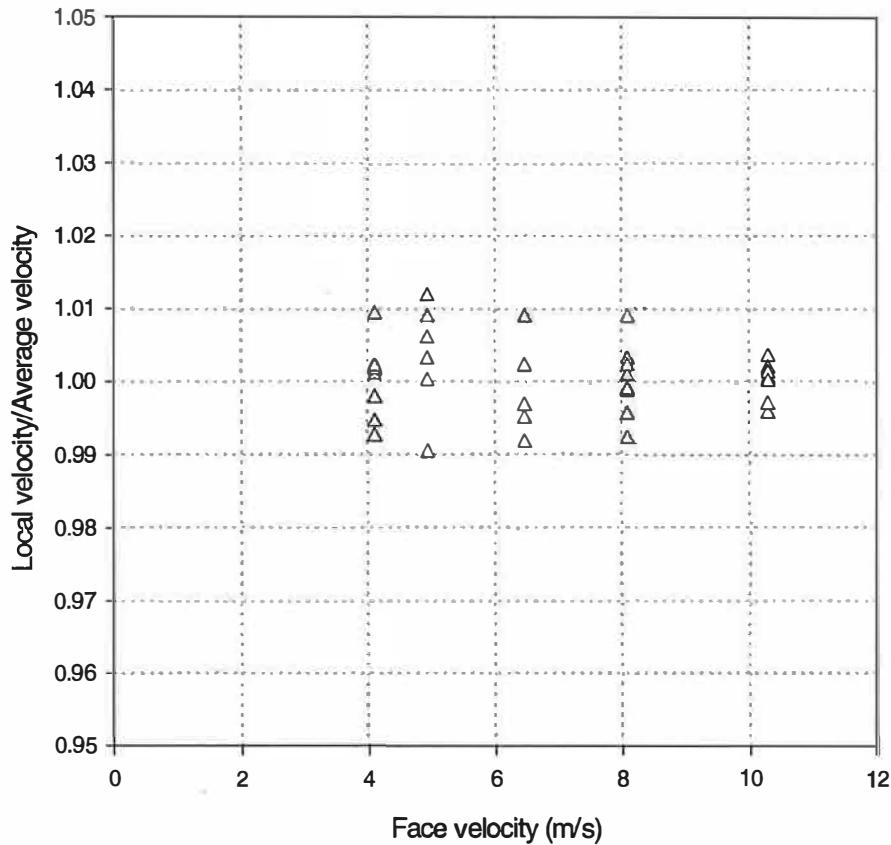


Figure (3.2) Air velocity fluctuation after modification

The air-side pressure drop across the tested sample was measured using four tappings upstream and two tappings downstream connected to a differential pressure transducer with a range of 0 to 250 mm of water. The pressure drop measurement at low velocities was improved through the addition of a pressure transducer with a measuring range from 0 to 20 mm of water. The newly fitted transducer, which has an accuracy of 1% for readings between 1 to 20 mm of water, Furness Control (type FC 044), was calibrated against an inclined manometer. The relationship between the pressure and the voltage output obtained from the calibration is shown in figure (3.3). The output linearity was confirmed over the differential pressure range of 0 to 30 mm of water.

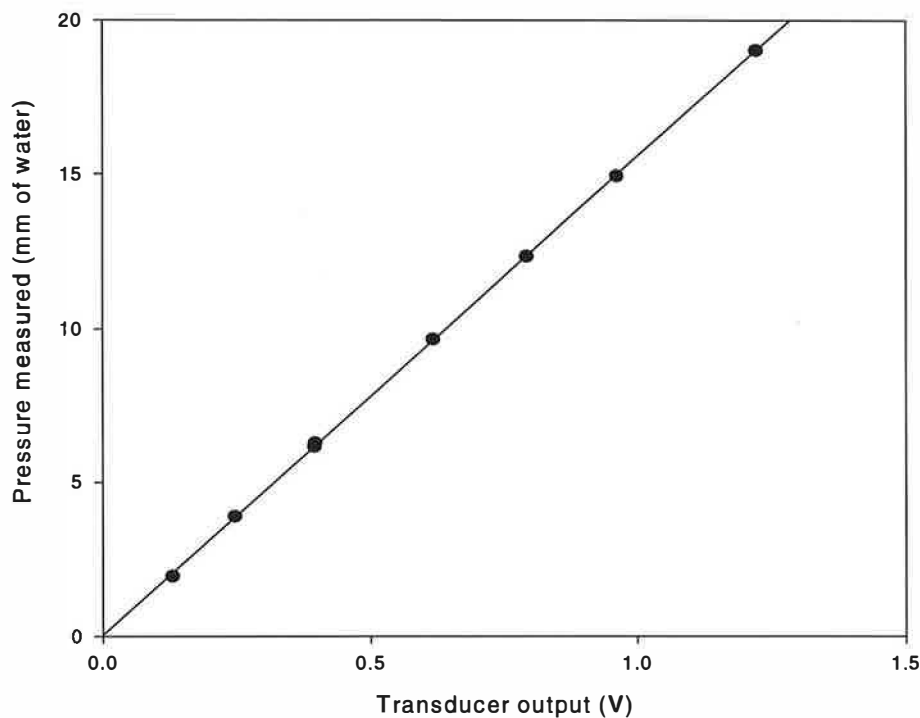


Figure (3.3) Low air pressure drop transducer calibration

The relationship between the transducer output, V_o in volts, and the pressure drop measured Δp was:

$$\Delta p = 15.5407V_o + 0.03204 \quad (\text{mm H}_2\text{O}) \quad (3.1)$$

A Pitot static tube located upstream of the working section was used to determine the air velocity used. Two pressure transducers, with ranges of 0 to 20 mm of water and 0 to 250 mm of water, were connected to the Pitot tube to cover the wide range of air velocities. The temperature of the hot water at inlet was measured during the heat transfer rate tests as a reference parameter. Other temperatures were calculated from measurement of the temperature difference for the water flow. A thermocouple was used to measure the inlet air temperature during the isothermal pressure drop tests. A thermopile was used to measure the temperature difference between the hot water at inlet and the air at inlet. This was used to calculate the air on temperatures during heat transfer tests. The differential temperature across the sample was measured

using 9 x 9 thermopile made of type K, chromel/ alumel junctions. The thermopile was fixed in a uniform grid upstream and downstream to produce a signal amplified by factor of nine to improve accuracy and the effects of any temperature distribution. More details of the instrumentation calibration can be found in Achaichia (1987).

3.4 Water-side flow measurement

Hot water was circulated through the test sample using a centrifugal pump in a closed circuit. The water temperature was regulated by use of a thyristor controlled electric heater element placed in a 500 litre tank. The water flow rate was controlled using two gate valves and a by-pass tube around the centrifugal pump. The tank and pipe line, connecting the tank to the pump and to the test sample, were insulated with polystyrene and rubber foam. The water differential temperature across the heat exchanger sample was measured using a 4 x 4 thermopile made of similar materials to those used on the air-side. An orifice plate connected to a differential pressure transducer was used to measure the water flow rates.

3.5 Data acquisition hardware and software

The data acquisition process is fully automated thereby reducing operator errors and facilitating repetitive calculations. The original wind tunnel data acquisition system was based on a data logger controlled by a BBC microcomputer. However, this computer was too slow and not user friendly by today's standards. Furthermore, monitoring, analysing and storing the data was a time consuming and inconvenient process. The microcomputer was replaced by a personal computer (PC) to overcome these difficulties and to read the newly installed differential pressure transducer.

A new data logger, type (D101/56) made by P.A. Hilton was installed. It is a multi-channel analogue and digital unit with both input and output capability. Commands and data are transferred via a 5-wire RS 232 serial link using ASCII character strings sent and received by the controlling computer with a 9600 baud rate and 8 data bits.

The microprocessor and memory inside the logger can be used to set-up the system to return data from transducers and thermocouples in the required form.

A new software routine , `LOGGER`, was written and used to establish communication between the PC and the logger. The analogue signals from the thermocouples measuring differential temperatures and from the pressure transducers were converted into digital form in the data logger. The data logger was used to acquire the temperatures of air-on and water-on from the thermocouple signals.

The main body of the software, developed using BBC Basic language by previous researcher, was rewritten, `THERMTUN.BAS`, in Quick Basic language for the PC. Changes made included data acquisition, format of data storage and addition of calibration and information verifying routines.

The zero offset of pressure transducers measuring air velocity and air pressure drop were determined using `CALIBRATE` routine which was executed before starting any new tests either hot or cold. The zero offsets of the thermopile measuring the air and water differential temperatures were determined for hot tests only. These data together with the test serial number, sample identity name and atmospheric pressure were stored on the hard disk as a data file called `CALIBRATE.DAT`. This allowed a temporary suspension of the experiment and subsequent resumption with consistent parameters.

When `THERMTUN.BAS` is executed, five options are displayed as follows: Reset calibrated values, cold test, hot test, show stored results on screen and exit, figure (3.4). `RESETCALIB` routine, which operates under option 1, resets all zero offset calibration values to zero. This was implemented before starting the calibration procedure for a new test. It is recommended, for practical reasons, to start the experiment by performing the cold test followed by the hot test. However, the routine `CALIBRATE` was called at the beginning of each new test made whether cold or hot. Once one of these two options was selected, communication was established between the computer and the data logger to reset the gain and output

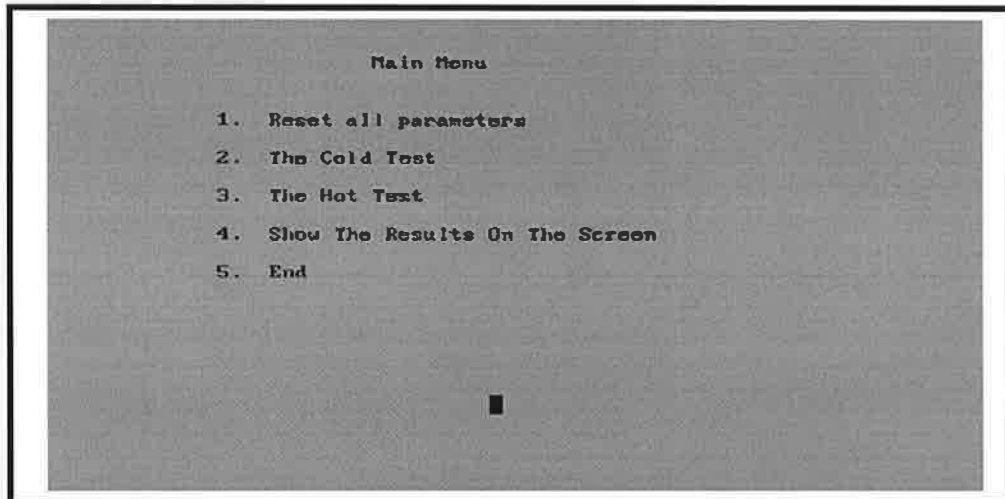


Figure (3.4) Wind tunnel software main menu

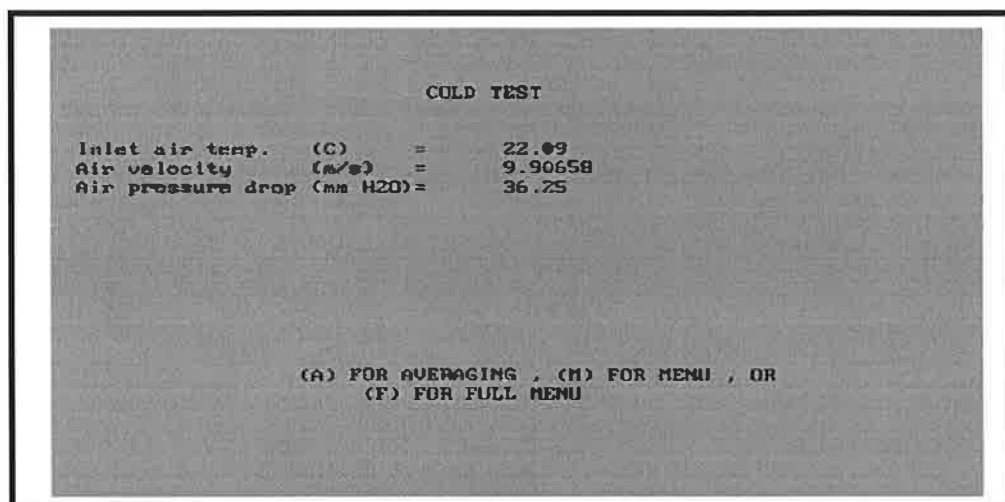


Figure (3.5) Cold test output screen

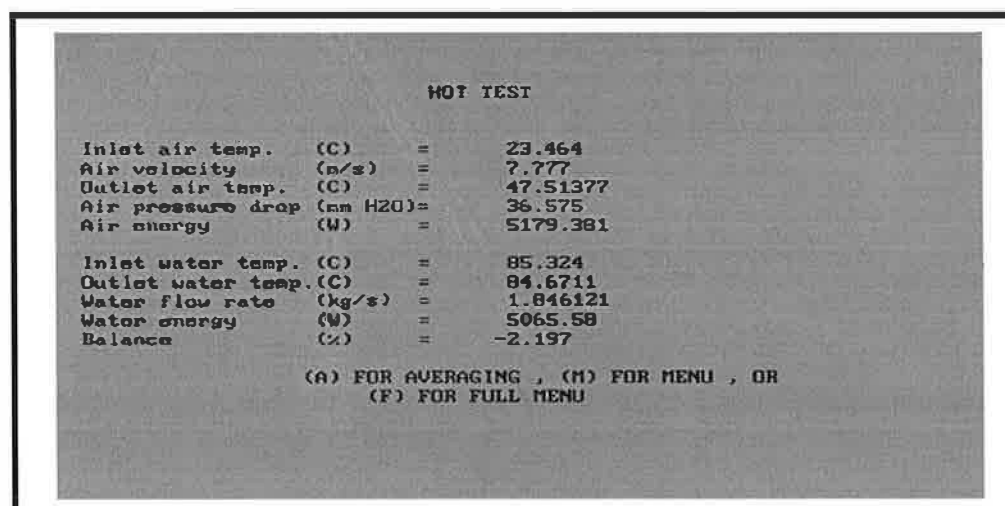


Figure (3.6) Hot test output screen

units for all channels used. The channels were scanned continuously and readings were shown on the screen as long as the output screen was displayed. Figures (3.5) and (3.6) shows the screen display for cold tests and hot tests respectively. When steady state conditions were obtained the readings were averaged and stored on the hard disk. The stored results were saved as a data file initialled by the letter T followed by the test serial number. Since the air velocity is the main parameter varied in the experiment, the initial output screen displayed the air velocity only thereby allowing the operator to set it to the required value more quickly. Once the required velocity had been achieved, full output was displayed. For the cold tests, the output screen displayed air velocity, air pressure drop and air on temperature numerically. For the hot tests, the output screen displayed the extra parameters measured, air off temperature, water on and off temperatures, water flow rate, energy transfer for water and air and heat balance for the energy transferred. Option number four allowed the operator to display the contents of the result file, at that stage, on the screen.

3.6 Experimental procedure

During experimentation, the sample was placed in a fixed position and the working section was kept shut using two spring loaded locking mechanisms. Rubber seals were used to provide an air tight seal on the sample. Masking tape was used for further air tightness between the working section and the sample under test. Two rubber hoses with clamps were used to connect the sample inlet and exit headers to the main hot water circuit. Polystyrene foam was used to insulate the rubber hoses and the sample during heat transfer tests.

The experiment settings stored in the file CALIBRATE.DAT were defaulted at the start of any new isothermal pressure drop tests or heat transfer tests. All pressure transducers measuring air velocity and pressure drop were then calibrated. Experimental settings, such as atmospheric pressure, sample name and test number were then entered.

During the isothermal pressure drop tests, use of the axial flow and centrifugal fans at different motor speeds enabled the test to be carried out over the total range of air flow velocities. Readings averaged over a period of 40 seconds were stored in a data file on the computer hard disk. The air velocities were adjusted using the two fans and throttle valve to cover the desired range of velocities.

The electric heaters were switched on 1 hour before starting any heat transfer tests to allow the water temperature to rise and stabilise at 85°C. With air flowing over the external surface, the zero point of the air differential temperature thermopile was measured. This was taken before filling the heat exchanger sample with hot water. Similarly, the zero point of the thermopile measuring the water differential temperature was determined after filling the sample with water and turning the circulating pump on without air flow across the finned surface.

Two gate valves were used to isolate the main section of the water circuit, containing the pump and orifice plate. Two drain valves, installed before and after the sample, were used for filling with water and bleeding air from the system.

3.7 Geometries considered

Two types of heat exchangers, typical of those used in automotive air-conditioning systems, were considered in this study; round tubes with plate fins and flat tubes with corrugated fins. The samples were made with 1, 2 and 4 rows of tubes with a face dimension of 152 mm x 152 mm. All samples were constructed as a single-pass configuration with the tubes connected to a header tank at each end.

3.7.1 Round tube and plate fin heat exchangers

Round tube and plate fins are used widely in heating, ventilation, refrigeration and air-conditioning systems. These heat exchangers consist of round tubes expanded into a block of parallel continuous plate fins. In total, 31 samples with copper tubes in staggered arrangements and aluminium fins were tested in the wind tunnel. Tubes

with an external diameter of 9.525 mm and thickness of 0.406 mm were used in all of the samples. The tubes were mechanically expanded with ratio of 4% to provide better contact between fins and tubes. Three groups of tube and row spacing were used, 25.4 mm x 22 mm, 25 mm x 16 mm and 19 mm x 16.5 mm. Two types of fins configuration were considered in this study, flat plate fins and corrugated plate fins, figure (3.7).

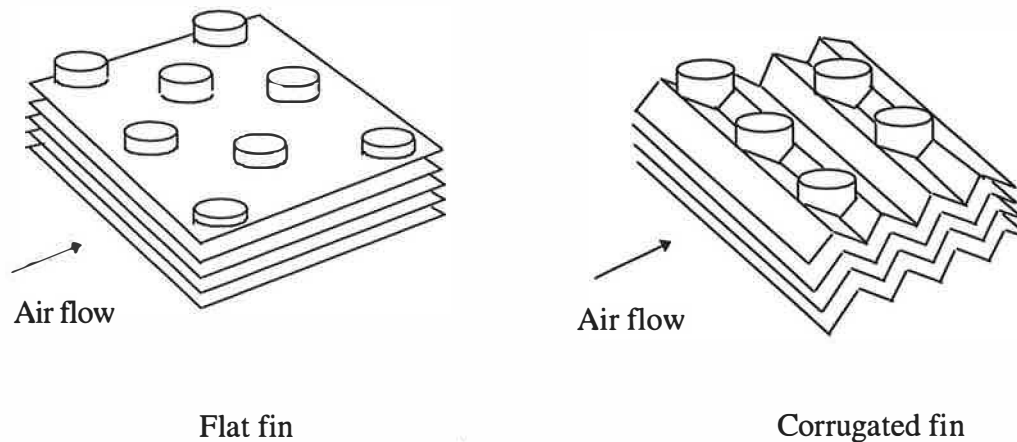
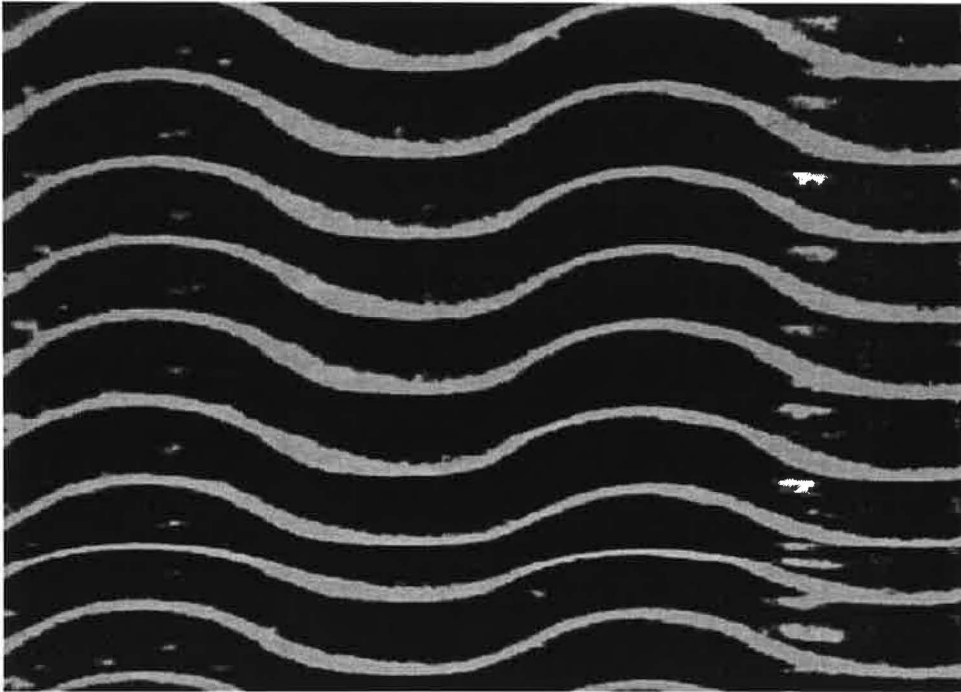
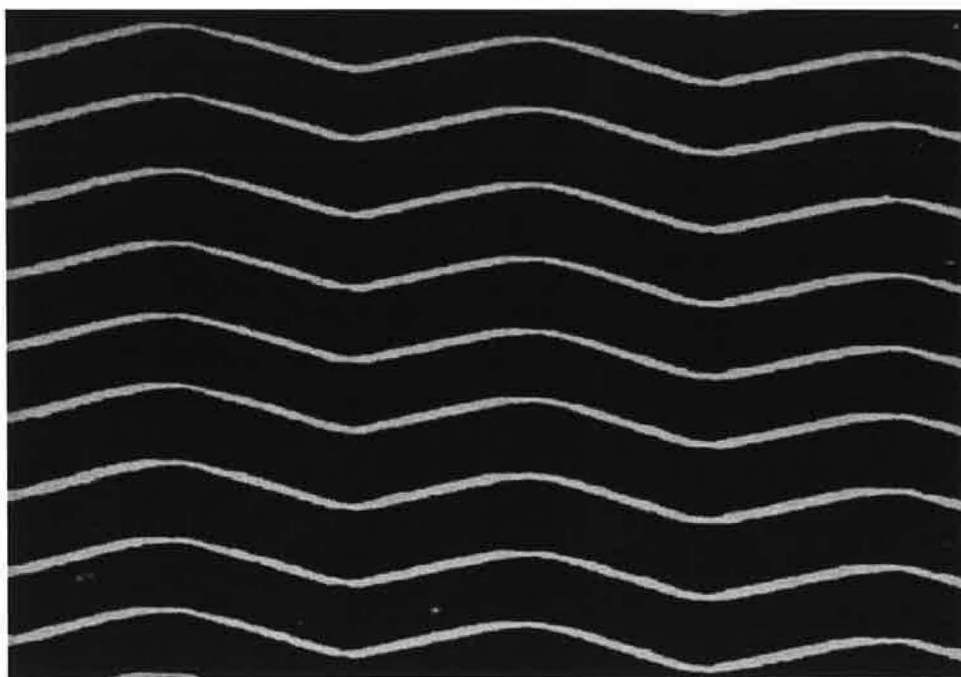


Figure (3.7) Round tube and plate fin configurations

The corrugated fins had a corrugation cycle of half the row spacing, formed in the air flow direction. The samples were divided into two groups according to their fin configuration. Table (3.1) shows the identity name and the geometries for samples of group 1. Group 1 contained 17 samples with flat fins, 1, 2 and 4 rows, fin spacings varied from 1.587 mm to 2.54 mm with fin thicknesses of 0.12 mm and 0.13 mm. The leading and trailing edges of the fins were modified to help remove condensed water when used as evaporators. The last column of tables (3.1) and (3.2) shows the edge type for each sample, straight (S), curved (C) or rippled (R). Figure (3.8) shows a picture of the types of modified edges used; curved and rippled.



Fins with curved edge



Fins with rippled edge

Figure (3.8) Fins with modified edge

Sample name	No. rows	Fin Thickness (mm)	Fin spacing (mm)	Tube spacing. (mm)	Row spacing. (mm)	Edge
2138	2	0.13	2.620	25.4	22	S
2144	2	0.13	1.833	25.4	22	S
2147	4	0.13	1.847	25.4	22	S
12	1	0.12	1.859	25.4	16	C
13	4	0.12	1.615	25.4	16	C
15	1	0.12	1.635	25.4	16	C
16	4	0.12	2.500	25.4	16	C
17	2	0.12	2.543	25.4	16	C
18	1	0.12	2.586	25.4	16	C
19	4	0.12	1.843	19	16.5	C
23	2	0.12	1.640	19	16.5	C
25	4	0.12	2.646	19	16.5	C
26	2	0.12	2.593	19	16.5	C
2152	2	0.13	2.541	19	16.5	C
2153	4	0.13	2.545	19	16.5	C
2154	2	0.13	1.953	19	16.5	C
2156	4	0.13	1.963	19	16.5	C

Table (3.1) Geometry of group 1 samples (with flat fin)

Table (3.2) shows the identity name and the geometries for the samples of group 2. Group 2 contains 13 samples with corrugated fins, 2 and 4 rows, fin spacings between 1.814 mm and 4.23 mm and fin thicknesses varied from 0.2 mm to 0.12 mm.

Sample name	No. rows	Fin Thickness (mm)	Fin spacing (mm)	Tube spacing. (mm)	Row spacing. (mm)	Edge
GR	4	0.2	4.129	25.4	22	R
AR	2	0.2	4.018	25.4	22	R
HR	4	0.12	2.548	25.4	22	R
ES	2	0.12	2.543	25.4	22	S
JS	4	0.12	1.820	25.4	22	S
FS	2	0.12	1.838	25.4	22	S
2137	2	0.13	2.612	25.4	22	S
2140	4	0.13	2.567	25.4	22	R
2143	2	0.13	1.827	25.4	22	S
2145	4	0.13	1.853	25.4	22	R
2148	2	0.13	2.589	25.4	16	R
2149	4	0.13	2.586	25.4	16	R
2151	4	0.13	2.122	25.4	16	R

Table (3.2) Geometry of group 2 samples (with corrugated fin)

3.7.2 Flat tube and corrugated fin heat exchangers

Flat tube and corrugated fin heat exchangers have been used increasingly in automotive applications such as radiators, oil coolers, condensers or evaporators because they are more compact, efficient and lighter than the traditional round tubes and flat fin heat exchangers. However, the internal fluid pressure drop for flat tubes is much higher than that for round tubes thereby increasing the pumping power required. Furthermore, when louvered fins are used on the external surface, the air-side pressure drop is higher than that for plate fins. Figure (3.9) shows a sketch of this type of heat exchanger.

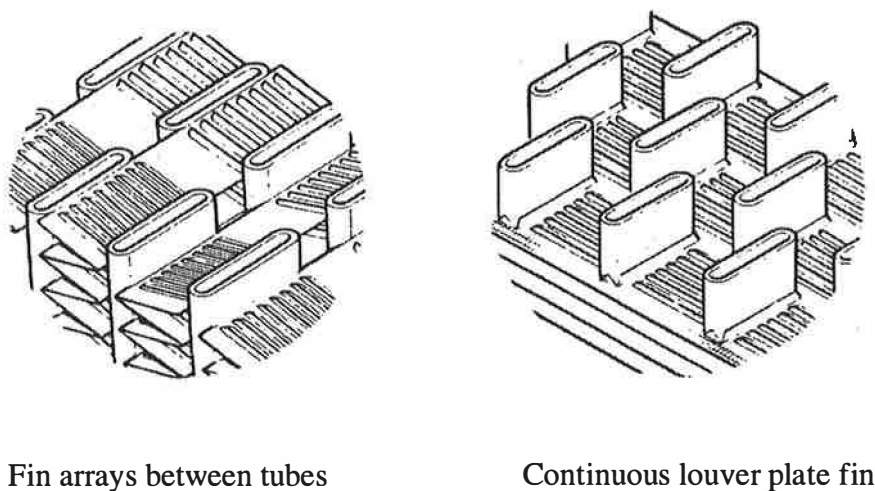


Figure (3.9) Flat tube heat exchanger

The sample considered in this study consisted of flat tubes made of aluminium, with corrugated aluminium fin arrays inserted between the tubes. The contact area was increased through brazing one of the flat surfaces of the corrugated fins to the tube wall. The contact area between the fins and tubes with the corrugated fins used was increased by using a flat section at right angle to the tube, figure (3.10).



Figure (3.10) Picture of corrugated fin used with flat tube heat exchangers

One heat exchanger of this type was tested in the wind tunnel. The sample was made with two rows of parallel tubes with tube width of 2 mm and fin length of 9.3 mm and tube spacing of 11.3 mm. The tube depth was 18.2 mm and the total heat exchanger depth was 44.5 mm. This left a gap of 8.1 mm between the two tube rows. The geometry used is specified in table (3.3).

Tube width (mm)	2
No. rows	2
Fin thickness (mm)	0.1
Fin spacing (mm)	3.38
Tube spacing. (mm)	11.3
Gap between tubes (mm)	8.1
Tube thickness (mm)	0.3
Tube depth (mm)	18.2

Table (3.3) Geometry of group 3 sample

CHAPTER 4

Condenser model

4.1 Introduction

This chapter describes a general model to design most cross flow type condensers found in automotive and domestic air-conditioning systems. The refrigerant enters the condenser from the compressor as superheated vapour and leaves as subcooled liquid. The condenser, therefore, consists of three heat transfer regions, single-phase superheating and subcooling and two-phase condensing. The heat transfer and pressure drop equations are used in the effectiveness-number of transfer units method. The refrigerant and air properties are calculated using a separate purposely built sub-model. The refrigerant-side heat transfer coefficients and pressure drops are calculated for the different phases within the condenser from general correlations found in the literature. The air-side heat transfer and pressure drop are determined from an empirical correlation derived from the wind tunnel tests. The condenser can be constructed of the traditional round tube and plate fins or the more compact flat tube and corrugated fins. The design model can be used for sizing and rating condensers from a given operating conditions or condenser size

4.2 Configurations

The function of the condenser is to change the phase of the working fluid from a superheated vapour to a subcooled liquid through heat transfer to the surrounding atmosphere. Methods for the determination of heat transfer include:

- a. Whole region. Each region of the condenser may be treated as a whole with the use of an overall heat transfer coefficient and fluid properties averaged between the inlet to and outlet from each region.

b. Row-by-row. Each row in a multi-pass condenser can be considered as a separate heat exchanger where the average heat transfer coefficient and local fluid properties can be applied.

c. Cell-by-cell. The heat exchanger is divided into discrete cells with local heat transfer and local fluid properties used.

The above analysis methods have been identified and used by previous investigators as described in chapter 2. However, the use of any of these methods will depend on the heat exchanger geometry and the equations used to determine heat transfer coefficients and pressure losses. Space considerations in automotive applications restrict the physical size of air-conditioning condensers. These are usually fitted in front of the radiator and the performance of the condenser influences the thermal performance of the radiator and engine. Compact heat exchangers are used in the restricted space to maximise performance. The flat tube and corrugated fin heat exchangers, so called parallel flow heat exchangers, can be made of a varied number of tubes for a varied number of passes. Examples are shown in figure (4.1).

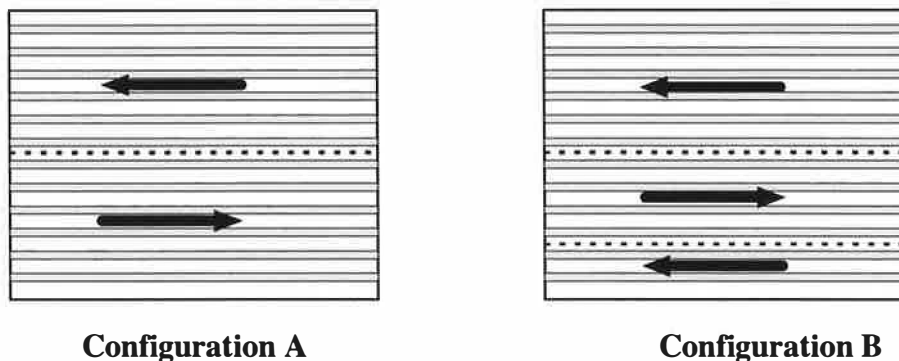


Figure (4.1) Parallel flow condenser configurations

The round tube and plate fin condensers may be constructed in various configurations. Examples are shown in figure (4.2).

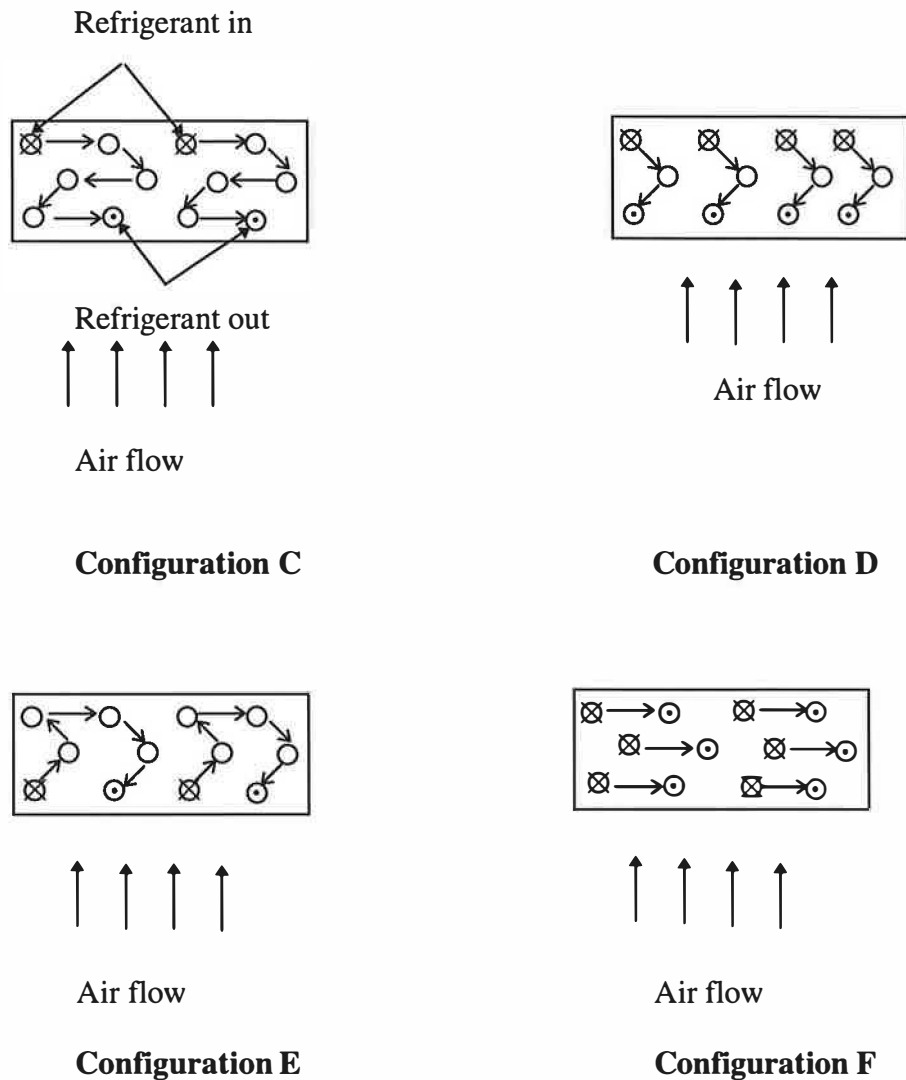


Figure (4.2) Round tube and plate fin heat exchanger configurations

An important criterion in the design of automotive condensers is the location of the two-phase region in relation to the air flow and to the single-phase regions. Figure (4.2) shows different flow configurations. If the refrigerant flow through the condenser is as shown in configurations C and D, then the subcooling region and part of the two-phase region will experience the same air on temperature. The remainder of the two-phase condensing region and the superheating region will have a higher air on temperature. This arrangement provides the maximum possible temperature difference between air and refrigerant for each of the three regions and for all rows. If the flow of refrigerant through the condenser is as shown in configuration F, then

the superheating, condensing and subcooling regions all experience the same air on temperature and the performance is more easily determined. Although not all heat exchanger rows provide the same performance and do not have the same refrigerant outlet conditions, it can be assumed in the model that the refrigerant will be fully mixed in the exit headers. This arrangement provides the maximum possible temperature difference between air and refrigerant for each of the three regions on the first row only. If the refrigerant flow through the condenser is as shown in configuration E, then both single-phase superheating and subcooling regions are ahead of the two-phase condensing region relative to the air flow through the condenser. This arrangement is more complicated and more difficult to model. However, this configuration can be assumed as one of the previous two configurations, based on the fact that the heat transfer in the single-phase regions is relatively small, typically 10% in automotive air-conditioning systems. Hence, it is more convenient to model these geometries as the two general configurations as shown in figure (4.3).

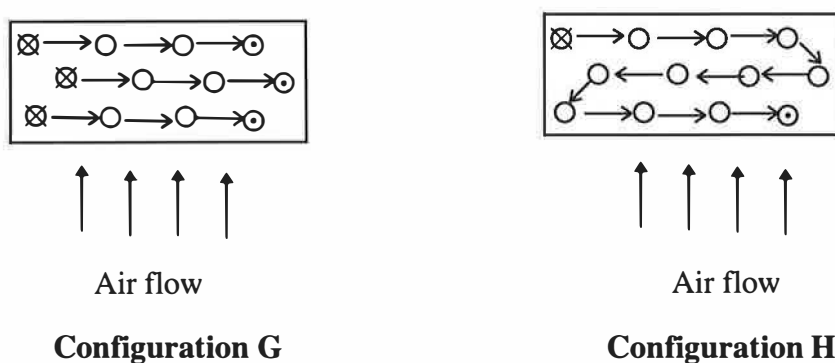


Figure (4.3) Simple configurations for round tube and plate fins heat exchangers

Configuration G in figure (4.3) assumes a heat exchanger with single-pass flow, where all regions experience the same air on temperature. Configuration H simulates the multi-pass heat exchanger with the single-phase subcooled region ahead of the two-phase condensing region, and the condensing region ahead of the single-phase superheating region relative to the air flow direction.

4.3 Heat transfer theory

The model developed to design condensers uses the Effectiveness-Number of transfer units (ϵ - Ntu) relation. The heat transfer rate from the condenser can be calculated from the inlet and outlet conditions for the air and refrigerant as follows;

$$Q_a = \dot{m}_a C_{p,a} \Delta T_a \quad (4.1)$$

$$Q_r = \dot{m}_r \Delta i_{ref} \quad (4.2)$$

These equations can also be used between any two points on the flow stream in order to divide the analysis into different regions or even a smaller part of each region. The number of transfer unit method has been used for both single-phase and two-phase regions. The effectiveness is calculated from a general equation as;

$$\epsilon = \frac{Q}{Q_{\max}} = \frac{\Delta T}{\Delta T_{\max}} \quad (4.3)$$

and the number of transfer unit from

$$Ntu = f(\epsilon, C, \text{flow arrangement}) \quad (4.4)$$

In most design cases the heat exchanger dimensions are required to be calculated (sizing). It is more convenient to express areas as non-dimensional ratios. For example the ratio of internal surface area to external surface area, R_5 , in the following equation.

$$Ntu = \frac{R_5 U_{all}}{C_{p,a} \rho_a u_a} \quad (4.5)$$

The overall heat transfer coefficient, U_{all} , is given from the thermal resistances as;

$$U_{all} = \frac{1}{\frac{1}{\eta_a h_a} + \frac{A_a \delta_f}{A_{t,m} k_t} + \frac{A_a}{A_i h_i}} \quad (4.6)$$

Where η_a is a function of the fin temperature effectiveness, η_f , and the ratio of the secondary area to total external area, A_a , (primary area and secondary area) as follow;

$$\eta_a = 1 - \frac{A_s}{A_a} (1 - \eta_f) \quad (4.7)$$

For heat transfer surfaces with straight fins and constant-conduction cross section, η_f is calculated as;

$$\eta_f = \frac{\tanh(ml)}{ml} \quad (4.8)$$

where m can be calculated for thin sheet fins as ;

$$m = \sqrt{\frac{2h_a}{k_f \delta_f}} \quad (4.9)$$

the fin length from root to centre, l , for hexagonal fins is given by Schmidt (1949) as;

$$l = \frac{d_o}{2}(1 - \tau)(1 + 0.35 \ln \tau) \quad (4.10)$$

where τ for hexagonal fin, shown in figure (4.4), is defined as;

$$\tau = 1.27\varphi(\gamma - 0.3)^{0.5} \quad (4.11)$$

$$\varphi = \frac{S_t}{d_o} \quad (4.12)$$

$$\gamma = \frac{y}{z} \quad (4.13)$$

where $\gamma \geq 1$.

$$y = \sqrt{S_r^2 + \left(\frac{S_t}{2}\right)^2} \quad (4.14)$$

$$z = \frac{S_t}{2} \quad (4.15)$$

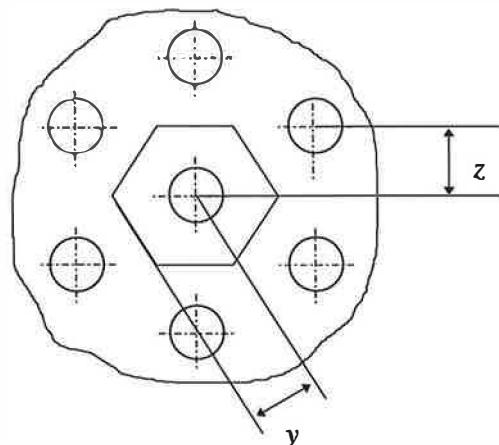


Figure (4.4) Hexagonal fin array

The parameter , m , is a function of the external heat transfer coefficient, h_a . An iterative process is used to evaluate the air-side heat transfer coefficient since it is related to the fin efficiency. This process is used when the external heat transfer coefficient is being calculated from the heat dissipation measured in the wind tunnel test. However, when h_a is known, during a design process, the fin efficiency is calculated directly from equation (4.8). The two main geometries of compact heat exchangers used in automotive applications namely, round tube and parallel flow heat exchangers, have been considered.

4.3.1 Refrigerant-side heat transfer coefficient

The superheated vapour from the compressor enters the condenser and leaves as subcooled liquid. The condenser has three regions, superheating, condensing and subcooling.

In the single-phase superheating and subcooling sections, the refrigerant-side heat transfer coefficients are calculated from the equation suggested by Dittus-Boelter for single-phase turbulent flow inside a tube. The equation which was described in chapter 2, equation (2.44), is expressed in a form easy to use. While local properties are used to determine the local heat transfer coefficient, average refrigerant properties between inlet and outlet are used to determine the overall value along the region.

General correlations for two-phase condensation heat transfer coefficient have been developed by many investigators as discussed in chapter 2. The correlation by Shah (1979) was developed from 777 data points for 10 different fluids for two-phase flow condensing inside horizontal, vertical and inclined tubes. In this study, the Shah correlation (1979) was used to calculate the two-phase condensing heat transfer coefficient. The correlation expresses the local heat transfer coefficient as a function of the refrigerant quality, pressure reduction and the liquid-phase heat transfer coefficient, equation (2.42).

It is sometimes more convenient to calculate the overall coefficient along the entire condensing region. Simple analysis can be used to obtain the overall value assuming linear quality change along the tube length, Shah (1979). The procedure involves integrating the equation for local heat transfer value between the saturated liquid line and the saturated vapour line.

The Shah correlation which calculates the local heat transfer coefficient was integrated over the total range of tube length to obtain the average heat transfer coefficient. The integration process assumes a linear vapour quality variation with the length and negligible change in transport properties of liquid-phase and pressure along the condenser tube length. Therefore, the average value of condensing heat transfer coefficient between vapour quality of x_i , x_o is calculated as;

$$h_{tp} = \frac{h_l}{(x_o - x_i)} \left[-\frac{(1-x)^{1.8}}{1.8} + 3.8 p_{re}^{-0.38} \left(\frac{x^{1.76}}{1.76} - \frac{0.04x^{2.76}}{2.76} \right) \right]_{x_i}^{x_o} \quad (4.16)$$

For complete condensation, vapour quality changes from 1 to 0, the overall heat transfer coefficient for condensation can be calculated as;

$$h_{tp} = h_l \left(0.55 + \frac{2.09}{p_{re}^{0.38}} \right) \quad (4.17)$$

The liquid-phase heat transfer coefficient, h_l , is calculated from the Dittus-Boelter correlation, equation (2.44).

4.3.2 Air-side heat transfer coefficient

The external surface performance of compact condensers has been studied by many investigators for different operating conditions, as described in chapter 2. These studies resulted in the development of empirical correlations for heat transfer and pressure drop performance in a non-dimensional form of j and f factors. The air-side heat transfer coefficient is calculated from j factor as follow;

$$h_a = \frac{j C_{p,a} \dot{G}_a}{P_r^{2/3}} \quad (4.18)$$

The published correlations, described in chapter 2, are restricted to flat finned heat exchangers and to a limited number of geometrical configurations. None of them reported plate fins with modified surfaces such as corrugated or sine wave. Use of these correlations in the model developed for automotive air-conditioning evaporators introduced errors as many of the configurations were outside the range of the correlations reported. A comprehensive experimental program was, therefore, undertaken with tests on 31 heat exchangers in a thermal wind tunnel to develop an empirical correlation for the j and f factors, Chapter 9. Although the overall heat transfer coefficient may vary over the surface of the heat exchanger owing to the varying fluid properties and flow conditions, it is sufficiently accurate for design purposes to employ an average value.

4.3.3 Air-side pressure drop

The air-side pressure drop is calculated from the core friction factor taking into account the change in air temperature and density as;

$$\Delta p = \frac{\dot{G}_a^2 v_{a,i}}{2} \left\{ \left[K_c + 1 - \left(\frac{A_{c,a}}{A_f} \right)^2 \right] - \left[1 - K_e - \left(\frac{A_{c,a}}{A_f} \right)^2 \right] \frac{v_{a,o}}{v_{a,i}} + \left(\frac{f A_a v_{a,m}}{A_{c,a} v_{a,i}} \right) + 2 \left(\frac{v_{a,o}}{v_{a,i}} - 1 \right) \right\} \quad (4.19)$$

The entrance and exit pressure drop coefficients are taken as zero for round tube and plate fin heat exchangers and, plate tube and corrugated fin heat exchangers. However, for interrupted fin surface such as louvre fins, the entrance and exit pressure drop coefficients, K_c and K_e , are calculated for Reynolds number, $Re = \infty$, from Kays and London (1984).

4.3.4 Refrigerant pressure drops

The refrigerant-side pressure drops in the condenser are calculated for the three different regions, superheating, two-phase condensing and subcooling, separately.

The total pressure drop from each region is calculated as the sum of momentum change pressure drops, frictional pressure drops and local pressure drops in headers and bends. The pressure drop estimates are carried out after calculating the required heat transfer areas and corresponding tube length for each region. An iteration process is used to recalculate the required heat transfer area taking into account the effect of refrigerant pressure drop on the outlet conditions and properties.

The single-phase superheated vapour and subcooled liquid frictional pressure drops are calculated from the friction factor using the Darcy-Weisbach equation as given in chapter 2, equations (2.48) to (2.51). While the momentum change pressure drop is calculated from the refrigerant mass flux and specific volume at inlet and outlet as shown in chapter 2, equation (2.52).

The two-phase frictional pressure drop is calculated from the single-phase vapour using modifiers to the vapour friction factor using the heterogeneous model. The work of Paliwoda (1989) was used to determine the modifiers. Paliwoda introduced a two-phase flow factor β and liquid/vapour gradient ratio θ . The work was based on Muller-Steinhagen and Heck (1986) correlation supported by extensive experimental data. The frictional pressure drops can be calculated as;

$$\left(\frac{\Delta p}{\Delta L}\right)_{tp,f} = \beta \left(\frac{\Delta p}{\Delta L}\right)_v \quad (4.20)$$

The two-phase flow factor, β , depends on the refrigerant quality and the pressure gradient ratio, θ , and is defined as;

$$\beta = (\theta + 2(1-\theta)x)(1-x)^{1/3} + x \quad (4.21)$$

An integration is used to estimate the mean value of the two-phase flow factor according to the inlet and outlet quality.

$$\beta_m = \frac{S}{(x_o - x_i)} \quad (4.22)$$

where the parameter, S , can be defined as;

$$S = \left[\frac{-3}{4}(1-x)^{4/3}(\theta + 2(1-\theta)x) + \frac{x^4}{4} - \frac{9}{14}(1-\theta)(1-x)^{7/3} \right]_{x_i}^{x_o} \quad (4.23)$$

This general equation can be applied to two-phase flow in condensers and evaporators. However, for complete condensation β_m depends only on the flow conditions and the pressure gradient. For laminar flow, $Re_v \leq 1187$, the two-phase flow factor becomes;

$$\beta_m = 0.5(1 - \theta) \quad (4.24)$$

In the case of turbulent flow, $Re_v > 1187$, β_m can be calculated as;

$$\beta_m = 0.36(1 - \theta) \quad (4.25)$$

The pressure gradient, θ , depends on the flow conditions. For laminar liquid flow and turbulent vapour flow the pressure gradient can be calculated as;

$$\theta = \frac{64}{0.3164} \frac{\mu_l}{\mu_v^{0.25}} \frac{v_l}{v_v} (\dot{G}d_h)^{-0.75} \quad (4.26)$$

For turbulent flow of liquid or vapour, the pressure gradient can be expressed as;

$$\theta = \frac{v_l}{v_v} \left(\frac{\mu_l}{\mu_v} \right)^{0.25} \quad (4.27)$$

For complete condensation, the total momentum change pressure drop can be reduced to;

$$\Delta p_{tp, mom} = \dot{G}^2 (v_l - v_v) \quad (4.28)$$

The pressure drop contribution of the local fittings to the total pressure drop in heat exchangers is very significant. Therefore, it is essential to evaluate this component accurately. Headers with many shapes are used in condensers to distribute and collect the refrigerant flow into and from the circuits. While the return bends, shown in figure (4.5), are used to connect one tube to another. The local fittings, headers and return bends, pressure drop in condensers is a function of the refrigerant flux, density and the local loss coefficient. The general equation given in Paliwoda (1992), calculates the local fitting pressure drop in single-phase flow as;

$$\Delta p_{local} = \lambda \frac{\dot{G}^2}{2\rho_v} \quad (4.29)$$

Where the local losses coefficient, λ , is calculated experimentally for the common local fitting used, some of these coefficients are given in Brooks (1993) and Paliwoda (1992). Tables (4.1) and (4.2) shows the local pressure coefficients for the fittings used in round tube heat exchangers. Table (4.2) is valid for heat exchangers with the number of tube circuits between 5 to 10.

Pressure coefficient, λ	r_b / d_i
0.28	1.0
0.21	1.25
0.19	1.5
0.175	1.75
0.16	2.0
0.14	2.5
0.13	3.0
0.12	4.0

Table (4.1) Return bend (180°) loss coefficients

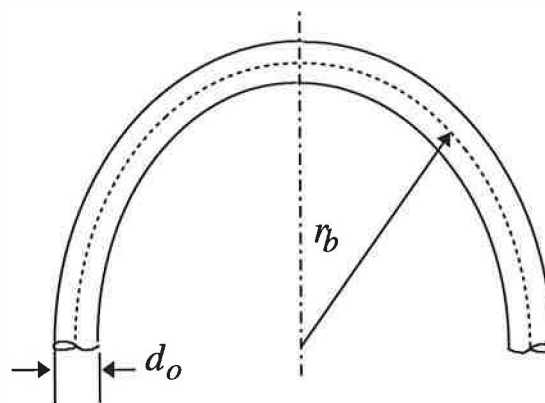


Figure (4.5) Return bend

	Pressure coefficient, λ	Position of inlet pipe to the header
Inlet header	2.5 to 3.2	Side connection
	6.0 to 10.0	Centre connection
Outlet header	2.8 to 3.5	Side connection
	8.0 to 12.0	Centre connection

Table (4.2) Headers loss coefficients

The previous equation can be modified to consider pressure drops caused by local fittings such as bends and headers during the two-phase condensing flow. The calculation of the header pressure losses in parallel flow condenser is a more complicated problem. These headers are manufactured with round cross sectional area and the tubes are inserted into the header. The local loss coefficient was determined from experimental measurements of the pressure drop across the whole sample. The same concept of two-phase flow factor, β , and liquid/vapour gradient ratio, θ , used to consider the two-phase flow pressure loss in straight tubes, was used for local fittings, Paliwoda (1992). The previous equation, therefore, can be written as;

$$\Delta p_{local} = \beta_c \lambda \frac{\dot{G}^2}{2\rho_v} \quad (4.30)$$

However, the pressure gradient for local resistance becomes;

$$\theta = \frac{v_l}{v_v} \quad (4.31)$$

and the two-phase flow factor can be determined as;

$$\beta_c = (\theta + C(1-\theta)x)(1-x)^{0.333} + x^{2.276} \quad (4.32)$$

The constant in equation (4.32) is determined from published experimental measurements for various components. For return bends and headers in round tube condensers and evaporators, the constant C , is given by Paliwoda (1992) as;

$$C = 3 \quad \text{For return bends}$$

$$C = 0.58 \quad \text{For round tubes heat exchanger's headers}$$

In round tube heat exchangers, each bend operates at a different refrigerant quality, x , through the heat exchanger. The pressure drop over each bend of the condenser coil, therefore, should be calculated at the actual refrigerant quality. Such an approach is complex and impractical. Instead the calculation has been made with the mean value of multiplier, β_m , determined for evaporators using the following equation;

$$\beta_m = \frac{S}{x_o - x_i} \quad (4.33)$$

where the parameter, S , for local pressure losses within condensers is calculated from the following equation;

$$S = \left[\theta x + (1 - \theta) \frac{x^{a+1}}{a+1} \right]_{x_i}^{x_o} \quad (4.34)$$

and the constant, a , which depends on the flow conditions, defined as follows;

$$a = 1 \quad \text{For laminar flow with } Re_v \leq 1187$$

$$a = 1.78 \quad \text{For turbulent flow, } Re_v > 1187$$

4.4 Condenser simulation

A general sub-model (Condens4.BAS) has been developed to simulate the round tube and the so called parallel flow condensers. The condensers are designed as single-pass and multi-pass cross flow heat exchangers. The air-side was assumed unmixed, while the refrigerant-side was assumed mixed for round tube condensers, and unmixed for the parallel flow condensers.

4.4.1 Round tube condensers with single-pass flow

This simple configuration can be simulated easily as the whole region method, identified above in figure (4.3), configuration G, using some assumptions. The three different regions within the condenser are considered separately where the analysis is based on the whole region. The total heat exchanger area is the sum of that for the three different regions. This method can be applied to condensers as the variations in air properties and surface temperatures between the rows are not significant.

Although the available data for the condenser designs may vary from one design case to another, there are basic geometric and operating parameters which needed to be specified. The geometric parameters cover fin and tube geometries such as fin thickness, fin spacing, row spacing, tube spacing, tube internal diameter, tube thickness and the number of circuits which the heat exchanger has been divided into. The refrigerant operating conditions through the condensers, such as inlet temperature and pressure and the outlet temperature are specified from the thermodynamic cycle. The air-side parameters required for the design include the face velocity and inlet temperature. The screen input format is shown in figure (4.6).

Figure (4.6) Condenser model input screen

Together with the previous details the designer needs three out of four of the main parameters. These parameters are finned length, finned height, number of rows and duty or refrigerant flow rate. Although the developed sub-model was constructed initially with the three last parameters as inputs, finned height, number of rows and condenser duty or refrigerant flow rate, suitable modifications were made to the

original model to consider other design cases. The initial design case is discussed in detail in this section, and a brief description given for the other design options.

4.4.1.1 Assumptions

An average refrigerant-side heat transfer coefficient has been assumed in each region. The refrigerant flow is assumed to be divided equally between the circuits and to be fully mixed in the outlet headers. The heat transfer rate and efficiency of each row may vary between one tube row and another, but this variation is assumed to be small. The face area and the air mass flow rate have been divided between the different regions. The average air-side heat transfer coefficient has been considered as constant over the heat exchanger.

4.4.1.2 Model description

In this configuration, the three different regions have the same air inlet temperature. After taking the input parameters from the design menu screen, the thermophysical and thermodynamics properties of the selected refrigerant are calculated. The constants of these equations are stored in an external data files. Refrigerant properties are calculated as described in appendix A. The thermophysical and transport properties are calculated at four different points for condensers, in the superheated vapour region at the condenser inlet, at the saturation vapour line, at the saturated liquid line and in the subcooled region at the condenser outlet. The initial estimation of the refrigerant properties assumes no pressure drops during the whole process throughout the condenser and the pressure is assumed constant between inlet and outlet.

The non-dimensional geometric ratios, which describe the heat exchanger geometry are calculated in the next step. This also involves an external data file with all the dimensions needed together with the performance of the selected geometry in terms of j and f factors. The heat transfer rate for each region can then be obtained from the refrigerant mass flow rate and enthalpy difference across each region. The

single-phase average heat transfer coefficients are calculated for superheated and subcooled regions using average properties between inlet and outlet. The two-phase condensing average heat transfer coefficient is calculated using the integrated form of Shah correlation, equation (4.17). External surface heat transfer coefficient can be determined from j factor based on equation (4.18) and the overall heat transfer coefficient can then be calculated. The condenser model is shown schematically in Figure (4.7).

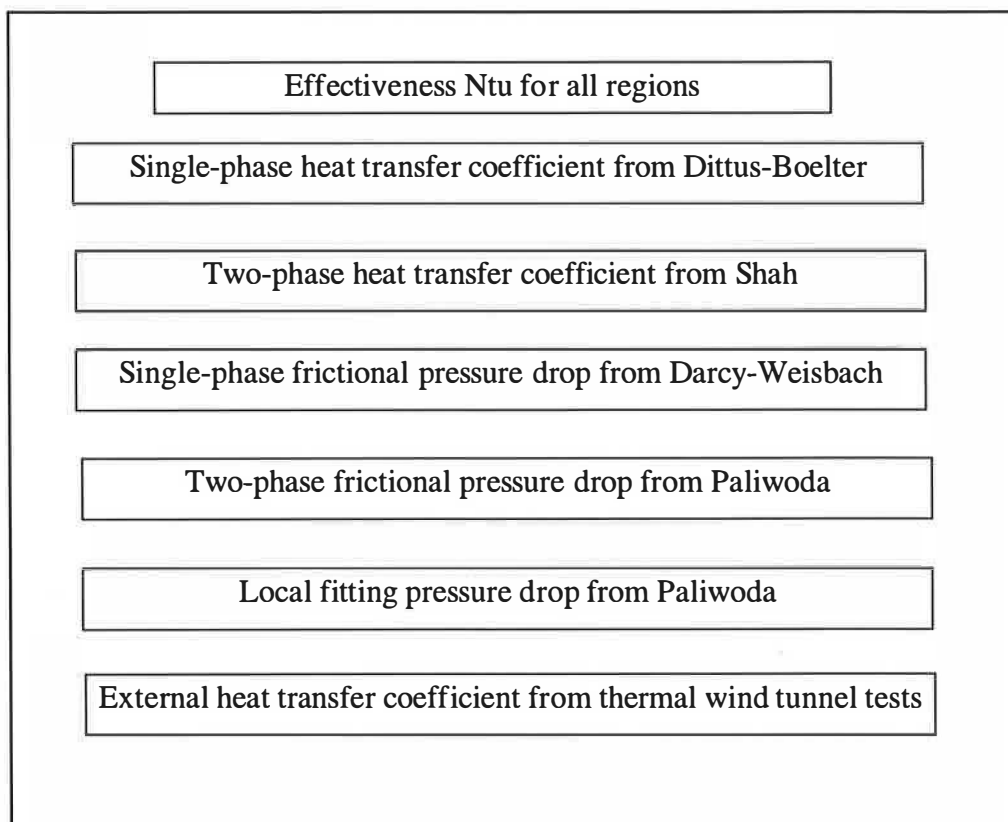


Figure (4.7) Schematic diagram of the condenser model

4.4.1.3 Calculation process

Initially, the required face area is estimated for each region of the single-pass heat exchanger for the whole unit. These areas are needed to estimate the air-side capacity ratio for each region. The initial estimate is made from the following equations taken from the Ntu method with a capacity ratio taken as zero.

$$\epsilon = 1 - \exp(-Ntu) \quad (4.35)$$

$$A_a = \frac{Q_a}{\epsilon C_{p,a} \rho_a u_a \Delta T_{\max}} \quad (4.36)$$

The finned length for each region can then be determined.

It is common practice to assume that the air has the minimum heat capacity ratio in cross flow compact heat exchangers. Although this assumption can be applied with phase change during condensing or evaporating, it is not always correct for the single-phase regions. Hence, for accurate calculations the fluid with minimum heat capacity should be correctly identified.

The single-phase superheating vapour and subcooling liquid regions are analysed using the Effectiveness, Number of transfer units method. The heat capacity ratio for both air and refrigerant are calculated and compared and the appropriate analysis used in each case. In the case where the air has the minimum heat capacity the Ntu is calculated from equation (4.5). The effectiveness, ϵ , can then be calculated from equation (4.4) and the required face area can be calculated from the air-side area obtained using equation (4.36). In the case where the refrigerant-side has the minimum capacity ratio, ϵ can be calculated from equation (4.3) and Ntu can be obtained from equation (4.4). The geometrical parameter, R_5 , can then be calculated using equation (4.5). The face area required can then be obtained. This case is most likely to occur if the refrigerant flux is small or if the enthalpy difference between inlet and outlet for this particular region is small.

In the two-phase region, Ntu is calculated from equation (4.5) assuming the air-side with the minimum heat capacity ratio. The effectiveness, ϵ , can then be calculated from equation (4.35) and the face area calculated in a similar way to that for the single-phase region. The calculated finned length is compared with the assumed one, and appropriate iteration is used to match the assumed value with the calculated one to the accuracy of 1 mm. Refrigerant pressure drops, due to momentum change, friction and return bends, if applicable, are calculated at this point for each region. The previous calculation process is repeated considering the effect of refrigerant

pressure drops on properties. An iteration procedure to match the calculated finned length comparing the pressure drop effect with the assumed one is then used. Once the iteration is within the specified accuracy (10 mm), the air-side pressure drop across the heat exchanger can be calculated based on equation (4.19). The calculation process is summarised schematically in figure (4.8).

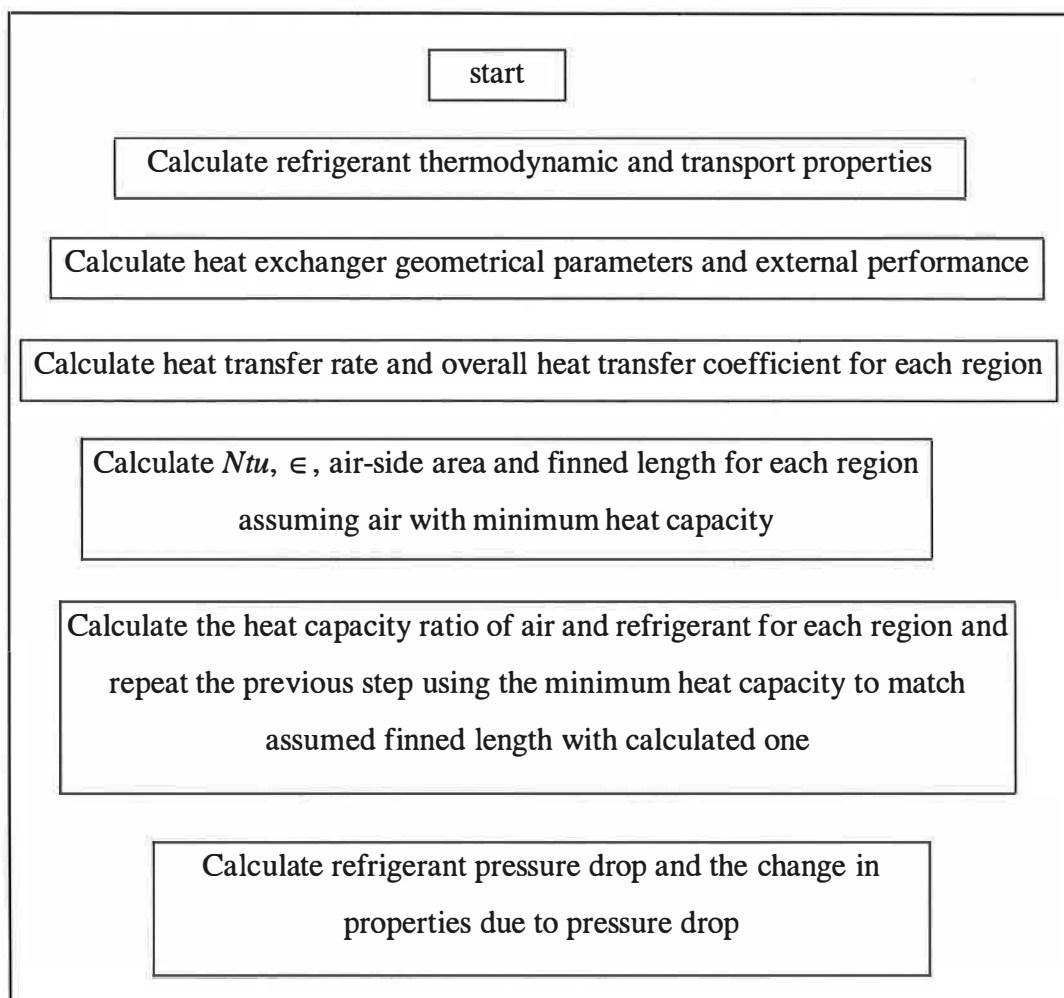


Figure (4.8) Calculation procedure for the condenser model

However, if the design process requires the number of rows to be calculated for a given face area, the number of rows is initially assumed to be equal to one. The finned length can then be calculated using the process above. An iteration is used with the assumed number of rows to match the calculated finned length with the selected value. Once the iteration converges to within 10 mm of the selected value,

the design is satisfied. The calculated number of rows to match the required duty could result in a part of a row. Therefore, the total number of rows is considered with complete number of rows and the maximum duty is calculated for the same operating conditions.

The last design option to be discussed here is rating, i.e. determining the duty for a given heat exchanger size, face dimensions and number of rows. The calculation process assumes an initial condenser duty of 0.5 kW for which the finned length is to be calculated. To match the selected face area with the calculated value, the assumed duty is corrected on the basis of the ratio of face area entered to face area calculated and duty assumed. Once the iteration converges, the refrigerant pressure drop is calculated, and the process repeated with the effect of pressure drop on the refrigerant properties included .

4.4.2 Parallel flow condensers with single and multi-pass flow

These heat exchangers are made of oval tubes with louvered fins or plane corrugated fins. To obtain low weight, the tubes and fins are made of aluminium. The tubes are normally divided into a number of channels varying from 6 to 12 channel per tube, as shown in figure (6.5). These heat exchangers are made of single row or two row arrays. These tubes permit flexibility in the design of heat exchangers by altering the number of parallel tubes per pass, but the configuration geometry is of one design as shown in figure (4.1), configuration A and B. Because the pressure drops for these tubes is high, the flow is normally divided into a large number of parallel tubes to form one pass. The number of parallel tubes per pass is easier to change than with round tubes, using a divider fixed into the headers. This can be used to overcome regions with poor heat transfer coefficients by increasing the refrigerant flux.

4.4.2.1 Assumptions

The heat exchanger is divided into a number of passes. Each pass is made of a number of parallel tubes and it is assumed that the headers will deliver equal

amounts of refrigerant to each tube on the same pass. Hence, the calculation can be performed on the basis of one tube per pass. The tubes are assumed to be divided into small cells. The cell width is considered to be equal to the tube spacing. The heat transfer and pressure drop is calculated for each cell assuming a complete element. These cells are linked together and the outlet refrigerant conditions from a cell is taken as inlet to the next one.

The air-side heat transfer coefficient and fin efficiency is calculated for the whole heat exchanger, as shown previously for round tubes. Although the overall heat transfer coefficient may vary over the surface of the heat exchanger due to varying the air properties and flow conditions, it is assumed that the air velocity is uniformly distributed on the heat exchanger face area. Hence, it is reasonable to employ an average value which will be equal to the local heat transfer coefficient for each cell. Unlike round tubes and flat fin heat exchangers, parallel flow heat exchangers have unmixed refrigerant as the flow is divided into a large number of narrow channels, and unmixed air, with corrugated plane fins, or mixed air with louvred fins.

4.4.2.2 Model description

The three different regions have the same air inlet temperature in a single row condenser. The air outlet temperature from a tube row is calculated by averaging the outlet temperature from each cell taking into account the number of tubes per pass and the number of passes per row. The analysis method and input parameters are similar to those for round tube heat exchangers. However, while the design options for round tube heat exchangers allow the calculation of the number of rows required for a given duty and face area, this option is not applicable to parallel flow ones. This is owing to the fact that these heat exchangers become inefficient with multi-row arrays, and they are limited to one or two rows only.

The refrigerant local heat transfer coefficients are calculated for each cell individually. The single-phase superheated and subcooled local heat transfer coefficients are calculated from Dittus-Boelter equation for each cell based on the properties determined at the inlet. The two-phase condensing heat transfer

coefficient is also calculated locally for each cell using the Shah correlation. The overall heat transfer coefficient for each cell is calculated based on equation (4.6).

4.4.2.3 Calculation process

The single-phase subcooled region is analysed first as it occupies part of the first row of the heat exchanger, for two row condensers, relative to the air flow. The two-phase condensing region is considered next as it occupies part of the first row. The calculation procedure for the two-phase region starts with the inlet vapour quality assumed to be 0.1%. Both air and refrigerant heat capacity ratios are calculated based on the cell face area and the refrigerant flow per tube. As the air-side area per cell is known, the effectiveness, ϵ , and Ntu are calculated from equations (4.35) and (4.5) respectively for both fluid unmixed. When the refrigerant is the fluid with the minimum heat capacity, the refrigerant outlet temperature is determined from the effectiveness, ϵ , as;

$$T_{ref,o} = T_{ref,i} - \epsilon (T_{ref,i} - T_{a,i}) \quad (4.37)$$

and hence, the heat transfer rate and air outlet temperature per cell can be calculated. If, however, the air is the fluid with the minimum heat capacity, air outlet temperature is calculated from the effectiveness based on equation (4.38), and the heat transfer rate and refrigerant outlet temperature from the cell can be determined.

$$T_{a,o} = T_{a,i} + \epsilon (T_{ref,i} - T_{a,i}) \quad (4.38)$$

The refrigerant properties at outlet are calculated from the resulting temperature and pressure and the refrigerant pressure drop is then determined from the friction and momentum change effect. The process is continued for each cell using the refrigerant outlet condition from previous cell as inlet to the next one. The analysis is continued until the refrigerant outlet temperature is equal to or greater than the specified outlet temperature. The difference between the calculated and specified refrigerant outlet temperature depends on the cell size. Therefore, it is more accurate to select a smaller cell size. On the other hand, smaller cell size results in a larger number of cells for the heat exchanger size and more computer time for the analysis.

The Ntu and ϵ for the two-phase region can be calculated in a similar way to that for round tube condensers, equations (4.35) and (4.36). The heat transfer rate is calculated from equation (4.3) for the air-side. The refrigerant outlet conditions are then determined for each cell, and the process repeated for the next cell until the outlet refrigerant becomes saturated vapour. The single-phase superheated vapour is then analysed in the same way used for subcooled liquid. For a two rows condenser, the outlet temperature from the first row, relative to the air flow, is used as inlet to the next row.

CHAPTER 5

Evaporator model

5.1 Introduction

A general evaporator model which deals with cross flow compact heat exchangers used in automotive and domestic air-conditioning units is described in this chapter. Fundamental heat transfer and pressure drop equations were used including the effectiveness-number of transfer units, logarithmic mean temperature differences and Lewis relation for mass transfer. The refrigerant and air properties and the air-side heat transfer and friction factor calculations are similar to those used for condensers. The refrigerant-side heat transfer coefficients and pressure drops are calculated for the different phases which exist within the evaporator from general correlations found in the literature. Evaporators used in air-conditioning applications have to transfer the heat from the cooled air by evaporating the refrigerant inside the heat exchanger tubes. The refrigerant enters the evaporator from the thermal expansion valve as a two-phase mixture of liquid and vapour and leaves as superheated vapour. The evaporator, therefore, has two distinct heat transfer regions: two-phase evaporation, and single-phase superheating regions. In automotive applications, evaporators are normally fitted inside the car cabin and are provided with a circulating fan to pump the air around the passengers compartment. In tropical and temperate summer climates, however, the air-conditioning system is required not only to transfer heat from the fresh make-up air and the recirculated air in the vehicle but also to reduce the relative humidity to a level in the comfort zone. The model developed may be used to determine the size required from a set of operating conditions or the heat transfer rate for a given geometry.

5.2 Configuration

The evaporator configuration considered in this study was the round tube and plate fin compact heat exchanger with multi-pass cross flow as shown in figure (4.3), configuration H. The single-phase superheated region is assumed to be ahead of the two-phase evaporating region relative to the air flow through the evaporator. This configuration includes the direct expansion evaporators widely used in refrigeration systems. Unlike condensers, the refrigerant flow in the evaporator is normally divided into a large number of circuits. This allows the reduction of the refrigerant flux within the evaporator and hence, a reduction of the refrigerant pressure drop. The methods for the determination of heat transfer described in chapter 4 are valid for evaporators.

5.3 Heat transfer calculations

The model developed to design evaporators uses the Effectiveness-Number of transfer units (ϵ - Ntu) relations, the overall heat and mass transfer coefficient and Lewis number analysis. The single-phase superheated vapour region is analysed using the ϵ - Ntu method. The overall heat and mass transfer coefficient is used to analyse the two-phase evaporating region. In the case where combined heat and mass transfer occurs, the mass transfer coefficient calculation is based on Lewis number. In designing evaporators with combined heat and mass transfer, it is common practice to plot the air inlet and desired air outlet conditions on a psychrometric chart and to joint the two state points by a straight line, Prince (1994). When this line is extrapolated to the saturation line the intersection determines the apparatus dew point temperature, figure (5.1). The evaporating temperature may then be specified at a value below the apparatus dew point temperature. Conversely, if the apparatus dew point temperature is known from the heat exchanger surface temperature, the straight line joining this point to the air inlet conditions can be used to determine the air outlet state for a specified duty. Condensation will only occur when the apparatus dew point temperature is below the dew point temperature of the air at inlet. If the evaporator surface temperature is below 0°C, frost will accumulate.

Looking at the heat transfer phenomena from air to refrigerant, one can realise that the dehumidification process will alter the heat transfer on the external surface of the finned tube, while other processes in the tube and refrigerant stay unaffected.

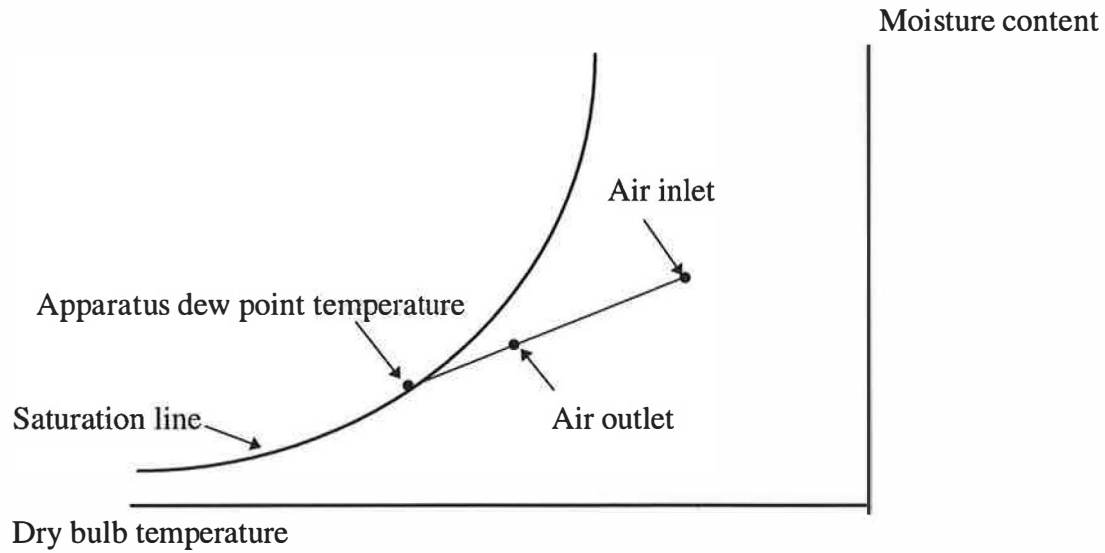


Figure (5.1) Psychrometric chart

The heat transfer rate from the moist air may be calculated as;

$$Q_a = \dot{m}_a (i_{a,i} - i_{a,o}) \quad (5.1)$$

The heat transfer rate resulting from the condensation on the heat exchanger surface is:

$$Q_w = m_a (\omega_i - \omega_o) i_w \quad (5.2)$$

and the total heat transfer rate;

$$Q_{total} = Q_{ref} = Q_a + Q_w \quad (5.3)$$

where the heat transfer rate from the refrigerant, Q_{ref} , can be calculated from the inlet and outlet conditions as follow;

$$Q_{ref} = \dot{m}_{ref} (i_{ref,o} - i_{ref,i}) \quad (5.4)$$

The model developed uses the overall heat and mass transfer coefficients and the Lewis number analysis to determine the heat transfer rate. The relationship for moist air at atmospheric pressure;

$$Le^{2/3} = \frac{h_a}{h_{a,m} C_{p,mix}} \quad (5.5)$$

is used to modify the dry surface heat transfer coefficient of the air, ASHRAE (1993). The Lewis number, Le , for air and water vapour mixture is given as 0.845, and, therefore, the left hand side of equation (5.5) is equal to 0.919. The total heat transfer rate can also be calculated from the overall heat transfer coefficient, the logarithmic mean temperature difference and the external surface area as;

$$Q_{total} = A_a U_{all} \Delta T \quad (5.6)$$

The overall heat transfer coefficient for the wet finned tube is determined as;

$$U_{all} = \frac{1}{\frac{1}{\eta_a h_a \left(1 + \frac{i_{fg} c}{0.919 C_{p,mix}}\right)} + \frac{A_a \delta_t}{A_{t,m} k_t} + \frac{A_a}{A_t h_t}} \quad (5.7)$$

The fin effectiveness for combined heat and mass transfer is calculated by a formula suggested by McQuiston (1975) using the ratio between the specific humidity difference and the dry bulb temperature difference;

$$c = \frac{\Delta \omega}{\Delta T_{db}} \quad (5.8)$$

The suggested formula for fin effectiveness is similar to that used for a dry surface, equation (4.7), but with the addition of a modified fin effectiveness parameter, m . For a wet fin and tube surface, the parameter m is calculated as follow;

$$m = \sqrt{\frac{2h_a}{k_f \delta_f} \left(1 + \frac{ci_{fg}}{0.919 C_{p,mix}}\right)} \quad (5.9)$$

Although the original equation suggested by McQuiston assumes that the left hand side of equation (5.5) is equal to one, the value of 0.919 was suggested to be more accurate, ASHRAE (1993), and was, therefore, used. With heat transfer only, $c = 0$ and the correlations (5.7) and (5.9) are reduced to that used for a dry surface only. The required surface area is determined from the equation;

$$A_a = \frac{Q_{total}}{U_{all} \Delta T} \quad (5.10)$$

Since the air is being cooled in the evaporator while the temperature of the refrigerant is essentially constant in the two-phase region, the wall temperature will decrease in the direction of airflow and may drop below the dew point.

In the case of multi-pass cross flow evaporator, the surface temperatures vary between rows. Therefore, in the design of evaporators subjected to heat and mass transfer on the external surface, the calculated duty or heat transfer surface area needs to be calculated on a row-by-row basis owing to the changes in surface temperature and air specific humidity. The use of a constant value for the ratio between the specific humidity difference and the dry bulb temperature difference leads to significant errors. The effect of water on the external surface was considered to take place only within the two-phase evaporating region.

5.3.1 Refrigerant-side heat transfer coefficient

The refrigerant enters the evaporator from the expansion device at qualities ranging from 20% to 40%, depending on the application and operating conditions, and leaves as superheated vapour. As in the condenser model, the required heat transfer surface area for the two-phase evaporating region and the superheating region are determined separately.

The Dittus-Boelter correlation, equation (2.44), recommended by Kandlikar (1990) for calculating the single-phase superheated vapour heat transfer coefficient, is used in the model. While average properties between inlet and outlet are used to determine the overall value along the superheated region, local properties are used to determine the local heat transfer coefficient.

The many correlations for calculating the forced convection evaporation heat transfer coefficient presented by the different investigators is discussed in chapter 2. The correlation by Kandlikar (1990) was developed from over 5000 data points for 10 different fluids for two-phase flow boiling inside horizontal and vertical tubes. Many researchers recommended the Kandlikar correlation; Khanpara et al. (1986)

and Webb et al. (1992). Additional factors were included in the correlation, Kandlikar (1991), to take into account the effect of the different geometries of compact evaporators and enhanced tubes. The correlation is presented in a simple form and is readily integrated to calculate the average heat transfer coefficient. The Kandlikar correlation, equations (2.24) to (2.27), is used in the model developed to calculate the local heat transfer coefficient during evaporation.

The average value of two-phase heat transfer coefficient during evaporation can be obtained by effectively integrating the local values over the length of the two-phase region. This may be simplified by assuming a negligible change in transport properties of the liquid-phase and pressure drop along the length of the tube, Shah (1979).

$$h_{tp}^- = \frac{1}{L} \int_0^L h_{tp} dL \quad (5.11)$$

If a linear quality change along the tube length is assumed, the average two-phase heat transfer coefficient may be calculated as the largest of $h_{tp,NBD}^-$ and $h_{tp,CBD}^-$.

With this assumption, equation (5.11) can be rewritten as;

$$h_{tp}^- = \frac{1}{(x_o - x_i)} \int_{x_i}^{x_o} h_{tp} dx \quad (5.12)$$

The nucleate boiling and convective boiling equations can be simplified and rewritten as;

$$h_{tp,NBD} = C_1 \frac{(1-x)^{0.64}}{x^{-0.16}} + C_2 (1-x)^{0.8} \quad (5.13)$$

$$h_{tp,NBD} = C_3 \frac{(1-x)^{0.08}}{x^{-0.72}} + C_4 (1-x)^{0.8} \quad (5.14)$$

The first part of both equations can be expanded using Maclaurin series, Stroud (1995), as follow;

$$h_{tp,NBD} = C_1 \left(x^{0.16} - 0.64x^{1.16} + \frac{0.64(-0.36)x^{2.16}}{2!} - \frac{0.64(-0.36)(-1.36)x^{3.16}}{3!} + \dots \right) + C_2 (1-x)^{0.8} \quad (5.15)$$

$$h_{tp,CBD} = \frac{C_3 \left(x^{0.72} - 0.08x^{1.72} + \frac{0.08(-0.92)x^{2.72}}{2!} - \frac{0.08(-0.92)(-1.92)x^{3.72}}{3!} + \dots \right) + C_4(1-x)^{0.8}}{C_4(1-x)^{0.8}} \quad (5.16)$$

This simplifies the integration based on equation (5.12) as follow;

$$h_{tp,NBD} = \frac{1}{(x_o - x_i)} \left[C_1 \left(\frac{x^{1.16}}{1.16} - \frac{0.64x^{2.16}}{2.16} - \frac{0.2304x^{3.16}}{6.32} - \frac{0.3133x^{4.16}}{24.96} \right) - C_2 \frac{(1-x)^{1.8}}{1.8} \right]_{x_o}^{x_i} \quad (5.17)$$

$$h_{tp,CBD} = \frac{1}{(x_o - x_i)} \left[C_3 \left(\frac{x^{1.72}}{1.72} - \frac{0.08x^{2.72}}{2.72} - \frac{0.0736x^{3.72}}{7.44} - \frac{0.1413x^{4.72}}{28.32} \right) - C_4 \frac{(1-x)^{1.8}}{1.8} \right]_{x_o}^{x_i} \quad (5.18)$$

For vertical tubes and for horizontal tubes with Froude number, $Fr_l > 0.04$ the terms

$C_1..C_4$ are defined as;

$$C_1 = 0.6683 \left(\frac{\rho_v}{\rho_l} \right)^{-0.1} h_l \quad (5.19)$$

$$C_2 = 1058Bo^{0.7} F_{fl} h_l \quad (5.20)$$

$$C_3 = 1.136 \left(\frac{\rho_v}{\rho_l} \right)^{-0.45} h_l \quad (5.21)$$

$$C_4 = 667.2Bo^{0.7} F_{fl} h_l \quad (5.22)$$

However, for horizontal tubes with Froude number, $Fr_l \leq 0.04$ the terms $C_1..C_3$ become;

$$C_1 = 0.6683 \left(\frac{\rho_v}{\rho_l} \right)^{-0.1} h_l (25Fr_l)^{0.3} \quad (5.23)$$

$$C_3 = 1.136 \left(\frac{\rho_v}{\rho_l} \right)^{-0.45} h_l (25F_{rl})^{0.3} \quad (5.24)$$

The Dittus-Boelter correlation was employed by Kandlikar (1990) to calculate the single-phase heat transfer coefficients for a liquid inside smooth tubes and was, therefore, used in this study. Dittus-Boelter equation for forced convection flow is as given in chapter 2, equation (2.44).

The fluid dependent parameter, F_{fl} , used in the correlation depends on the tube material. For copper tubes used in automotive evaporators, the fluid dependent parameter given by Kandlikar (1991) for some of the fluids in common use are shown in Table (5.1).

Fluid	fluid dependent parameter
Water	1.00
R11	1.30
R12	1.50
R13B1	1.31
R22	2.20
R113	1.30
R114	1.24
R134a	1.63
R152a	1.10

Table (5.1) Fluid dependent parameters, Kandlikar (1991).

The dimensionless boiling number, Bo , and the convection number, Co , proposed by Shah (1976) are given in chapter 2.

5.3.2 Air-side heat transfer coefficient and pressure drop

The external surface performance of compact evaporators has been studied by many investigators for different operating conditions, as described in chapter 2. Most of the studies, including this research programme, were of dry surface conditions with

single phase heat transfer. The external heat transfer coefficients, derived from the thermal wind tunnel tests, were corrected using the Lewis number, Le , to take the effect of mass transfer into consideration. It is assumed that all moisture removal takes place in the two-phase region only. The air-side heat transfer coefficient is calculated from j factor for dry surface based on equation (4.18). The air-side pressure drop is calculated from the core friction factor using the same procedure used in the condenser simulation model, equation (4.19).

5.3.3 Refrigerant-side pressure drop

The refrigerant-side pressure drops in the evaporator are calculated for the two regions, superheating and two-phase evaporating, separately. The total pressure drop from each region, like the condenser, is calculated as the sum of momentum change pressure drops, frictional pressure drops and local pressure drops in headers and bends. The pressure drop estimates are carried out after calculating the required heat transfer areas and correspondent tube length for each region. An iteration process is used to recalculate the required heat transfer area taking into account the effect of refrigerant pressure drop on the outlet conditions and properties.

The single-phase superheated vapour frictional pressure drop in straight tube is calculated, using Darcy-Weisbach equation, from the friction factor as given in chapter 2, equations (2.48) to (2.51). While the momentum change pressure drop is calculated from the refrigerant mass flux and specific volume at inlet and outlet as shown in chapter 2, equation (2.52).

The two-phase frictional pressure drop in a straight tube is calculated from the single-phase vapour using modifiers to the vapour friction factor assuming the heterogeneous model, equation (4.20), chapter 4. The work of Paliwoda (1989) was used to determine the two-phase modifiers for two-phase evaporating flow. The mean value of the two-phase flow factor, β_m , and the parameter, S , are calculated as shown in chapter 4, from equations (4.22) and (4.23) respectively. The pressure gradient, θ , is calculated for laminar liquid flow and turbulent vapour flow from

equation (4.26). For turbulent flow of liquid or vapour, the pressure gradient is calculated from equation (4.27).

The refrigerant enters the evaporator as a mixture of liquid and vapour. Therefore, the momentum change pressure drop during evaporation is calculated taking into account the inlet quality from equation (2.52). As the refrigerant specific volume increases during evaporation, the momentum change pressure drop, therefore, increases the total pressure drop in the evaporators. However, unlike the evaporator, the specific volume decreases during condensation. The resulting momentum change pressure drop during condensation, therefore, decreases the total pressure drop in condensers.

The local fitting pressure drop during single-phase and two-phase flow contribution to the total pressure drop in evaporators is calculated based on the same method used for the condenser, equations (4.29) and (4.30). The local loss coefficient, λ , is taken from tables (4.1) and (4.2) for return bends and inlet and outlet headers respectively. However, the mean value of the two-phase flow factor during evaporation is calculated from equation (4.33), where the parameter, S , for local pressure losses is calculated from the following equation;

$$S = \left[\left(\frac{3}{2}\theta - \frac{9}{4} \right) (1-x)^{4/3} + \frac{9}{7} (1-\theta)(1-x)^{7/3} + \frac{x^{3.276}}{3.276} \right]_{x_i}^{x_o} \quad (5.25)$$

5.4 Round tube evaporator simulation model

A general sub-model (Evaporator.bas) has been developed to simulate round tube evaporators. The evaporator in this case is designed as a cross flow heat exchanger with mixed flow on the refrigerant-side and unmixed flow on the air-side. The most common evaporator configuration, including direct expansion heat exchangers, was modelled based on multi-pass round tube with plate fin heat exchanger, identified in configuration H, figure (4.3), in chapter 4.

The calculation method used assumed that the evaporator consists of equivalent parallel refrigerant circuits. Since the heat exchanger is modelled as several equivalent parallel refrigerant circuits (the actual number being specified with the input data), the air-side total mass flow rate and the estimated total refrigerant mass flow rate are apportioned equally between the circuits. Each parallel flow sub-circuit is a complete heat exchanger in itself, and it is, therefore, necessary to model only one sub-circuit in order to determine the total heat exchanger behaviour. In each one of these circuits, the air inlet temperature will vary from row to row. A row-by-row analysis is, therefore, applied using the heat transfer coefficients and properties for each region. Average heat transfer coefficient on the refrigerant-side is assumed for each zone.

This method considers the variation in surface temperature and air properties across each row. The average air-side heat transfer coefficient has been considered as constant over the coil. The analysis is based on designing the heat exchanger row-by-row, where the outlet conditions from one row are used as inlet to the next. The total heat exchanger area is the sum of that for the two different regions found in evaporators, two-phase evaporating and single-phase superheating.

The main input parameters and the design options are the same as those described in the condenser model in chapter 4. The calculation procedure is similar to that used for condensers but with some modification to consider the condensing water vapour on the external surface. These modifications introduced in the evaporator model are summarised below. The refrigerant operating conditions through the evaporator, such as inlet vapour quality and pressure and the outlet temperature are specified from the thermodynamic cycle. The air-side parameters required for the design includes face velocity and inlet dry bulb and wet bulb temperatures. The screen input format is shown in figure (5.2).

Figure (5.2) Evaporator model input screen

5.4.1 Model description

In this configuration, the superheated vapour region occupies part of the first row, relative to the air flow, followed by the two-phase evaporating region. The average air outlet temperature from the first row is taken as inlet to the next. The refrigerant properties are calculated at three different points for evaporators, on the saturated liquid line, the saturated vapour line and in the superheated vapour region at the evaporator outlet. The superheated vapour average heat transfer coefficient is calculated using average properties between inlet and outlet. The two-phase evaporating average heat transfer coefficient is calculated using the integrated form of Kandlikar correlation, equations (5.17) and (5.18). This requires the knowledge of the tube length of the two-phase region. The tube length is, therefore, assumed initially, and an iteration process is used to match the assumed value with the calculated one. The overall heat transfer coefficient can then be calculated from equation (5.7). The evaporator model is shown schematically in Figure (5.3).

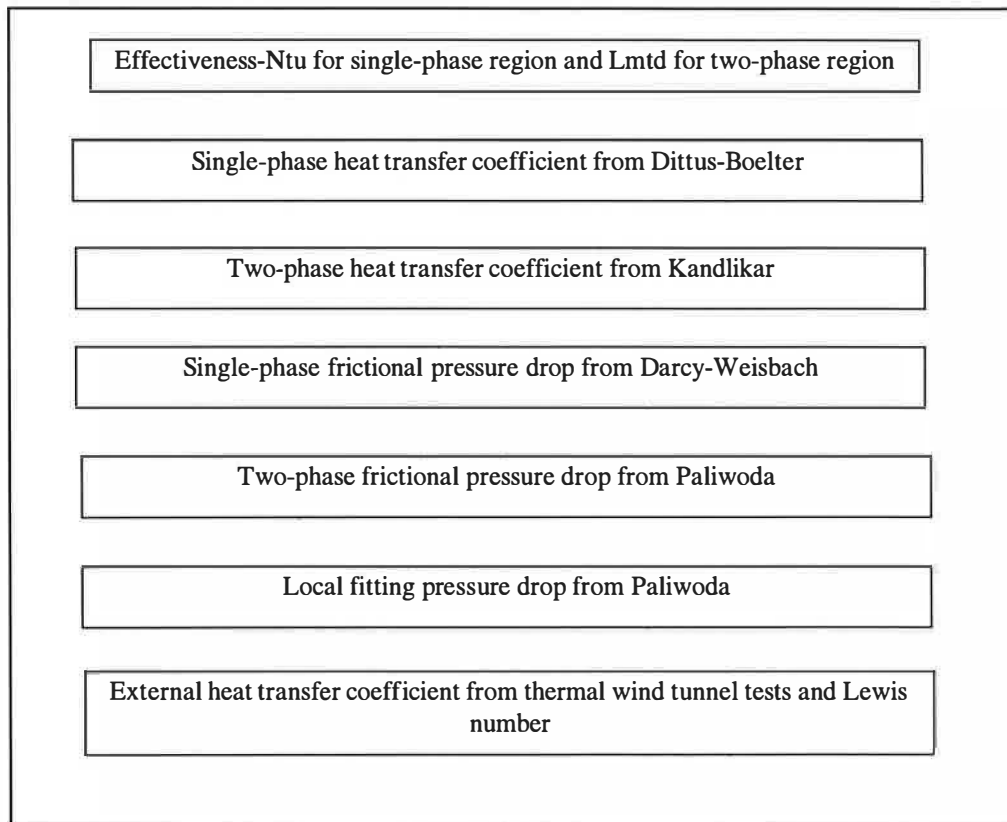


Figure (5.3) Schematic diagram of the evaporator model

5.4.2 Calculation procedure

The single-phase superheated vapour is analysed first as it occupies part of the first row of the heat exchanger, relative to the air flow. The analysis is based on the effectiveness, ϵ , and Ntu method, as described in the condenser model, where the required face area is calculated. The two-phase evaporating region is considered next as it occupies part of the first row. The heat transfer rate dissipated in the first row from the two-phase region is calculated. The process is continued for the next row using the air outlet condition from previous row as inlet to the next one. The analysis is continued until the sum of the heat transfer rates dissipated on each row is equal to the total heat transfer rate specified. The calculation process is summarised schematically in figure (5.4).

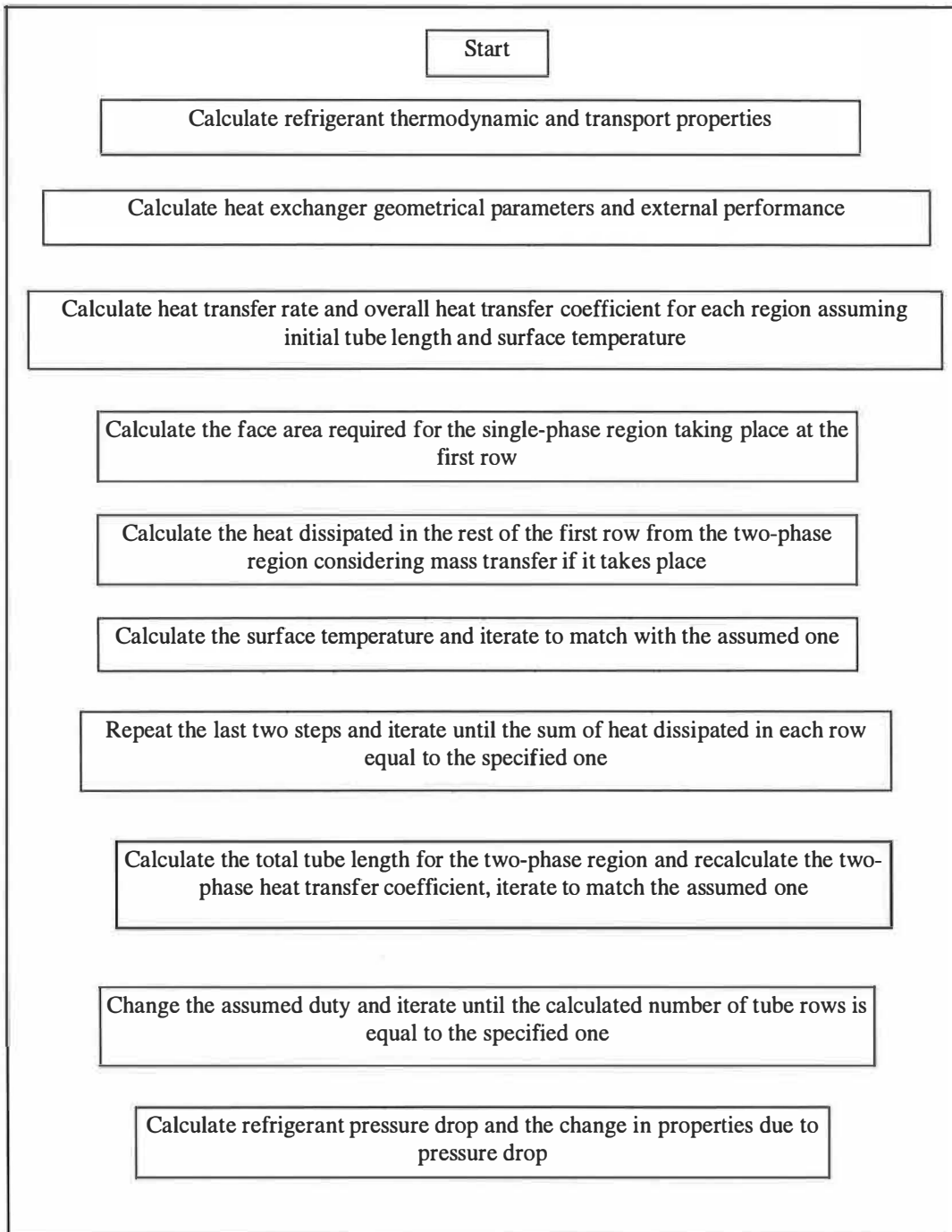


Figure (5.4) Calculation procedure for the evaporator model

CHAPTER 6

External heat transfer coefficient and geometry description

6.1 Introduction

This chapter describes the heat exchanger geometries tested in the wind tunnel. The method used to determine the Colburn factor, j , friction factor, f , and Reynolds number, Re , from the test results are described. The geometrical parameters for different types of heat transfer surfaces used in the analysis are also discussed.

6.2 Analysis

6.2.1 Colburn factor

The analysis of heat exchanger thermal performance is based on the fundamental heat transfer theory using the Effectiveness-Number of Transfer Units (ϵ - Ntu) method. Where the effectiveness is calculated from a general equation as;

$$\epsilon = \frac{Q}{Q_{max}} \Big|_{C_{min}} = \frac{\Delta T}{\Delta T_{max}} \Big|_{C_{min}} \quad (6.1)$$

And the Number of transfer unit is defined as;

$$Ntu = f(\epsilon, C, \text{flow arrangement}) \quad (6.2)$$

The capacity rate ratio, C , is defined as the ratio of the minimum to the maximum fluid thermal capacities;

$$C = \frac{C_{min}}{C_{max}} \quad (6.3)$$

The Number of transfer units can be calculated also from the overall heat transfer coefficient, air-side area and C_{min} as;

$$Ntu = \frac{A_a U_{all}}{C_{min}} \quad (6.4)$$

When the air-side has the minimum capacity, the Number of transfer units can be rewritten as;

$$Ntu = \frac{R_5 U_{all}}{C_{p,a} \rho_a V_a} \quad (6.5)$$

R_5 is the ratio between the heat exchanger total external area and face area. The overall heat transfer coefficient, U_{all} , is given from the thermal resistances as;

$$U_{all} = \frac{1}{\frac{1}{\eta_a h_a} + \frac{A_a \delta_t}{A_{t,m} k_t} + \frac{A_a}{A_i h_i}} \quad (6.6)$$

Equation (6.6) may be re-written as;

$$U_{all} = \frac{1}{\frac{R_1}{h_a} + \frac{R_2}{k_t} + \frac{R_3}{h_i}} \quad (6.7)$$

The air-side heat transfer coefficient is determined from equation (6.6) after calculating the other variables. The determination of the internal heat transfer coefficient, h_i , for fluid flow inside a tube is well established in the literature. Dittus-Boelter equation can be used to calculate h_i for turbulent flow ($Re > 10000$) as;

$$h_i = \frac{k_i}{d_{h,t}} 0.023 Re^{0.8} Pr^{0.3} \quad (6.8)$$

The parameters, R_2 and R_3 depend on the heat exchanger geometries. However, R_1 depends on the air-side heat transfer coefficient, and a suitable iteration is used to establish the value of h_a . More details are given by Achaichia (1987).

Colburn factor, j , is calculated from the Stanton number, St , and the Prandtl number, Pr_a , as;

$$j = St Pr_a^{2/3} \quad (6.9)$$

Where Pr_a represents the air-side thermophysical properties and is defined as;

$$Pr_a = \frac{\dot{m}_a C_{p,a}}{k_a} \quad (6.10)$$

The Stanton number, based on the minimum free flow area of a heat exchanger, is given by;

$$St = \frac{h_a}{C_{p,a} \dot{G}_a} \quad (6.11)$$

where;

$$\dot{G}_a = \frac{\dot{m}_a}{A_{c,a}} \quad (6.12)$$

The mass velocity, \dot{G}_a , based on the minimum free flow area, is recommended for the calculation of the Reynolds number, the Stanton number and the friction factor, Kays and London (1984). By rearranging equation (6.12), \dot{G}_a can be written as;

$$\dot{G}_a = u_a \rho_a R_4 \quad (6.13)$$

6.2.2 Friction factor

The total pressure losses across a heat transfer surface can be divided into three components as follows, inlet and exit pressure losses, momentum change pressure loss and core friction pressure loss.

$$\Delta p = \frac{\dot{G}_a^2 v_{a,i}}{2} \left\{ \left[K_c + 1 - \left(\frac{A_{c,a}}{A_f} \right)^2 \right] - \left[1 - K_e - \left(\frac{A_{c,a}}{A_f} \right)^2 \right] \frac{v_{a,o}}{v_{a,i}} + \left(\frac{f A_a v_{a,m}}{A_{c,a} v_{a,i}} \right) + 2 \left(\frac{v_{a,o}}{v_{a,i}} - 1 \right) \right\} \quad (6.14)$$

The inlet and exit pressure losses were ignored in calculating the friction factor. They are considered as part of the periodic flow characteristics of round tube and plate fin heat exchangers, Kays and London (1984). The momentum change effects were also ignored since the pressure drop was measured in an isothermal test and the air-side specific volume at entrance and exit were equal. Therefore, the core friction factor can be obtained as;

$$f = \frac{2 \rho_a A_{c,a} \Delta p}{\dot{G}_a^2 A_a} \quad (6.15)$$

Equation (6.15) can be written as;

$$f = \frac{2 \Delta p}{\rho_a u_a^2 R_4^3 R_5} \quad (6.16)$$

6.2.3 Reynolds number

The thermal performance and pressure losses for a heat transfer surface were measured for a range of air velocities. The air flow over the external surface can be described in the non-dimensional form of Reynolds number. Reynolds number, based on the hydraulic diameter, is defined as

$$Re = \frac{\dot{G} d_{h,a}}{\mu_a} \quad (6.17)$$

Equation (6.17) can also be written as;

$$Re = \frac{\rho_a u_a R_6}{\mu_a} \quad (6.18)$$

6.3 Geometrical parameters ($R_1 \dots R_8$)

The geometrical parameters $R_1 \dots R_8$ used in the analysis can be derived from the heat exchanger geometries, independent of the heat exchanger face dimensions. The fin and tube geometries such as the tube internal diameter and thickness, tube spacing, row spacing, number of rows and the fins spacing and thickness are used to derive expressions for the two types of heat transfer surfaces considered in this study.

6.3.1 Round tube and plate fin heat exchangers

This type of heat exchanger is shown in figure (6.1). For heat exchangers with extended surfaces, temperature gradients occur along the extended surface and influence the reduction of the temperature effectiveness of the surface. R_1 represents the heat exchanger surface temperature effectiveness, η_a , as follow;

$$R_1 = 1/\eta_a \quad (6.19)$$

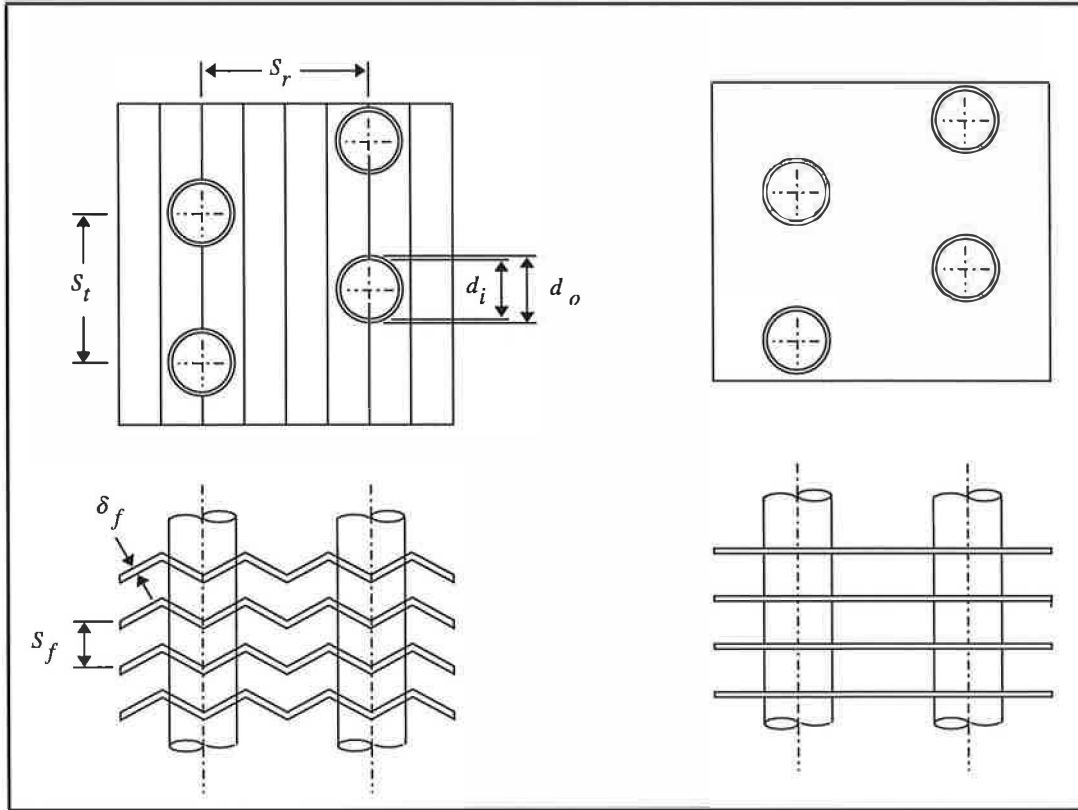


Figure (6.1) Round tube with flat and corrugated fins

where η_a is calculated from equations (4.7) to (4.10) as given in chapter 4.

R_2 appears in the tube wall thermal resistance and is defined as;

$$R_2 = \frac{A_a \delta_t}{A_{t,m}} \quad (6.20)$$

The tube wall mean area, $A_{t,m}$, the tube heat transfer area at a mean distance $(d_i + \delta_t)$, figure (6.2), is calculated as;

$$A_{t,m} = \pi(d_i + \delta_t)L_t N_t \quad (6.21)$$

The total air-side heat transfer area, A_a , is defined as the summation of the primary area and the secondary area;

$$A_a = A_p + A_s \quad (6.22)$$

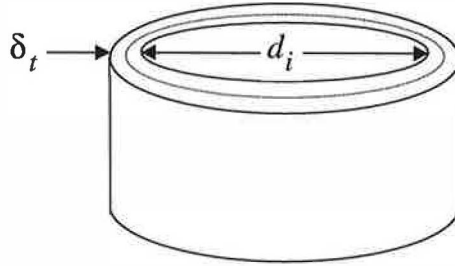


Figure (6.2) Tube diameter at mean distance

The primary area of a heat exchanger is defined as the tube outside area in contact with the air, and is calculated as;

$$A_p = \pi d_o (L_t - N_f \delta_f) N_t \quad (6.23)$$

The total tube outside area is reduced by the fact that the fins are in contact with the tubes and hence reduce the primary area in contact with air.

The secondary area is defined as the total fin surface area taking into account the tube slot area and the fin edge area, and is calculated as;

$$A_s = 2N_f \left(L_f D_f - N_t \frac{\pi d_o^2}{4} + L_f \delta_f \right) \quad (6.24)$$

Where the heat exchanger face dimensions, L_f, L_t are calculated as follow;

$$L_f = N_t / r S_t \quad (6.25)$$

$$L_t = N_f S_f \quad (6.26)$$

and the heat exchanger depth, D_f , is defined as;

$$D_f = S_r N_r \quad (6.27)$$

The total number of tubes for a heat exchanger is calculated as;

$$N_t = N_t / r N_r \quad (6.28)$$

By rearranging equation (6.20), R_2 can be expressed as;

$$R_2 = \frac{\delta_t}{d_i + \delta_t} \left[d_o \left(1 - \frac{\delta_f}{S_f} \right) + 2 \frac{S_t S_r}{\pi S_f} - \frac{d_o^2}{2 S_f} + \frac{2 \delta_f S_t}{\pi S_f N_r} \right] \quad (6.29)$$

Or

$$R_2 = \frac{d_i \delta_t}{d_i + \delta_t} R_3 \quad (6.30)$$

The internal surface of the tubes used in this study was plane without internal fins. Hence, the temperature effectiveness for the internal surface was taken as unity. R_3 can be defined as the ratio of the total air-side heat transfer area and the tube internal surface area;

$$R_3 = \frac{A_a}{A_i} \quad (6.31)$$

A_i represents the total area of the tube internal surface in contact with the internal fluid and is defined as;

$$A_i = \pi d_i N_t L_t \quad (6.32)$$

By rearranging equation (6.31) we get;

$$R_3 = \frac{d_o}{d_i} \left(1 - \frac{\delta_f}{S_f} \right) + 2 \frac{S_t R_{sp}}{\pi d_i S_f} - \frac{d_o^2}{2 d_i S_f} + \frac{2 \delta_f S_t}{\pi d_i S_f N_r} \quad (6.33)$$

R_4 represents the blockage of a heat exchanger face area created by tubes and fins and is defined as the ratio between the heat exchanger face area and the air free flow area;

$$R_4 = \frac{A_f}{A_{c,a}} \quad (6.34)$$

$1/R_4$ is known as the heat exchanger porosity. The free flow area for a heat exchanger can be defined as the minimum area through which the air flows. Assuming that the heat exchanger face area is divided into a number of smaller cells where each cell face dimensions are tube spacing and fin spacing, figure (6.3), R_4 for one cell, equal to that for the heat exchanger, is calculate as;

$$R_4 = \frac{S_f S_t}{(S_t - d_o)(S_f - \delta_f)} \quad (6.35)$$

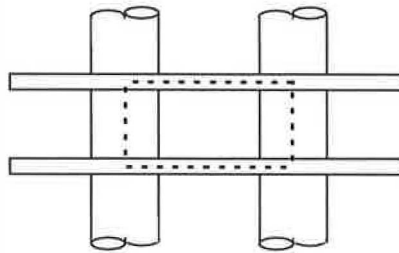


Figure (6.3) One cell of round tube heat exchanger

The ratio between the heat exchanger total external area and face area is described by

R_5 ;

$$R_5 = \frac{A_a}{A_f} \quad (6.36)$$

R_5 depends strongly on the number of tube rows and is calculated as;

$$R_5 = \frac{\pi N_r d_o \left(1 - \frac{\delta_f}{S_f}\right)}{S_t} + \frac{N_r}{S_f} \left(2S_r - \frac{\pi d_o^2}{2S_t} + \frac{2\delta_f}{N_r}\right) \quad (6.37)$$

Therefore, the ratio between the heat transfer surface area for one row and the face area, $R_{5,1}$, is:

$$R_{5,1} = \frac{R_5}{N_r} \quad (6.38)$$

R_6 is used in the calculation of the air-side Reynolds number and is defined as,

$$R_6 = \frac{A_f d_{h,a}}{A_{c,a}} \quad (6.39)$$

Where the air-side hydraulic diameter, $d_{h,a}$, is defined as ;

$$d_{h,a} = \frac{4D_f A_{c,a}}{A_a} \quad (6.40)$$

And R_6 , base on the global measurement of the sample dimensions, is calculated as;

$$R_6 = \frac{4S_r N_r}{R_5} \quad (6.41)$$

R_7 is defined as the ratio between the secondary area and the total external area;

$$R_7 = \frac{A_s}{A_a} \quad (6.42)$$

By rearranging equation (6.42), we get;

$$R_7 = \frac{1}{1 + \frac{2\pi d_o (S_f - \delta_f)}{4S_t S_r - \pi d_o^2 + \frac{4S_t \delta_f}{N_r}}} \quad (6.43)$$

Or

$$R_7 = \frac{1}{1 + R_8} \quad (6.44)$$

Where R_8 is the ratio between the primary and the secondary areas and is calculated as;

$$R_8 = \frac{A_p}{A_s} = \frac{2\pi d_o (S_f - \delta_f)}{4S_t S_r - \pi d_o^2 + \frac{4S_t \delta_f}{N_r}} \quad (6.45)$$

6.3.2 Flat tube and corrugated fin, parallel flow, heat exchangers

The geometry of flat tubes and corrugated fin heat exchangers, shown in figure (6.4), can be simplified on the same basis as in the analysis described in section (6.3.1). The flat tubes used in these types of heat exchanger are divided into a number of internal channels, figure (6.5). The number of channels may vary from 6 to 12 channels per tube depending on the tube depth.

The calculation of R_2 is based on equation (6.20) where the tube heat transfer area at a mean distance is calculated as;

$$A_{t,m} = [2(D_t - 2r) + \pi(2r - \delta_t)]L_t N_t \quad (6.46)$$

The calculation of tube length is based on equation (6.26).

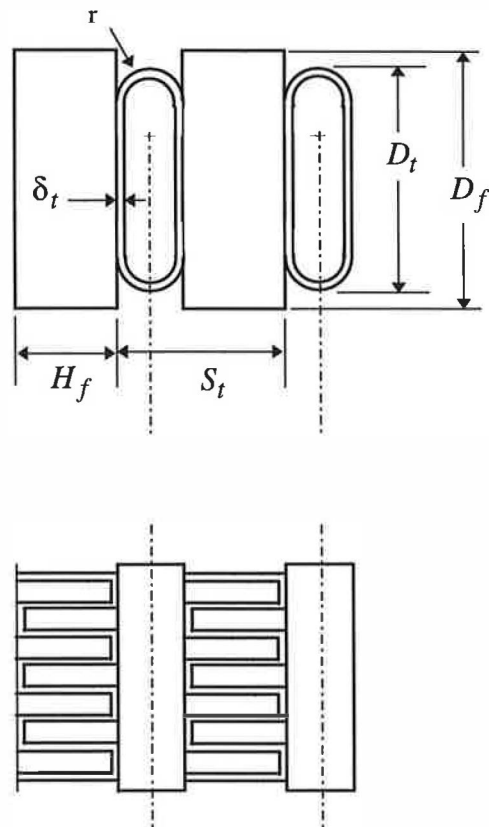


Figure (6.4) Plate tube and corrugated fins, parallel flow, heat exchangers

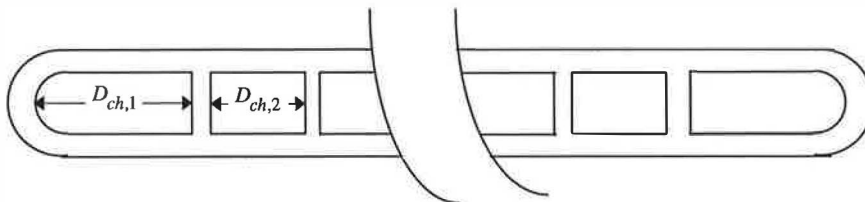


Figure (6.5) Multi channels flat tube

The calculation of the heat exchanger total external area is based on equation (6.22) where the primary area is defined as the tube total external area minus the contact area between tubes and fins. The primary area is calculated as;

$$A_p = 2\pi r L_t N_t + L_t N_t (D_t - 2r) \quad (6.47)$$

The secondary area is obtained as follow;

$$A_s = 2D_f H_f N_t / r N_f + D_f S_f N_t / r N_f + S_f N_t N_f (D_f - N_r D_t) + 2\delta_f N_t N_f (S_f + H_f) \quad (6.48)$$

R_2 may then be expressed as;

$$R_2 = \frac{\delta_t [2D_f H_f + D_f S_f + S_f N_r (D_f - N_r D_t) + 2\delta_f N_r (S_f + H_f)]}{N_r [2(D_t - 2r) + \pi(2r - \delta_t)]} + \frac{\delta_t [2\pi r + (D_t - 2r)]}{2(D_t - 2r) + \pi(2r - \delta_t)} \quad (6.49)$$

The calculation of R_3 is based on equation (6.31), where the total heat exchanger internal surface area is defined as the tube length times the total wetted perimeter;

$$A_i = w p_{t, total} L_t \quad (6.50)$$

The total wetted perimeter for the heat exchanger is calculated as;

$$w p_{t, total} = w p_t N_t / r N_r \quad (6.51)$$

The internal surface wetted perimeter for one tube is given by;

$$w p_t = 4[D_{ch,1} - (r - \delta_t) + 2(r - \delta_t)] + 2\pi(r - \delta_t) + 2(N_{ch} - 2)[D_{ch,2} + 2(r - \delta_t)] \quad (6.52)$$

The ratio between the total external surface area and the internal surface area, R_3 , is calculated as;

$$R_3 = \frac{2D_f H_f + D_f S_f + S_f N_r (D_f - N_r D_t) + 2\delta_f N_r (S_f + H_f)}{w p_t N_r S_f} + \frac{2\pi r + (D_t - 2r)}{w p_t} \quad (6.53)$$

R_4 is evaluated in the same way for round tube and plate fin heat exchangers as;

$$R_4 = \frac{S_f S_t}{[S_t - (2r + \delta_f)](S_f - \delta_f)} \quad (6.54)$$

The ratio between the face area and the total external area, R_5 , is calculated from equation (6.36) where the face area is given as follow;

$$A_f = L_t S_t N_t / r \quad (6.55)$$

R_5 is then given as;

$$R_5 = \frac{2D_f H_f + D_f S_f + S_f N_r (D_f - N_r D_t) + 2\delta_f N_r (S_f + H_f)}{S_t S_f} + \frac{2\pi r S_f N_r + S_f N_r (D_t - 2r)}{S_f S_t} \quad (6.56)$$

R_6 is defined in the same way used for round tubes and plate fin heat exchangers and is calculated as;

$$R_6 = \frac{2S_f S_t}{[S_t - (2r + \delta_f)] + (S_f - \delta_f)} \quad (6.57)$$

The ratio between the secondary area and the total external area, R_7 , can be calculated from equation (6.44).

The ratio between the primary area and the secondary area, R_8 , is calculated as;

$$R_8 = \frac{2\pi r S_f N_r + S_f N_r (D_t - 2r)}{2D_f H_f + D_f S_f + S_f N_r (D_f - N_r D_t) + 2\delta_f N_r (S_f + H_f)} \quad (6.58)$$

The tube-side hydraulic diameter in equation (6.8) is calculated for the whole tube rather than one channel to overcome the problem of different channel sizes within the same tube.

$$d_{h,T} = \frac{4A_{c,t}}{wp_t} \quad (6.59)$$

Equation (6.59) can be used to define the tube-side hydraulic diameter where the tube wetted perimeter is calculated from equation (6.52).

The cross sectional area for a tube is calculated from;

$$A_{c,t} = \pi(r - \delta_t)^2 + 4[D_{ch,1} - (r - \delta_t)](r - \delta_t) + 2D_{ch,2}(N_{ch} - 2)(r - \delta_t) \quad (6.60)$$

6.4 Software for data analysis

The thermal wind tunnel results are stored in an external file for each test. Each file name begin with the letter "T" followed by the test number with the extension ".RES". The first line of each file contains the test details including the number of runs for the cold test and the hot test, the sample identity name, the wind tunnel serial test number and the atmospheric pressure. The collected results for cold test and hot test are then follow.

In order to eliminate human error in transferring and analysing the data, the analysis process were performed automatically. A newly constructed programme (JF-ALL.BAS), written in Quick Basic, was used to determine the non-dimensional j factor, f factor and Reynolds number from the wind tunnel test data. When (JF-ALL.BAS) is run, it only requires the cold and hot test numbers for the tested sample. The sample identity names are compared, to insure similarity, when cold test and hot test numbers are different. Then the test results are automatically transferred, from the test result file, and analysed. The heat exchanger sample geometries needed to calculate the parameters $R_1 \dots R_8$ are stored in a data file (FIN-GEOM.DAT). This enabled the calculation of Reynolds number, based on the various geometrical parameters, to establish the best correlation fit to the results. The analysis outputs are saved in a format suitable for graphic presentation as (JF-XXXX.RES), where XXXX is the sample identity name.

Chapter 7

Model validation

7.1 Introduction

This chapter contains a validation of the condenser and evaporator models developed. The accuracy of the model was tested by comparison of the model predictions against a large experimental databank derived from manufacturers, literature and previous tests at the University. The comparison was carried out using typical heat exchanger geometries and operating conditions.

7.2 Evaporator model validation

The evaporator model was validated against two different sources of data, experimental data for the evaporator with R12 and experimental data with chilled water. The first source of data was collected from experimental tests carried out on a demonstration air-conditioning unit built by PA Hilton. The Hilton unit was charged with refrigerant R12 and was run with varying dry bulb and wet bulb temperatures and air velocities. The unit was fitted with a staggered round tube evaporator; the evaporator geometry is shown in table (7.1).

The air-conditioning unit was run with nine different inlet conditions as shown in table (7.2). During each run, the refrigerant temperature and pressure were measured at the inlet and exit of each component to allow the calculation of heat transfer rate and pressure loss from the evaporator. The air dry bulb and wet bulb temperatures at the evaporator inlet and outlet, condensed water flow rate and air volume flow were also measured. The balance between air heat transfer rate and refrigerant heat transfer rate was within 6 %. The refrigerant heat transfer rate was believed to be more accurate and was, therefore, considered in the comparison. The thermal

performance of the external surface was obtained from correlation developed by Gray and Webb (1986) for similar geometry to that used in experiment.

Face area	255 mm x 255 mm
Tube external diameter	15.8 mm
Tube thickness	0.7112 mm
Fin spacing	4 mm
Fin thickness	0.2 mm
Tube spacing	50.8 mm
Row spacing	37.5 mm
Number of rows	4
Number of circuits	1

Table (7.1) Evaporator geometry used in Hilton air-conditioning unit

Test number	Inlet dry bulb temp. (°C)	Inlet wet bulb temp. (°C)	Air velocity (m/s)
1	36	26	1.98
2	29	24	2.07
3	23	20	2.07
4	24	20	1.49
5	23	17	1.49
6	39	21.5	2.17
7	23	16	0.93

Table (7.2) Test operating conditions used in Hilton air-conditioning unit

The model was used to predict the duty and air outlet conditions using the same geometry and operating conditions taken from the experiment. Figure (7.1) shows the percentage difference between experiment and model prediction. The majority of

heat transfer rate data were predicted within 10 %, and 86 % of the temperatures were predicted within 6 %.

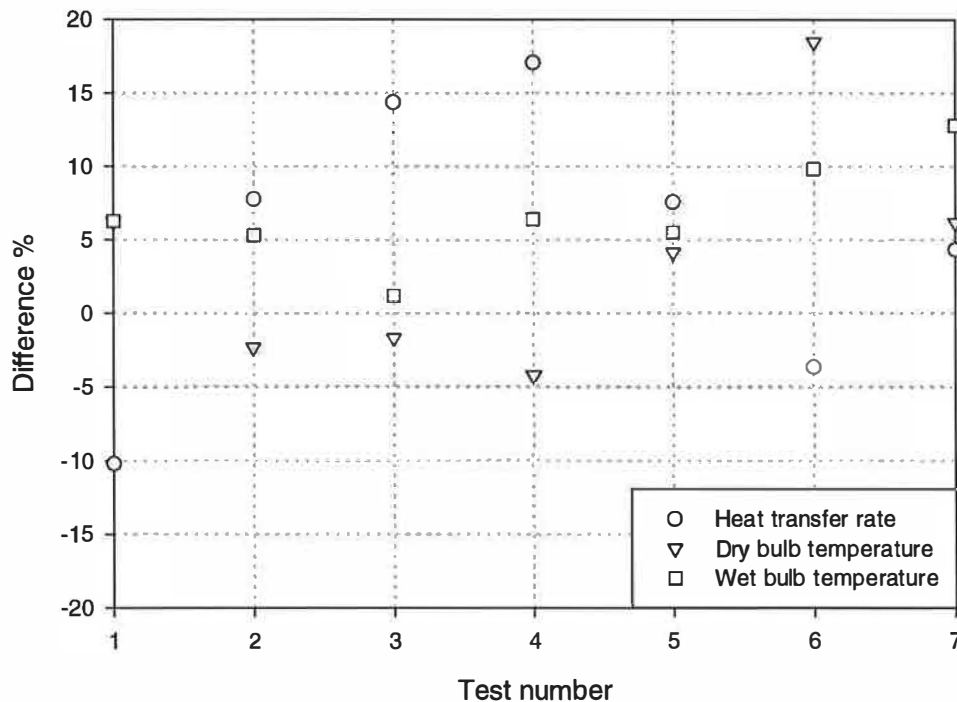


Figure (7.1) Comparison of the evaporator model prediction and Hilton air-conditioning unit

The second source of data was experimental test results published in the literature by El-Mahdy and Biggs (1978) for 4 and 8 row coils. The heat exchanger geometries and operating conditions are shown in table (7.3). Although the experiment was carried out using chilled water, the data was found to provide useful and accurate measurement on the air side performance. The thermal performance of the external surface was obtained from correlation developed by Gray and Webb (1986) for similar geometry to that used in experiment. A subroutine of the thermodynamic and transport properties for water was, therefore, included in the model in place of the properties for refrigerants. The average water heat transfer coefficient is evaluated

from the Ditts-Boelter equation. The water flow rate was obtained from the experimentally reported duty and water temperature difference.

Face area	608 mm x 611 mm
Tube external diameter	15.9 mm
Tube thickness	0.65 mm
Fin spacing	2.15 mm
Fin thickness	0.165 mm
Tube spacing	38 mm
Row spacing	32.8 mm
Number of rows	4, 8
Number of circuits	16

Table (7.3) Heat exchanger geometries and operating conditions from El-Mahdy and Biggs (1978)

To obtain similarity between experimental and calculated results, a cross-counter flow heat exchanger, was used. The experimental water outlet temperature of El-Mahdy and Biggs was used to evaluate the thermal performance of the last row together with a given air inlet condition. The water inlet temperature to the row and the air outlet conditions were then evaluated from the total heat transferred. This process was continued row-by-row. Calculations based on the outlet fluid temperature rather than the mean value may lead to small errors in performance with large temperature differences between the inlet and the outlet conditions. However, this effect is not significant with heat exchangers using the refrigerants.

Figures (7.2) and (7.3) show the percentage difference in the calculated water inlet temperature, air outlet temperature, outlet moisture content and duty for the two heat exchangers.

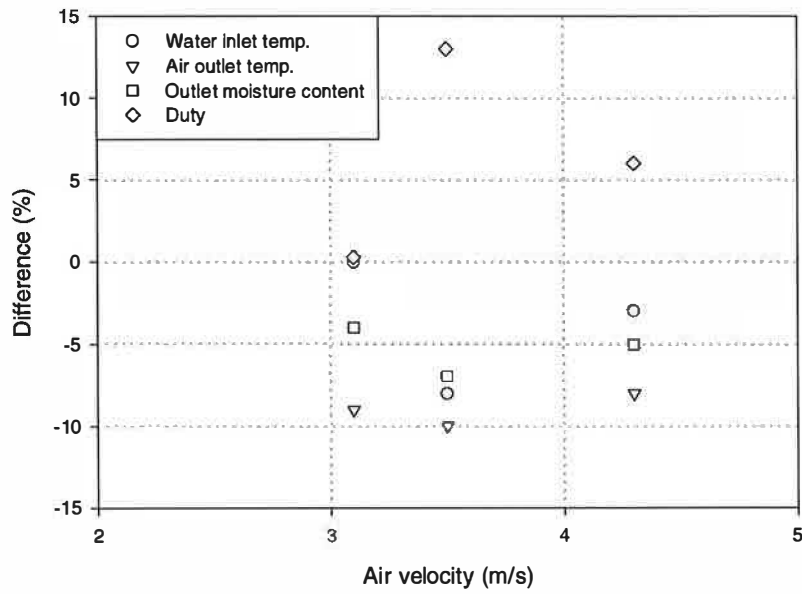


Figure (7.2) Percentage difference for 4-row heat exchanger results

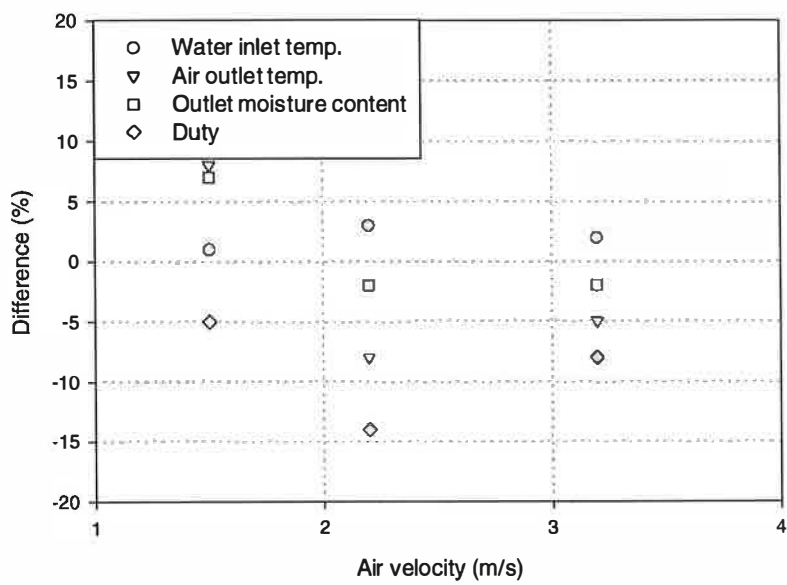


Figure (7.3) Percentage difference for 8-row heat exchanger results

The result shows good overall agreement between the experimental and the calculated values. The water outlet temperature is predicted to within 8 % for the 4-row heat exchanger and 4 % for the 8-row one. The prediction of duty is higher at a maximum of 12 % for the 4-row whereas this is lower at about 14 % for the 8-row. The calculated air outlet temperature was between 7 to 10% lower than measured temperatures for the 4-row and within $\pm 8\%$ for the 8-row. The outlet moisture is predicted within $\pm 7\%$ for both heat exchangers.

7.3 Condenser model validation

The condenser model was validated against experimental data supplied by heat exchangers manufacturers for the refrigerants R134a and R12. Both round tube and parallel flow condensers were included in the validation. One parallel flow condenser unit was tested experimentally with varying refrigerant operating conditions, air velocities and inlet temperatures. Measurements were taken to calculate the heat transfer rate from air and refrigerant. The condenser geometry is shown below in table (7.4).

Face area	570 mm x 409 mm
Tube thickness	0.4 mm
Fin spacing	1.3 mm
Fin thickness	0.115 mm
Tube spacing	11.12 mm
Number of rows	1
Number of passes	2
Number of circuits	21, 15

Table (7.4) Parallel flow condenser geometry

The condenser described above was tested at typical operating conditions found in automotive applications. The condensing pressure was fixed at 1.62 MPa (gauge) and saturation temperature of 61°C. The refrigerant inlet condition to the condenser

was taken as superheated vapour and the outlet was taken as subcooled liquid; the values of superheat and subcool being 25 K and 5 K respectively. Air velocities were varied between 2 m/s and 4 m/s with fixed air inlet temperature at 35°C. The heat transfer rate predicted from the model was compared against those taken from experiment. Figure (7.4) shows the percentage difference over the range of air velocities.

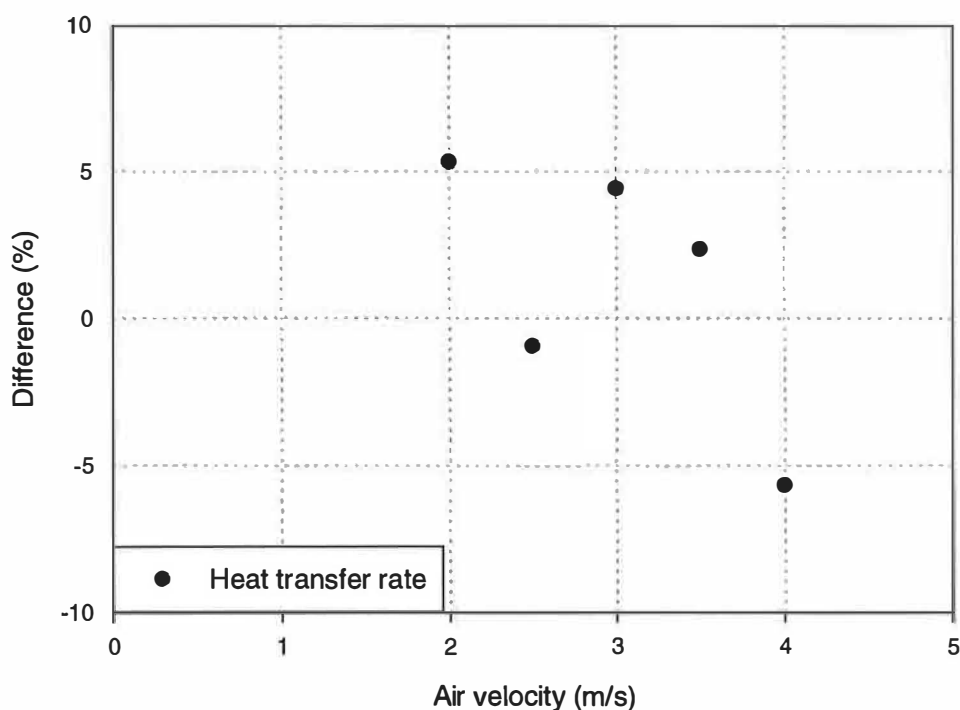


Figure (7.4) Difference between experiment and prediction for heat transfer rate for parallel flow condenser

The results show good agreement between the experimental and calculated values. The heat transfer rate is predicted within $\pm 5.5\%$ over the typical range of air velocities.

The round tube condenser prediction was compared with the manufacturer's data using refrigerant R12. The heat transfer rate and air pressure drop were compared

for one condenser geometry at a condensing temperature of 65°C, 10 K superheat and 5 K subcooling. The air velocity was varied between 1 m/s and 11 m/s with a fixed inlet temperature at 40°C. The condenser geometry is shown in table (7.5).

Face area	480 mm x 275 mm
Tube thickness	0.4 mm
Tube diameter	9 mm
Fin spacing	2.82 mm
Fin thickness	0.13 mm
Tube spacing	25 mm
Row spacing	16 mm
Number of rows	4
Number of circuits	2

Table (7.5) Round tube condenser geometry

The comparison, expressed as a percentage difference between the manufacturers data and the model, is shown in figure (7.5). The air pressure drop was predicted to within 7.6% over the entire range of air velocity. This was expected as the manufacturer pressure drop data were based on isothermal conditions, while the predicted one was calculated taking into account the effect of temperature change between inlet and outlet. The prediction of heat transfer rate was higher with a maximum difference of 3.6% at low air velocities and was lower at a maximum of 0.7% with the higher air velocities. This is a consequence of the effect of error in measurement at low air speeds.

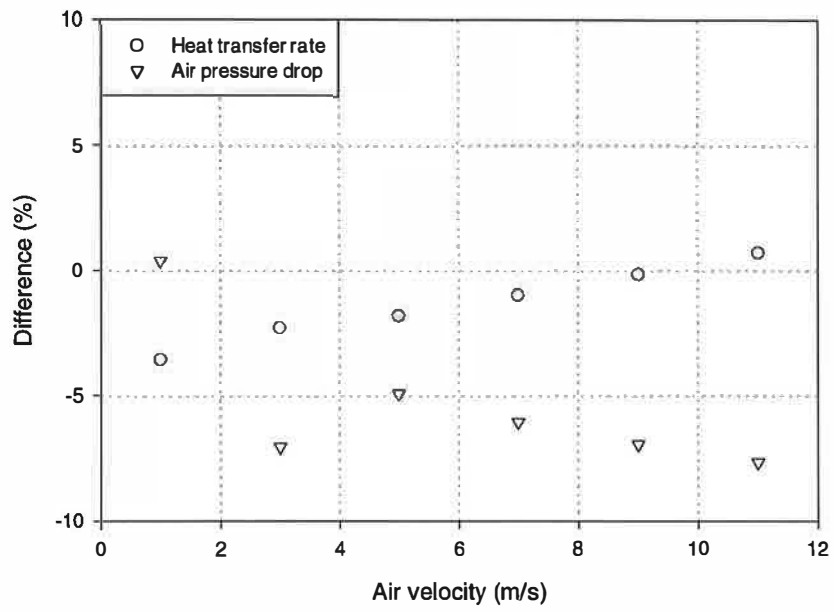


Figure (7.5) Round tube condenser model validation

Chapter 8

Effect of refrigerant properties

8.1 Introduction

The effect of refrigerant properties on the thermal performance and pressure losses in condensers and evaporators is described in this chapter. The effect of refrigerant properties on heat transfer coefficients and pressure losses with different flow regimes and tube configurations has been studied by many investigators. These are described in chapter 2. However the reported observations do not include directly the effect of refrigerant properties on the overall performance of the compact heat exchangers used for air-conditioning. The effect of refrigerant properties on the actual performance of typical heat exchangers with different flow phases, single-phase liquid, single-phase vapour and two-phase liquid and vapour for condensing and evaporating, therefore, needed to be investigated. The models developed for the condenser and evaporator were used to compare the thermal performance and pressure losses of heat exchangers with typical operating conditions. These comparisons, as one of the aims of this project, provided a better understanding and useful information for the retrofitting of refrigerants in existing refrigeration and air-conditioning systems. Comparisons were made between R12 and its replacement R134a, and R22 and its replacement R407C. Various operating conditions, geometries and fluid properties were covered; including air-on temperature and velocity, refrigerant saturation temperature, heat transfer only and combined heat and mass transfer.

8.2 Comparison between R12 and R134a performance

The model was used to study the effect of refrigerant properties on the heat transfer and pressure drop in both round tube condensers and evaporators, and parallel flow condensers. Typical operating conditions and geometries were used to predict the

heat exchanger duties, refrigerant pressure drops and refrigerant mass velocity. In the case of the condenser in automotive applications the heat transfer from the refrigerant is to the surrounding air in an “under bonnet” environment. The worst case being experienced in stop and go rush hour traffic in a hot, humid tropical environment. The evaporator is required to “draw-down” the temperatures inside vehicles quickly and to provide adequate cooling at the same “hostile” conditions. The model was run with the air-on velocity varied between 1 m/s and 5 m/s at temperatures of between 35°C and 40°C.

8.2.1 Effect of refrigerant properties on the performance of round tube condenser

A single-pass condenser with 3 staggered tube rows was used to compute the comparisons between the refrigerants R12 and R134a. The heat exchanger geometry and operating conditions are shown in table (8.1).

Face area	406 mm x 560 mm
Tube internal diameter	9 mm
Fin spacing	1.81 mm
Fin thickness	0.13 mm
Tube spacing	25.4 mm
Row pitch	16 mm
Tube	round copper
Fins	sine wave aluminium
Number of rows	3
Number of circuits	3
Inlet air temperature	35°C to 40°C
Condensing temperature	61°C
Superheat	25 K
Subcool	5 K

Table (8.1) Condenser operating conditions and geometry

The model was run with a condensing saturation temperature of 61°C. The refrigerant inlet condition to the condenser was taken as superheated vapour and the outlet was taken as subcooled liquid; values of superheat and subcool being 25 K and 5 K respectively. The predicted condenser duties are compared for the two refrigerants in figure (8.1) for air inlet temperatures of 35°C and 40°C.

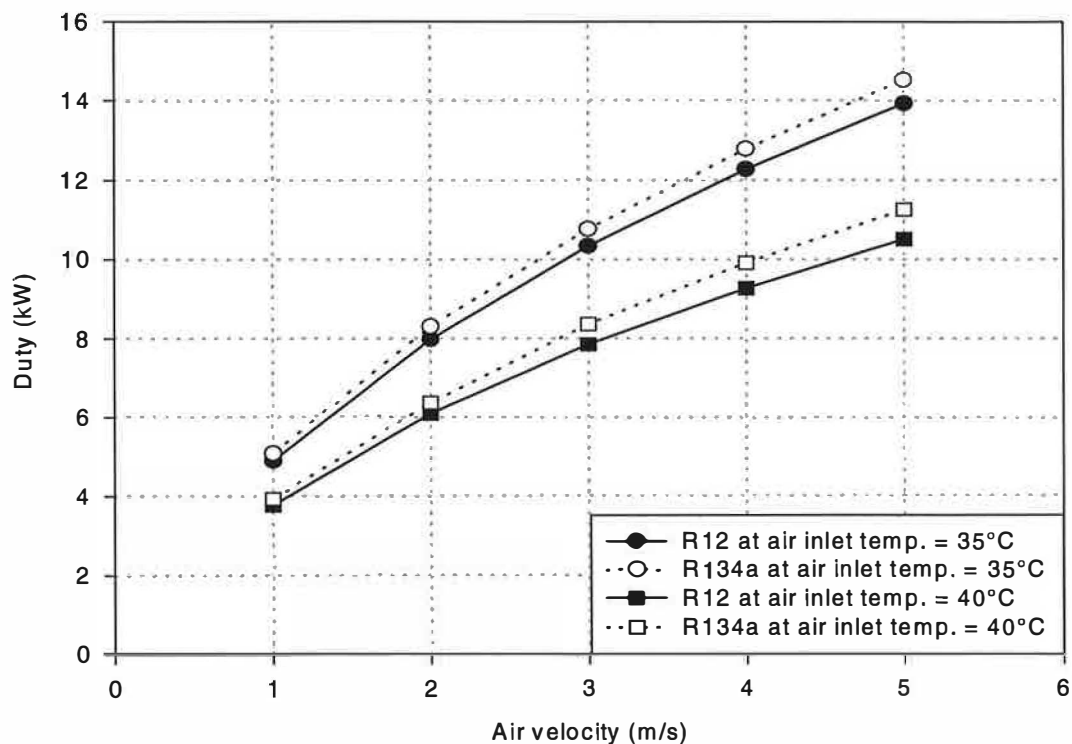


Figure (8.1) Comparison of refrigerant performance in round tube condenser with R12 and R134a

The results show a comparative duties of the condenser as retrofitted with R134a in place of R12. There is an increase in duty of about 6% when R134a is used. This is explained by the comparable refrigerant heat transfer coefficient calculated for both refrigerants. The refrigerant mass velocity and refrigerant pressure drop were compared for R12 and its replacement R134a as shown in figures (8.2) and (8.3) respectively.

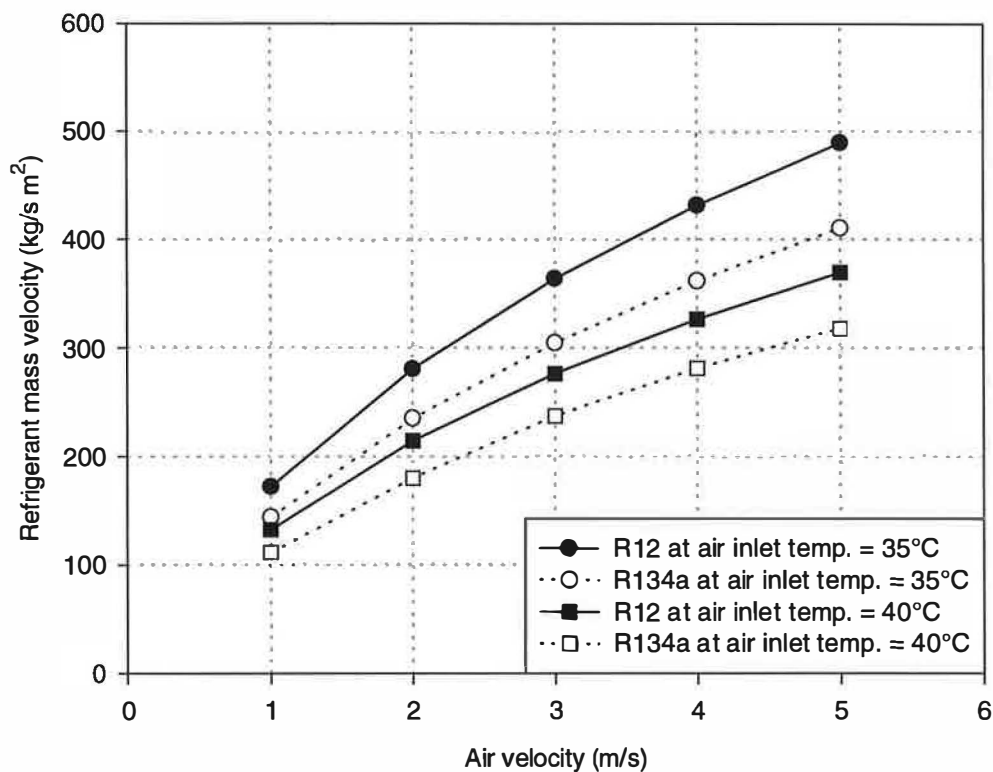


Figure (8.2) Comparison of refrigerant mass velocity in round tube condenser with R12 and R134a

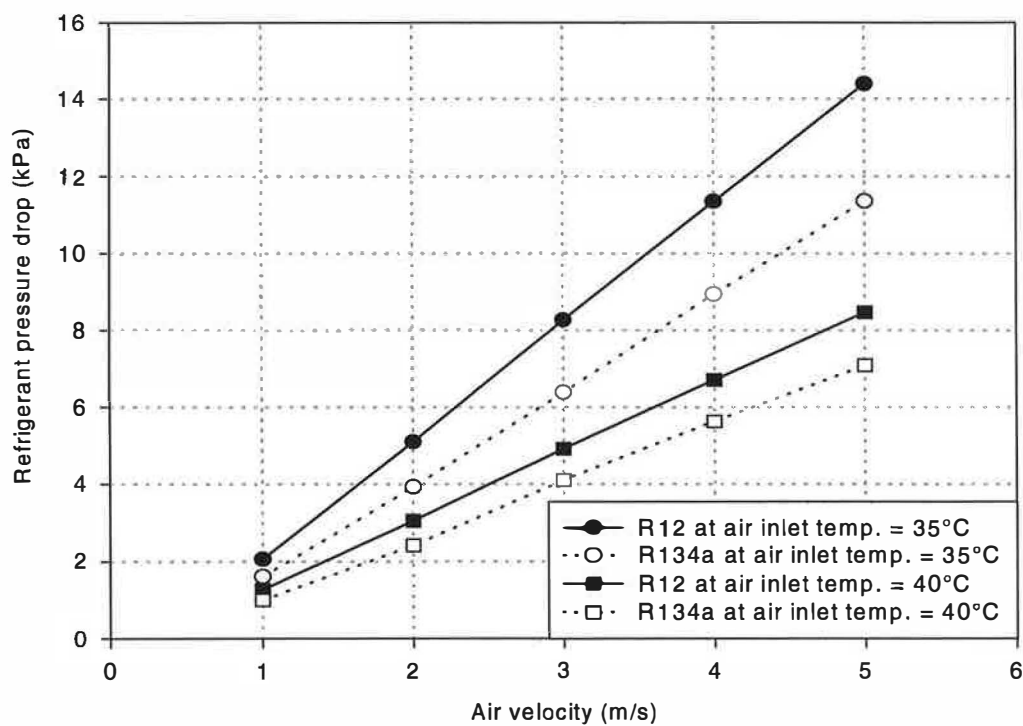


Figure (8.3) Comparison of refrigerant pressure drop in round tube condenser with R12 and R134a

Replacing R12 with R134a in the same heat exchanger results in a reduction in the refrigerant mass velocity and associated pressure drop for the same duty. The main reason behind this is the fact that R134a has a larger specific enthalpy of condensation, therefore, requiring a lower refrigerant flow for the same duty. As a result of the reduction in refrigerant mass flow, the associated pressure drop is reduced. The refrigerant mass velocity per unit duty was compared for R12 and R134a in figure (8.4).

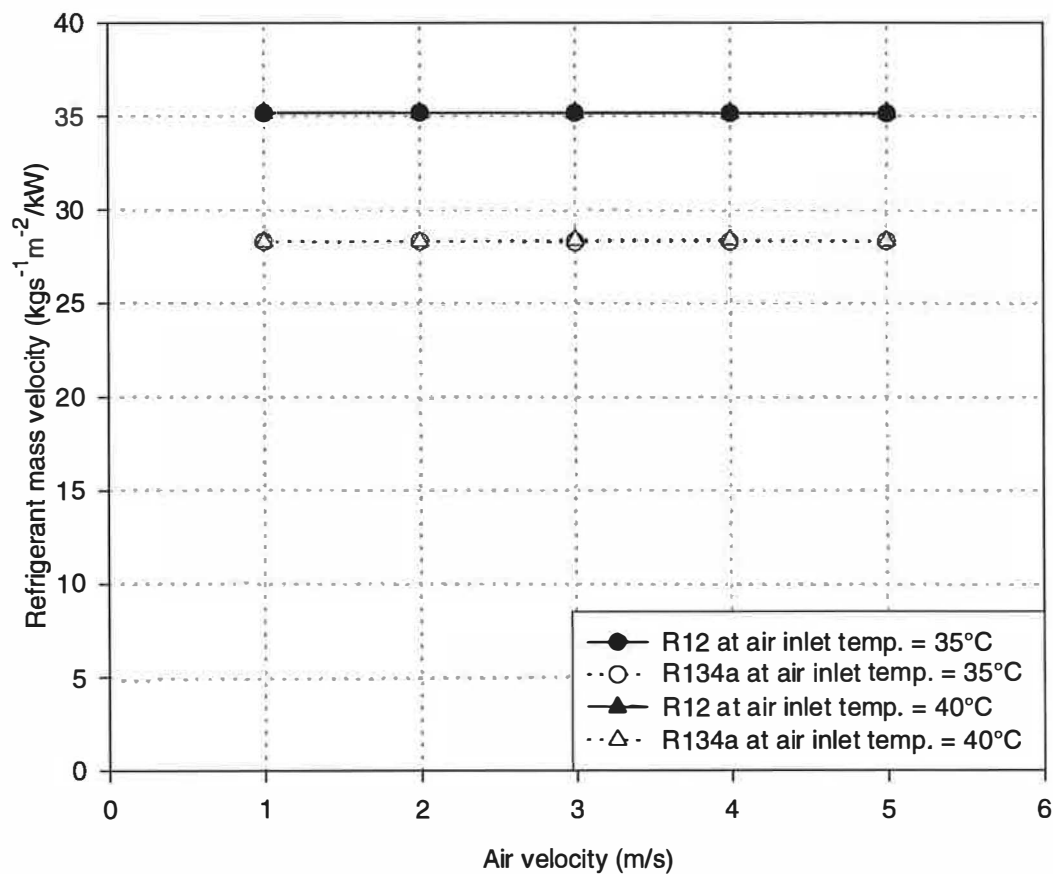


Figure (8.4) Comparison of refrigerant mass velocity per unit duty in round tube condenser with R12 and R134a

The results show a reduction in refrigerant mass velocity per unit duty when using R134a of approximately 20% due to the reasons mentioned above. The air inlet temperature had little effect on the refrigerant mass velocity per unit duty. The

refrigerant pressure drop per unit duty is compared for the two refrigerants in figure (8.5) for air inlet temperature of 35°C and 40°C.

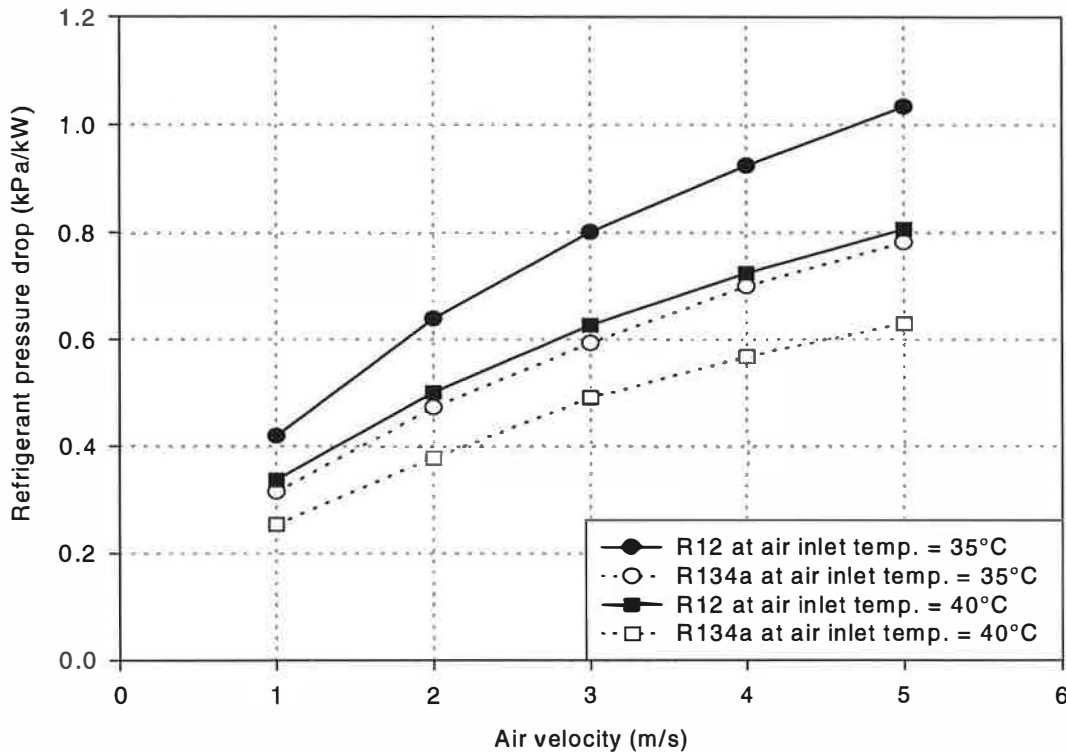


Figure (8.5) Comparison of refrigerant pressure drop per unit duty in round tube condenser with R12 and R134a

The refrigerant pressure drop per unit duty is reduced with R134a by approximately 24% corresponding to the reduction in refrigerant mass velocity per unit duty.

8.2.2 Effect of refrigerant properties on the performance of a parallel flow condenser

The condenser performance was compared when R12 is replaced by R134a in a parallel flow condenser. The refrigerant inlet and outlet conditions and the air inlet temperature were maintained at the same values as those used for round tube condenser. The air inlet velocity was varied between 1.5 m/s and 5 m/s. The heat exchanger geometry and operating conditions are shown in table (8.2). The refrigerant mass velocity per unit duty and pressure drop per unit duty are compared for R12 and R134a in figures (8.6) and (8.7) respectively.

Face area	342 mm x 560 mm
Core depth	16 mm
Fin spacing	1.3 mm
Fin thickness	0.12 mm
Tube spacing	11.4 mm
Number of tubes per pass	15
Tube	oval aluminium
Fins	louvre aluminium
Number of rows	1
Number of tube pass	3

Table (8.2) Parallel flow condenser operating conditions and geometry

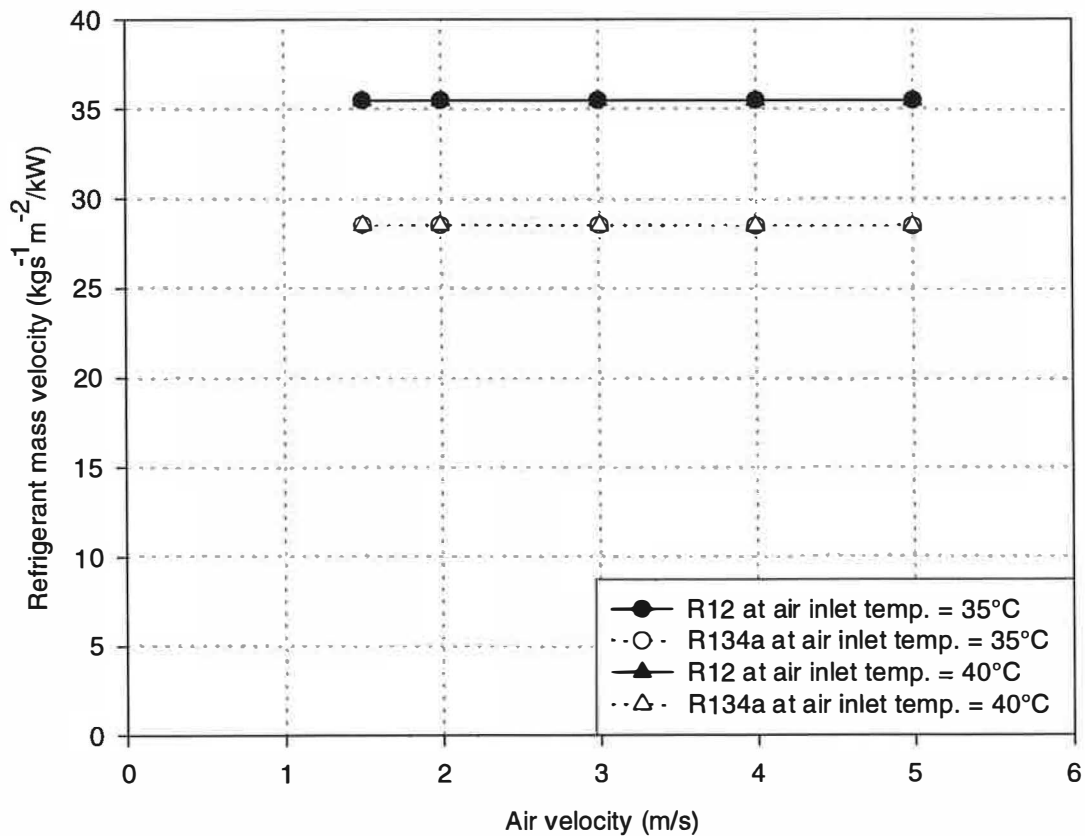


Figure (8.6) Comparison of refrigerant mass velocity per unit duty in parallel flow condenser with R12 and R134a

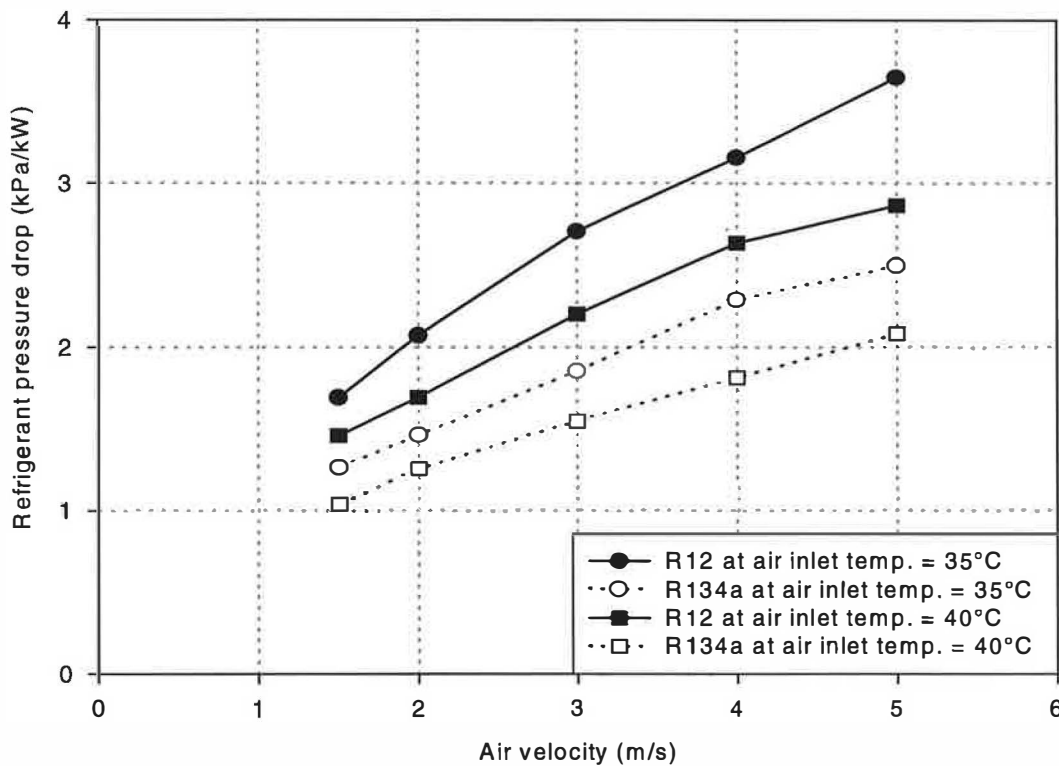


Figure (8.7) Comparison of refrigerant pressure drop per unit duty in parallel flow condenser with R12 and R134a

The results for the parallel flow condenser were very similar to that for round tube condenser. The refrigerant mass velocity per unit duty is lower with R134a by approximately 20%. The air inlet temperature had little effect on the refrigerant mass velocity per unit duty. The refrigerant pressure drop per unit duty is reduced with R134a by approximately 29% corresponding to the reduction in refrigerant mass velocity per unit duty.

8.2.3 Effect of refrigerant properties on evaporator performance

A multi-pass evaporator with 3 staggered tube rows was used to compute the comparisons between the refrigerants R12 and R134a. Both heat and mass transfer occur in evaporators. The evaporator may be operating with heat transfer only or combined heat and mass transfer. The combined heat and mass transfer is most likely to occur in evaporators working in hot and humid conditions and therefore,

was considered in this comparison. The heat exchanger geometry and operating conditions are shown in table (8.3).

Face area	305 mm x 350 mm
Tube internal diameter	9 mm
Fin spacing	2.11 mm
Fin thickness	0.13 mm
Tube spacing	25.4 mm
Row pitch	16 mm
Tube	round copper
Fins	sine wave aluminium
Number of rows	3
Number of circuits	6
Inlet air temperature, dry bulb	35°C to 40°C
Inlet air relative humidity	80%
Evaporating temperature	0°C
Inlet vapour quality	40%
Superheat	5 K

Table (8.3) Evaporator operating conditions and geometry

The model was run with an evaporating saturation temperature of 0°C, over a range of air velocities from 1 m/s to 5 m/s. The refrigerant inlet condition was taken as two-phase mixture with a vapour quality of 40%. The outlet condition was taken as superheated vapour with a superheat of 5 K. The inlet air relative humidity was fixed at 80% with two dry bulb air inlet temperatures of 35°C and 40°C. The corresponding wet bulb air inlet temperatures were 32°C and 37°C respectively. The predicted evaporator duties are compared for the two refrigerants in figure (8.8) for air inlet temperatures of 35°C and 40°C and 80% relative humidity. The results show a lower performance of the evaporator as retrofitted with R134a in place of R12. This was owing to the higher heat transfer coefficient when the refrigerant R12 was used. The refrigerant mass velocity and refrigerant pressure drop were compared for R12 and its replacement R134a as shown in figures (8.9) and (8.10) respectively.

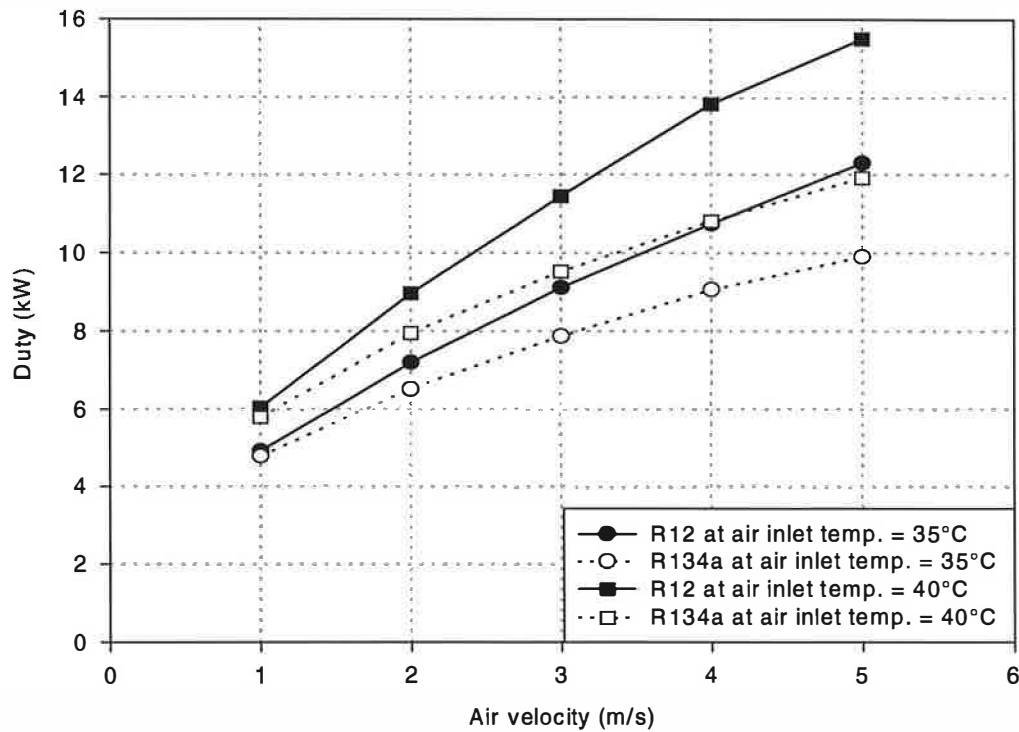


Figure (8.8) Comparison of refrigerant performance in evaporator with R12 and R134a

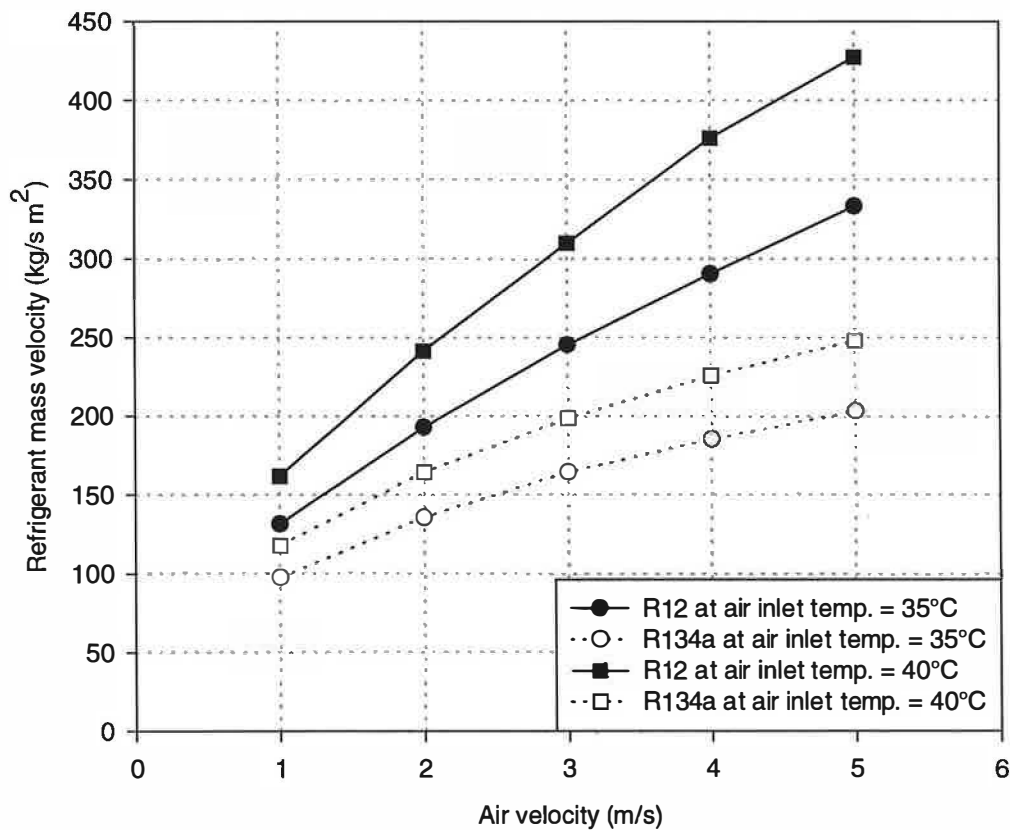


Figure (8.9) Comparison of refrigerant mass velocity in evaporator with R12 and R134a

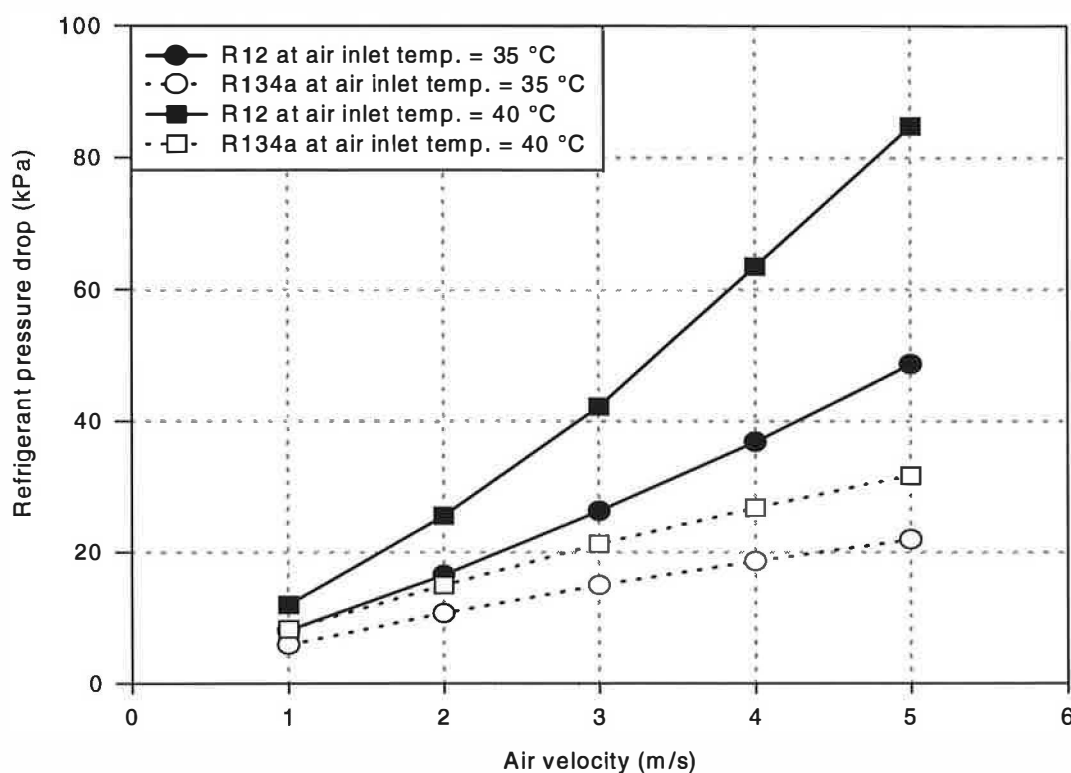


Figure (8.10) Comparison of refrigerant pressure drop in evaporator with R12 and R134a

Replacing R12 with R134a in the same heat exchanger results in a reduction in the refrigerant mass velocity and associated pressure drop. This was owing to the higher specific enthalpy of evaporation for R134a at the same saturation temperature. The refrigerant mass velocity per unit duty is compared for R12 and R134a in figure (8.11).

The results show a reduction in refrigerant mass velocity per unit duty when using R134a of approximately 24%. The air inlet temperature had little effect on the refrigerant mass velocity per unit duty. The duty of the evaporator was evaluated by balancing the air side thermal resistance and the refrigerant side thermal resistance. It should be noted that the heat transfer coefficient for R134a is higher than that for R12 if the same mass flow was maintained, Eckels and Pate (1990) and (1991). They reported heat transfer coefficients of 1.35 to 1.41 times higher for condensation with R134a, while the heat transfer coefficient for R134a was higher by 1.28 to 1.34 comparing with that for R12 for evaporation. The corresponding specific enthalpy of

evaporation for R134a is 1.13 and 1.32 times higher than that for R12 during condensation and evaporation. This increase results in a reduction of the specific mass velocity when R12 is replaced by R134a by approximately 1.25 and 1.31 during condensation and evaporation respectively. Therefore, for the condenser, the reduction in specific mass velocity for R134a has been compensated by the increase in heat transfer coefficient resulting into a similar refrigerant heat transfer coefficient and duty. For the evaporator, however, the reduction in specific mass velocity for R134a was even greater and the increase in heat transfer coefficient was smaller which resulted into a decrease in the refrigerant heat transfer coefficient and duty for R134a. The refrigerant pressure drop per unit duty is compared for the two refrigerants in figure (8.12) for air inlet temperature of 35°C and 40°C. The refrigerant pressure drop per unit duty is reduced with R134a, by approximately 25% at the low velocities to as much as 51% at the high velocities, corresponding to the reduction in refrigerant mass velocity per unit duty.

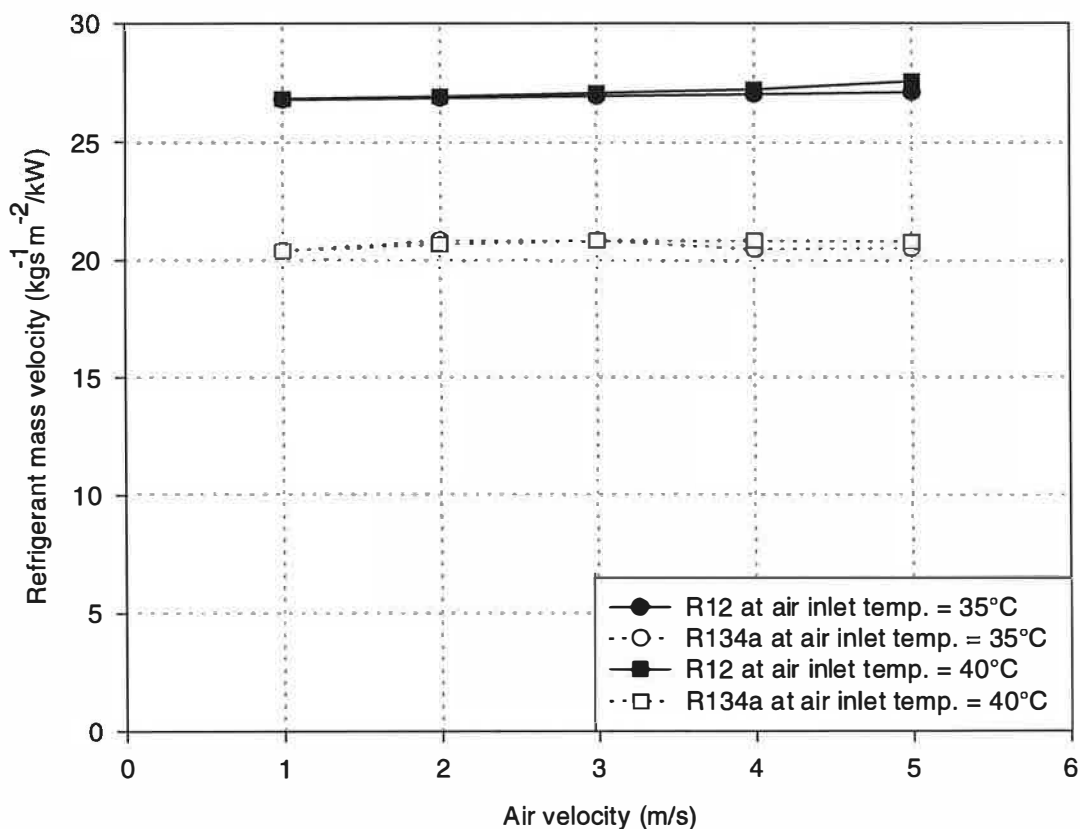


Figure (8.11) Comparison of refrigerant mass velocity per unit duty in evaporator with R12 and R134a

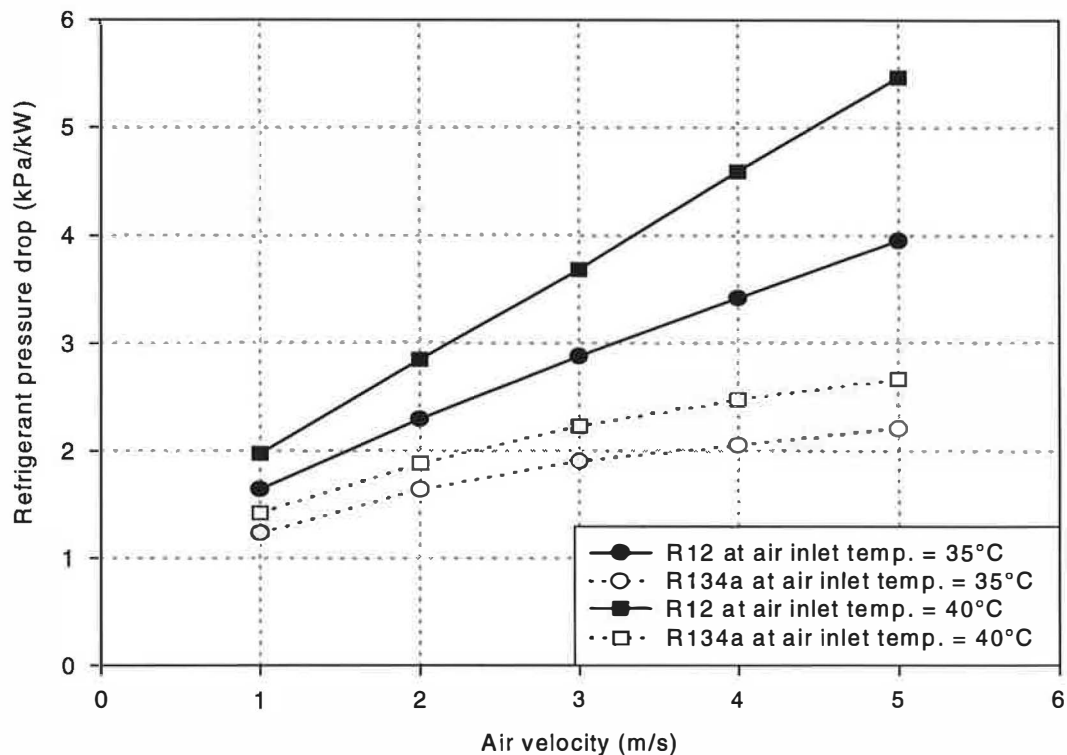


Figure (8.12) Comparison of refrigerant pressure drop per unit duty in evaporator with R12 and R134a

8.3 Comparison between R22 and R407C performance

Although R22 is not being used in automotive application it is widely used in various domestic and industrial applications which require a lower evaporating temperature and higher condensing temperature. Therefore, a comparison was made of the performance of R22 and its replacement R407C due to the lack of such data in the literature.

8.3.1 Effect of refrigerant properties on condenser performance

The comparison was made using the same round tube condenser geometry and operating conditions for R12 and R134a. For R407C, which is an azeotropic blend, the temperature decreases during condensation at constant pressure. Condensation at constant pressure commences at the dew point temperature (saturated vapour) which is higher than that at the bubble point temperature (saturated liquid). The bubble

point temperature has been used to reference the “condensing temperature”. The simulation model was used to predict the heat exchanger duty, refrigerant pressure drop and refrigerant mass velocity with various air-on velocities between 1 m/s and 5 m/s. The refrigerant mass velocity per unit duty is compared for R22 and R407C in figure (8.13).

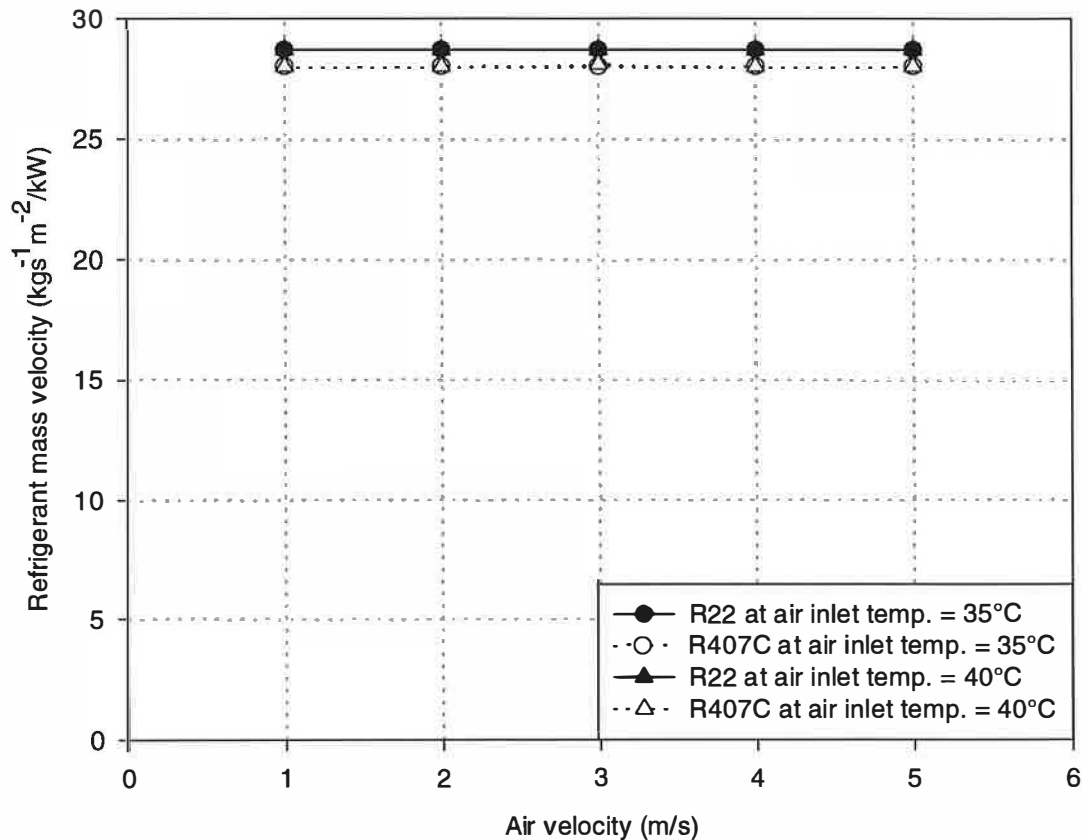


Figure (8.13) Comparison of refrigerant mass velocity per unit duty in condenser with R22 and R407C

Replacing R22 with R407C in the same heat exchanger results in a comparative refrigerant mass velocity per unit duty (within 2.5%). This is owing to the similar specific enthalpy of evaporation for both refrigerants. Again, the air inlet temperature had little effect on the refrigerant mass velocity per unit duty. The refrigerant pressure drop per unit duty is compared for the two refrigerants in figure (8.14) for air inlet temperatures of 35°C and 40°C.

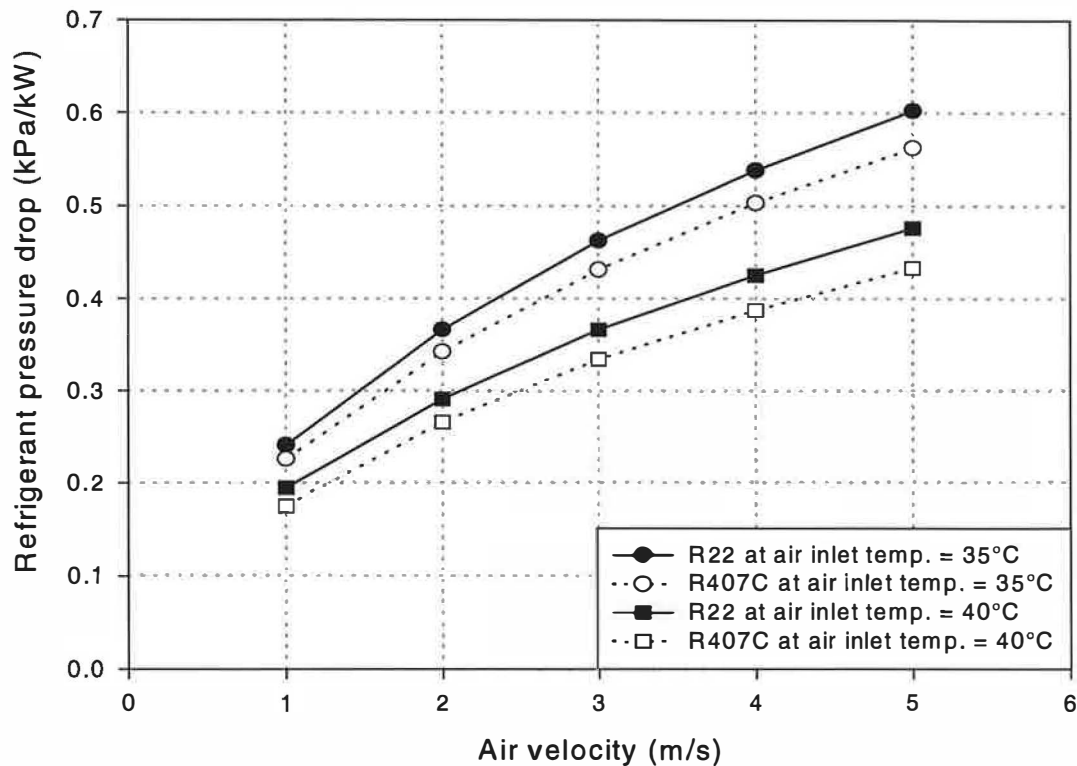


Figure (8.14) Comparison of refrigerant pressure drop per unit duty in condenser with R22 and R407C

The refrigerant pressure drop per unit duty is reduced with R407C by approximately 6% to 9%. This is a consequence of the reduction in mass velocity.

8.3.2 Effect of refrigerant properties on evaporator performance

The model was used to compute the performance of an evaporator using the refrigerant R407C in place of R22. The refrigerant inlet and outlet conditions, heat exchanger geometry and air inlet conditions were similar to that used for the refrigerants R12 and R134a shown in table (8.3). For R407C, the mid-point temperature was taken as 0°C. The refrigerant mass velocity per unit duty is compared for R22 and its replacement R407C as shown in figure (8.15)

The results show a reduction in refrigerant mass velocity when using R407C in place of R22 of approximately 11%. Although the specific enthalpy of evaporation for R407C is similar to that for R22 at a condensing temperature of 61°C, it increases by

up to 11.5% during evaporating, at a temperature of 0°C, for R407C. This increase in the enthalpy of evaporation is the main reason why there is a decrease in mass flux per unit duty. No effect was found for air inlet temperature on the refrigerant mass velocity per unit duty.

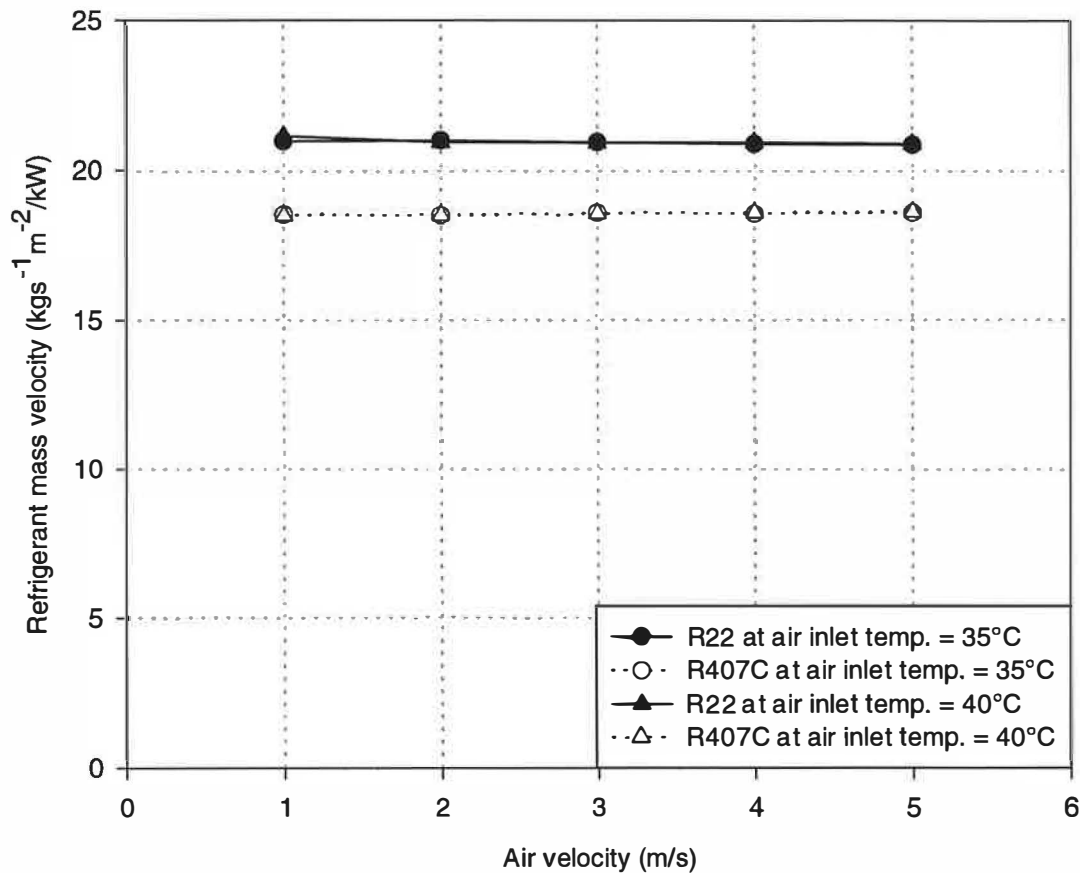


Figure (8.15) Comparison of refrigerant mass velocity per unit duty in evaporator with R22 and R407C

The refrigerant pressure drop per unit duty is compared for the two refrigerants in figure (8.16). The refrigerant pressure drop per unit duty is reduced with R407C, by approximately 8% at the low velocities to as much as 19% at the high velocities, as a result of the reduction in refrigerant mass velocity per unit duty.

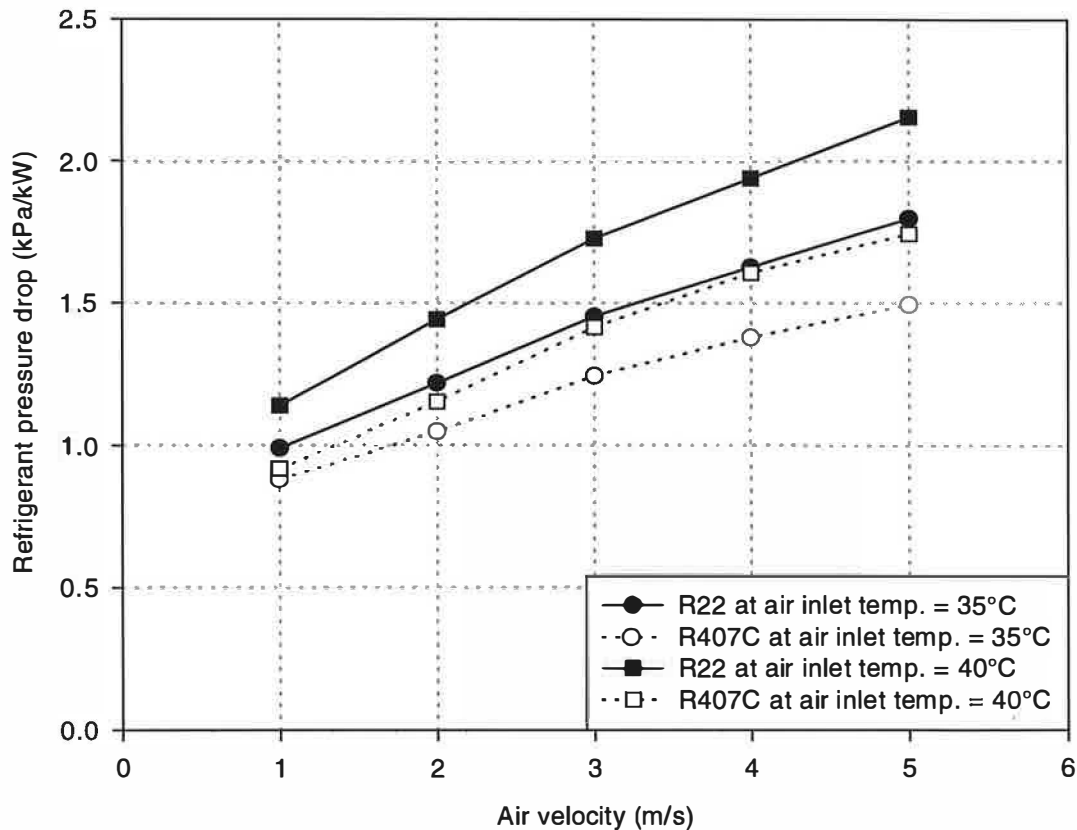


Figure (8.16) Comparison of refrigerant pressure drop per unit duty in evaporator with R22 and R407C

8.4 Summary

The simulation model developed in this study evaluates the performance of compact heat exchangers without reference to the other components of a vapour compression refrigeration system. The model was used to study the effect of refrigerant properties on the performance of condensers and evaporators. Two condenser geometries and one evaporator geometry were used, by way of example, to compare the performance of R12 when it is replaced by R134a. Results are also presented for R22 and R407C in a condenser and an evaporator. The focus of this comparison has been the changes in performance of a typical condenser and evaporator when R12 and R22 are replaced by R134a and R407C respectively. The refrigerant mass velocity was determined from heat transfer considerations with fixed refrigerant inlet and outlet conditions, fixed air-on conditions and fixed heat exchanger geometry. No account has been taken of the characteristics of compressors or expansion valves. In practice,

however, the refrigerant volumetric flow rate is fixed by the compressor displacement and regulated by the expansion valve. The results produced above do, therefore, need to be interpreted with care when considering the complete system performance. Based on the results shown above, the refrigerant mass velocity and pressure drop per unit duty were reduced when R12 is being replaced by R134a in both condenser and evaporator. The same conclusion was found for evaporator when R22 is being replaced by R407C. Replacing R22 by R407C in the condenser showed a reduction in the refrigerant mass velocity and pressure drop per unit duty but with smaller percentages.

CHAPTER 9

Geometry effects and performance correlations

9.1 Introduction

The heat exchanger performance test results are analysed in this chapter. The thermal performance and associated pressure loss are presented in a non-dimensional form of j and f factors against Reynolds number. The effects of fin and tube geometries on the thermal performance and pressure losses are considered. The parameters for the geometries are fin type, fin spacing, fin thickness and number of tube rows. The test results for round tube and plate fin heat exchangers were correlated to derive a general equation using a multiple regression analysis. New equations were developed to predict j and f factors for flat fin and corrugated fin heat exchangers with one, two or four rows of tubes. The effect of the number of rows for both types of fins was also incorporated in the modelling using the multiple regression analysis. The equations developed are compared with existing data in the literature. The equations derived were used in the condenser and evaporator simulation models to predict air-side external heat transfer coefficients and associated pressure losses. The analysis of the test results for flat tubes and corrugated fins is also included using a third order polynomial regression line.

9.2 Effect of geometry

Thirty one samples with varying fin and tube geometries were tested in this study of their effects on the heat exchanger thermal performance and air-side pressure loss. The geometry effects can be categorised into four parameters; fin type, fin spacing, fin thickness and the number of tube rows. The effect of each parameter was investigated by testing heat exchanger samples with varying values of the parameter in question with all others parameters kept constant.

9.2.1 Effect of fin type

The effect of fin surface type on the thermal and fluid dynamic performance was studied by comparing the thermal wind tunnel test results for the flat fin heat exchangers (group 1) with results for samples of corrugated fins with similar geometries (group 2). The effect of leading and trailing edges was included. Figures (9.1) to (9.3) show the effect of fin type on the thermal performance and pressure drop for 16 samples. Figure (9.1) compares the performance of flat and corrugated fin with a straight edges. Samples (2138 and 2137), presented in plots 1 and 2 respectively, have two rows, a tube spacing of 25.4 mm, a row spacing of 22 mm, a fin spacing of 2.62 mm and a fin thickness of 0.13 mm. The graphs show an increase in j and f factors when corrugated fins, plot number 2, were used in place of flat fins, plot number 1. Samples with smaller fin spacing show the same trend. Plots number 3 and 4 shows the performance of samples (2144 and 2143) with geometries similar to that used in plots 1 and 2 but with a fin spacing of 1.83 mm. The graph shows an increase in the j and f factors when the corrugated fins, plot number 3, were used. This may be due to the fact that corrugated fins accelerate the air flow and intensify the turbulence of the air flow between them, thereby enhancing the heat transfer rate. This results in an increase in pressure drop and corresponding increase in the friction factor.

The effect of the type of fin edge was investigated by considering two types of edges, straight and rippled. The performance of 12 samples of corrugated fins (group 2) are compared in figures (9.2) and (9.3) for samples with geometries that include two and four rows respectively. Plots 1 and 2 in figure (9.2) shows the performance of samples (DS and DR) with tube spacing of 25.4 mm, a row spacing of 22 mm, a fin thickness of 0.2 mm and a fin spacing of 4.02 mm. The graph shows comparable j and f factors for both types of edges. Plots 3 and 4 shows the performance of samples (ES and ER) with a smaller fin thickness of 0.12 mm and a smaller fin spacing of 2.54 mm. Plot number 4 shows superior j factor with a rippled edge at high Reynolds number. The edge effect on j factor for samples (2143 and 2142) is not as significant as the fin spacing is reduced to 1.83 mm and the fin thickness is

increased to 0.13 mm, plots 5 and 6. This maybe due to the difference in fin spacing between samples ES, ER and 2143, 2142. Plots 3, 4 and 5, 6 shows comparable friction factor with both edges at high Reynolds number, similar to that found for plots 1, 2. However, the rippled edge has higher friction factor at low Reynolds number.

The effect of the edge type on the performance of samples with 4 row are shown in figure (9.3). The graph shows comparable friction factor with both edges for samples (HS and HR) with a tube spacing of 25.4 mm, a row spacing of 22, a fin spacing of 2.65 and a fin thickness of 0.12 mm, plots (3 and 4). The graph shows similar trend in f factor for samples (2141 and 2140) as the fin thickness increase to 0.13 mm, plots 5 and 6. Samples (GS and GR) with increased fin spacing to 4.13 mm and increased fin thickness to 0.2 mm have superior friction factor when rippled edge is used in place of straight edge, plots 1 and 2. The j factor was found to be similar for both type of edges at low Reynolds number for plots 1,2 and 3,4. While at the higher Reynolds number the rippled edge have increased j factor. For plots 5 and 6, a comparable j factor was found for both edges over the entire range of Reynolds number. From figures (9.2) and (9.3) it could be noticed that most of the f factor results shows negligible effect for the edge type. While the increase in j with rippled edges was mainly owing to the difference in fin spacing rather than the edge type.

9.2.2 Effect of fin spacing

The performance of 11 samples with flat fin (group 1) were compared to study the effect of fin spacing on the thermal performance and friction factor in figures (9.4) to (9.6). The results for samples (15, 12 and 18) with one tube row, a tube spacing of 25.4 mm, a row spacing of 16.5 and a fin thickness of 0.12 mm is shown in figure (9.4). The graph shows a comparable j and f factors for samples with increased fin spacing from 1.63 mm to 1.86 mm, plots 1 and 2 respectively. But, as the fin spacing increase to 2.58 mm, plot 3, the j factor increase as the Reynolds number is reduced. The friction factor has also increased with the increase in fin spacing at

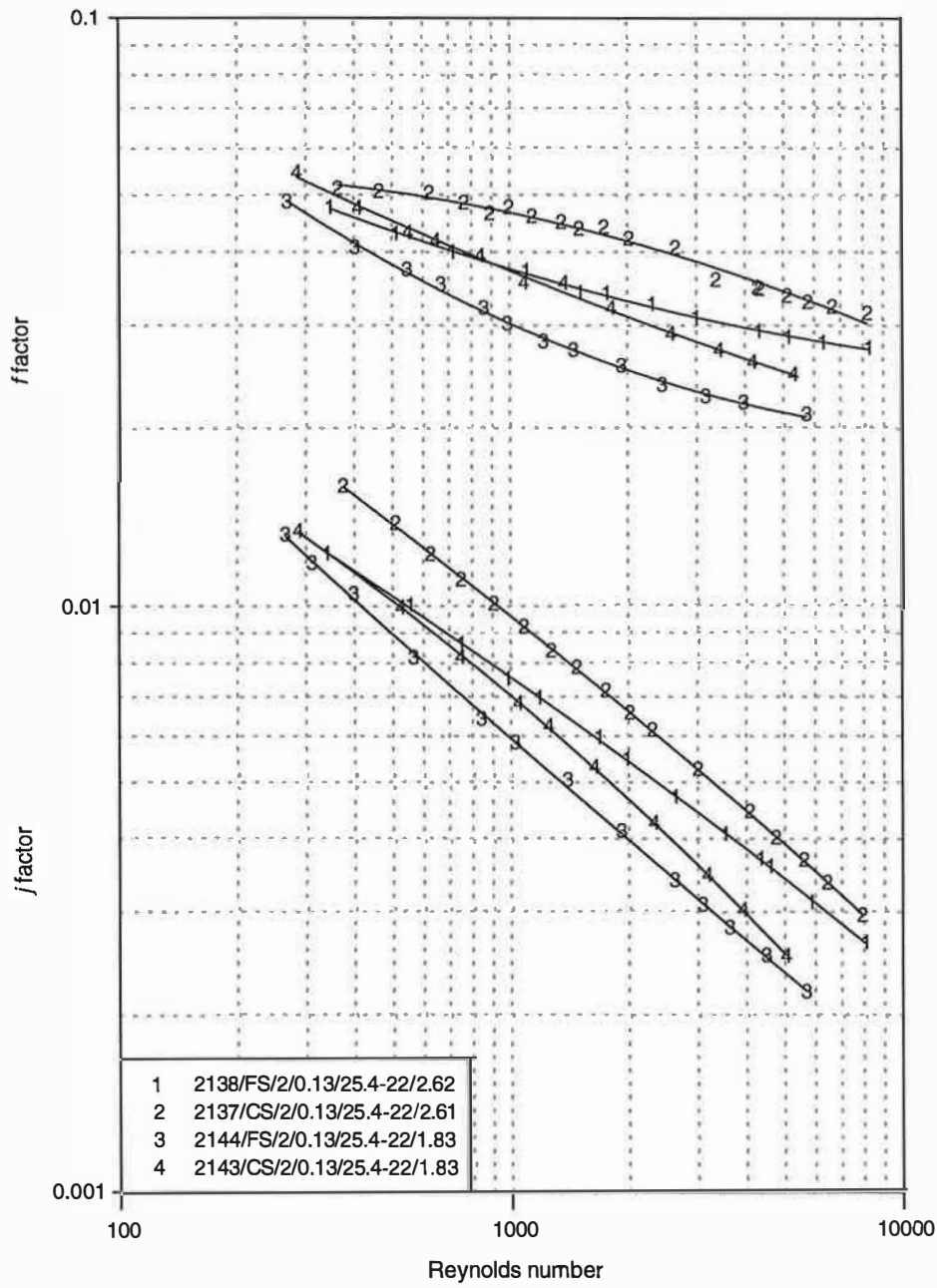


Figure (9.1) Fin surface type effect

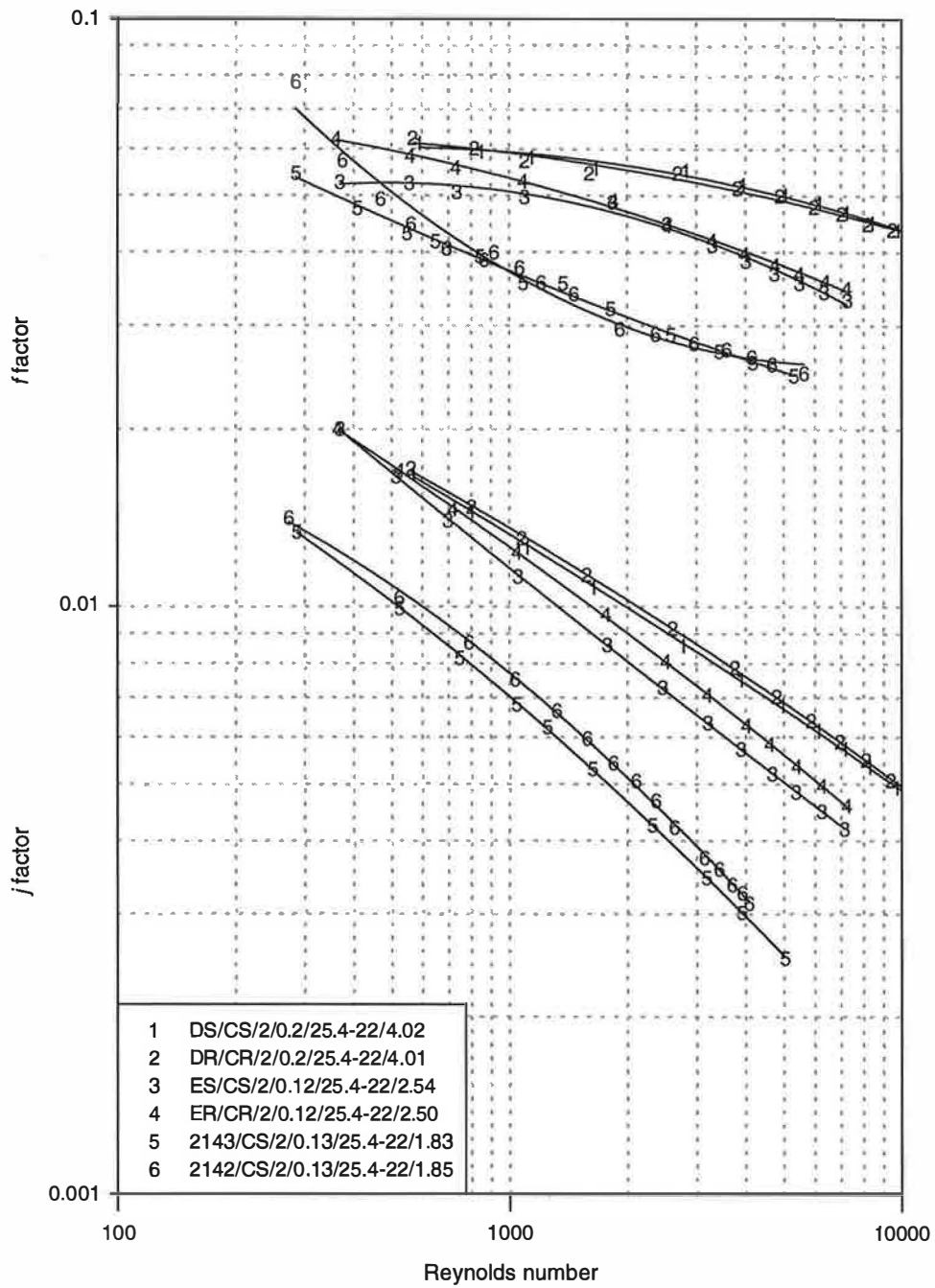


Figure (9.2) Fin edge effect, samples of group (2) with 2-row

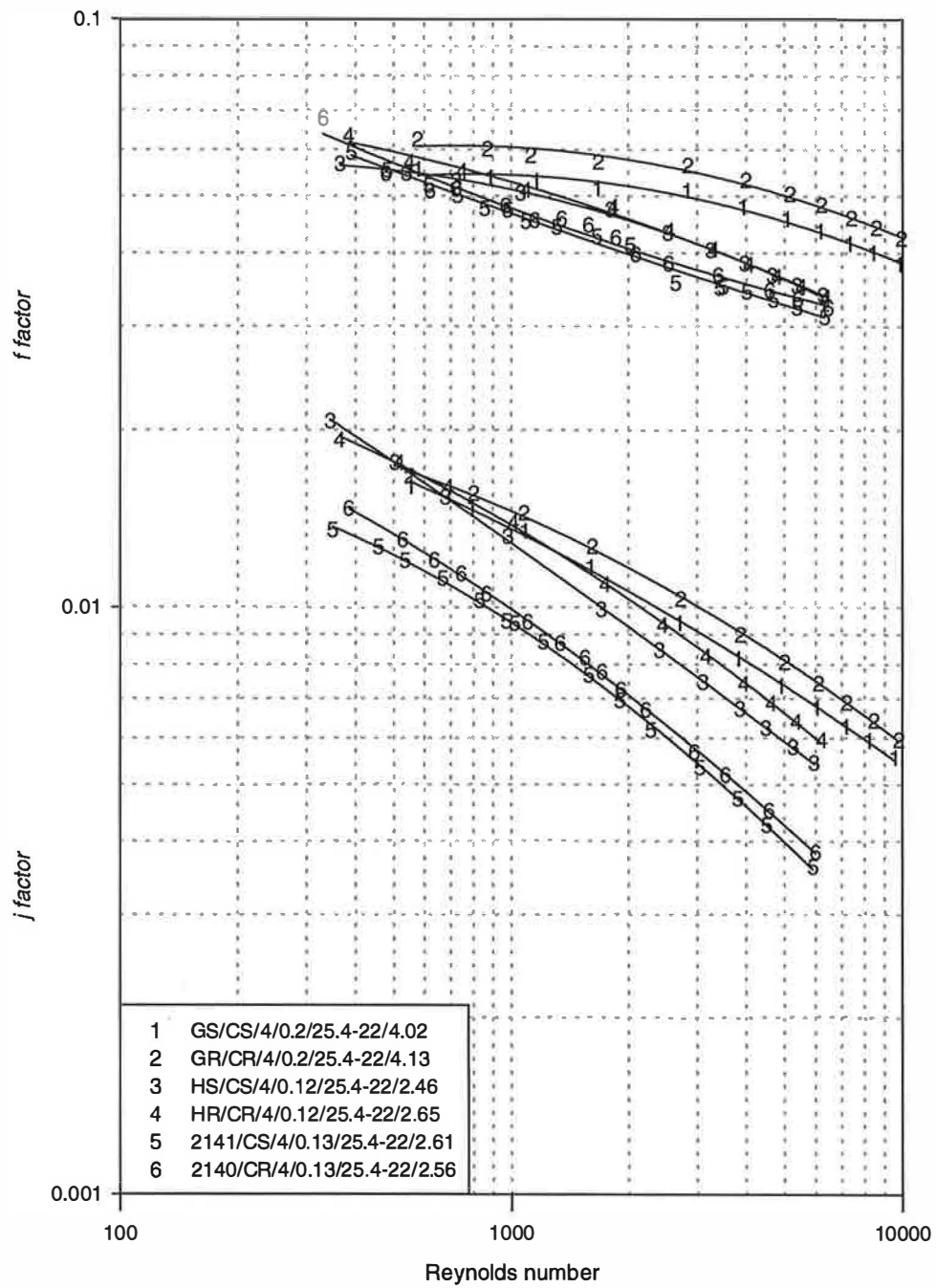


Figure (9.3) Fin edge effect, samples of group (2) with 4-row

high Reynolds number. Figure (9.5) shows the performance of 2-row samples with different fin spacings. Plots 1 and 2 show the performance of samples (2144 and 2138) with tube spacing of 25.4 mm, a row spacing of 22 mm and a fin thickness of 0.13 mm. The j and f factors have increased with the increase of fin spacing from 1.83 mm to 2.62 mm. Similar result was found for samples (23 and 26) with reduced tube and row spacings of 19 and 16.5 mm respectively, and a smaller fin thickness of 0.12 mm for increased fin spacing from 1.64 mm to 2.59 mm, plots 3 and 4 respectively. Samples with increased fin thickness showed the trend. Plots number 5 and 6 are for samples (2154 and 2152) with larger fin thickness, 0.13 mm, than that for plots 3 and 4. The graph shows superior j and f factors with increased fin spacing from 1.91 mm to 2.54 mm. The friction factors in both figures (9.4) and (9.5) seems to be influenced mainly by the fin spacing regardless what the other geometries are. Figure (9.6) shows an increased j and f factors for samples (19 and 25) with 4-rows, a tube spacing of 19 mm, a row spacing of 16,5 mm and a fin thickness of 0.12 mm when the fin spacing was increased from 1.84 mm to 2.64 mm. This is the result of a smaller fin spacing increasing the number of fins for the same face area and hence increasing the total heat transfer area. The air-side pressure drop has correspondingly increased with the reduced spacing between fins and the increased surface area.

The performance of 10 samples with corrugated fin (group 2) were compared to study the effect of fin spacing on the thermal performance and friction factor in figures (9.7) to (9.8). The results were similar to that found for flat fins. The increase of fin spacing was found to enhance j and as a result of that the f factor was increased. This is a consequence of a increase in the Reynolds number due to the increase in the hydraulic diameter.

9.2.3 Effect of fin thickness

The effect of fin thickness on the heat transfer and pressure drop was studied by comparing the performance of 12 samples of groups 1 and 2. Two fin thicknesses of 0.12 mm and 0.13 mm were considered in this comparison. Figure (9.9) show the thermal performance and friction factor for 4 samples of group (1) with 2 and 4 tube

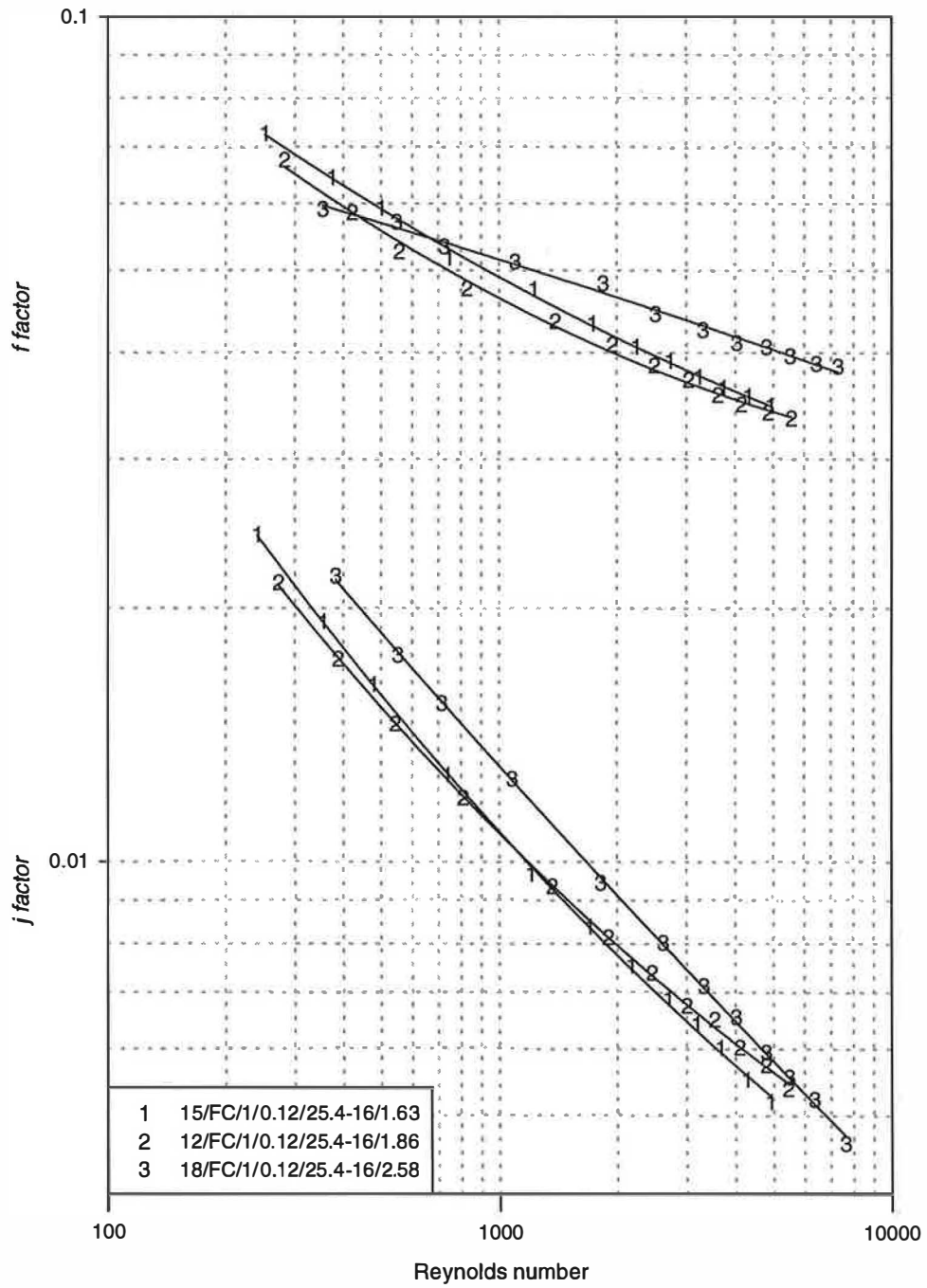


Figure (9.4) Fin spacing effect, samples of group (1) with 1-row

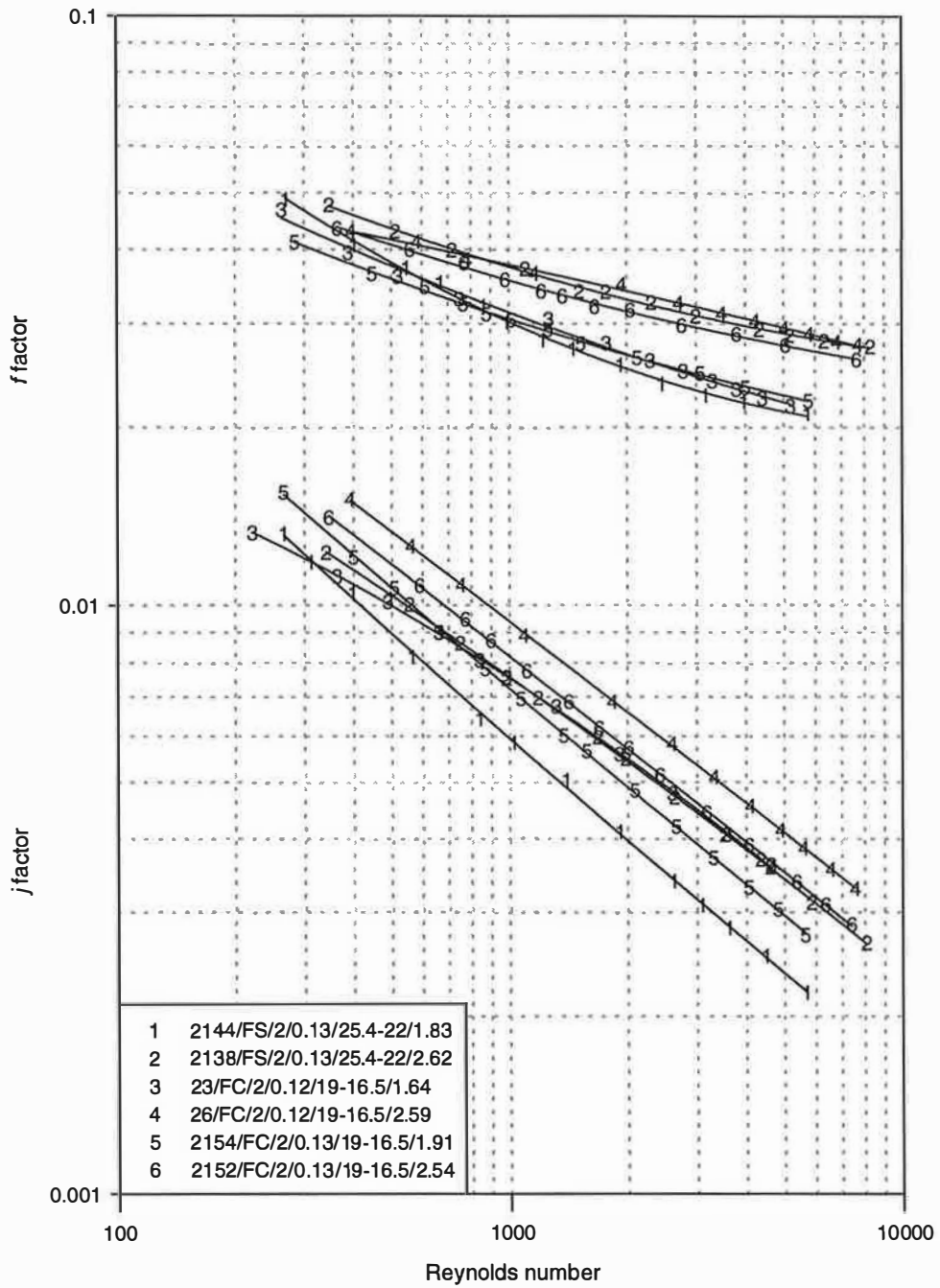


Figure (9.5) Fin spacing effect, samples of group (1) with 2-row

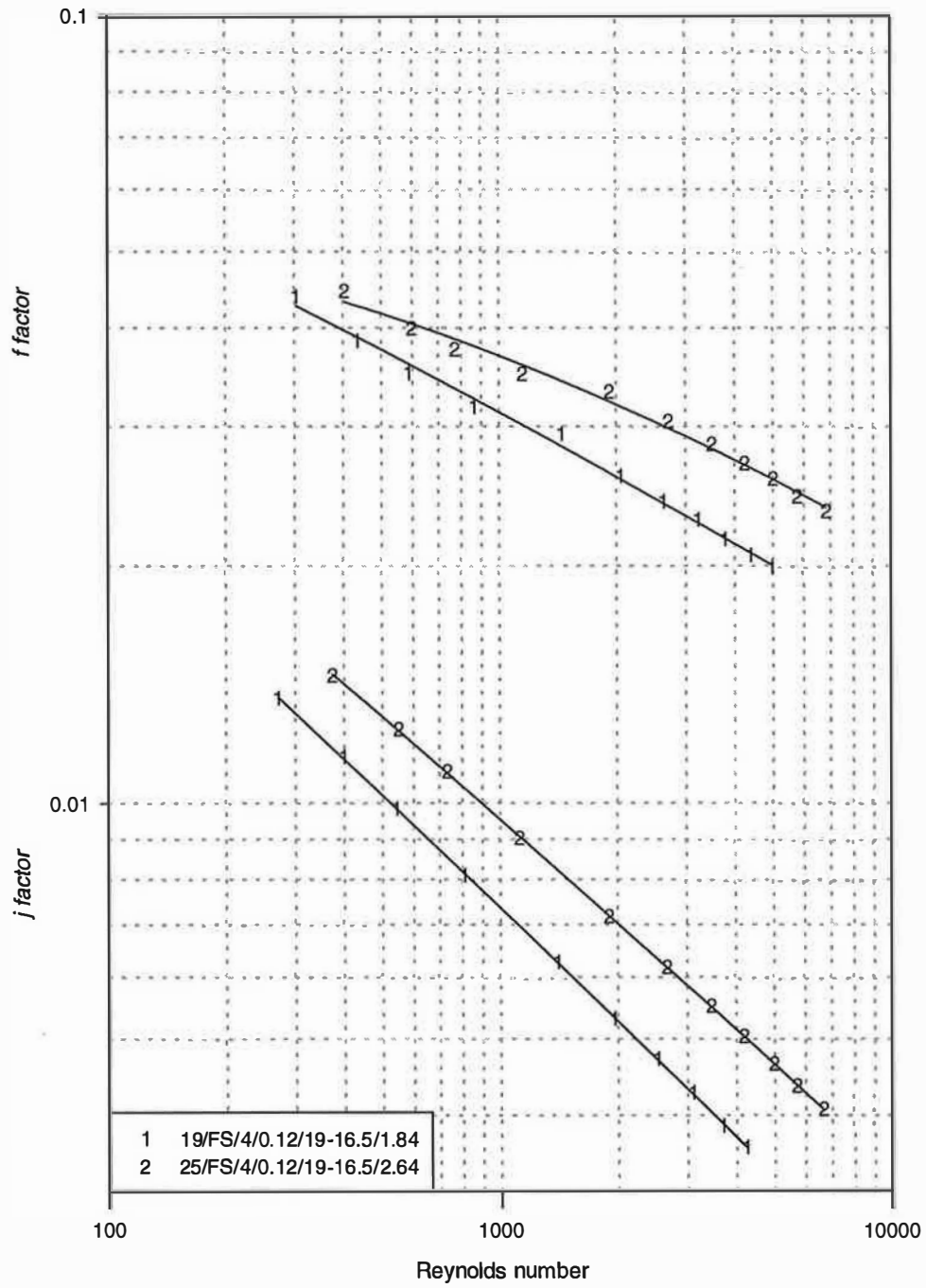


Figure (9.6) Fin spacing effect, samples of group (1) with 4-row

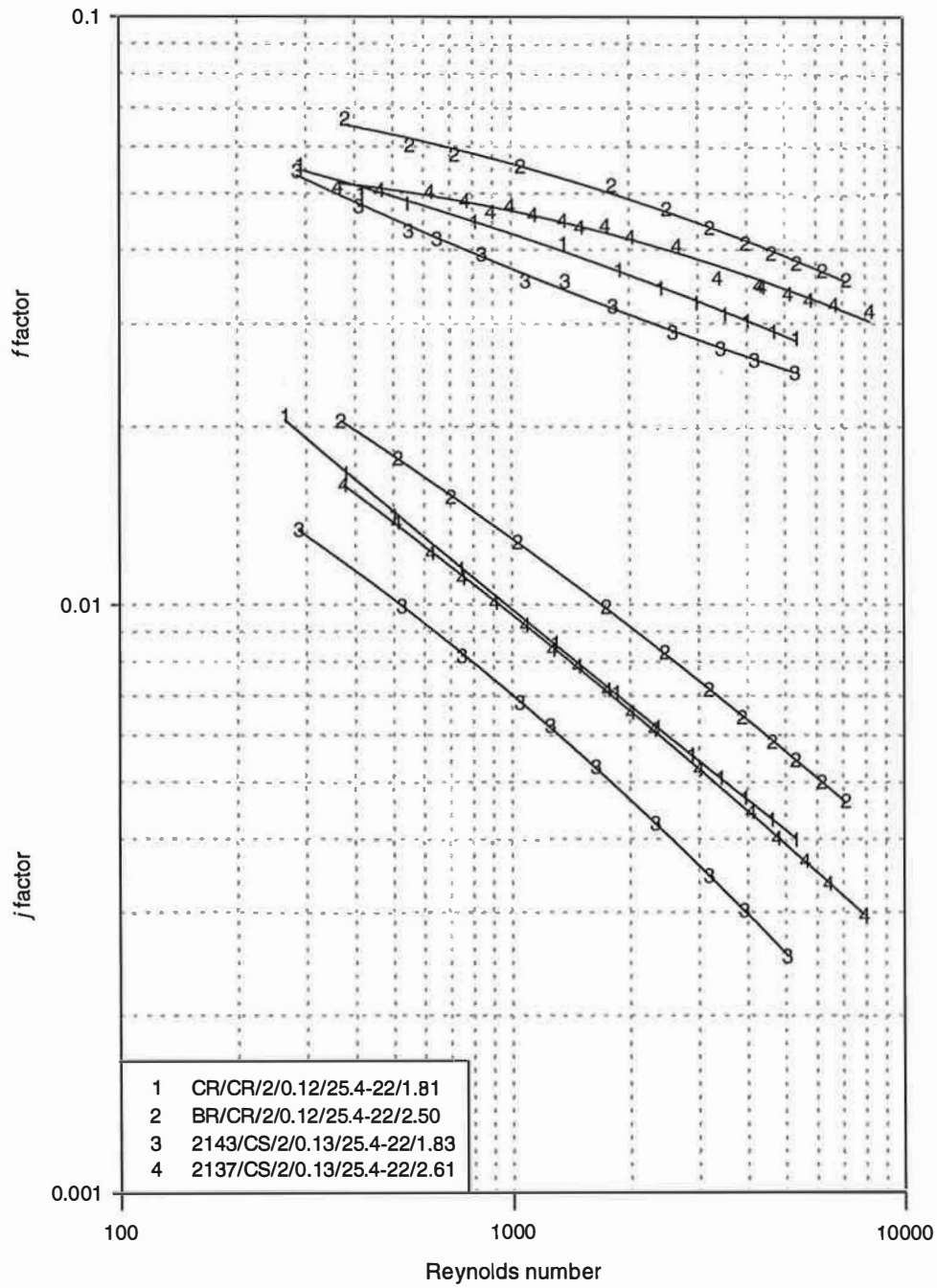


Figure (9.7) Fin spacing effect, samples of group (2) with 2-row

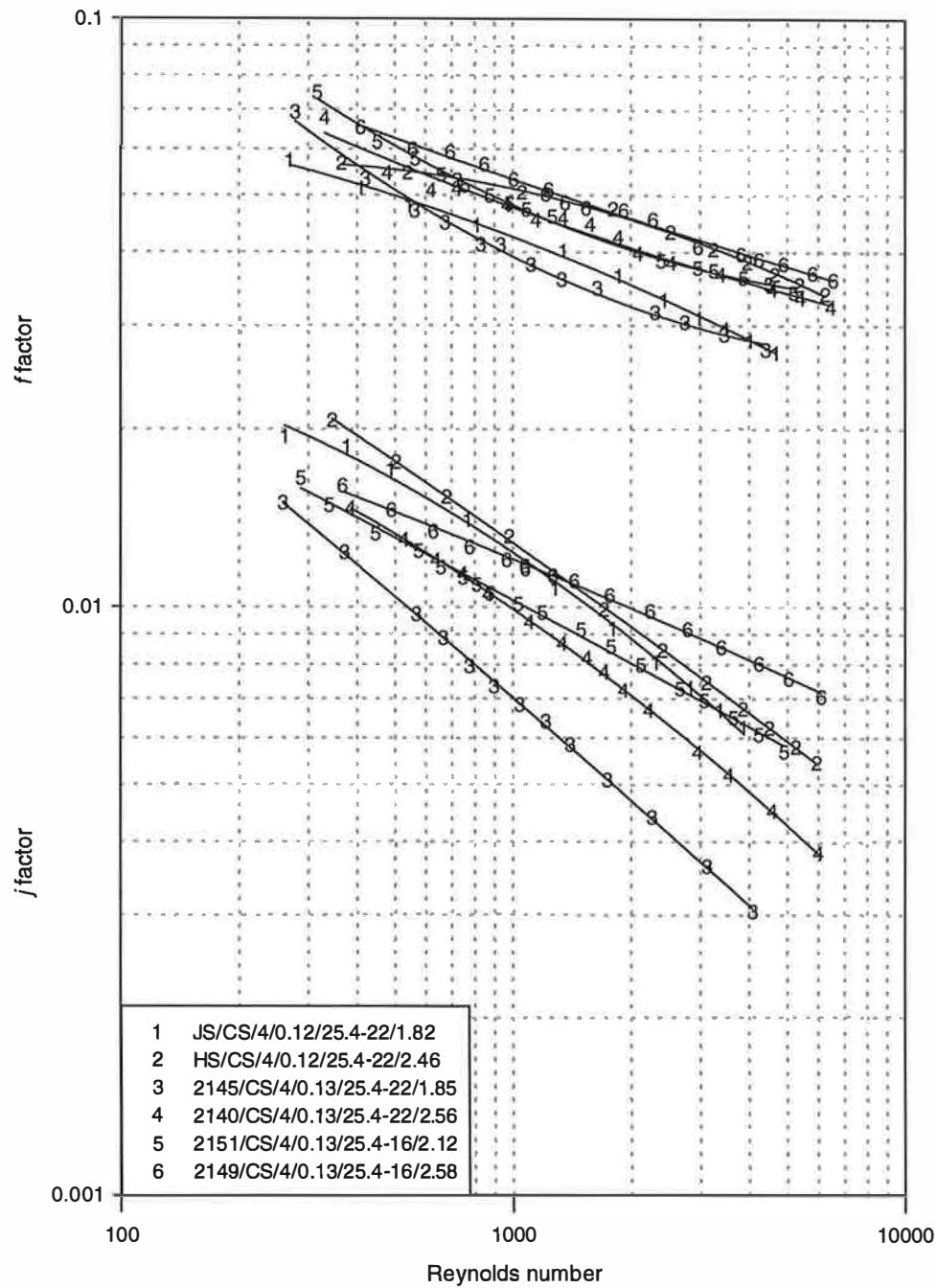


Figure (9.8) Fin spacing effect, samples of group (2) with 4-row

rows. Plots 1 and 2 shows a larger j factor with reduced fin thickness for samples (26 and 2152) with 2 rows, a tube spacing of 19 mm, a row spacing of 16.5 mm, a fin spacing of 2.59 and fin thickness of 0.12 mm and 0.13 mm respectively. The same result was found for j factor with similar geometry but with 4-rows, samples (25 and 2153). However, the friction factor was not as not influenced by the change in fin thickness for both 2 and 4 rows samples.

Figure (9.10) shows the performance of 8 samples of group (2) with 2 and 4 tube rows. The shows an increase in the j factor with reduction in the fin thickness. As expected, the friction factors were comparable for both thicknesses.

9.3 Colburn and friction factor correlations for round tube heat exchangers

Many empirical correlations have been developed by different investigators to calculate the j and f factors, as described in chapter 2. Most of the published correlations are restricted to flat finned heat exchangers and to a limited number of geometrical configurations. Modified fins such as corrugated and sine waves are widely used with round tube heat exchangers. Use of these correlations in a model developed for automotive air-conditioning heat exchangers introduced errors as many were outside the range of geometries. Therefore, it was necessarily to develop empirical correlations to calculate the thermal performance and pressure drop for the geometries considered.

The software package, Sigma Plot, was used to correlate the experimental data based on the Colburn and friction factors and Reynolds number. A multiple regression analysis, used by Sigma Plot, was used to predict the different variables in the suggested correlation. The coefficient of determination, R^2 , was used to evaluate the accuracy of the correlation. The empirical correlations for Colburn and friction factors were assumed as follow;

$$j, f = C_0 Re^{C_1} f(x) \quad (9.1)$$

Where $f(x)$ represent the geometrical parameters in a non-dimensional form affecting the performance, and can be given as;

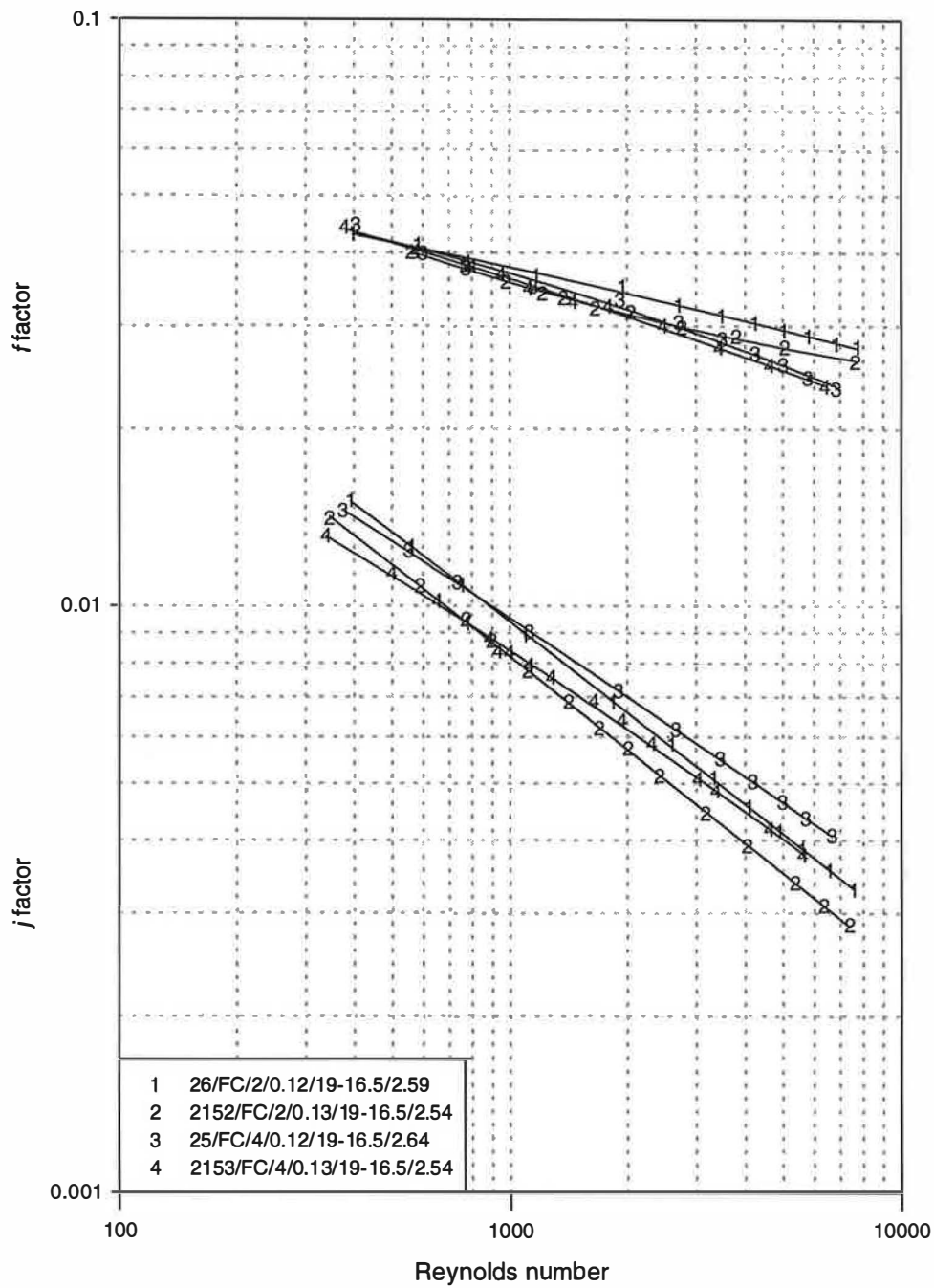


Figure (9.9) Fin thickness effect, samples of group (1)

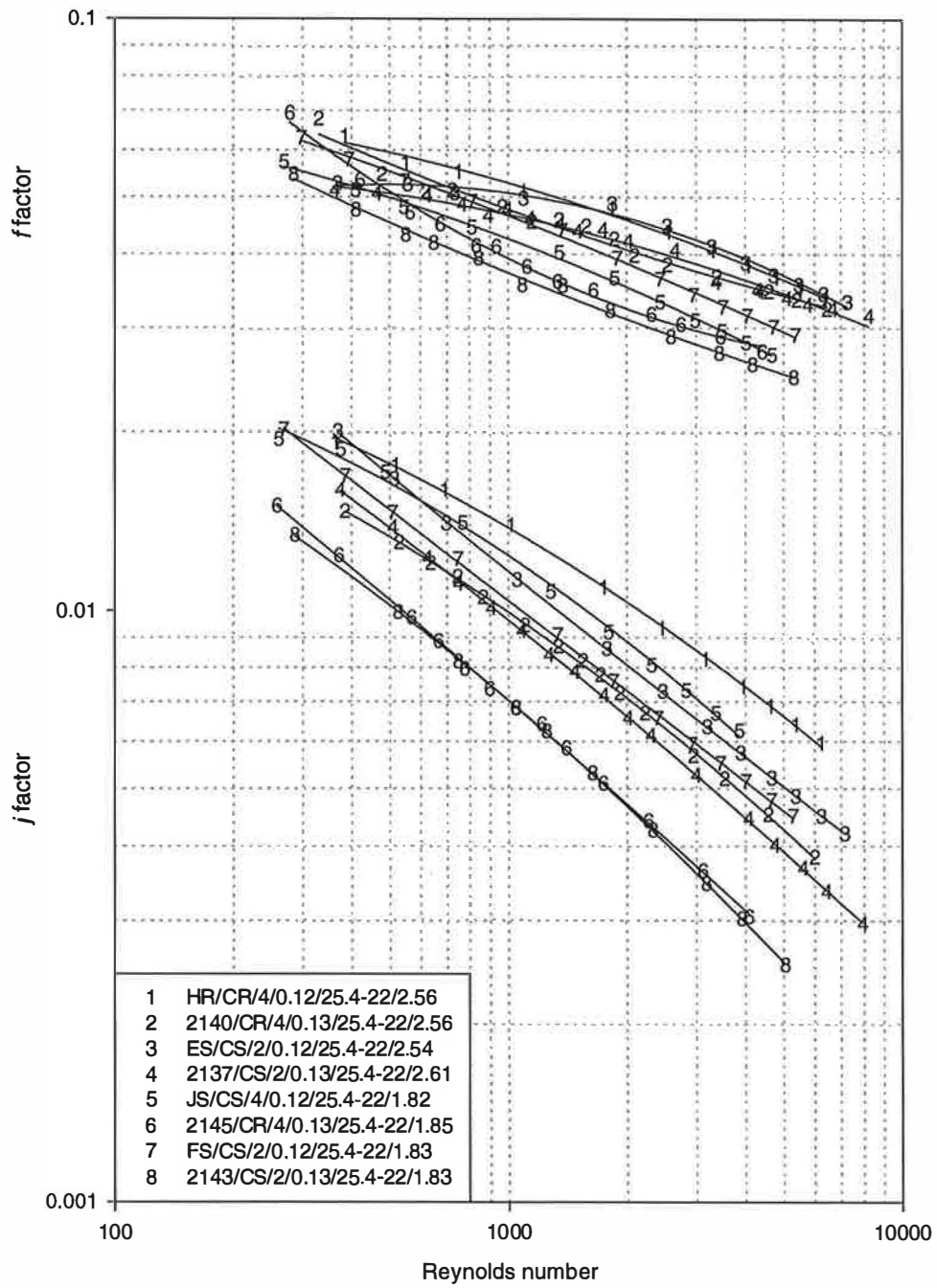


Figure (9.10) Fin thickness effect, samples of group (2)

$$f(x) = S_1^{n_1} S_2^{n_2} \dots S_i^{n_i} \quad (9.2)$$

The geometrical parameters used in the multiple regression analysis includes areas such as face area, tube internal area, total external area, primary area, secondary area, and free flow area, and parameters such as fin spacing, tube spacing, row spacing, fin thickness and tube diameter. These parameters were used in a non-dimensional form by taking the ratios between two parameters. In this study a fundamental approach to heat transfer has been used to establish the effects of the geometric factors on the thermal and frictional performance. The determination of correlations for Colburn, j , and friction, f , factors was carried out in two stages. Various combinations of correlating variables were used to identify the influence of the geometric ratios and to produce a correlation with high accuracy. The initial correlation was undertaken on the experimental data obtained for the four tube row samples. The effect of the number of tube rows was then superimposed for 1 and 2 rows. The two types of fin were considered separately.

9.3.1 Colburn and friction factors for heat exchangers with 4-rows

The regression analysis of the Colburn and friction factors evaluated from the experimental results was undertaken using the Sigma Plot software. Multiple regression analysis was used to identify the influence of the geometric factors, R_n , on the thermal performance and the friction factor. Those of little influence were excluded from the correlation. Both fin types, flat and corrugated, were considered separately as they perform differently (explained in section 9.2.1). A generic equation, which includes the significant geometric factors, was obtained:

$$j = Re^{C_1} R_4^{C_2} R_{5,1}^{C_3} R_7^{C_4} \left(\frac{S_r}{d_o} \right)^{C_5} \quad (9.3)$$

The values of the indices for 4-row heat exchangers with flat and with corrugated fins are shown in Table (9.1).

Type of fin	C_1	C_2	C_3	C_4	C_5
j Flat	-0.44	-3.07	0.37	-6.14	-2.13
f Flat	-0.25	-1.43	1.37	1.65	-3.05
j Corrugated	-0.44	-11.4	1.25	-21.4	-0.47
f Corrugated	-0.25	-1.15	0.70	1.24	-1.12

Table (9.1) Indices for four row heat exchangers.

The same multiple regression analysis was used to correlate the friction factor results. The friction factor can thus be calculated as;

$$f = Re^{C_1} R_4^{C_2} R_{5,1}^{C_3} \left(\frac{S_f}{d_o} \right)^{C_4} \left(\frac{S_r}{d_o} \right)^{C_5} \quad (9.4)$$

Where the values of the indices, C_n , for 4-row heat exchangers with flat and corrugated fins are shown in Table (9.1) above. The coefficient of determination was between 98.4% to 93.9% with an rms error of 1.9% to 3.6%. The friction factor for both types of fins was based on a similar correlation used for Colburn j factor with coefficient of determination varying between 98.1% and 92.7% with an rms error of 1.2% and 2.8% for flat and corrugated fins respectively. The limits of equations (9.3) and (9.4) are shown in Table (9.2).

Type of fin	R_4	$R_{5,1}$	R_7	S_f / d_o	S_r / d_o
Flat	1.77 - 2.25	11.0 - 21.8	0.86 - 0.95	0.16 - 0.27	1.60 - 2.21
Corrugated	1.73 - 1.77	10.4 - 22.1	0.89 - 0.95	0.18 - 0.41	1.60 - 2.21

Table (9.2) Limits of 4-row heat exchangers correlations.

The correlation developed for flat fin and tube heat exchangers was validated against the previously published data of McQuiston (1978a) for one geometry. The sample had a tube spacing of 25.4 mm, fin spacing of 1.814 mm, row spacing of 22 mm, fin thickness of 0.1524 mm, tube outside diameter of 9.956 mm and 4 tube rows. The predicted j and f factors were plotted against the experimentally predicted ones in figure (9.11). This showed an overall agreement of +11% and +5% for j factor, while the f factor was predicted within +11% and -8%.

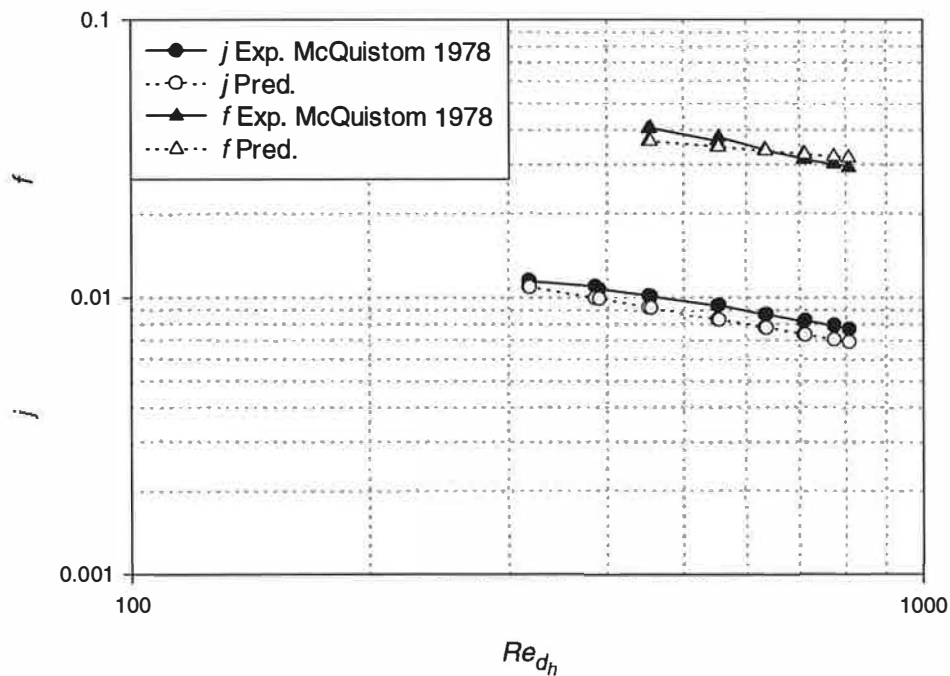


Figure (9.11) Validation of flat fin correlation

9.3.2 Correlation for the effect of the number of tube rows

Previous studies, McQuiston (1978b) and Gray and Webb (1986), used the database of Rich (1975) to derive a factor to account for the effect of a different number of rows in the correlation. One heat exchanger configuration was used, circular flat fins

on round tubes. In the above studies the only factor reported as influencing the thermal performance through the effect of the number of tube rows was Reynolds number. The number of rows had little influence on the friction factor.

In this study, 10 samples with 5 different geometries of corrugated fins and 14 samples with 6 different geometries of flat fins were used to establish the influence of the number of tube rows on the thermal performance. A regression analysis was used to establish the influence of the number of tube rows on the Colburn factor from the experimental data in the form:

$$\frac{j_{N_r=4}}{j_{N_r}} = a_0 + a_1 Re^{a_2} N_r^{a_3} R_3^{a_4} R_{5,1}^{a_5} \quad (9.5)$$

The values of the constants and indices (a_n) for equation (9.5) are given in table (9.3) below and the limits of equation (9.5) are given in table (9.4). The results show that the tube row effect is influenced by the heat exchanger geometries as well as the Reynolds number. A regression analysis of the experimental data showed that the number of tube rows had little effect on the friction factor.

Type of fin	a0	a1	a2	a3	a4	a5
Flat	0.87	1.43E-5	0.55	-0.67	-3.13	4.95
Corrugated	-1.08	0.23	0.03	2.62	-0.14	0.21

Table (9.3) Constants and indices for effect of number of rows.

Type of fin	N_r	R_3	$R_{5,1}$	Re
Flat	1 - 4	7.26 - 19.34	11.03 - 21.78	200 - 6000
Corrugated	2 - 4	9.38 - 19.45	10.68 - 22.08	250 - 5000

Table (9.4) Limits of number of rows effect correlation.

9.4 Correlations for the Colburn and friction factors for flat tube heat exchangers

The multiple regression analysis method used for the analysis of round tube and plate fins cannot be used here. Only one geometry of flat tubes was tested. The equation suggested by Yu (1992) was used to correlate the friction and Colburn factors for the flat tube and corrugated fin samples tested. This equation is suitable to correlate the performance of a single heat exchanger geometry. The friction factor and the Colburn factor were related to the Reynolds number using a third order polynomial regression line in the form:

$$\log(f) = 9.140 - 9.243(\text{Log } Re) + 2.810(\text{Log } Re)^2 - 0.289(\text{Log } Re)^3 \quad (9.6)$$

$$\log(j) = 6.731 - 8.089(\text{Log } Re) + 2.575(\text{Log } Re)^2 - 0.281(\text{Log } Re)^3 \quad (9.7)$$

The fit of these correlations is described by the coefficient of determination (R^2) and is equal to 99% for both f factor and j factor correlations. Figure (9.12) shows the curve fitted to the experimental data points of f and j factors. Equations (9.6) and (9.7) are valid only to the test samples with the geometry shown in table (3.3) and air Reynolds number between 260 and 4100. The lack of information about this type of heat exchanger made it difficult to compare the test data and the derived correlation with that from other studies.

9.5 Error analysis

The uncertainties associated with the experimental measurements were considered to establish the accuracy of the results. The procedure of evaluating the uncertainties for the Reynolds number, j and f factors, described by Achaichia (1987) and Yu (1992) was followed. The procedure involves identifying the errors in the measured parameters caused by its measuring device. A complicated effect was found for the measured parameters on the Reynolds number, j and f factors. The wind tunnel results, therefore, were re-analysed using the values of the measured parameters, modified by the percentage of the expected error. The percentage errors, E_i , caused

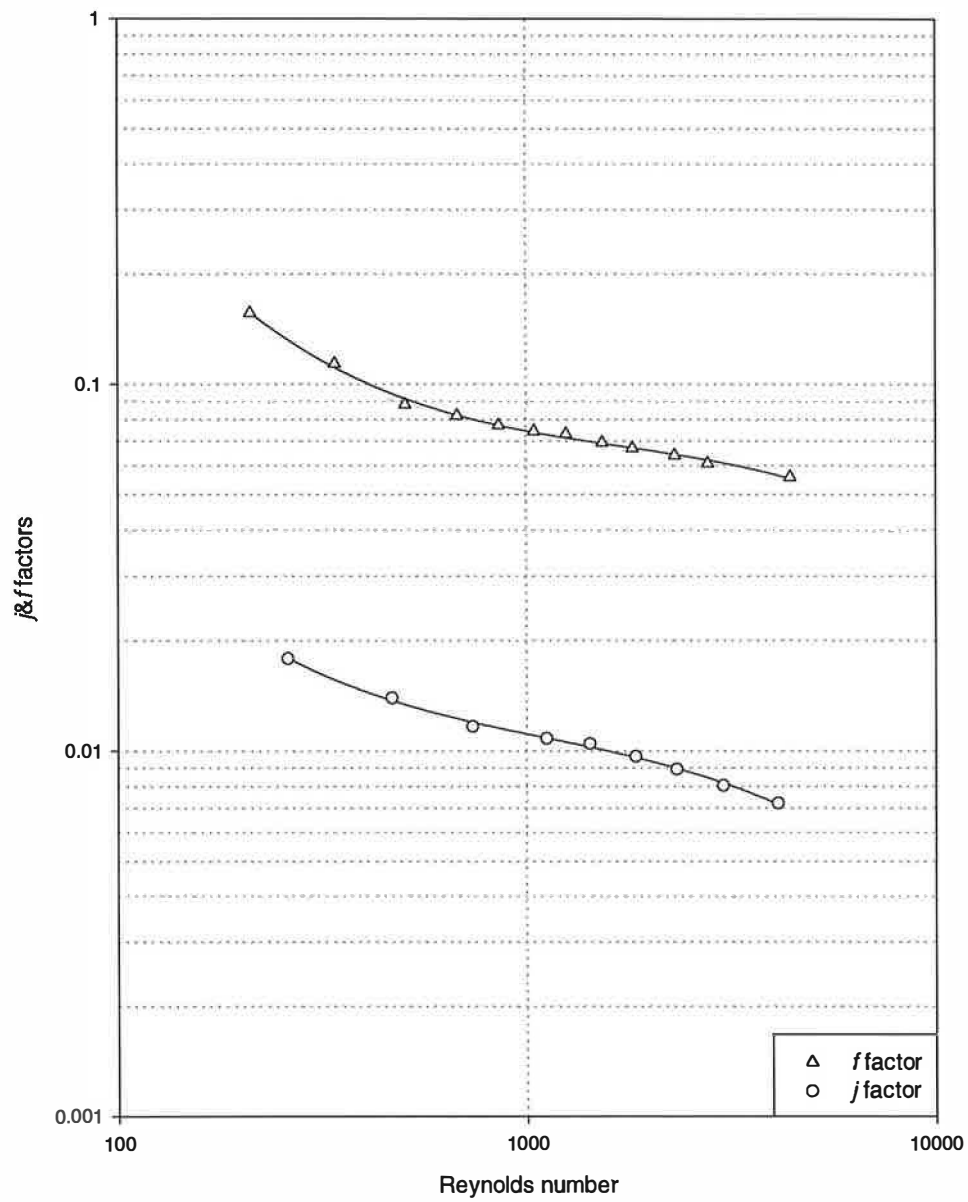


Figure (9.12) Colburn and friction factors for flat tube heat exchange

by each parameter were calculated and the total percentage error, E , calculated as follow;

$$E = \sqrt{\sum_{i=1}^n E_i^2} \quad (9.8)$$

The experimental tests were carried out at different air velocities, 1 to 20 m/s, and the accuracy had to be evaluated at both ends of the velocity range. The low accuracy of the pressure drop measurements experienced in the early design of the wind tunnel, up to $\pm 10\%$ resulted into $\pm 15\%$ error in the f factor at low air velocity Achaichia (1987), was improved by using an additional pressure transducer. The parameters that contribute to the uncertainties in the evaluation of j factor are the air velocity, water mass flow, the air temperature difference, the inlet water-air temperature difference and the water inlet temperature. The uncertainties in evaluating the f factor are the contribution of air velocity, air pressure drop and air inlet temperature. And finally, the uncertainties in evaluating the Reynolds number are the contribution of the air velocity, water inlet temperature and the inlet water-air temperature difference. Table (9.5) shows a list of the instruments error at low and high velocities. Table (9.6) shows an example of the percentage of uncertainty, E_i , of the measured parameters caused by its measuring device, readings are for sample number "2147".

Parameter	error
air velocity low	2 %
air velocity high	1 %
pressure drop low	1 %
pressure drop high	1 %
air in temp.	0.1 K
water in temp.	0.1 K
water in - air in	0.5 K
air out - air in	0.08 K
water flow	1 %

Table (9.5) Instrument errors

	Reynolds number		<i>j</i> factor		<i>f</i> factor	
	low	high	low	high	low	high
air velocity	2%	1%	0.35%	0.41%	4.12%	2.03%
pressure drop	/	/	/	/	1%	1%
air in temp.	/	/	/	/	0.03%	0.03%
water in temp.	0.06%	0.06%	0.01%	0.03%	/	/
water in - air in	0.28%	0.29%	4.27%	1.40%	/	/
air out - air in	/	/	0.71%	0.72%	/	/
water flow	/	/	0.09%	0.22%	/	/

Table (9.6) Uncertainties caused by the different measured parameters for sample “2147”.

The error in Reynolds number was mainly due to error in air velocity with a maximum errors of 2% and 1% for high and low air velocities respectively. A maximum error of 4.2% was obtained for *f* factor at low air velocities and 2.2% at high air velocities. The main reason behind this is again due to the measurement of air velocities. The error in the *j* factor was mainly attributed to the uncertainty in the measurement of the inlet water-air temperature difference. A maximum error of 3.2% was obtained over the range of air velocities.

9.6 Summary

Experimental results are presented for a number of round tube and plate fin heat exchangers of different geometric configurations with both flat and corrugated fins. Correlation equations for the *j* and *f* factors are presented as functions of Reynolds number, based on the hydraulic diameter, and geometric parameters of the heat exchangers. These equations are believed to be more accurate than earlier correlations with a broader scope of applications. A novel approach was developed for deriving the geometric ratios in the correlation equations based on consideration of the heat transfer and fluid flow relations for the heat exchanger surfaces. The

correlation equations show good agreement with published test data for round tube and plate fin heat exchangers.

It was found that the fin type affects the heat transfer and friction factor, whilst the number of tube rows have a negligible effect on the friction factor. The number of tube rows effect was found to be influenced by the fin and tube geometries as well as the Reynolds number. The j factor increased with the decrease of fin thickness. The fin thickness has negligible effect on the friction factor.

Chapter 10

Conclusion and further work

10.1 Conclusion

The objective of this study was to develop a simulation model for the heat exchangers in automotive air-conditioning systems. The model developed, from the work of previous researchers and experimental wind tunnel tests by the author can be used to design condensers and evaporators using the new non-ozone depletion refrigerants. Validation against experimental results and manufacturer's test showed the model to be sufficiently accurate for design purposes. The model has been used successfully by four heat exchanger manufacturers and by researchers to improve the understanding of the behaviour of condensers and evaporators with varying geometries, refrigerants and operating conditions. The development of the model involved two main steps. The first step was the simplification of heat transfer and pressure drop calculations by introducing geometrical parameters. These parameters were derived for the two types of heat exchanger used in automotive application, round tube with plate fins and parallel flow heat exchangers, from the basic fin and tube geometries.

The second step involved the development of accurate heat transfer and pressure drop correlations from experimentation for use in the developed model. The geometrical parameters derived from the theory have been used to describe the influence of fin and tube geometries on the heat exchange and pressure loss performance. The effect of the number of tube rows described in the literature for one geometry has been extended for a number of fin and tube geometries. The use of corrugated fins has been found to give a higher heat transfer performance and higher pressure drop owing to the vortices generated in the wake of the corrugation. The fin edge type was found to have negligible effect on the thermal performance. Heat exchangers with reduced fin thickness were found to have higher heat transfer

performance. The fin spacing effects were found to be in agreement with studies reported in the literature.

Studies into the retrofitting of R12 with R134a in the same condenser showed a reduction in the refrigerant mass velocity per unit duty owing to the increase of the specific enthalpy of condensation for R134a. The refrigerant pressure drop per unit duty was reduced with R134a corresponding to the reduction in refrigerant mass velocity per unit duty. Comparable results were found in evaporators retrofitting with R134a in place of R12. Using R407C in place of R22 in the same condenser resulted in a comparable refrigerant mass velocity per unit duty. This is explained by the comparable specific enthalpy of condensation for both refrigerants. The refrigerant pressure drop per unit duty reduced slightly with R407C as a consequence of the small reduction in mass velocity per unit duty. The specific enthalpy of vaporisation was reduced for R407C resulting in a reduction of the specific mass velocity and specific pressure drop in the same evaporator.

This investigation developed a simple method for describing the heat exchanger geometries and the heat transfer and pressure drop theory, using the suggested geometrical parameters. It is shown that these geometrical parameters can also be used to describe the effect fin and tube geometries in correlating the Colburn factor and friction factor. This development can be extended to cover different types of heat exchanger geometry.

10.2 Further work

The heat exchanger simulation is an important element in the design of condensers and evaporators for energy saving and optimisation purposes. It can be used to study the effect of different fin and tube geometries on the thermal and pressure drop performance of condensers and evaporators. Further, the model can provide valuable data to improve the understanding of retrofitting existing air-conditioning and refrigeration systems with new refrigerants.

The newly introduced non-ozone depleting refrigerants need more attention. Accurate heat transfer coefficient and pressure drop data are needed for single-phase and two-phase flow particularly with the use of new lubricating oils.

The thermal performance and pressure drop for the new generation of tubes, with the internal micro-fins used in the parallel flow condensers needs to be investigated. These tubes have higher heat transfer coefficients, but data on the enhancement factor and the effect of micro-fin on the pressure drops are not readily available. Further, although the pressure drop in the header tanks is very significant, no data were found for the local pressure loss coefficient to evaluate total pressure drop on the refrigerant side. This need an extensive experimental investigation to produce accurate data for inclusion in the model.

The other two basic components found in air-conditioning and refrigeration systems, the compressor and the expansion valve, need to be included in the model to create an overall simulation that can be used for the steady state performance evaluation of the complete system. Performance data and theoretical models are needed for the types of compressors and expansion valves used in automotive application.

Appendix A

Refrigerant properties

1	Introduction	A-1
2	Specific enthalpy	A-2
3	Density	A-6
4	Specific heat capacity	A-8
5	Thermal conductivity and viscosity	A-10
6	Saturated pressure and temperature	A-13

1 Introduction

Much of the software used for the simulation of heat exchangers, described in chapter 2, were developed for one or two specific refrigerants such as R12 and R22. However, the phase out of the ozone depletion refrigerant R12 resulted in the consideration of many alternatives. Therefore, one of the aims of this project was to include the performance of a wide range of refrigerants in the modelling. The refrigerant thermodynamic properties are required at several points in the vapour compression cycle. These points include the inlet and outlet of each flow region, superheated vapour region, two phase region and subcooled liquid region. These are necessary for the determination of the refrigerant mass flow rates or the heat transfer rates. The thermophysical properties are also required for the calculation of non-dimensional numbers, heat transfer coefficients and pressure losses.

The accuracy of the simulation model will depend on the accuracy of the calculated properties as well as other factors. Therefore, accurate predictions of the refrigerant properties are important. Many software packages are available commercially for the prediction of the refrigerant thermodynamic and thermophysical properties. Most of the software is limited to a strict inputs. Further, the output of most of these packages cannot be accessed by other software to allow the automatic and fast performance prediction calculations process. The limitations of known input properties used to determine the other properties makes the use of the commercial software unsuitable in a heat exchanger simulation model. Therefore, it was decided to build a separate sub-model to calculate the refrigerant properties.

The refrigerant properties required by the heat exchanger simulation software includes specific enthalpy, enthalpy of vaporisation, specific heat capacity, saturation pressure and temperature, critical pressure and temperature, density, viscosity and thermal conductivity. These are required for the three regions existing in the heat exchangers; superheated vapour, two phase and subcooled liquid. The bubble point temperature (the saturated liquid line), the mid point temperature and the dew point temperature (the saturated vapour line) are also required for the near azeotropic

refrigerant mixtures. The single phase refrigerant properties requires not more than two different properties on each point to calculate the others. Most of the properties are presented in tabular form for varied temperature or pressure. However, as the use of personal computers has increased rapidly in the past ten years, many investigators and refrigerant manufacturers have used sets of equations to describe these properties.

Four refrigerants were considered in this study. These include the two main refrigerants used in air conditioning and refrigeration, R12 and R22, and their replacements R134a and R407C. The molecular weight, critical temperature and pressure for these refrigerants are given in table (A.1)

Refrigerant	R12	R22	R134a	R407C
Molecular weight	120.914	86.469	102.03	86.17
Critical temperature K	385.2	369.16	374.23	359.2
Critical pressure M Pa	4.1249	4.977	4.0603	4.652

Table (A.1) Refrigerants critical properties

The refrigerant properties given as equations have been used in the heat exchanger simulation model. For the properties where no equations were found and tabulated data were given instead, a least mean squares analysis was used to correlate the tabulated data. However, for the properties which were required in the initial estimation only, an alternative method was used to determine these properties. A full description of the refrigerant thermodynamic and thermophysical properties calculation procedures is given below.

2 Specific enthalpy

The specific enthalpy difference between inlet and outlet of the heat exchanger is used to calculate the heat transfer rate from the refrigerant mass flow rate. The specific enthalpy of the liquid is calculated assuming that the liquid is saturated. The

error resulting from this assumption is usually less than 2%, Heikal (1990). The specific enthalpy of saturated liquid is given by many investigators as a function of the temperature. The specific enthalpy values of saturated liquid are given in ASHRAE Handbook (1993) for most of the refrigerants. A polynomial equation has been used to fit the tabulated data within the range of -90°C and -150°C for R12 and R22 respectively to the critical point. The resulting formulae have been used to calculate the value for the refrigerants R12 and R22 from the liquid temperature in Celsius as follow,

$$i_l = a_0 + a_1T + a_2T^2 + a_3T^3 + a_4T^4 + a_5T^5 \quad (\text{A.1})$$

For the refrigerants R134a and R407C, the formula given in ICI (1994) data sheet have been used to calculate the liquid specific enthalpy as;

$$i_l = a_0 + a_1H + a_2H^2 + a_3H^3 + a_4H^4 + a_5H^5 \quad (\text{A.2})$$

Where

$$H = \left(1 - \left(\frac{T}{T_C} \right) \right)^{1/3} \quad (\text{A.3})$$

The SI system of units has been used throughout the development of the property formulations. The temperature in equation (A.3) is taken as the bubble point temperature for the refrigerant R407C. The constants for calculating the liquid enthalpy from equations (A.1) and (A.2) is given in table (A.2).

Refrigerant	R12	R22	R134a	R407C
a_0	200.012	200.823	289.676	131.771
a_1	940.8E-3	116.72 E2	-120.933	122.47E1
a_2	869.9E-6	-741.4E-7	581.62E-1	-421.24E1
a_3	-326.9E-8	419.1E-8	-610.826	504.513E1
a_4	304E-10	290E-9	166.658	-252.85E1
a_5	991.2E-12	172.6E-11	0	0

Table (A.2) Liquid enthalpy constants

The specific enthalpy of saturated and superheated vapour was derived from the fundamental thermodynamic relations. Heikal (1991) calculated the vapour specific enthalpy from the ideal gas specific heat capacity at constant pressure and the equation of state for the refrigerant R134a. The process requires the integration of the equation of state to the temperature and specific volume. This was applied to the other refrigerants considered in this study, R12, R22 and R407C. Many forms of the equation of states have been suggested by investigators in the literature. The Martin-Hou equation of state has been widely used by refrigerant's manufacturers.

The Martin-Hou equation of state, given in ASHRAE (1987), was used for the refrigerants R12 and R22. For the refrigerant R134a, the Martin-Hou equation of state given in DUPONT (1994) data sheet was used. The equation of state for R407C given in ICI (1994) data sheet was used with some modification to match the form used for the other refrigerants. The Martin-Hou equation of state is defined as follow;

$$p = \frac{RT}{v - B} + \sum_{i=1}^4 \frac{(A_i + B_i T + C_i \exp(-KT_r))}{(v - B)^{i+1}} + \frac{(A_5 + B_5 T + C_5 \exp(-KT_r))}{(1 + C' \exp(vu)) \exp(vu)} \quad (\text{A.4})$$

Table (A.3) contains the equation of state constants for the various refrigerants considered.

The enthalpy of saturated vapour is calculated for a given temperature and specific volume using Maxwell's relation, Heikal (1990), as follow;

$$di = C_p dT + \left(T \left(\frac{dp}{dT} \right)_v + v \left(\frac{dp}{dv} \right)_T \right) dv_T \quad (\text{A.5})$$

The specific enthalpy is, therefore, calculated by integrating the above equation where the three terms in the right hand-side are considered separately. The integration of the first term in the right hand side, the ideal gas specific heat capacity at constant pressure described below in section (A.4), is given as;

$$i_1 = I_1 T + \frac{I_2 T^2}{2} + \frac{I_3 T^3}{3} + \frac{I_4 T^4}{4} - \frac{I_5}{T} + \frac{I_6 T^5}{5} + I_7 \ln(T) \quad (\text{A.6})$$

Refrigerant	R12	R22	R134a	R407C
A_1	-133.951E-2	-874.661E-3	-890.946E-4	-224.292E-3
B_1	112.741E-5	870.543E-6	440.865E-7	374.9E-6
C_1	-222.992E-1	-885.337E-2	-207.483E-2	-251.721E-3
A_2	178.633E-3	-189.399E-4	-101.688E-5	360.1E-6
B_2	-100.328E-6	148.906E-6	257.452E-8	-600E-9
C_2	388.881E-2	160.916E-2	214.282E-4	-402.72E-5
A_3	-122.829E-4	135.242E-4	177.807E-7	-300E-9
B_3	0	-379.962E-7	-401.E-10	0
C_3	0	0	-297.791E-6	0
A_4	0	-117.687E-5	-748E-10	296.035E-11
B_4	105.499E-8	304.638E-8	167.028E-12	0
C_4	-429.827E-5	-583.074E-5	125.592E-8	-300E-9
A_5	0	940.018E3	0	0
B_5	0	-207.579E1	0	0
C_5	0	0	0	0
K	547.5E-2	4.2	459.996E-2	547.5E-2
u	0	101.554	0	0
C'	0	0	0	0
R	831.256E-5	831.369E-5	831.4E-5	831.4E-5
b	491.354E-4	107.961E-4	375.567E-6	0

Table (A.3) Martin-Hou equation of state constants

The second and third terms are obtained from the equation of state, described above, a follow;

$$i_2 = T \left[\frac{R}{mw} \ln(v-b) - \sum_{i=1}^4 \frac{B_i - C_i \left(\frac{K}{T_c} \right) \exp(-KT_r)}{i(v-b)^i} \right] \quad (\text{A.7})$$

$$\begin{aligned}
i_3 = & -\frac{RT}{mw} \ln(v-b) + \frac{RTb}{mw} + \frac{2(A_1 + B_1T + C_1 \exp(-KT_r))}{(v-b)} + \\
& \frac{2b(A_2 + B_2T + C_2 \exp(-KT_r)) + 3(A_3 + B_3T + C_3 \exp(-KT_r))}{2(v-b)^2} + \\
& \frac{3b(A_3 + B_3T + C_3 \exp(-KT_r)) + 4(A_4 + B_4T + C_4 \exp(-KT_r))}{3(v-b)^3} + \\
& \frac{4b(A_4 + B_4T + C_4 \exp(-KT_r)) + 5(A_5 + B_5T + C_5 \exp(-KT_r))}{4(v-b)^4} + \\
& \frac{5b(A_5 + B_5T + C_5 \exp(-KT_r))}{5(v-b)^5}
\end{aligned} \tag{A.8}$$

The specific enthalpy of vapour is calculated as follow;

$$i_v = i_1 + i_2 + i_3 + IC \tag{A.9}$$

where IC is the integration constant which is calculated from the specific enthalpy of vaporisation.

3 Density

The density or specific volume is used mainly in the calculation of pressure losses and vapour specific enthalpy. The liquid density is described in a polynomial fitted correlation as a function of the temperature. For the refrigerant R134a, the formula given in ICI (1994) data sheet has been used to calculate the liquid density. The equation suggested by ASHRAE (1986) has been used, with some modifications to match the equation used for R134a, to calculate the liquid density for the refrigerants R12 and R22. The liquid density for R12, R22 and R134a were calculated from the liquid temperature as follow;

$$\rho_l = a_0 + a_1H + a_2H^{1.5} + a_3H^2 + a_4H^3 + a_5H^4 + a_6H^6 \tag{A.10}$$

Where H is calculated from equation (A.3). However, for the refrigerant R407C, the polynomial curve fitted correlation, equation (A.2), given in ICI (1994) data sheet has been used to calculate the liquid density. The temperature in equation (A.3) is taken as the bulb point temperature for the refrigerant R407C. The constants for the liquid density equation are given in Table (A.4).

Refrigerant	R12	R22	R134a	R407C
a_0	558.084	524.764	528.1464	-650.458
a_1	854.469	875.159	755.1834	786.165E1
a_2	352.165	0	0	-153.123E2
a_3	0	588.661	1028.676	157.057E2
a_4	299.433	-357.092	-949.1172	-573.419E1
a_5	0	327.950	593.566	0
a_6	-504.828E-1	0	0	#

Table (A.4) coefficient of liquid density equations

The specific volume of superheated vapour is calculated using Maxwell relation from the Martin-Hou equation of state, Heikal (1990). For a given vapour pressure and temperature, the specific volume is calculated as follow;

$$v = \frac{RT}{p} \quad (\text{A.11})$$

$$F = p - \frac{RT}{v-B} - \sum_{i=1}^4 \frac{(A_i + B_i T + C_i \exp(-KT_r))}{(v-B)^{i+1}} - \frac{(A_5 + B_5 T + C_5 \exp(-KT_r))}{(1 + C' \exp(vu)) \exp(vu)} \quad (\text{A.12})$$

$$F' = \left. \frac{dF}{dv} \right|_{T,p} \quad (\text{A.13})$$

$$F' = \frac{RT}{(v-B)^2} + \sum_{i=1}^4 (i+1) \frac{(A_i + B_i T + C_i \exp(-KT_r))}{(v-B)^{i+2}} - \frac{(A_5 + B_5 T + C_5 \exp(-KT_r))}{(1 + C' \exp(vu)) \exp(vu)} \quad (\text{A.14})$$

$$v = v_{\text{initial}} - \frac{F}{F'} \quad (\text{A.15})$$

An initial value for the specific volume is assumed using the ideal gas equation, equation (A.11), then the new value, calculated from equation (A.15), is obtained through an iterative process to the accuracy of 0.0001 residual.

The specific volume of saturated vapour for the refrigerants R12, R22 and R134a is calculated using the superheated vapour sets of correlations. However for R407C, the equation given in ICI (1994) data sheet is used to calculate the density of saturated vapour. The polynomial fitted equation is based on the form used in equation (A.2) where the temperature in equation (A.3) is taken as the dew point temperature for the refrigerant R407C.

4 Specific heat capacity

The specific heat capacity at constant pressure is used mainly for the initial estimation of heat transfer rate, fluid capacity and effectiveness-Number of transfer units. In air to refrigerant heat exchangers, such as condensers and evaporators, the heat transfer analysis is carried out on the fluid with minimum fluid capacity, namely air. Therefore, accurate predictions of the specific heat capacity is not necessarily significant. The specific enthalpy of vapour is calculated using the ideal gas heat capacity, while the Effectiveness-Number of transfer units is calculated using the capacity rate ratio.

The saturated liquid and saturated vapour specific heat capacity values are given in ASHRAE Handbook (1993) for most of the refrigerants. A fifth order polynomial equation has been used to fit the tabulated data against the temperature. The resulting formulae have been used to calculate the value for the refrigerants R12, R22 and R134a from the vapour temperature based on equation (A.1). The coefficients for specific heat capacity at constant pressure, based on equation (A.1), are given in tables (A.5), (A.6) for saturated liquid and saturated vapour respectively. For the refrigerant R407C, no data were found for the subcooled and saturated liquid specific heat capacity. Therefore, the specific heat capacities at constant pressure were calculated from the specific enthalpy difference. The ideal gas heat capacity formula, given in ICI (1994) data sheet have been used to calculate the specific heat capacity of saturated vapour.

Refrigerant	R12	R22	R134a
a_0	928.971	117.271E1	891.489
a_1	185.02E-2	290.5E-2	444.81E-2
a_2	111.0E-4	181E-4	16E-4
a_3	496.1E-7	-838.1E-7	819E-7
a_4	164.6E-8	506.E-8	940.1E-8
a_5	151.9E-10	957.8E-10	728.9E-10

Table (A.5) Specific heat capacity at constant pressure coefficients for saturated liquid

Refrigerant	R12	R22	R134a
a_0	634.2437	747.254	133.618E1
a_1	238.23E-2	426.7E-2	329.2E-2
a_2	98E-4	223E-4	147.0E-4
a_3	970.7E-7	371.7E-6	-240.1E-6
a_4	248.1E-8	880.7E-8	432.1E-8
a_5	209.4E-10	563.1E-10	924.3E-10

Table (A.6) Specific heat capacity at constant pressure for saturated vapour coefficients

The specific heat capacity at constant pressure for superheated vapour is calculated assuming that the fluid is an ideal gas. The ideal gas heat capacity at constant pressure can be described as a function of the temperature as follow;

$$C_{p, Ideal} = I_1 + I_2T + I_3T^2 + I_4T^3 + \frac{I_5}{T^2} + I_6T^4 + \frac{I_7}{T} \quad (\text{A.16})$$

The coefficients given in ASHRAE (1986) for R12 and R22 and in DUPONT (1994) data sheet for R134a were used with some modifications while the coefficients given in ICI (1994) data sheet were used for the refrigerant R407C.

Table (A.7) coefficients for the ideal gas specific heat capacity at constant pressure, equation (A.16).

Refrigerant	R12	R22	R134a	R407C
I_1	338.894E-4	117.767E-3	190.146E-3	-838.430E-4
I_2	250.697E-5	169.970E-5	253.387E-5	321.516E-5
I_3	-327.445E-8	-883.030E-9	-127.085E-8	-194.062E-8
I_4	164.170E-11	0	0	0
I_5	0	332.536	0	0
I_6	0	0	0	0
I_7	0	0	0	363.565E-1
IC	270.469	310.367	168.169	30

Table (A.7) Coefficients for the ideal gas specific heat capacity at constant pressure

5 Thermal conductivity and viscosity

The thermal conductivities of the refrigerants are used in calculating the heat transfer coefficient through the Nusselt number correlation. The viscosity is used in calculating both the heat transfer coefficient and pressure losses through the Reynolds number and Prandtl number. A polynomial was fitted to the tabulated data given in ASHRAE (1993) for R12 and R22 at the saturation conditions. The fifth order polynomial equation given above, equation (A.1), was used to calculate the thermal conductivity and viscosity from the saturated temperature.

The equations given in ICI (1994) data sheet for R134a, for the thermal conductivity and viscosity of saturated liquid have been used based on equation (A.2). The thermal conductivity and viscosity of saturated vapour for the same refrigerant, taken from ICI (1994) data sheet, were calculated using equation (A.1). The formulas given in ICI (1994) data sheet for the refrigerant R407C was used to calculate the saturated liquid and saturated vapour thermal conductivity and viscosity as follow;

$$K_{lorV} = a_0 + a_1T + a_2T^2 + \frac{a_3}{T} \quad (A.17)$$

The mid point and the dew point temperatures were used with R407C for the saturated liquid and saturated vapour respectively.

The superheated vapour and subcooled liquid thermal conductivities were calculated assuming saturated conditions. In the case of superheated vapour for R407C the calculation was based on equation (A.1). The coefficients used with equations (A.1), (A.2) and (A.17) to calculate the liquid and vapour thermal conductivities are given in tables (A.8) and (A.9) respectively. The coefficients used with equations (A.1), (A.2) and (A.17) to calculate the liquid and vapour viscosities are given in tables (A.10) and (A.11) respectively.

Refrigerant	R12	R22	R134a	R407C
a_0	771.108 E-4	961.723E-4	785.73E-4	118.98E-3
a_1	-367.2E-6	-424.5E-6	-146.406E-3	0
a_2	169.4E-9	425.6E-9	265.347E-3	-671.955E-9
a_3	-146.0E-13	489.9E-12	0	903.994E-2
a_4	353.5E-14	-209.8E-13	0	0
a_5	0	-419.2E-15	0	0

Table (A.8) Liquid thermal conductivity

Refrigerant	R12	R22	R134a	R407C saturated	R407C superheated
a_0	857.47E-5	950.55E-5	-126.05E-4	425.38E-3	-355.65E-5
a_1	541.0E-7	608.0E-7	109.279E-6	-.00156445	358.48E-7
a_2	120.8E-9	-454.3E-10	-160.487E-9	208.498E-8	774.837E-10
a_3	120.4E-11	368.9E-12	303.615E-12	-385.464E-1	
a_4	-888.6E-16	226.3E-14	0		
a_5	0	435.2E-16	0		

Table (A.9) Vapour thermal conductivity

Refrigerant	R12	R22	R134a	R407C
a_0	257.737E-6	210.125E-6	-852.527 E-2	156.644E-1
a_1	-279.1E-8	-227.81E-8	298.469E1	-128.305E1
a_2	188.E-10	114E-10	-275.736E3	-615.04E-4
a_3	-715.7E-13	380.8E-14	0	581.907E-7
a_4	-118.2E-16	-775.2E-15	0	0
a_5	0	772.8E-17	0	0

Table (A.10) Liquid viscosity

Refrigerant	R12	R22	R134a	R407C saturated	R407C superheated
a_0	119.879E-7	118.0E-7	-498.811E-4	375.554E-6	-137.24E-8
a_1	514.E-10	4E-8	623.980E-6	-136.789E-8	535.9E-10
a_2	112.4E-12	-735.1E-17	-221.507E-8	177.845E-11	-153.12E-13
a_3	245.1E-14	-689.7E-19	282.25E-11	-333.749E-4	
a_4	108.4E-18	217.4E-19	0		
a_5	0	309.2E-21	0		

Table (A.11) Vapour viscosity

6 Saturated pressure and temperature

One equation was used to describe the saturated liquid and saturated vapour lines for the pure refrigerants R12, R22 and R134a. The saturation pressure was calculated from the saturation temperature based on equation given by ASHRAE (1986) for R12 and R22. The equation given in ICI (1994) data sheet for R134a was used with some modification, to match that used, found in ASHRAE, to calculate the saturation pressure. The formula used to calculate the saturation pressure for R12, R22 and R134a from the saturation temperature is:

$$\begin{aligned} \text{Log}(p) = & a_0 + \frac{a_1}{T} + \frac{a_2}{T^2} + a_3 \text{Log}(T) + a_4 T + a_5 T^2 + a_6 T^3 + \\ & a_7 \left(\frac{a_8 - T}{T} \right) \text{Log}((a_8 - T)a_9) \end{aligned} \quad (\text{A.18})$$

No equations were found for the saturated temperatures. Therefore, a fifth order polynomial equation was used to correlate the tabulated data given in ASHRAE (1993). However, the resulting equation produced large inaccuracies. This has been overcome through use of an iteration process. The coefficients for equation (A.18) are given in table (A.12).

Refrigerant	R12	R22	R134a
a_0	345.386E-1	251.893E-1	406.988E-1
a_1	-190.924E1	-213.621E1	-236.254E1
a_2	0	0	0
a_3	-124.715E-1	-786.103E-2	-130.688E-1
a_4	851.479E-5	394.369E-5	761.600E-5
a_5	0	0	0
a_6	0	0	0
a_7	0	445.746E-3	234.256E-3
a_8	500	381.166	376.111
a_9	18E-1	18E-1	1

Table (A.12) Saturation pressure

The saturation temperatures were estimated using equation (A.1), where the coefficients are given in table (A.13).

Refrigerant	R12	R22	R134a
a_0	-46.7856	-54.2465	-43.8835
a_1	189.7898	154.4898	187.2723
a_2	-162.757	-112.9977	-169.9693
a_3	79.1813	46.0326	85.4248
a_4	-18.3749	-8.8756	-20.3291
a_5	1.5987	.6394	1.8083

Table (A.13) Saturation temperature

Three different equations were used to describe the bubble point temperatures, mid point temperatures and dew point temperatures for refrigerant mixtures, such as

R407C. The equations given in ICI (1994) data sheet for R407C were used to calculate these temperatures from the saturation pressure as follows;

$$T_{B \text{ or } M \text{ or } D} = a_0 + a_1H + a_2H^2 + a_3H^3 \quad (\text{A.19})$$

$$H = \text{Ln}(p_{\text{saturation}}) \quad (\text{A.20})$$

The coefficients of equation (A.19) are given in table (A.14).

Refrigerant	Bubble point	Mid point	Dew point
a_0	228.9073	232.490	236.0528
a_1	209.983E-1	206.426E-1	203.760E-1
a_2	185.538E-2	204.796E-2	217.732E-2
a_3	377.83 E-3	308.296E-3	250.429 E-3

Table (A.14) R407C bubble point, mid point and dew point temperatures

The saturation pressure was correlated accurately from the tabulated data given in ICI (1994) data sheet for R407C. The resulting formula, based on equation (A.1), calculates the saturation pressure from the dew point temperature.

Refrigerant	R407C
a_0	-228.230222
a_1	417.366E-2
a_2	-305.522E-4
a_3	113.412E-6
a_4	-219.851E-9
a_5	187.3356E-12

Table (A.15) Saturation pressure for R407C

Appendix B

PROGRAM LISTINGS

- 1 The program written in Quick Basic for monitoring the thermal wind tunnel tests and analysing the results (THERMAL.BAS). **B-1**

- 2 The program written in Visual Basic for simulating the condensers performance (CONDENSE.BAS). **B-16**

- 3 The program written in Visual Basic for simulating the evaporator performance (EVAPORAT.BAS). **B-46**

- 4 The program written in Visual Basic for calculating the refrigerants properties (FORMULA.BAS). **B-60**

- 5 The program written in Visual Basic for calculating the properties of air and water (FUNCTION.BAS). **B-65**

[THERMAL.BAS]

' THERMTUN.BAS

' To run thermal wind tunnel

' for cold & hot test

' By Mahmoud Abu-Madi

' 1997

```

DECLARE SUB CalcHTC (Option$, BP, TAI, taO, AV, PD, airen, twi, two, Q, waten, bal, ACp,
ACon, AVis, ADenIn, WDen, WCp, WVis, WCon)
DECLARE SUB CalcPDC (Option$, BP, TAI, AV, PD)
DECLARE SUB CalcVelIne (Option$, BP, TAI, AV)
DECLARE SUB Calibrate (Option$, DTWVI, DTAVI, VVHI, VVLI, PDVHI, PDVLI, BP, Sample$,
TestNo$, NoColdRun)
DECLARE SUB ConRead (A$())
DECLARE SUB ConSet (A$())
DECLARE SUB Contenuie ()
DECLARE SUB DisplyResultHTC (TAI, AV, taO, PD, airen, twi, two, Q, waten, bal)
DECLARE SUB DisplyResultPDC (TAI, AV, PD)
DECLARE SUB DisplyTable (Option$)
DECLARE SUB HighPD (PD1, PD2, PD)
DECLARE SUB HighVel (V1, V2, ADenIn, AV)
DECLARE SUB Logger (KeyInput$, modeminput$)
DECLARE SUB LoggerRead (Option$, A$(), B())
DECLARE SUB LowPD (PD3, PD4, PD)
DECLARE SUB LowVel (V3, V4, ADenIn, AV)
DECLARE SUB Main (Option$)
DECLARE SUB ShowRes (Sample$, TestNo$, BP, NoHotRun, NoColdRun, NoOutHot, NoOutCold,
OutptHot(), OutptCold())
DECLARE SUB StrtColdT (Option$, Sample$, TestNo$, BP, VVLI, VVHI, PDVLI, PDVHI,
DTWVI, DTAVI, NoColdRun)
DECLARE SUB StrtHotT (Option$, Sample$, TestNo$, BP, VVLI, VVHI, PDVLI, PDVHI,
DTWVI, DTAVI, NoColdRun)
DECLARE SUB STim (T%)
DECLARE SUB Stor (Sample$, TestNo$, BP, NoHotRun, NoColdRun, NoOutHot, NoOutCold,
OutptHot(), OutptCold())
DECLARE SUB StorCalib (NoOutCalb, Sample$, TestNo$, InitialVolt())
DECLARE SUB TableOfCalib (Sample$, TestNo$, BP, VVLI, VVHI, PDVLI, PDVHI, DTWVI,
DTAVI, CHANGCALB)
DECLARE FUNCTION FunACp (T)
DECLARE FUNCTION FunADen (T, B)
DECLARE FUNCTION FunAThermal (T)
DECLARE FUNCTION FunAVis (T)
DECLARE FUNCTION FunTemp (v)
DECLARE FUNCTION FunWCp (T)
DECLARE FUNCTION FunWDen (T)
DECLARE FUNCTION FunWThermal (T)
DECLARE FUNCTION FunWVis (T)
DIM SHARED A$(10), B(10), C(500), Q(500), OutptHot(40, 40), OutptCold(30, 30), InitialVolt(9)
DIM SHARED DTWVI, DTAVI, VVHI, VVLI, PDVHI, PDVLI, CON(14), Sample$, ADenIn

1 CALL Main(Option$)
  IF Option$ = "2" THEN
    CALL StrtColdT(Option$, Sample$, TestNo$, BP, VVLI, VVHI, PDVLI, PDVHI, DTWVI,
DTAVI, NoColdRun)
    CALL TableOfCalib(Sample$, TestNo$, BP, VVLI, VVHI, PDVLI, PDVHI, DTWVI, DTAVI,
CHANGCALB)
    IF CHANGCALB = 10 THEN GOTO 1
  
```

```

CLS
LOCATE 10, 15
PRINT " Now left the cover and switch on the fan "
CALL Contenuc
ELSEIF Option$ = "3" THEN
  CALL StatrHotT(Option$, Sample$, TestNo$, BP, VVLI, VVHI, PDVLI, PDVHI, DTWVI,
DTAVI, NoColdRun)
  CALL TableOfCalib(Sample$, TestNo$, BP, VVLI, VVHI, PDVLI, PDVHI, DTWVI, DTAVI,
CHANGCALB)
  IF CHANGCALB = 10 THEN GOTO 1
  CLS
  LOCATE 10, 15
  PRINT " Now lift the cover and switch on the fan"
  CALL Contenuc
ELSEIF Option$ = "1" THEN
  DO
    CLS
    LOCATE 4, 30
    PRINT "Warning "
    LOCATE 6, 25
    PRINT "ARE YOU SURE ? Y/N"
    LOCATE 21, 35
    LINE INPUT OptREST$
    LOOP UNTIL OptREST$ = "Y" OR OptREST$ = "N"
    IF OptREST$ = "Y" THEN
      VVLI = 0: VVHI = 0: PDVLI = 0: PDVHI = 0: DTAVI = 0: DTWVI = 0
      Sample$ = "": TestNo$ = "": BP = 0: NoColdRun = 0: NoHotRun = 0
      FOR I = 1 TO 7
        InitialVolt(I) = 0
      NEXT I
    END IF
    GOTO 1
  ELSEIF Option$ = "4" THEN
    CALL ShowRes(Sample$, TestNo$, BP, NoHotRun, NoColdRun, NoOutHot, NoOutCold,
OutptHot(), OutptCold())
    GOTO 1
  ELSE
    END
  END IF
2 CLS
TAIa = 0: TAOa = 0: AVa = 0: PDa = 0: AirEna = 0: TWIa = 0
TWOa = 0: Qa = 0: WatEna = 0: Bala = 0
ACpa = 0: ACona = 0: AVisa = 0: ADenina = 0
WDena = 0: WCpa = 0: WVisa = 0: WCona = 0
CALL DisplyTable(Option$)
' TO DISPLAY AIR VELOCITY ONLY
IF Option$ = "3" THEN Option$ = "13"
IF Option$ = "2" THEN Option$ = "12"
DO
  CALL CalcVelIne(Option$, BP, TAI, AV)
  CALL DisplyResultPDC(TAI, AV, 0)
  FullScreen$ = INKEY$
LOOP UNTIL FullScreen$ = "F"
IF Option$ = "13" THEN Option$ = "3"
IF Option$ = "12" THEN Option$ = "2"
' TO DISPLAY FULL SCREEN
DO
  IF Option$ = "3" THEN ' Heat Transfer test

```

```

CALL CalcHTC(Option$, BP, TAI, taO, AV, PD, airen, twi, two, Q, waten, bal, ACp, ACon,
AVis, ADenIn, WDen, WCp, WVis, WCon)
CALL DisplyResultHTC(TAI, AV, taO, PD, airen, twi, two, Q, waten, bal)
ELSE ' Pressure Drop test
CALL CalcPDC(Option$, BP, TAI, AV, PD)
CALL DisplyResultPDC(TAI, AV, PD)
END IF
MenuOrAve$ = INKEY$
LOOP UNTIL MenuOrAve$ = "M" OR MenuOrAve$ = "A"
IF MenuOrAve$ = "M" THEN
CALL TableOfCalib(Sample$, TestNo$, BP, VVLI, VVHI, PDVLI, PDVHI, DTWVI, DTAVI,
CHANGCALB)
IF CHANGCALB = 10 THEN
GOTO 1
ELSE
GOTO 2
END IF
ELSE ' averaging results
IF Option$ = "3" THEN ' Heat Transfer test
FOR I% = 1 TO 5
CALL CalcHTC(Option$, BP, TAI, taO, AV, PD, airen, twi, two, Q, waten, bal, ACp, ACon,
AVis, ADenIn, WDen, WCp, WVis, WCon)
TAIa = TAIa + TAI: TAOa = TAOa + taO: AVa = AVa + AV
PDa = PDa + PD: AirEna = AirEna + airen: TWIa = TWIa + twi
TWOa = TWOa + two: Qa = Qa + Q: WatEna = WatEna + waten
Bala = Bala + bal: ACpa = ACpa + ACp: ACona = ACona + ACon
AVisa = AVisa + AVis: ADenina = ADenina + ADenIn: WDena = WDen + WDen
WCpa = WCpa + WCp: WVisa = WVisa + WVis: WCona = WCona + WCon
LOCATE 21, 30: PRINT " Averaging the results"
LOCATE 22, 40: PRINT I% * 20; "%"
CALL DisplyResultHTC(TAI, AV, taO, PD, airen, twi, two, Q, waten, bal)
NEXT I%
TAI = TAIa / 5: taO = TAOa / 5: AV = AVa / 5: PD = PDa / 5
airen = AirEna / 5: twi = TWIa / 5: two = TWOa / 5: Q = Qa / 5
waten = WatEna / 5: bal = Bala / 5
CALL DisplyResultHTC(TAI, AV, taO, PD, airen, twi, two, Q, waten, bal)
ELSE ' Pressure Drop test
FOR I% = 1 TO 5
CALL CalcPDC(Option$, BP, TAI, AV, PD)
TAIa = TAIa + TAI: AVa = AVa + AV: PDa = PDa + PD
LOCATE 21, 30: PRINT " Averaging the results"
LOCATE 22, 40: PRINT I% * 20; "%"
CALL DisplyResultPDC(TAI, AV, PD)
NEXT I%
TAI = TAIa / 5: AV = AVa / 5: PD = PDa / 5
CALL DisplyResultPDC(TAI, AV, PD)
END IF
CALL Contenuue
DO
CLS
LOCATE 10, 15
PRINT " Do you want to store the data Y/N ....."
LOCATE 16, 35
LINE INPUT ST$
LOOP UNTIL ST$ = "Y" OR ST$ = "N"
IF ST$ = "N" THEN
CALL TableOfCalib(Sample$, TestNo$, BP, VVLI, VVHI, PDVLI, PDVHI, DTWVI, DTAVI,
CHANGCALB)

```

```

IF CHANGCALB = 10 THEN
  GOTO 1
ELSE
  GOTO 2
END IF
ELSE
  IF Option$ = "3" THEN    ' Heat Transfer test
    NoHotRun = NoHotRun + 1
    OutptHot(NoHotRun, 1) = TAI: OutptHot(NoHotRun, 2) = taO: OutptHot(NoHotRun, 3) =
AV
    OutptHot(NoHotRun, 4) = PD: OutptHot(NoHotRun, 5) = airen: OutptHot(NoHotRun, 6) =
twi
    OutptHot(NoHotRun, 7) = two: OutptHot(NoHotRun, 8) = Q: OutptHot(NoHotRun, 9) =
waten
    OutptHot(NoHotRun, 10) = bal: OutptHot(NoHotRun, 11) = ACp: OutptHot(NoHotRun, 12)
= ACon
    OutptHot(NoHotRun, 13) = AVis: OutptHot(NoHotRun, 14) = ADenIn: OutptHot(NoHotRun,
15) = WDen
    OutptHot(NoHotRun, 16) = WCp: OutptHot(NoHotRun, 17) = WVis: OutptHot(NoHotRun,
18) = WCon
    NoOutHot = 18
  ELSE                      ' Pressure Drop test
    NoColdRun = NoColdRun + 1
    OutptCold(NoColdRun, 1) = TAI: OutptCold(NoColdRun, 2) = AV: OutptCold(NoColdRun,
3) = PD
    NoOutCold = 3
  END IF
  CALL Stor(Sample$, TestNo$, BP, NoHotRun, NoColdRun, NoOutHot, NoOutCold,
OutptHot(), OutptCold())
  END IF
  CALL TableOfCalib(Sample$, TestNo$, BP, VVLI, VVHI, PDVLI, PDVHI, DTWVI, DTAVI,
CHANGCALB)
  IF CHANGCALB = 10 THEN
    GOTO 1
  ELSE
    GOTO 2
  END IF
END IF

```

```

SUB CalcHTC (Option$, BP, TAI, taO, AV, PD, airen, twi, two, Q, waten, bal, ACp, ACon, AVis,
ADenIn, WDen, WCp, WVis, WCon)
  CALL LoggerRead(Option$, A$, B())
  twi = B(8)
  DTWV = (B(9) - DTWVI) / 4
  DTW = FunTemp(DTWV)
  two = twi - DTW
  DTWA = FunTemp(B(10))
  TAI = twi - DTWA
  DTAV = (B(7) - DTAVI) / 9
  DTA = FunTemp(DTAV)
  taO = TAI + DTA
  TWa = (twi + two) / 2
  TAa = (TAI + taO) / 2
  ADenIn = FunADen(TAI, BP)
  ADenO = FunADen(taO, BP)
  ADenA = FunADen(TAa, BP)
  ACp = FunACp(TAa)
  AVis = FunAVis(TAa)

```

```

ACon = FunAThermal(TAa)
WVis = FunWVis(twi)
WDen = FunWDen(twi)
WCp = FunWCp(TWa)
WCon = FunWThermal(TWa)
IF B(2) > .063 THEN
  CALL HighVel(B(2), VVHI, ADenIn, AV)
ELSE
  CALL LowVel(B(1), VVLI, ADenIn, AV)
END IF
AMFR = AV * ADenIn * .023226      ' air mass flow rate
airen = AMFR * ACp * DTA
PW = B(5) * 5.744 - 91.912
I% = 0
C(I%) = .6053
3 Q(I%) = SQR(133.333 * PW * 2 * WDen) * C(I%) * 4.37635E-04
I% = I% + 1
C(I%) = C(0) + 1.723 * (WVis / Q(I% - 1)) ^ .75
IF ABS(C(I%) - C(I% - 1)) > .001 THEN GOTO 3
Q = Q(I% - 1)
waten = Q * DTW * WCp
bal = (waten - airen) * 100 / airen
IF B(4) > .089 THEN
  CALL HighPD(B(4), PDVHI, PD)
ELSE
  CALL LowPD(B(3), PDVLI, PD)
END IF
END SUB

```

```

SUB CalcPDC (Option$, BP, TAI, AV, PD)
  CALL LoggerRead(Option$, A$, B())
  TAI = B(6)
  ADenIn = FunADen(TAI, BP)
  ACp = FunACp(TAI)
  AVis = FunAVis(TAI)
  IF B(2) > .063 THEN
    CALL HighVel(B(2), VVHI, ADenIn, AV)
  ELSE
    CALL LowVel(B(1), VVLI, ADenIn, AV)
  END IF
  IF B(4) > .089 THEN
    CALL HighPD(B(4), PDVHI, PD)
  ELSE
    CALL LowPD(B(3), PDVLI, PD)
  END IF
END SUB

```

```

SUB CalcVelIne (Option$, BP, TAI, AV)
  CALL LoggerRead(Option$, A$, B())
  TAI = B(6)
  ADenIn = FunADen(TAI, BP)
  IF B(2) > .063 THEN
    CALL HighVel(B(2), VVHI, ADenIn, AV)
  ELSE
    CALL LowVel(B(1), VVLI, ADenIn, AV)
  END IF
END SUB

```

SUB Calibrate (Option\$, DTWVI, DTAVI, VVHI, VVLI, PDVHI, PDVLI, BP, Sample\$, TestNo\$, NoColdRun)

' to set the data logger

IF NoColdRun > 0 THEN GOTO 4

CLS

COLOR 5, 7

LOCATE 5, 20

PRINT " Do not switch on the fan"

LOCATE 7, 20

PRINT " Close all the openings of the tunnel"

CALL Contenu

COLOR 5

LOCATE 4, 30

PRINT "System calibration"

LOCATE 6, 26

PRINT "The process will take 5 minutes"

CALL ConSet(A\$())

' set logger

FOR I = 1 TO 10

CHAN\$ = A\$(I)

OPEN "COM1:9600,N,8,1,OP,CD0,DS0,CS0" FOR RANDOM AS #1 LEN = 256

PRINT #1, CHAN\$

SLEEP 2

CLOSE

NEXT I

CALL STim(120)

CALL ConRead(A\$())

' calibrate velocity and pressure Transducer

DTWVI = 0: DTAVI = 0

VVHI = 0: VVLI = 0: PDVHI = 0: PDVLI = 0

FOR J% = 1 TO 20

FOR I = 1 TO 4

CHAN\$ = A\$(I)

CALL Logger(CHAN\$, RED\$)

B(I) = VAL(RED\$)

NEXT I

COLOR 4

LOCATE 11, 22: PRINT "VVLI="; B(1): VVLI = VVLI + B(1)

LOCATE 13, 22: PRINT "VVHI="; B(2): VVHI = VVHI + B(2)

LOCATE 15, 22: PRINT "PDVLI="; B(3): PDVLI = PDVLI + B(3)

LOCATE 17, 22: PRINT "PDVHI="; B(4): PDVHI = PDVHI + B(4)

NEXT J%

VVLI = VVLI / 20

VVHI = VVHI / 20

PDVLI = PDVLI / 20

PDVHI = PDVHI / 20

LOCATE 11, 22: PRINT "Average VVLI="; VVLI

LOCATE 13, 22: PRINT "Average VVHI="; VVHI

LOCATE 15, 22: PRINT "Average PDVLI="; PDVLI

LOCATE 17, 22: PRINT "Average PDVHI="; PDVHI

InitialVolt(1) = VVLI

InitialVolt(2) = VVHI

InitialVolt(3) = PDVLI

InitialVolt(4) = PDVHI

LOCATE 19, 22

PRINT " Calibration finished"

4 CALL Contenu

IF Option\$ = "3" THEN ' hot test

```

CLS
COLOR 5
LOCATE 5, 20
PRINT " Now switch on the axial fan and open "
LOCATE 7, 20
PRINT " the tunnel entrance and exit fully "
PRINT
CALL Contenu
COLOR 5
LOCATE 4, 30
PRINT "System calibration"
PRINT
PRINT "          The process will take 5 minutes"
CALL STim(150)
' calibrate air temperature difference
DTAVI = 0
FOR J% = 1 TO 20
  CHAN$ = A$(7)
  CALL Logger(CHAN$, RED$)
  B(7) = VAL(RED$)
  COLOR 4
  LOCATE 14, 22: PRINT "DTAVI="; B(7): DTAVI = DTAVI + B(7)
NEXT J%
DTAVI = DTAVI / 20
LOCATE 14, 22: PRINT "Average DTAVI="; DTAVI
InitialVolt(5) = DTAVI
LOCATE 21, 22
PRINT " Calibration finished"
CALL Contenu
COLOR 5
LOCATE 2, 15
PRINT "  Second stage calibration finished "
LOCATE 4, 15
PRINT "  Now flood the sample with hot water"
LOCATE 6, 15
PRINT "  Switch off the fan"
LOCATE 8, 15
PRINT "  Close the entrance and exit, and turn the pump on "
PRINT
CALL Contenu
COLOR 5
LOCATE 4, 30
PRINT "System calibration"
PRINT
PRINT "          The process will take 20 minutes"
CALL STim(900)
' calibrate water temperature difference
DTWVI = 0
FOR J% = 1 TO 20
  CHAN$ = A$(9)
  CALL Logger(CHAN$, RED$)
  B(9) = VAL(RED$)
  COLOR 4
  LOCATE 14, 22: PRINT "DTWVI="; B(9): DTWVI = DTWVI + B(9)
NEXT J%
DTWVI = DTWVI / 20
LOCATE 14, 22: PRINT "Average DTWVI="; DTWVI
InitialVolt(6) = DTWVI

```



```

END IF
LOCATE 16, 22
PRINT " Calibration finished"
IF NoColdRun > 0 THEN GOTO 5
LOCATE 18, 22
INPUT " Enter Sample Name           "; Sample$
LOCATE 19, 22
INPUT " Enter test number           "; TestNo$
LOCATE 20, 22
INPUT " Enter Barometric Pressure in mm Hg ", BP
TestNo = VAL(TestNo$)
InitialVolt(7) = BP           ' Barometric Pressure
5 NoOutCalb = 7
CALL StorCalib(NoOutCalb, Sample$, TestNo$, InitialVolt())
END SUB

```

```

SUB ConRead (A$())
' set the Units
A$(1) = "0V1": A$(2) = "0V2": A$(3) = "0V3": A$(4) = "0V4"
A$(5) = "0D1": A$(6) = "0D2": A$(7) = "0D3": A$(8) = "0D4"
A$(9) = "0D5": A$(10) = "0D6"
' B(1) = Low Air Velocity           0V1
' B(2) = High Air Velocity          0V2
' B(3) = Low Pressure Drop          0V3
' B(4) = High Pressure Drop         0V4
' B(5) = Water Flow Rate            0D1
' B(6) = Air Temperature In         0D2
' B(7) = Air Temperature Difference 0D3
' B(8) = Water Temperature In       0D4
' B(9) = Water Temperature Difference 0D5
' B(10) = Water-Air Temperature Difference 0D6
END SUB

```

```

SUB ConSet (A$())
' set the Format the Number of Decimal places
A$(1) = "0V1ZR:GR:M=D:R=H:F=69": A$(2) = "0V2ZR:GR:M=D:R=H:F=69"
A$(3) = "0V3ZR:GR:M=D:R=H:F=69": A$(4) = "0V4ZR:GR:M=D:R=H:F=69"
A$(5) = "0D1ZR:GR:M=D:R=L:F=49": A$(6) = "0D2ZR:GR:M=K:R=L:F=49"
A$(7) = "0D3ZR:GR:M=D:R=H:F=49": A$(8) = "0D4ZR:GR:M=K:R=L:F=49"
A$(9) = "0D5ZR:GR:M=D:R=L:F=49": A$(10) = "0D6ZR:GR:M=D:R=L:F=49"
END SUB

```

```

SUB Contenuc
DO
LOCATE 23, 22
COLOR 2
PRINT " Press space bar to continue ....."
LOOP UNTIL INKEY$ = CHR$(32)
CLS
END SUB

```

```

SUB DisplyResultHTC (TAI, AV, taO, PD, airen, twi, two, Q, waten, bal)
COLOR 4
LOCATE 7, 35: PRINT TAI; "           "
LOCATE 8, 35: PRINT AV; "           "
LOCATE 9, 35: PRINT taO; "          "
LOCATE 10, 35: PRINT PD; "          "
LOCATE 11, 35: PRINT airen; "         "

```

```

LOCATE 13, 35: PRINT twi; "          "
LOCATE 14, 35: PRINT two; "         "
LOCATE 15, 35: PRINT Q; "          "
LOCATE 16, 35: PRINT waten; "       "
LOCATE 17, 35: PRINT bal; "         "
END SUB

SUB DisplyResultPDC (TAI, AV, PD)
  COLOR 4
  LOCATE 7, 35: PRINT TAI; "        "
  LOCATE 8, 35: PRINT AV; "         "
  LOCATE 9, 35: PRINT PD; "         "
END SUB

SUB DisplyTable (Option$)
  CLS
  COLOR 5
  PRINT
  IF Option$ = "3" THEN
    LOCATE 4, 30
    PRINT "HOT TEST"
    PRINT : PRINT
    PRINT " Inlet air temp. (C) = "
    PRINT " Air velocity (m/s) = "
    PRINT " Outlet air temp. (C) = "
    PRINT " Air pressure drop (mm H2O)= "
    PRINT " Air energy (W) = "
    PRINT
    PRINT " Inlet water temp. (C) = "
    PRINT " Outlet water temp.(C) = "
    PRINT " Water flow rate (kg/s) = "
    PRINT " Water energy (W) = "
    PRINT " Balance (%) = "
  ELSE
    LOCATE 4, 30
    PRINT "COLD TEST"
    PRINT : PRINT
    PRINT " Inlet air temp. (C) = "
    PRINT " Air velocity (m/s) = "
    PRINT " Air pressure drop (mm H2O)= "
  END IF
  LOCATE 19, 20: PRINT "(A) "; "FOR AVERAGING , "; "(M) "; "FOR MENU , OR"
  LOCATE 20, 25: PRINT "(F) "; "FOR FULL MENU"
END SUB

FUNCTION FunACp (T)
  ' FUNCTION TO CALCULATE THE AIR SPECIFIC HEAT in J/kgK from T in 'C
  FunACp = (1.00401 + .0000147071# * T + 5.247691E-07 * T ^ 2 - 3.96964E-10 * T ^ 3 -
5.42824E-15 * T ^ 4) * 1000
END FUNCTION

FUNCTION FunADen (T, B)
  ' FUNCTION TO CALCULATE THE AIR DENSITY in kg/m3 from T in 'C and B in mmHg
  FunADen = .4642 * B / (273.15 + T)
END FUNCTION

FUNCTION FunAThermal (T)
  ' FUNCTION TO CALCULATE THE AIR THERMAL CONDUCTIVITY in W/mK from T in 'C

```

```

FunAThermal = .00229 + .00008 * (T + 273.15)
END FUNCTION

```

```

FUNCTION FunAVis (T)
' FUNCTION TO CALCULATE THE AIR VISCOSITY in Pa s from T in 'C
FunAVis = (1.71621 + .00493372# * T - 3.90801E-06 * T ^ 2 + 3.552622E-09 * T ^ 3 - 1.62902E-
12 * T ^ 4) * 10 ^ (-5)
END FUNCTION

```

```

FUNCTION FunTemp (v)
' FUNCTION TO CONVERT THE TEMPERATURE FROM VOLT TO 'C
FunTemp = .020307 + 25.313 * v - .37915 * v ^ 2 + .038239 * v ^ 3
END FUNCTION

```

```

FUNCTION FunWCp (T)
' FUNCTION TO CALCULATE THE WATER SPECIFIC HEAT in J/kgK from T in 'C
FunWCp = 4213.46 - 2.4711 * T + .057686 * T ^ 2 - .00052186# * T ^ 3 + .0000019724# * T ^ 4
END FUNCTION

```

```

FUNCTION FunWDen (T)
' FUNCTION TO CALCULATE THE WATER DENSITY in kg/m3 from T in 'C
FunWDen = 999.85 + .05214 * T - .007619 * T ^ 2 + .00004367# * T ^ 3 - 1.444E-07 * T ^ 4
END FUNCTION

```

```

FUNCTION FunWThermal (T)
' FUNCTION TO CALCULATE THE water THERMAL CONDUCTIVITY in W/mK from T in 'C
FunWThermal = .56197 + .0021233 * T - 1.1101E-05 * T ^ 2 - 4.556E-08 * T ^ 3 + 1.2236E-09 *
T ^ 4 - 6.3079E-12 * T ^ 5
END FUNCTION

```

```

FUNCTION FunWVis (T)
' FUNCTION TO CALCULATE THE WATER VISCOSITY in Pa s from T in 'C
FunWVis = .0017908 - 5.9282E-05 * T + 1.2919E-06 * T ^ 2 - 1.7531E-08 * T ^ 3 + 1.289E-10 *
T ^ 4 - 3.8535E-13 * T ^ 5
END FUNCTION

```

```

SUB HighPD (PD1, PD2, PD)
PD = 250 * (PD1 - PD2) ' [mm H2O] PDVH - PDVHI MANUFACTURER
END SUB

```

```

SUB HighVel (V1, V2, ADenIn, AV)
' CONVERT HIGH VELOCITY
VV = V1 - V2 ' VVH - VVHI
AV = SQR(2 * 187.75 * VV / ADenIn) / 1.0223 ' OLD CALIB
END SUB

```

```

SUB Logger (KeyInput$, modeminput$)
' to communicate with data logger
OPEN "COM1:9600,N,8,1,OP,CD0,DS0,CS0" FOR RANDOM AS #1 LEN = 256
PRINT #1, KeyInput$
SLEEP 1
IF NOT EOF(1) THEN
modeminput$ = INPUT$(LOC(1), #1)
END IF
CLOSE
END SUB

```

```

SUB LoggerRead (Option$, A$(), B())

```

```

' to read from the data logger all parameters
IF Option$ = "12" OR Option$ = "13" THEN ' VELOCITY ONLY
  CHAN$ = "0V1"
  CALL Logger(CHAN$, RED$)
  B(1) = VAL(RED$)
  CHAN$ = "0V2"
  CALL Logger(CHAN$, RED$)
  B(2) = VAL(RED$)
  CHAN$ = "0D2"
  CALL Logger(CHAN$, RED$)
  B(6) = VAL(RED$)
ELSE
  CALL ConRead(A$())          ' set units
  IF Option$ = "3" THEN
    Limit = 10                ' heat transfer channels to be read
  ELSE
    Limit = 6                  ' pressure drop channels to be read
  END IF
  FOR I = 1 TO Limit
    CHAN$ = A$(I)
    CALL Logger(CHAN$, RED$)
    B(I) = VAL(RED$)
  NEXT I
END IF
END SUB

SUB LowPD (PD3, PD4, PD)
  PD = -.00762 + 20.0857 * (PD3 - PD4) ' [mm H2O] MANUFACTURER
END SUB

SUB LowVel (V3, V4, ADenIn, AV)
  ' CONVERT LOW AND MEDIUM VELOCITY
  VV = V3 - V4 ' VVM - VVLI
  AV = SQR(2 * 28.515 * VV / ADenIn) / 1.0223 ' OLD CALIB
END SUB

SUB Main (Option$)
  DO
    CLS
    SCREEN 9
    COLOR 5, 7
    LOCATE 4, 30
    PRINT "Main Menu"
    PRINT : PRINT
    PRINT "      1. Reset all parameters"
    PRINT
    PRINT "      2. The Cold Test"
    PRINT
    PRINT "      3. The Hot Test"
    PRINT
    PRINT "      4. Show The Results On The Screen"
    PRINT
    PRINT "      5. End"
    LOCATE 21, 35
    LINE INPUT Option$
  LOOP UNTIL Option$ = "1" OR Option$ = "2" OR Option$ = "3" OR Option$ = "4" OR Option$
= "5"
END SUB

```

```
SUB ShowRes (Sample$, TestNo$, BP, NoHotRun, NoColdRun, NoOutHot, NoOutCold, OutptHot(),
OutptCold())
```

```
' TO SHOW STORED RESULTS ON SCREEN
```

```
NoOutCold = 3
```

```
NoOutHot = 18
```

```
DIM Filenum AS INTEGER
```

```
filename$ = "c:\T" + TestNo$ + ".RES"
```

```
Filenum% = FREEFILE
```

```
OPEN filename$ FOR INPUT AS Filenum%
```

```
INPUT #Filenum%, NoColdRun, NoHotRun, TIM$, DAT$, Sample$, TestNo$, BP
```

```
IF NoColdRun > 0 THEN
```

```
FOR K = 1 TO NoColdRun
```

```
INPUT #Filenum%, L$ ' space
```

```
FOR I = 1 TO NoOutCold
```

```
INPUT #Filenum%, OutptCold(K, I)
```

```
NEXT I
```

```
NEXT K
```

```
INPUT #Filenum%, L$ ' space
```

```
END IF
```

```
IF NoHotRun > 0 THEN
```

```
FOR K = 1 TO NoHotRun
```

```
INPUT #Filenum%, L$ ' space
```

```
FOR I = 1 TO NoOutHot
```

```
INPUT #Filenum%, OutptHot(K, I)
```

```
NEXT I
```

```
NEXT K
```

```
END IF
```

```
CLOSE Filenum%
```

```
' To print RESULTS on the screen
```

```
CLS
```

```
PRINT NoColdRun; "/"; NoHotRun; "/"; TIM$; "/"; DAT$; "/"; Sample$; "/"; TestNo$; "/"; BP
```

```
PRINT ' space
```

```
FOR K = 1 TO NoColdRun
```

```
FOR I = 1 TO NoOutCold
```

```
PRINT OutptCold(K, I); "/";
```

```
IF I = 5 THEN PRINT
```

```
NEXT I
```

```
NEXT K
```

```
IF NoColdRun > 0 AND NoHotRun > 0 THEN
```

```
INPUT SSS
```

```
CLS
```

```
END IF
```

```
FOR K = 1 TO NoHotRun
```

```
FOR I = 1 TO NoOutHot
```

```
PRINT OutptHot(K, I); "/";
```

```
IF I = 28 THEN PRINT
```

```
NEXT I
```

```
NEXT K
```

```
INPUT SSS
```

```
END SUB
```

```
SUB StatrColdT (Option$, Sample$, TestNo$, BP, VVLI, VVHI, PDVLI, PDVHI, DTWVI, DTAVI,
NoColdRun)
```

```
DO
```

```
CLS
```

```
LOCATE 4, 30
```

```
PRINT "Pressure Drop Test"
```

```

PRINT : PRINT
PRINT "      1. Calibrate "
PRINT
PRINT "      2. Start The Test"
LOCATE 21, 35
LINE INPUT Optcol$
LOOP UNTIL Optcol$ = "1" OR Optcol$ = "2"
IF Optcol$ = "1" THEN
    CALL Calibrate(Option$, DTWVI, DTAVI, VVHI, VVLI, PDVHI, PDVLI, BP, Sample$,
TestNo$, NoColdRun)
END IF
END SUB

SUB StatrHotT (Option$, Sample$, TestNo$, BP, VVLI, VVHI, PDVLI, PDVHI, DTWVI, DTAVI,
NoColdRun)
CLS
DO
    LOCATE 4, 30
    PRINT "Thermal Test"
    PRINT : PRINT
    PRINT "      1. Calibrate "
    PRINT
    PRINT "      2. Start The Test"
    LOCATE 21, 35
    LINE INPUT Optcol$
    LOOP UNTIL Optcol$ = "1" OR Optcol$ = "2"
    IF Optcol$ = "1" THEN
        CALL Calibrate(Option$, DTWVI, DTAVI, VVHI, VVLI, PDVHI, PDVLI, BP, Sample$,
TestNo$, NoColdRun)
    END IF
END SUB

SUB STim (T%)
    SLEEP T%
END SUB

SUB Stor (Sample$, TestNo$, BP, NoHotRun, NoColdRun, NoOutHot, NoOutCold, OutptHot(),
OutptCold())
    'To save the time, date, sample name and test number on the first line,
    ' and then to save the test data for each air velocity.
    ' under file name = "TEST" + sample name + "RES"
    CLS
    A$ = "T"
    filename$ = "T" + TestNo$ + ".RES"
    Filenum% = FREEFILE
    OPEN filename$ FOR OUTPUT AS Filenum%
    PRINT #Filenum%, NoColdRun;
    PRINT #Filenum%, " , ";
    PRINT #Filenum%, NoHotRun;
    PRINT #Filenum%, " , ";
    PRINT #Filenum%, TIME$;
    PRINT #Filenum%, " , ";
    PRINT #Filenum%, DATE$;
    PRINT #Filenum%, " , ";
    PRINT #Filenum%, Sample$;
    PRINT #Filenum%, " , ";
    PRINT #Filenum%, TestNo$;
    PRINT #Filenum%, " , ";

```

```

PRINT #Filenum%, BP
' pressure drop results
IF NoColdRun > 0 THEN
  FOR I = 1 TO NoColdRun
    PRINT #Filenum%,      ' space
    FOR J = 1 TO NoOutCold
      PRINT #Filenum%, OutptCold(I, J);
      IF J < NoOutCold THEN
        PRINT #Filenum%, " , ";
      END IF
    NEXT J
    PRINT #Filenum%,      ' space
  NEXT I
  PRINT #Filenum%, ' space
END IF
' thermal results
IF NoHotRun > 0 THEN
  FOR K = 1 TO NoHotRun
    PRINT #Filenum%,      ' space
    FOR L = 1 TO NoOutHot
      PRINT #Filenum%, OutptHot(K, L);
      IF L < NoOutHot THEN
        PRINT #Filenum%, " , ";
      END IF
    NEXT L
    PRINT #Filenum%,      ' space
  NEXT K
END IF
CLOSE Filenum%
END SUB

```

```

SUB StorCalib (NoOutCalb, Sample$, TestNo$, InitialVolt())

```

```

  CLS
  filename$ = "Calibrat.DAT"
  Filenum% = FREEFILE
  OPEN filename$ FOR OUTPUT AS Filenum%
  PRINT #Filenum%, Sample$, " , ";
  PRINT #Filenum%, TestNo$, " , ";
  FOR J = 1 TO NoOutCalb
    PRINT #Filenum%, InitialVolt(J);
    IF J < NoOutCalb THEN
      PRINT #Filenum%, " , ";
    END IF
  NEXT J
  CLOSE Filenum%
END SUB

```

```

SUB TableOfCalib (Sample$, TestNo$, BP, VVLI, VVHI, PDVLI, PDVHI, DTWVI, DTAVI,
CHANGCALB)

```

```

  ' To open (Calibrat) , read values from file and print them on the screen
6 DO
  CLS
  filename$ = "C:\calibrat.DAT"
  Filenum% = FREEFILE
  OPEN filename$ FOR INPUT AS Filenum%
  INPUT #Filenum%, Sample$
  INPUT #Filenum%, TestNo$
  FOR I = 1 TO 7

```

```

    INPUT #Filenum%, InitialVolt(I)
  NEXT I
CLOSE Filenum%
PRINT
PRINT " 1 - SAMPLE NAME :"; Sample$
PRINT
PRINT " 2 - TEST NUMBER :"; TestNo$
PRINT
PRINT " 3 - VVLI      :"; InitialVolt(1): VVLI = InitialVolt(1)
PRINT
PRINT " 4 - VVHI      :"; InitialVolt(2): VVHI = InitialVolt(2)
PRINT
PRINT " 5 - PDVLI     :"; InitialVolt(3): PDVLI = InitialVolt(3)
PRINT
PRINT " 6 - PDVHI     :"; InitialVolt(4): PDVHI = InitialVolt(4)
PRINT
PRINT " 7 - DTAVI     :"; InitialVolt(5): DTAVI = InitialVolt(5)
PRINT
PRINT " 8 - DTWVI     :"; InitialVolt(6): DTWVI = InitialVolt(6)
PRINT
PRINT " 9 - BP        :"; InitialVolt(7): BP = InitialVolt(7)
PRINT
PRINT " 10 - Return to Menu"
PRINT
INPUT " ENTER NUMBER TO CHANGE VALUE OR 0 TO END"; CHANGCALB
LOOP UNTIL CHANGCALB >= 0 AND CHANGCALB < 11
IF CHANGCALB = 1 THEN
  CLS
  LOCATE 10, 10
  INPUT "ENTER NEW SAMPLE NAME "; Sample$
  CALL StorCalib(7, Sample$, TestNo$, InitialVolt())
  GOTO 6
ELSEIF CHANGCALB = 2 THEN
  CLS
  LOCATE 10, 10
  INPUT "ENTER NEW TEST NUMBER "; TestNo$
  CALL StorCalib(7, Sample$, TestNo$, InitialVolt())
  GOTO 6
ELSEIF CHANGCALB > 2 AND CHANGCALB < 10 THEN
  CLS
  LOCATE 10, 10
  INPUT "ENTER NEW VALUE "; InitialVolt(CHANGCALB - 2)
  CALL StorCalib(7, Sample$, TestNo$, InitialVolt())
  GOTO 6
END IF
END SUB

```


[CONDENSE.BAS]

```
'      CONDENSER MODEL
'
'      BY
'      MAHMOUD ABU-MADI
'      UNIVERSITY OF BRIGHTON
'
'      1997
'
'      Version III
```

```
Global CEqStatA(6), CEqStatb(6), CEqStatc(6), k, u
Global cc, b, Temp_Critical, r, x, mw, CSatPress(12)
Global CLiqDen(7), Temp(6)
Global Liq_S_Vol, SH_Vap_SVol, CIdeCp(7), IC, V, P_sat_v
Global aa1, aa2, AA3, AA4, AA5, AA6, CP1, CP2, CP3, CP4, Refrig$
Global CLiqViscos(6), CVapViscos(7)
Global CLiqTherCon(6), CVapTherCon(7)
Global CliqCp(6)
Global CVapCp(6)
Global CLiqEnth(6), CSatTemp(8)
Global vol(6), Inth(6), HeatCap(6), v_SH_m
Global Cp_SH_m, Visco(6), m_SH_m, TherCon(6), k_SH_m
Global Press(6), PressCritical
Global Dens_air, Cp_Air, m_air_SH, Vel_Air
Global Re_v, Re_SH, Re_L, Pr_SH, Pr_V, Pr_L, mr
Global L_SH, L_TP, l_l, No_of_Tube_Cir, Tube_Pitch, Dp(3)
Global Q_SH, Q_TP1, C, Q_l, NoRows_ass, R5, R51, DP_tot
Global R1, R3, E_TP, E_SH, E_L, NTU_SH, NTU_TP, NTU_L, Uall_TP, Uall_SH
Global Uall_SC, BtwHead_SH, BtwHead_TP, BtwHead_L, DFL, Acs, ha, htpm, hl, hSH
Global AF_SH, F_TP, AF_l, dinhyd, Gr, BtwHead_CAL, fs, DTM_CS, DTM_TP, DTM_SH
Global Taout_SH, C_air_SH, Taout, AF_TP1, AF_SC, No_Tube_Row
Global C_TP, m_air_TP, C_air_TP, C_SH, BtwHead_SH_E, BtwHead_SH_ASS, BtwHead_TP_ASS
Global Ta_TP(40), Q_TP(40), Q_TP_E(40), AF_E(40), AF_TP(40), TL, Q_TP_S_I
Global Q_TP_S_II, TDP, NoRows_TP_S, NoRows_TP_Sl, xi, Xo, Tainw1, Taout_TP
Global Tain2, Q_TP_E_I, Fay_out, ifg_ref, TL_cal_l, PwsDP, ha_m, win
Global CVapVol(5), T_m
Global Q_TP_E1, Trm, Q_S_L, Ti, Wi, INI, Tain10
Global CLiqPress(6), DT(2), ffl, NDTS, Opt, T_Sat, Win1, DTM_SC, Q_SC, E_SC
Global BtwHead_SC_ASS, BtwHead_SC, C_SC, C_air_SC, Re_SC, L_SC, C_Ref_SH, C_Ref_SC
Global DT1$(3), BtwHead_CAL_(800), DpHv, DpHl, ifg_air, Lmwd, Lmtd, Dpa, R4
Global fFACTOR, jFACTOR, Rea, F_H, FinCond, ll, Findensity, Tubedensity, TubeWeight_P_M
Global row_space
Global Tao(800), np_in, SameEnd$, Acs_T, NoRows_SH, R7, Twbout, Waout, Np_row(5)
Global No_Cell_row(800), NC(100), Temp_Avr(6), Tth, Stream_screen
Global Config As String
```

```
Sub ASSUMPTION (R51, NoRows_ass, Uall_SH, Uall_SC, Uall_TP, DTM_SH, DTM_SC,
DTM_TP, Q_SH, Q_TP1, Q_SC, Cp_Air, win, Dens_air, Vel_Air, OvFins, BtwHead_SH,
BtwHead_SC, BtwHead_TP)
```

```
On Error GoTo Assumption_Error
```

```
' To calculate approximate Between Headers for super heated and condensed
' vapour at the condenser { to start the design with it } assuming that
' the air side with the minimum heat capacity for both SH & TP
```

```
R5 = R51 * NoRows_ass
```

```
NTU_SH = R5 * Uall_SH / ((Cp_Air + win * 1805) * Dens_air * Vel_Air)
```

```
NTU_TP = R5 * Uall_TP / ((Cp_Air + win * 1805) * Dens_air * Vel_Air)
```

```
NTU_SC = R5 * Uall_SC / ((Cp_Air + win * 1805) * Dens_air * Vel_Air)
```

```
E_SH = 1 - Exp(-NTU_SH)
```

```
E_TP = 1 - Exp(-NTU_TP)
```

```
E_SC = 1 - Exp(-NTU_SC)
```

```

AF_SH = Q_SH / (E_SH * (Cp_Air + win * 1805) * Dens_air * Vel_Air * DTM_SH)
AF_TP1 = Q_TP1 / (E_TP * (Cp_Air + win * 1805) * Dens_air * Vel_Air * DTM_TP)
AF_SC = Q_SC / (E_SC * (Cp_Air + win * 1805) * Dens_air * Vel_Air * DTM_SC)
BtwHead_SH = AF_SH / OvFins
BtwHead_TP = AF_TP1 / OvFins
BtwHead_SC = AF_SC / OvFins
Exit Sub
Assumption_Error:
  Error_Flag = 46
  Resume Next
End Sub

Sub condenser_a (Opt)
  On Error GoTo Condenser_A_Error
  ' Programme for condenser design case I [ single pass ]
  Orig_Rows = Norows
  Pwsdb = STEAM_PRESS(AirInlet)
  Pwdb = Pwsdb * .5 ' assuming 50% relative humidity
  win = Wsat(Pwdb)
  Call read_prop(Refrig$, CEqStatA(), CEqStatb(), CEqStatc(), k, u, cc, r, b, mw, Temp_Critical,
  PressCritical, ffl, CSatPress(), CLiqDen(), CVapVol(), CIdeCp(), IC, CVapViscos(), CLiqViscos(),
  CVapTherCon(), CLiqTherCon(), CVapCp(), CliqCp(), CLiqEnth(), CSatTemp())
  Call Ref_Proper(Refrig$, T_Sat, DT(), Press(), vol(), Inth(), Visco(), TherCon(), HeatCap(),
  CEqStatA(), CEqStatb(), CEqStatc(), k, u, cc, r, b, mw, Temp_Critical, PressCritical, ffl, CSatPress(),
  CLiqDen(), CIdeCp(), CVapViscos(), CLiqViscos(), CVapTherCon(), CLiqTherCon(), CVapCp(),
  CliqCp(), CLiqEnth(), CSatTemp())
  If Opt = 1 Or Opt = 2 Or Opt = 9 Then
    NoRows_ass = 1
  Else
    NoRows_ass = Norows
  End If
  Norows = NoRows_ass
  Call AIR_PROP(AirInlet, Dens_air, Cp_Air)
  Call read_Geomtry(AirInlet, win, Vel_Air, ConfigType, dinhyd, Dout, FinPtch, FperM, fs, Fth,
  Tube_Pitch, rsp, R3, R4, R51, R6, R7, R8, ll, fFACTOR, ha, Acs_T, Orig_Rows)
  Acs = Acs_T * Nostream
  If Error_Flag <> 0 Then Exit Sub
  If Opt = 1 Or Opt = 3 Then
    Call fluxses(Gr, Acs, Inth(), HeatCap(), DT(), mr, ReqDis, Q_SH, Q_TP1, Q_SC, C_Ref_SH,
  C_Ref_SC)
  ElseIf Opt = 9 Then
    NoRows_ass = Orig_Rows
    Norows = NoRows_ass
    ReqDis = .1 ' KW ASSUMPTION
    Call Duties(ConfigType, Inth(), ReqDis, HeatCap(), Acs, mr, Gr, Q_SH, Q_TP1, Q_SC,
  C_Ref_SH, C_Ref_SC)
  Else
    Call Duties(ConfigType, Inth(), ReqDis, HeatCap(), Acs, mr, Gr, Q_SH, Q_TP1, Q_SC,
  C_Ref_SH, C_Ref_SC)
  End If
  Call Non_Dim_No(ha, Fth, FinCond, ll, R3, R7, Visco(), TherCon(), vol(), HeatCap(), Gr, dinhyd,
  PressCritical, Press(), Temp(), AirInlet, Refrig$, Uall_SH, Uall_SC, Uall_TP, DTM_SH, DTM_SC,
  DTM_TP)
  Call ASSUMPTION(R51, NoRows_ass, Uall_SH, Uall_SC, Uall_TP, DTM_SH, DTM_SC,
  DTM_TP, Q_SH, Q_TP1, Q_SC, Cp_Air, win, Dens_air, Vel_Air, OvFins, BtwHead_SH,
  BtwHead_SC, BtwHead_TP)
1 Call fin_length
  If Error_Flag <> 0 Then Exit Sub

```

```

If Opt = 3 Or Opt = 4 Then
  BtwHead = BtwHead_CAL
ElseIf Opt = 9 Then
  BtwHead_CAL_New = BtwHead_CAL
  If Abs(BtwHead - BtwHead_CAL) < .001 Then
    ElseIf BtwHead > BtwHead_CAL Then
      ReqDis_New = ReqDis * BtwHead / BtwHead_CAL
      Delta_ReqDis = ReqDis_New - ReqDis
      ReqDis = ReqDis_New
      BtwHead_CAL_old = BtwHead_CAL
      Call Duties(ConfigType, Inth(), ReqDis, HeatCap(), Acs, mr, Gr, Q_SH, Q_TP1, Q_SC,
C_Ref_SH, C_Ref_SC)
      Call Non_Dim_No(ha, Fth, FinCond, ll, R3, R7, Visco(), TherCon(), vol(), HeatCap(), Gr,
dinhyd, PressCritical, Press(), Temp(), AirInlet, Refrig$, Uall_SH, Uall_SC, Uall_TP, DTM_SH,
DTM_SC, DTM_TP)
      GoTo 1
    End If
    ReqDis = ReqDis - Delta_ReqDis * (BtwHead_CAL_New - BtwHead) / (BtwHead_CAL_New -
BtwHead_CAL_old)
  Else
    If DFL < .01 Then
      Norows = NoRows_ass
    Else
      If DFL > .01 Then
        NoRows_ass = NoRows_ass * BtwHead_CAL / BtwHead
        GoTo 1
      Else
        NoRows_ass = NoRows_ass * 1.1 * BtwHead_CAL / BtwHead
        GoTo 1
      End If
    End If
  End If
  End If
  AF_tot = AF_TP1 + AF_SH + AF_SC
  R5 = R51 * Norows
  L_SH = (AF_SH * R5) / (3.1415927 * dinhyd * R3)
  L_TP = (AF_TP1 * R5) / (3.1415927 * dinhyd * R3)
  L_SC = (AF_SC * R5) / (3.1415927 * dinhyd * R3)
  If DT(1) > 0 Then Call D_Press_SH_Con(vol(), Re_SH, Gr, L_SH, dinhyd, Nostream, Dp(),
No_of_Bends_Cir_SH)
  If DT(2) > 0 Then Call D_Press_SC(vol(), Re_SC, Gr, L_SC, dinhyd, Nostream, Dp(),
No_of_Bends_Cir_SC)
  Call D_Press_TP(No_of_Bends_Cir_SH, No_of_Bends_Cir_SC)
  DL_SH = Abs(L_SH - L_SH_P)
  DL_TP = Abs(L_TP - L_TP_P)
  DL_SC = Abs(L_SC - L_SC_P)
  If DL_TP > .01 Or DL_SH > .01 Or DL_SC > .01 Then
    L_SH_P = L_SH
    L_TP_P = L_TP
    L_SC_P = L_SC
    Call Ref_Proper(Refrig$, T_Sat, DT(), Press(), vol(), Inth(), Visco(), TherCon(), HeatCap(),
CEqStatA(), CEqStatb(), CEqStatc(), k, u, cc, r, b, mw, Temp_Critical, PressCritical, ffl, CSatPress(),
CLiqDen(), CLideCp(), CVapViscos(), CLiqViscos(), CVapTherCon(), CLiqTherCon(), CVapCp(),
CLiqCp(), CLiqEnth(), CSatTemp())
    If Opt = 1 Or Opt = 3 Or Opt = 11 Then
      Call fluxses(Gr, Acs, Inth(), HeatCap(), DT(), mr, ReqDis, Q_SH, Q_TP1, Q_SC, C_Ref_SH,
C_Ref_SC)
    Else

```

```

    Call Duties(ConfigType, Inth(), ReqDis, HeatCap(), Acs, mr, Gr, Q_SH, Q_TP1, Q_SC,
C_Ref_SH, C_Ref_SC)
    End If
    Call Non_Dim_No(ha, Fth, FinCond, ll, R3, R7, Visco(), TherCon(), vol(), HeatCap(), Gr,
dinhyd, PressCritical, Press(), Temp(), AirInlet, Refrig$, Uall_SH, Uall_SC, Uall_TP, DTM_SH,
DTM_SC, DTM_TP)
    If Error_Flag <> 0 Then Exit Sub
    GoTo 1
    End If
    DP_tot = Dp(1) + Dp(2) + Dp(3) + DpHv + DpHI
    Call D_Press_Air(AirInlet, Taout, fFACTOR, Vel_Air, R4, R51, Norows, Dpa)
    Exit Sub
Condenser_A_Error:
    Error_Flag = 4
    Resume Next
End Sub

Sub connew (Opt)
    On Error GoTo Connew_Error
    ' Programme for parallel flow condenser design [ single pass ]
    ' Dim Orig_Rows
    Pwsdb = STEAM_PRESS(AirInlet)
    Pwdb = Pwsdb * .5 ' assuming 50% relative humidity
    win = Wsat(Pwdb)
    Orig_Rows = Norows
    Call read_prop(Refrig$, CEqStatA(), CEqStatb(), CEqStatc(), k, u, cc, r, b, mw, Temp_Critical,
PressCritical, ffl, CSatPress(), CLiqDen(), CVapVol(), CIdeCp(), IC, CVapViscos(), CLiqViscos(),
CVapTherCon(), CLiqTherCon(), CVapCp(), CliqCp(), CLiqEnth(), CSatTemp())
    Call Ref_Proper(Refrig$, T_Sat, DT(), Press(), vol(), Inth(), Visco(), TherCon(), HeatCap(),
CEqStatA(), CEqStatb(), CEqStatc(), k, u, cc, r, b, mw, Temp_Critical, PressCritical, ffl, CSatPress(),
CLiqDen(), CIdeCp(), CVapViscos(), CLiqViscos(), CVapTherCon(), CLiqTherCon(), CVapCp(),
CliqCp(), CLiqEnth(), CSatTemp())
    NoRows_ass = Norows
    Call AIR_PROP(AirInlet, Dens_air, Cp_Air)
    Call read_Geomtry(AirInlet, win, Vel_Air, ConfigType, dinhyd, Dout, FinPtch, FperM, fs, Fth,
Tube_Pitch, rsp, R3, R4, R51, R6, R7, R8, ll, fFACTOR, ha, Acs_T, Orig_Rows)
    If Error_Flag <> 0 Then Exit Sub
    For i = 1 To 100 'for parallel flow condensers and not for develop
        NC(i) = NoStr(i)
        If NoStr(i) = 0 Then NC(i) = Nostream 'Np_row(nr)=Np_row(2)
    Next i
    Select Case Opt
    Case 24 ' to calculate between headers
        BtwHead = .8 ' assumption as minimum
    Case 25 ' to calculate over fins
        Np_row(NR) = 10 ' assumption
    Case 29 ' to calculate duty
        ReqDis = .5 ' KW ASSUMPTION
    End Select
    Acs = Acs_T * NC(1)' NoStream
    Call Duties(ConfigType, Inth(), ReqDis, HeatCap(), Acs, mr, Gr, Q_SH, Q_TP1, Q_SC,
C_Ref_SH, C_Ref_SC)
    Call fin_length_NEW(win)
    Call D_Press_Air(AirInlet, Taout, fFACTOR, Vel_Air, R4, R51, Norows, Dpa)
    Exit Sub
Connew_Error:
    Error_Flag = 4
    Resume Next

```

End Sub

```

Sub D_Press_SC (vol(), Re_SC, Gr, L_SC, dinhyd, Nostream, Dp(), No_of_Bends_Cir_SC)
  ' To calculate SC liquid pressure drop in plain tube { no bends are considered }
  v_SC_m = (vol(3) + vol(4)) / 2
  ' friction
  If Re_SC < 1187 Then
    Frec_SC = 64 / Re_SC
  ElseIf Re_SC < 100000 Then
    Frec_SC = .3164 / Re_SC ^ .25
  Else
    Frec_SC = .0032 + .221 / Re_SC ^ .237
  End If
  If Opt = 1 Or Opt = 2 Or Opt = 3 Or Opt = 4 Or Opt = 9 Then ' case I
    L_SC_Tubes_Cir = L_SC / Nostream
  Else ' case II
    L_SC_Tubes_Cir = L_SC
  End If
  No_of_Tube_Cir = L_SC_Tubes_Cir / BtwHead
  If No_of_Tube_Cir > Int(No_of_Tube_Cir) Then No_of_Tube_Cir = Int(No_of_Tube_Cir) + 1
  No_of_Bends_Cir_SC = (No_of_Tube_Cir - 1)
  L_SC_Bends_Cir = No_of_Bends_Cir_SC * 3.1415927 * Tube_Pitch / 2
  L_SC_Cir = L_SC_Tubes_Cir + L_SC_Bends_Cir
  DP_SC_f = Gr ^ 2 * Frec_SC * L_SC_Cir * v_SC_m / (2 * dinhyd)
  ' momentum
  DP_SC_m = Gr ^ 2 * (vol(4) - vol(3))
  ' bend effect
  fay = .19712
  If No_of_Bends_Cir_SC > 0 Then
    Dp_SC_bend = Gr ^ 2 * v_SC_m * .5 * No_of_Bends_Cir_SC * fay
  Else
    Dp_SC_bend = 0
  End If
  Dp(3) = DP_SC_f + DP_SC_m + Dp_SC_bend
End Sub

```

```

Sub D_Press_SH_Con (vol(), Re_SH, Gr, L_SH, dinhyd, Nostream, Dp(), No_of_Bends_Cir_SH)
  ' To calculate SH vapour pressure drop in plain tube { no bends are considered }
  v_SH_m = (vol(1) + vol(2)) / 2
  ' friction
  If Re_SH < 1187 Then
    Frec_SH = 64 / Re_SH
  ElseIf Re_SH < 100000 Then
    Frec_SH = .3164 / Re_SH ^ .25
  Else
    Frec_SH = .0032 + .221 / Re_SH ^ .237
  End If
  If Opt = 1 Or Opt = 2 Or Opt = 3 Or Opt = 4 Or Opt = 9 Then ' case I
    L_SH_Tubes_Cir = L_SH / Nostream
  Else ' case II
    L_SH_Tubes_Cir = L_SH
  End If
  No_of_Tube_Cir = L_SH_Tubes_Cir / BtwHead
  If No_of_Tube_Cir > Int(No_of_Tube_Cir) Then No_of_Tube_Cir = Int(No_of_Tube_Cir) + 1
  No_of_Bends_Cir_SH = (No_of_Tube_Cir - 1)
  L_SH_Bends_Cir = No_of_Bends_Cir_SH * 3.1415927 * Tube_Pitch / 2
  L_SH_Cir = L_SH_Tubes_Cir + L_SH_Bends_Cir
  DP_SH_f = Gr ^ 2 * Frec_SH * L_SH_Cir * v_SH_m / (2 * dinhyd)

```

```

' momentum
DP_SH_m = Gr ^ 2 * (vol(2) - vol(1))
' bend effect
fay = .19712
If No_of_Bends_Cir_SH > 0 Then
  Dp_SH_bend = Gr ^ 2 * v_SH_m * .5 * No_of_Bends_Cir_SH * fay
Else
  Dp_SH_bend = 0
End If
Dp(1) = DP_SH_f + DP_SH_m + Dp_SH_bend
End Sub

Sub D_Press_TP (No_of_Bends_Cir_SH, No_of_Bends_Cir_SC)
' To calculate TP condensing pressure drop { from Paliwoda equation }
' friction and bends
' friction
If Re_v < 1187 Then
  Frec_v = 64 / Re_v
ElseIf Re_v < 100000 Then
  Frec_v = .3164 / Re_v ^ .25
Else
  Frec_v = .0032 + .221 / Re_v ^ .237
End If
If Opt = 1 Or Opt = 2 Or Opt = 3 Or Opt = 4 Or Opt = 9 Then ' case I
  L_TP_Tubes_Cir = L_TP / Nostream
  No_Tube_Row = CInt(OvFins / Tube_Pitch)
Else ' case II
  L_TP_Tubes_Cir = L_TP
  No_Tube_Row = CInt(Nostream * OvFins / Tube_Pitch)
End If
No_of_Tube_Cir = No_Tube_Row * Norows / Nostream
If Re_v < 1187 Then
  Factor = .5
  A = 1
Else
  Factor = .36
  A = 1.78
End If
' No of ( 180°) bends / cir. = No of tubes per circuit - 1
' No of tubes per circuit = tube length for TP / Between Headers
No_of_Bends_Cir = (No_of_Tube_Cir - 1)
No_of_Bends_Cir_TP = No_of_Bends_Cir - (No_of_Bends_Cir_SH + No_of_Bends_Cir_SC)
L_TP_Bends_Cir = No_of_Bends_Cir_TP * 3.1415927 * Tube_Pitch / 2
L_TP_Cir = L_TP_Tubes_Cir + L_TP_Bends_Cir
If Re_L <= 1187 Then
  Theta = 64 * vol(3) * Visco(3) / (.3164 * vol(2) * Visco(2) ^ .25 * (Gr * dinhyd) ^ .75)
Else
  Theta = (vol(3) / vol(2)) * (Visco(3) / Visco(2)) ^ .25
End If
Bm = Factor * (Theta + 1)
Dp_TP_f = Frec_v * Bm * Gr ^ 2 * vol(2) * L_TP_Cir / (2 * dinhyd)
' momentum
Dp_TP_m = Gr ^ 2 * (vol(3) - vol(2))
' bend effect
fay = .19712
Theta = (vol(3) / vol(2))
If No_of_Bends_Cir_TP > 0 Then
  x = 0

```

```

so = Theta * x + (1 - Theta) * (x ^ (A + 1) / (A + 1))
x = 1
si = Theta * x + (1 - Theta) * (x ^ (A + 1) / (A + 1))
ss = so - si
Bm = ss / (-1)
Dp_TP_bend = Gr ^ 2 * vol(2) * .5 * No_of_Bends_Cir_TP * fay * Bm
Else
  Dp_TP_bend = 0
End If
Dp(2) = Dp_TP_f + Dp_TP_m + Dp_TP_bend
' inlet manifold
DpHv = .5 * vol(1) * 3.5 * Gr ^ 2
' outlet manifold
DpHl = .5 * vol(4) * 3.2 * Gr ^ 2
End Sub

Sub Duties (ConfigType, Inth(), ReqDis, HeatCap(), Acs, mr, Gr, Q_SH, Q_TP1, Q_SC, C_Ref_SH,
C_Ref_SC)
' To calculate condenser ReqDis from SH & TP
mr = ReqDis / (Inth(1) - Inth(4))
If ConfigType <> 3 Then Gr = mr / Acs
Q_SH = 1000 * (Inth(1) - Inth(2)) * mr
Q_TP1 = 1000 * (Inth(2) - Inth(3)) * mr
Q_SC = 1000 * (Inth(3) - Inth(4)) * mr
C_Ref_SH = mr * (HeatCap(2) + HeatCap(1)) / 2
C_Ref_SC = mr * (HeatCap(4) + HeatCap(3)) / 2
End Sub

Sub E_NTU_SC_I (Opt, Taout_SC, R51, NoRows_ass, Uall_SC, DTM_SC, Temp(), AirInlet, Q_SC,
Cp_Air, Dens_air, win, Vel_Air, OvFins, BtwHead_SC, C_Ref_SC)
' To calculate SC vapour heat transfer area for air with max. or
' min. heat capacity
Do
  BtwHead_SC_ASS = BtwHead_SC
  m_air_SC = BtwHead_SC_ASS * OvFins * Dens_air * Vel_Air
  C_air_SC = m_air_SC * (Cp_Air + win * 1805)
  C_SC = C_Ref_SC / C_air_SC
  If C_SC < 1 Then
    Call ENTU_SC_R_I(Opt, Taout_SC, R51, NoRows_ass, Uall_SC, DTM_SC, Temp(),
AirInlet, Q_SC, C_SC, C_Ref_SC, C_air_SC, Cp_Air, Dens_air, win, Vel_Air, OvFins,
BtwHead_SC)
  Else
    C_SC = C_air_SC / C_Ref_SC ' C_air_SC = C_min
    Call ENTU_SC_A_I(Opt, Taout_SC, R51, NoRows_ass, Uall_SC, DTM_SC, AirInlet, Q_SC,
Cp_Air, Dens_air, win, Vel_Air, OvFins, BtwHead_SC, C_SC)
  End If
  DFL_SC = Abs(BtwHead_SC_ASS - BtwHead_SC)
  Loop_Count1 = Loop_Count1 + 1
  If Loop_Count1 > 100000 Then
    Error_Flag = 2
    Exit Sub
  End If
Loop Until DFL_SC <= .01
End Sub

Sub E_NTU_SH_I (Opt, Taout_SH, R51, NoRows_ass, Uall_SH, DTM_SH, Temp(), AirInlet,
Q_SH, Cp_Air, Dens_air, win, Vel_Air, OvFins, BtwHead_SH, C_Ref_SH)
On Error GoTo E_NTU_SH_I_Error

```

```

' To calculate SH vapour heat transfer area for air with max. or
' min. heat capacity
Do
  BtwHead_SH_ASS = BtwHead_SH
  m_air_SH = BtwHead_SH_ASS * OvFins * Dens_air * Vel_Air
  C_air_SH = m_air_SH * (Cp_Air + win * 1805)
  C_SH = C_Ref_SH / C_air_SH
  If C_SH < 1 Then
    Call ENTU_SH_R_I(Opt, Taout_SH, R51, NoRows_ass, Uall_SH, DTM_SH, Temp(),
AirInlet, Q_SH, C_SH, C_Ref_SH, C_air_SH, Cp_Air, Dens_air, win, Vel_Air, OvFins,
BtwHead_SH)
  Else
    C_SH = C_air_SH / C_Ref_SH ' C_air_SH = C_min
    Call ENTU_SH_A_I(Opt, Taout_SH, R51, NoRows_ass, Uall_SH, DTM_SH, AirInlet,
Q_SH, Cp_Air, Dens_air, win, Vel_Air, OvFins, BtwHead_SH, C_SH)
  End If
  DFL_SH = Abs(BtwHead_SH_ASS - BtwHead_SH)
  Loop_Count1 = Loop_Count1 + 1
  If Loop_Count1 > 100000 Then
    Error_Flag = 2
    Exit Sub
  End If
Loop Until DFL_SH <= .001
Exit Sub
E_NTU_SH_I_Error:
  Error_Flag = 15
  Resume Next
End Sub

Sub E_NTU_TP (R51, NoRows_ass, Uall_TP, DTM_TP, AirInlet, Q_TP1, Cp_Air, win, Dens_air,
Vel_Air, OvFins, BtwHead_TP, C_air_TP)
  On Error GoTo E_NTU_TP_Error
  ' To calculate condensing heat transfer area { air is C_maximum }
  R5 = R51 * NoRows_ass
  NTU_TP = R5 * Uall_TP / ((Cp_Air + win * 1805) * Dens_air * Vel_Air)
  E_TP = 1 - Exp(-NTU_TP)
  AF_TP1 = Q_TP1 / (E_TP * (Cp_Air + win * 1805) * Dens_air * Vel_Air * DTM_TP)
  BtwHead_TP = AF_TP1 / OvFins
  m_air_TP = BtwHead_TP * OvFins * Dens_air * Vel_Air
  C_air_TP = m_air_TP * (Cp_Air + win * 1805)
  Taout_TP = AirInlet + (Q_TP1 / C_air_TP)
  Taout = Taout_TP
Exit Sub
E_NTU_TP_Error:
  Error_Flag = 1
  Resume Next
End Sub

Sub ENTU_SC_A_I (Opt, Taout_SC, R51, NoRows_ass, Uall_SC, DTM_SC, AirInlet, Q_SC,
Cp_Air, Dens_air, win, Vel_Air, OvFins, BtwHead_SC, C_SC)
  ' SC vapour CASE I for condensers
  ' with air as minimum heat capacity fluid
  R5 = R51 * NoRows_ass
  NTU_SC = R5 * Uall_SC / ((Cp_Air + win * 1805) * Dens_air * Vel_Air)
  E_SC = (1 / C_SC) * (1 - Exp(-C_SC * (1 - Exp(-NTU_SC))))
  AF_SC = Q_SC / (E_SC * (Cp_Air + win * 1805) * Dens_air * Vel_Air * DTM_SC)
  BtwHead_SC = AF_SC / OvFins
  If Opt <= 10 Then

```



```

    Taout_SC = AirInlet + E_SC * DTM_SC      ' condenser
Else
    Taout_SC = AirInlet - E_SC * DTM_SC      ' evaporator
End If
End Sub

Sub ENTU_SC_R_I (Opt, Taout_SC, R51, NoRows_ass, Uall_SC, DTM_SC, Temp(), AirInlet,
Q_SC, C_SC, C_Ref_SC, C_air_SC, Cp_Air, Dens_air, win, Vel_Air, OvFins, BtwHead_SC)
' SC vapour CASE I for condensers
' with refrigerant as minimum heat capacity fluid
R5 = R51 * NoRows_ass
E_SC = (Temp(3) - Temp(4)) / DTM_SC
If E_SC >= 1 Then E_SC = .999
logarithem = C_SC * Log(1 - E_SC)
If logarithem <= -1 Then logarithem = -.999
NTU_SC = -(1 / C_SC) * Log(1 + logarithem)
aair = NTU_SC * C_Ref_SC / Uall_SC
AF_SC = aair / R5
BtwHead_SC = AF_SC / OvFins
If Opt <= 10 Then
    Taout_SC = (Q_SC / C_air_SC) + AirInlet    ' condenser
Else
    Taout_SC = AirInlet - Q_SC / C_air_SC      ' evaporator
End If
End Sub

Sub ENTU_SH_A_I (Opt, Taout_SH, R51, NoRows_ass, Uall_SH, DTM_SH, AirInlet, Q_SH,
Cp_Air, Dens_air, win, Vel_Air, OvFins, BtwHead_SH, C_SH)
' SH vapour CASE I for condensers and evaporators
' with air as minimum heat capacity fluid (UNMIXED)
R5 = R51 * NoRows_ass
NTU_SH = R5 * Uall_SH / ((Cp_Air + win * 1805) * Dens_air * Vel_Air)
E_SH = (1 / C_SH) * (1 - Exp(-C_SH * (1 - Exp(-NTU_SH))))
AF_SH = Q_SH / (E_SH * (Cp_Air + win * 1805) * Dens_air * Vel_Air * DTM_SH)
BtwHead_SH = AF_SH / OvFins
If Opt <= 10 Then
    Taout_SH = AirInlet + E_SH * DTM_SH        ' condenser
Else
    Taout_SH = AirInlet - E_SH * DTM_SH        ' evaporator
End If
End Sub

Sub ENTU_SH_A_II (Opt, NoRows_I, Taout_SH, win)
' SH vapour CASE II for condensers and evaporators
' with air as minimum heat capacity fluid
' SHOULD BE CALLED AFTER E_NTU_SH_I(Opt,Taout_SH)
NoRows_ass = NoRows_I
Do
    R5 = R51 * NoRows_ass
    NTU_SH = R5 * Uall_SH / ((Cp_Air + win * 1805) * Dens_air * Vel_Air)
    E_SH = (1 / C_SH) * (1 - Exp(-C_SH * (1 - Exp(-NTU_SH))))
    AF_SH = Q_SH / (E_SH * (Cp_Air + win * 1805) * Dens_air * Vel_Air * DTM_SH)
    BtwHead_SH = AF_SH / OvFins
    Deff = Abs(BtwHead_SH - BtwHead)
    If Deff > .001 Then
        NoRows_ass = NoRows_ass * (BtwHead_SH / BtwHead)
    End If
Loop Until Deff <= .001

```

```

NoRows_SH = NoRows_ass
If Opt <= 10 Then
  Taout_SH = AirInlet + E_SH * DTM_SH      ' condenser
Else
  Taout_SH = AirInlet - E_SH * DTM_SH      ' evaporator
End If
End Sub

```

```

Sub ENTU_SH_NEW (Opt, A_Air_CELL, Uall, C, C_Ref, Cp_Ref, mr, C_Air, TRefIn, TRefOut,
Tain1, QiSH, C_MIN, Taoi, NC(), np)
  ' SH vapour or SC liquid CASE I for condensers and evaporators
  ' with air or refrigerant as minimum heat capacity fluid, with both fluids unmixed
  Ntu = A_Air_CELL * Uall / C_MIN
  effectiveness = 1 / (1 / (1 - Exp(-Ntu)) + C / (1 - Exp(-Ntu * C)) - 1 / Ntu) ' both fluids unmixed
  If C_Ref < C_Air Then
    TRefOut = TRefIn - effectiveness * (TRefIn - Tain1)
    Dh = (TRefIn - TRefOut) * Cp_Ref      ' Cp_Ref at inlet
    QiSH = mr * Dh / NC(np)
    Taoi = Tain1 + QiSH / C_Air
    QiSH = Abs(QiSH)
  Else
    Taoi = Tain1 + effectiveness * (TRefIn - Tain1)
    QiSH = C_Air * (Taoi - Tain1)
    Dh = QiSH / (mr / NC(np))
    TRefOut = TRefIn - Dh / Cp_Ref      ' Cp_Ref at inlet
    QiSH = Abs(QiSH)
  End If
End Sub

```

```

Sub ENTU_SH_R_I (Opt, Taout_SH, R51, NoRows_ass, Uall_SH, DTM_SH, Temp(), AirInlet,
Q_SH, C_SH, C_Ref_SH, C_air_SH, Cp_Air, Dens_air, win, Vel_Air, OvFins, BtwHead_SH)
  On Error GoTo ENTU_SH_R_I_Error
  ' SH vapour CASE I for condensers and evaporators --- temp(3)
  ' with refrigerant as minimum heat capacity fluid (MIXED)
  R5 = R51 * NoRows_ass
  E_SH = (Temp(1) - Temp(2)) / DTM_SH
  If E_SH >= 1 Then E_SH = .999
  logarithem = C_SH * Log(1 - E_SH)
  If logarithem <= -1 Then logarithem = -.999
  NTU_SH = -(1 / C_SH) * Log(1 + logarithem)
  aair = NTU_SH * C_Ref_SH / Uall_SH
  AF_SH = aair / R5
  BtwHead_SH = AF_SH / OvFins
  If Opt <= 10 Then
    Taout_SH = (Q_SH / C_air_SH) + AirInlet      ' condenser
  Else
    Taout_SH = AirInlet - Q_SH / C_air_SH      ' evaporator
  End If
Exit Sub
ENTU_SH_R_I_Error:
  Error_Flag = 14
  Resume Next
End Sub

```

```

Sub ENTU_SH_R_II (Opt, NoRows_I, Taout_SH)
  ' SH vapour CASE II for condensers and evaporators
  ' with refrigerant as minimum heat capacity fluid
  ' SHOULD BE CALLED AFTER E_NTU_SH_I(Opt,Taout_SH)

```

```

NoRows_ass = NoRows_I
Do
  R5 = R51 * NoRows_ass
  E_SH = (Temp(1) - Temp(2)) / DTM_SH
  logarithem = C_SH * Log(1 - E_SH)
  If logarithem <= -1 Then logarithem = -.999
  NTU_SH = -(1 / C_SH) * Log(1 + logarithem)
  aair = NTU_SH * C_Ref_SH / Uall_SH
  AF_SH = aair / R5
  BtwHead_SH = AF_SH / OvFins
  Deff = Abs(BtwHead_SH - BtwHead)
  If Deff > .001 Then
    NoRows_ass = NoRows_ass * (BtwHead_SH / BtwHead)
  End If
Loop Until Deff <= .001
NoRows_SH = NoRows_ass
If Opt <= 10 Then
  Taout_SH = (Q_SH / C_air_SH) + AirInlet ' condenser
Else
  Taout_SH = AirInlet - Q_SH / C_air_SH ' evaporator
End If
End Sub

Sub fin_length ()
  Call E_NTU_TP(R51, NoRows_ass, Uall_TP, DTM_TP, AirInlet, Q_TP1, Cp_Air, win, Dens_air,
Vel_Air, OvFins, BtwHead_TP, C_air_TP)
  If Error_Flag <> 0 Then Exit Sub
  If DT(1) > 0 Then Call E_NTU_SH_I(Opt, Taout_SH, R51, NoRows_ass, Uall_SH, DTM_SH,
Temp(), AirInlet, Q_SH, Cp_Air, Dens_air, win, Vel_Air, OvFins, BtwHead_SH, C_Ref_SH)
  If DT(2) > 0 Then Call E_NTU_SC_I(Opt, Taout_SC, R51, NoRows_ass, Uall_SC, DTM_SC,
Temp(), AirInlet, Q_SC, Cp_Air, Dens_air, win, Vel_Air, OvFins, BtwHead_SC, C_Ref_SC)
  If Error_Flag <> 0 Then Exit Sub
  BtwHead_CAL = BtwHead_TP + BtwHead_SH + BtwHead_SC
  DFL = Abs(BtwHead_CAL - BtwHead)
End Sub

Sub fin_length_NEW (win)
' for parallel flow condensers
If ConfigType = 3 Then OvFins = OvFins - F_H
On Error GoTo NTUTP_Error
Call FinEff(ha, Fth, FinCond, ll, R1, R7)
old_n = 0
7 Tdbi = AirInlet
NR = 1
For i = 1 To 6
  Temp_Avr(i) = 0
Next i
FLcalc = 0
DpTotal = 0
n = 1
m = 1
np = 1
Gr = mr / (Acs_T * NC(np))
BtwHead_Cell = .01
No_Cell_Pass = CInt(BtwHead / BtwHead_Cell)
No_Cell_row(NR) = CInt(No_Cell_Pass * Np_row(NR))
No_Pass_passed = Np_row(NR)
NoCells = 0

```

```

No_Pass_Orig = 0
No_Tube_Row = CInt(OvFins / Tube_Pitch)
For j = 1 To Norows
  NoCells = NoCells + CInt(No_Cell_Pass * Np_row(j))
  No_Pass_Orig = No_Pass_Orig + Np_row(j)
Next j
Cp_Air = Air_CP(AirInlet)
Dens_air = Air_Dens(AirInlet)
A_Air_CELL = R51 * BtwHead_Cell * Tube_Pitch
' DP-headers at outlet
'===== from Palywoda =====
Acs_Head = 3.14 * (.022 ^ 2) / 4
Gr_Head = mr / Acs_Head
DpHo = .5 * vol(4) * 20 * Gr_Head ^ 2 ' outlet coefficient vary from 2.8 to 3.5
'=====
DPHead = DpHo / 1000000 ' DpHead in MPa
DpTotal = DpTotal + DPHead
' DP-headers at inlet
'===== from Palywoda =====
DpHi = .5 * vol(1) * 15 * Gr_Head ^ 2 ' outlet coefficient vary from 2.8 to 3.5
'=====
DPHead = DpHi / 1000000 ' DpHead in MPa
DpTotal = DpTotal + DPHead
'=====
' Subcool region
' start from saturated liquid to subcooled liquid.
If DT(2) > 0 Then
  Tri = Temp(3)
  Pi = Press(3)
  VOLi = vol(3)
  Inthi = Inth(3)
  TherConi = TherCon(3)
  Viscoi = Visco(3)
  Cpi = HeatCap(3)
3 Call Ref_Prop_Liq(Refrig$, Tri, Pi, VOLi, Inthi, TherConi, Viscoi, Cpi)
  C_Ref_SC = mr * Cpi / NC(np)
  m_air = BtwHead_Cell * Tube_Pitch * Dens_air * Vel_Air
  C_Air = m_air * (Cp_Air + win * 1805)
  C_SC = C_Ref_SC / C_Air
  Re_SC = Gr * dinhyd / Viscoi
  Pr_SC = Viscoi * Cpi / TherConi
  hSC = .023 * Re_SC ^ .8 * Pr_SC ^ .4 * TherConi / dinhyd
  uu_SC = (R1 / ha) + (R3 / hSC)
  Uall_SC = 1 / uu_SC
  TRefIn = Tri
  If C_SC < 1 Then ' C_air = C_max
    C_MIN = C_Ref_SC
    Call ENTU_SH_NEW(Opt, A_Air_CELL, Uall_SC, C_SC, C_Ref_SC, Cpi, mr, C_Air,
TRefIn, TRefOut, Tdbi, Qi, C_MIN, Taoi, NC(), np)
  Else
    C_SC = C_Air / C_Ref_SC ' C_air = C_min
    C_MIN = C_Air
    Call ENTU_SH_NEW(Opt, A_Air_CELL, Uall_SC, C_SC, C_Ref_SC, Cpi, mr, C_Air,
TRefIn, TRefOut, Tdbi, Qi, C_MIN, Taoi, NC(), np)
  End If
  Tro = TRefOut
  Temp_Avr(NR) = Temp_Avr(NR) + Taoi * NC(np) / No_Tube_Row
' friction

```

```

If Re_SC < 1187 Then
  Frec_SC = 64 / Re_SC
ElseIf Re_SC < 100000 Then
  Frec_SC = .3164 / Re_SC ^ .25
Else
  Frec_SC = .0032 + .221 / Re_SC ^ .237
End If
DPf = Gr ^ 2 * Frec_SC * BtwHead_Cell * VOLi / (2 * dinhyd)
Po = Pi - DPf / 1000000
DPmt = 0
2  Call Ref_Prop_Liq(Refrig$, Tro, Po, VOLo, 0, 0, 0, 0)
  ' momentum
  DPm = Gr ^ 2 * (VOLo - VOLi)
  Dpi = (DPf + DPm) / 1000000
  Po = Pi - Dpi
  If Abs(DPm - DPmt) > .0001 Then
    DPmt = DPm
    GoTo 2
  End If
  FLcalc = FLcalc + BtwHead_Cell
  DpTotal = (DpTotal + Dpi) ' in MPa
  If DT(2) > (Temp(3) - Tro) Then ' Subcool region not finished
    If FLcalc < BtwHead Then ' total cells length < BtwHead
      n = n + 1 ' inlet condition to next cell = outlet form previous one
      m = m + 1
      Pi = Po
      Tri = Tro
      VOLi = VOLo
      GoTo 3
    ElseIf np < No_Pass_passed Then ' start new pass on the same row
      ' DP-headers
      '===== from Palywoda =====
      Acs_Head = 3.14 * (.022 ^ 2) / 4
      Gr_Head = mr / Acs_Head
      DpHo = .5 * VOLi * 20 * Gr_Head ^ 2 ' outlet coefficient vary from 2.8 to 3.5
      ' outlet manifold
      DpHi = .5 * VOLi * 15 * Gr_Head ^ 2 ' inlet coefficient vary from 2.5 to 3.2
      '=====
      DPHead = (DpHo + DpHi) / 1000000 ' DpHead in MPa
      DpTotal = DpTotal + DPHead
      Po = Po - DPHead
      n = n + 1
      m = m + 1
      np = np + 1 ' new number of circuits
      Pi = Po
      Gr = mr / (Acs_T * NC(np))
      Tri = Tro
      VOLi = VOLo
      FLcalc = 0
      GoTo 3
    Else ' start new pass on a new row
      NR = NR + 1
      No_Cell_row(NR) = CInt(No_Cell_Pass * Np_row(NR))
      No_Pass_passed = No_Pass_passed + Np_row(NR)
      np = np + 1 ' NC (np) new number of circuits
      Gr = mr / (Acs_T * NC(np))
      n = n + 1
      m = 1

```

```

Tdbi = Temp_Avr(NR - 1) / No_Cell_Pass
Cp_Air = Air_CP(Tdbi)
Dens_air = Air_Dens(Tdbi)
' DP-headers
'===== from Palywoda =====
Acs_Head = 3.14 * (.022 ^ 2) / 4
Gr_Head = mr / Acs_Head
DpHo = .5 * VOLi * 20 * Gr_Head ^ 2 ' outlet coefficient vary from 2.8 to 3.5
' outlet manifold
DpHi = .5 * VOLi * 15 * Gr_Head ^ 2 ' inlet coefficient vary from 2.5 to 3.2
'=====
DPHead = (DpHo + DpHi) / 1000000 ' DpHead in MPa
DpTotal = DpTotal + DPHead
Po = Po - DPHead
Pi = Po
Tri = Tro
VOLi = VOLo
FLcalc = 0
GoTo 3
End If
Else ' subcooled finished.
NoCells_SC = n 'sub cool region NUMBER OF CELLS
DpSC = DpTotal ' in MPa
n = n + 1
m = m + 1
End If
Else ' no subcooled liquid
FLcalc = 0
DpSC = 0
NoCells_SC = 0
End If
Tro = Temp(3) ' outlet conditions from two phase
Po = Press(3)
'=====
' Two phase region
' start from saturated liquid to saturated vapour
Xo = .001 ' assumption
4 If n > 1 Then
region$ = "TP"
Call Ref_Prop_Vap(Refrig$, Tro, Po, vol(2), Inth(2), TherCon(2), Visco(2), HeatCap(2),
region$, n)
Call Ref_Prop_Liq(Refrig$, Tro, Po, vol(3), Inth(3), TherCon(3), Visco(3), HeatCap(3))
End If
hifgi = (Inth(2) - Inth(3)) * 1000
Re_L = Gr * dinhyd / Visco(3) ' dinhyd is hydraulic diameter
' ===== Martilene equation =====
Re_v = Gr * dinhyd / Visco(2) ' dinhyd is hydraulic diameter
Re_q = Re_v * (Visco(2) / Visco(3)) * (vol(2) / vol(3)) ^ .5 + Re_L
Visco_r = Visco(3) * (1 - Xo) + Visco(2) * Xo
heatCap_r = HeatCap(3) * (1 - Xo) + HeatCap(2) * Xo
TherCon_r = TherCon(3) * (1 - Xo) + TherCon(2) * Xo
Pr_q = Visco_r * heatCap_r / TherCon_r
Nu = .05 * (Re_q ^ .8) * (Pr_q ^ .3)
htpm = Nu * TherCon_r / dinhyd
' =====
' ===== shah equation =====
Pr_L = Visco(3) * HeatCap(3) / TherCon(3)
hl = .023 * Re_L ^ .8 * Pr_L ^ .4 * TherCon(3) / dinhyd

```

```

PressRatioi = Po / PressCritical
htpm = hl * ((1 - Xo) + 3.8 * Xo ^ .76 * (1 - Xo) ^ .04 / PressRatioi ^ .38)
uu_TP = (R1 / ha) + (R3 / htpm)
Ualli = 1 / uu_TP
Ntu = R51 * Ualli / (Dens_air * Vel_Air * (Cp_Air + win * 1805))
effectivness = 1 - Exp(-Ntu)
Taoi = Tdbi + effectivness * (Tro - Tdbi)
m_air = BtwHead_Cell * Tube_Pitch * Dens_air * Vel_Air ' based on cell face area
Qi = m_air * (Cp_Air + win * 1805) * (Taoi - Tdbi)
Dh = Qi / (mr / NC(np))
DXi = Dh / (hifgi) ' hifgi is based on outlet conditions
xi = Xo + DXi
Temp_Avr(NR) = Temp_Avr(NR) + Taoi * NC(np) / No_Tube_Row
If n = 1 Then
  VOLo = vol(3) * (1 - Xo) + Xo * vol(2)
End If
VOLi = vol(3) * (1 - xi) + xi * vol(2)
' friction
Re_v = Gr * dinhyd / Visco(2)
If Re_v < 1187 Then
  Frec_v = 64 / Re_v
ElseIf Re_v < 100000 Then
  Frec_v = .3164 / Re_v ^ .25
Else
  Frec_v = .0032 + .221 / Re_v ^ .237
End If
If Re_L <= 1187 Then
  Theta = 64 * vol(3) * Visco(3) / (.3164 * vol(2) * Visco(2) ^ .25 * (Gr * dinhyd) ^ .75)
Else
  Theta = (vol(3) / vol(2)) * (Visco(3) / Visco(2)) ^ .25
End If
If xi > 1 Then
  xi = .9999
End If
'===== PALIWODA =====
so = ((3 * Theta / 2) - (9 / 4)) * (1 - Xo) ^ (4 / 3) + (9 / 7) * (1 - Theta) * (1 - Xo) ^ (7 / 3) + (Xo ^
(3.276)) / 3.276
si = ((3 * Theta / 2) - (9 / 4)) * (1 - xi) ^ (4 / 3) + (9 / 7) * (1 - Theta) * (1 - xi) ^ (7 / 3) + (xi ^
(3.276)) / 3.276
ss = so - si
Bm = ss / (Xo - xi)
DPf = Frec_v * Bm * Gr ^ 2 * vol(2) * BtwHead_Cell / (2 * dinhyd)
' momentum
DPm = Gr ^ 2 * (VOLo - VOLi)
Dpi = (DPf + DPm) / 1000000 ' total pressure drop
Pi = Po + Dpi ' pressure at outlet
Call SatTemperature(Pi, Refrig$, CSatTemp(), CSatPress(), xi, Tri) ' for R-12, R-22, R134a and
R66 only
If Error_Flag <> 0 Then Exit Sub
FLcalc = FLcalc + BtwHead_Cell
DpTotal = (DpTotal + Dpi) ' in MPa
If xi < .9999 Then ' condensing region not finished
  If FLcalc < BtwHead Then ' total cells length < BtwHead
    n = n + 1 ' inlet condition to next cell = outlet form previous one
    m = m + 1
    Xo = xi
    Po = Pi
    Tro = Tri

```

```

VOLo = VOLi
GoTo 4
ElseIf np < No_Pass_passed Then ' start new pass on the same row
' DP-headers from outlet of the existing pass and inlet to the next pass
' inlet manifold
'===== from Palywoda =====
Acs_Head = 3.14 * (.022 ^ 2) / 4
Gr_Head = mr / Acs_Head
Theta = vol(3) / vol(2) 'two phase
Bc = (Theta + 3 * (1 - Theta) * xi) * (1 - xi) ^ .333 + xi ^ 2.276
DpHo = .5 * Bc * VOLi * 20 * Gr_Head ^ 2 ' outlet coefficient vary from 2.8 to 3.5
' outlet manifold
DpHi = .5 * Bc * VOLi * 15 * Gr_Head ^ 2 ' inlet coefficient vary from 2.5 to 3.2
'=====
DPHead = (DpHo + DpHi) / 1000000 ' DpHead in MPa
Pi = Pi + DPHead
DpTotal = DpTotal + DPHead
'===== orifice
acS_orific = 3.14 * (.02 ^ 2) / 4
Gr_orific = mr / acS_orific
dens_vap = 1 / VOLi
DPORIFIC = 0.5 * Bc * Voli * 40 * Gr_orific ^ 2 ' inlet coefficient vary from 2.5 to 3.2
'DPORIFIC = Bc * .1 * .5 * (Gr_Head ^ 2) / (Acs_Head ^ 2 * dens_vap)
DpTotal = DpTotal + DPORIFIC / 1000000
Pi = Pi + DPORIFIC / 1000000
xi = Xo' + DX 'DX from new pressure and the same enthalpy
'=====
Call SatTemperature(Pi, Refrig$, CSatTemp(), CSatPress(), xi, Tri)' for R-12, R-22, R134a
and R66 only
If Error_Flag <> 0 Then Exit Sub
n = n + 1
m = m + 1
np = np + 1 'NC (np) new number of circuits
Po = Pi
Gr = mr / (Acs_T * NC(np))
Xo = xi
Tro = Tri
VOLo = VOLi
FLcalc = 0
GoTo 4
Else ' start new pass on a new row
NR = NR + 1
No_Cell_row(NR) = CInt(No_Cell_Pass * Np_row(NR))
No_Pass_passed = No_Pass_passed + Np_row(NR)
' DP-headers
'===== from Palywoda =====
Acs_Head = 3.14 * (.022 ^ 2) / 4
Gr_Head = mr / Acs_Head
Theta = vol(3) / vol(2)
Bc = (Theta + 3 * (1 - Theta) * xi) * (1 - xi) ^ .333 + xi ^ 2.276
DpHo = .5 * vol(2) * Bc * 20 * Gr_Head ^ 2 ' outlet coefficient vary from 2.8 to 3.5
' outlet manifold
DpHi = .5 * vol(2) * Bc * 15 * Gr_Head ^ 2 ' inlet coefficient vary from 2.5 to 3.2
'=====
DPHead = (DpHo + DpHi) / 1000000 ' DpHead in MPa
Pi = Pi + DPHead
DpTotal = DpTotal + DPHead
Acs_Bend = 3.14 * (.009 ^ 2) / 4

```



```

Gr_Bend = mr / Acs_Bend
Sita = (.24 + .691 + .458) ' from bend, inlet to the bend and exit from the bend
DPBend = .5 * vol(2) * (Gr_Bend ^ 2) * Sita * Bc
DpTotal = DpTotal + (DPBend / 1000000)
Pi = Pi + (DPBend / 1000000)
xi = Xo
Call SatTemperature(Pi, Refrig$, CSatTemp(), CSatPress(), xi, Tri)' for R-12, R-22, R134a
and R66 only
If Error_Flag <> 0 Then Exit Sub
Po = Pi
np = np + 1 ' NC (np) new number of circuits
Gr = mr / (Acs_T * NC(np))
n = n + 1
m = 1
Tro = Tri
VOLo = VOLi
FLcalc = 0
Tdbi = Temp_Avr(NR - 1) / No_Cell_Pass
Cp_Air = Air_CP(Tdbi)
Dens_air = Air_Dens(Tdbi)
GoTo 4
End If
Else ' condensing finished.
Po = Pi
Tro = Tri
VOLo = VOLi
DpTP = DpTotal - DpSC ' in MPa
NoCells_TP = n - NoCells_SC ' TWO PHASE REGION NUMBER OF CELLS
FLTP = NoCells_TP * BtwHead_Cell
n = n + 1
m = m + 1
End If
=====
===
If DT(1) > 0 Then ' superheated region
Psat_v = Pi ' condensing pressure at the vapour line
Temp(2) = Tri ' condensing temperature at the vapour line
Temp(1) = Tri + DT(1) ' inlet temperature to the condenser
Tri = Temp(1) ' start at superheat vapour to saturated vapour
6 region$ = "SH"
Call Ref_Prop_Vap(Refrig$, Tri, Pi, VOLi, Inthi, TherConi, Viscoi, Cpi, region$, n)
m_air = BtwHead_Cell * Tube_Pitch * Dens_air * Vel_Air
C_Air = m_air * (Cp_Air + win * 1805)
C_Ref_SH = mr * Cpi / NC(np)
C_SH = C_Ref_SH / C_Air
Re_SH = Gr * dinhyd / Viscoi
Pr_SH = Viscoi * Cpi / TherConi
hSH = .023 * Re_SH ^ .8 * Pr_SH ^ .4 * TherConi / dinhyd
uu_SH = (R1 / ha) + (R3 / hSH)
Uall_SH = 1 / uu_SH
TRefIn = Tri
If C_SH < 1 Then ' C_air = C_max
C_MIN = C_Ref_SH
Call ENTU_SH_NEW(Opt, A_Air_CELL, Uall_SH, C_SH, C_Ref_SH, Cpi, mr, C_Air,
TRefIn, TRefOut, Tdbi, Qi, C_MIN, Taoi, NC(), np)
Else
C_SH = C_Air / C_Ref_SH ' C_air = C_min
C_MIN = C_Air

```

```

Call ENTU_SH_NEW(Opt, A_Air_CELL, Uall_SH, C_SH, C_Ref_SH, Cpi, mr, C_Air,
TRefIn, TRefOut, Tdbi, Qi, C_MIN, Taoi, NC(), np)
End If
Tro = TRefOut
Temp_Avr(NR) = Temp_Avr(NR) + Taoi * NC(np) / No_Tube_Row
If Re_SH < 1187 Then
  Frec_SH = 64 / Re_SH
ElseIf Re_SH < 100000 Then
  Frec_SH = .3164 / Re_SH ^ .25
Else
  Frec_SH = .0032 + .221 / Re_SH ^ .237
End If
DPf = Gr ^ 2 * Frec_SH * BtwHead_Cell * VOLi / (2 * dinhyd)
Po = Pi - DPf / 1000000
DPmt = 0
5 Call Ref_Prop_Vap(Refrig$, Tro, Po, VOLo, 0, 0, 0, 0, region$, n)
' momentum
DPm = Gr ^ 2 * (VOLo - VOLi)
Dpi = (DPf + DPm) / 1000000
Po = Pi - Dpi
If Abs(DPm - DPmt) > .001 Then
  DPmt = DPm
  GoTo 5
End If
FLcalc = FLcalc + BtwHead_Cell
DpTotal = (DpTotal + Dpi) ' in MPa
If DT(1) > (Temp(1) - Tro) Then ' superheated region not finished
  If FLcalc < BtwHead Then ' total cells length < BtwHead
    n = n + 1 ' inlet condition to next cell = outlet form previous one
    m = m + 1
    Pi = Po
    Tri = Tro
    VOLi = VOLo
    GoTo 6
  ElseIf np < No_Pass_passed Then ' start new pass on the same row
    ' DP-headers
    '===== from Palywoda =====
    Acs_Head = 3.14 * (.022 ^ 2) / 4
    Gr_Head = mr / Acs_Head
    DpHo = .5 * VOLi * 20 * Gr_Head ^ 2 ' outlet coefficient vary from 2.8 to 3.5
    ' outlet manifold
    DpHi = .5 * VOLi * 15 * Gr_Head ^ 2 ' inlet coefficient vary from 2.5 to 3.2
    '=====
    DPHead = (DpHo + DpHi) / 1000000 ' DpHead in MPa
    DpTotal = DpTotal + DPHead
    Po = Po - DPHead
    n = n + 1
    m = m + 1
    np = np + 1
    Pi = Po
    Gr = mr / (Acs_T * NC(np))
    Tri = Tro
    VOLi = VOLo
    FLcalc = 0
    GoTo 6
  Else ' start new pass on a new row
    NR = NR + 1
    No_Cell_row(NR) = CInt(No_Cell_Pass * Np_row(NR))

```

```

No_Pass_passed = No_Pass_passed + Np_row(NR)
np = np + 1      ' NC (np) new number of circuits
Gr = mr / (Acs_T * NC(np))
n = n + 1
m = 1
Tdbi = Temp_Avr(NR - 1) / No_Cell_Pass
Cp_Air = Air_CP(Tdbi)
Dens_air = Air_Dens(Tdbi)
' DP-headers
'===== from Palywoda =====
Acs_Head = 3.14 * (.022 ^ 2) / 4
Gr_Head = mr / Acs_Head
DpHo = .5 * VOLi * 20 * Gr_Head ^ 2  ' outlet coefficient vary from 2.8 to 3.5
' outlet manifold
DpHi = .5 * VOLi * 15 * Gr_Head ^ 2  ' inlet coefficient vary from 2.5 to 3.2
'=====
DPHead = (DpHo + DpHi) / 1000000  ' DpHead in MPa
DpTotal = DpTotal + DPHead
Po = Po - DPHead
Pi = Po
Tri = Tro
VOLi = VOLo
FLcalc = 0
GoTo 6
End If
Else      ' superheating finished.
NoCells_SH = n - (NoCells_TP + NoCells_SC) ' TOTAL NUMBER OF CELLS
DpSH = DpTotal - (DpSC + DpTP)  ' in MPa
FLSH = NoCells_SH * BtwHead_Cell
End If
Else      ' no superheat
DpSC = 0
NoCells_SH = 0
End If

'=====
DP_tot = 1000000 * DpTotal
NoCells_Total = n      ' Total calculated NUMBER OF CELLS
If Opt = 24 Then      ' to calculate between headers
BtwHead_CAL = n * BtwHead_Cell / No_Pass_Orig 'assumption
BtwHead_CAL = Int(BtwHead_CAL * 100) / 100
BtwHead = (BtwHead_CAL + BtwHead) / 2
BtwHead = CInt(BtwHead * 100) / 100
If Abs(old_n - n) = 1 Then ' finish
ElseIf old_n <> n Then
old_n = n
GoTo 7
End If
BtwHead = BtwHead_CAL
ElseIf Opt = 25 Then  ' to calculate over fins
If khl = 1 Then GoTo 8
khl = 0
BtwHead_CAL = n * BtwHead_Cell / No_Pass_Orig 'assumption
BtwHead = CInt(BtwHead * 100) / 100
khl = 1
GoTo 7
8  BtwHead_CAL = n * BtwHead_Cell / No_Pass_Orig 'assumption
If Abs(BtwHead_CAL - BtwHead) > .001 Then

```

```

    BtwHead = (BtwHead_CAL + BtwHead) / 2
    BtwHead = CInt(BtwHead * 100) / 100
    GoTo 7
End If
BtwHead = BtwHead_CAL
Elseif Opt = 29 Then ' to calculate duty
    ncell_New = NoCells_Total
    If NoCells > NoCells_Total Then
        ReqDis_New = ReqDis * NoCells / NoCells_Total
        Delta_ReqDis = ReqDis_New - ReqDis
        ReqDis = ReqDis_New
        ncell_old = NoCells_Total
        Call Duties(ConfigType, Inth(), ReqDis, HeatCap(), Acs, mr, Gr, Q_SH, Q_TP1, Q_SC,
C_Ref_SH, C_Ref_SC)
        GoTo 7
    End If
    ReqDis = ReqDis - Delta_ReqDis * (ncell_New - NoCells) / (ncell_New - ncell_old)
End If
Taout = Temp_Avr(Norows) / No_Cell_Pass
xtra = (OvFins + F_H) / OvFins
ReqDis = ReqDis * xtra
OvFins = F_H + OvFins
Exit Sub
NTUTP_Error:
    Error_Flag = 7
    Resume Next
End Sub

Sub FinEff (ha, Fth, FinCond, ll, R1, R7)
    ' to calculate fin efficiency
    mm = Sqr(2 * ha / (Fth * FinCond))
    ef = (Exp(mm * ll) - Exp(-mm * ll)) / (mm * ll * (Exp(mm * ll) + Exp(-mm * ll)))
    R1 = 1 / (1 - R7 * (1 - ef))
End Sub

Sub fluxses (Gr, Acs, Inth(), HeatCap(), DT(), mr, ReqDis, Q_SH, Q_TP, Q_SC, C_Ref_SH,
C_Ref_SC)
    mr = Gr * Acs
    ReqDis = mr * (Inth(1) - Inth(4))
    Q_SC = 1000 * (Inth(3) - Inth(4)) * mr
    Q_SH = 1000 * (Inth(1) - Inth(2)) * mr
    Q_TP1 = 1000 * (Inth(2) - Inth(3)) * mr
    C_Ref_SH = mr * (HeatCap(2) + HeatCap(1)) / 2
    C_Ref_SC = mr * (HeatCap(4) + HeatCap(3)) / 2
End Sub

Sub IdeialCp (A(), mw, x, Y)
    ' To calculate ideal specific heat capacity
    ' for all refrigerants "generalised equation"
    Y = A(1) + A(2) * x + A(3) * x ^ 2 + A(4) * x ^ 3 + A(5) / x ^ 2 + A(6) * x ^ 4 + A(7) / x
End Sub

Sub Non_Dim_No (ha, Fth, FinCond, ll, R3, R7, Visco(), TherCon(), vol(), HeatCap(), Gr, dinhyd,
PressCritical, Press(), Temp(), AirInlet, Refrig$, Uall_SH, Uall_SC, Uall_TP, DTM_SH, DTM_SC,
DTM_TP)
    ' to calculate refrigerant heat transfer coefficient
    On Error GoTo Non_Dim_No_Error2
    mm = Sqr(2 * ha / (Fth * FinCond))

```

```

ef = (Exp(mm * ll) - Exp(-mm * ll)) / (mm * ll * (Exp(mm * ll) + Exp(-mm * ll)))
R1 = 1 / (1 - R7 * (1 - ef))
m_SH_m = (Visco(1) + Visco(2)) / 2
k_SH_m = (TherCon(1) + TherCon(2)) / 2
v_SH_m = (vol(1) + vol(2)) / 2
Cp_SH_m = (HeatCap(1) + HeatCap(2)) / 2
m_SC_m = (Visco(3) + Visco(4)) / 2
k_SC_m = (TherCon(3) + TherCon(4)) / 2
v_SC_m = (vol(3) + vol(4)) / 2
Cp_SC_m = (HeatCap(3) + HeatCap(4)) / 2
Re_L = Gr * dinhyd / Visco(3)
Re_SH = Gr * dinhyd / m_SH_m
Re_v = Gr * dinhyd / Visco(2)
Re_SC = Gr * dinhyd / m_SC_m
Pr_L = Visco(3) * HeatCap(3) / TherCon(3)
Pr_SH = m_SH_m * Cp_SH_m / k_SH_m
Pr_V = Visco(2) * HeatCap(2) / TherCon(2)
Pr_SC = m_SC_m * Cp_SC_m / k_SC_m
PressRatio = Press(2) / PressCritical
' Heat transfer coefficient for refrigerant
hSH = .023 * Re_SH ^ .8 * Pr_SH ^ .4 * k_SH_m / dinhyd
hl = .023 * Re_L ^ .8 * Pr_L ^ .4 * TherCon(3) / dinhyd
htpm = hl * (.55 + (2.09 / (PressRatio ^ .38)))
hSC = .023 * Re_SC ^ .8 * Pr_SC ^ .4 * k_SC_m / dinhyd
' superheat
uu_SH = (R1 / ha) + (R3 / hSH)
Uall_SH = 1 / uu_SH
' two-phase
uu_TP = (R1 / ha) + (R3 / htpm)
Uall_TP = 1 / uu_TP
' Subcool
uuL = (R1 / ha) + (R3 / hSC)
Uall_SC = 1 / uuL
DTM_SH = Temp(1) - AirInlet
DTM_SC = Temp(3) - AirInlet
If Refrig$ = "407c" Then
    DTM_TP = (Temp(2) + Temp(3)) / 2 - AirInlet
Else
    DTM_TP = Temp(2) - AirInlet
End If
Exit Sub
Non_Dim_No_Error2:
    Error_Flag = 45
    co = 14
    Resume Next
End Sub

Sub r345 (Dout, dinhyd, FperM, Fth, Tube_Pitch, rsp, R3, R4, R51, R6, R7, R8, ll)
' to calculate the constant R3,4,51,6,7,8,ll
R3 = (Dout / dinhyd) * (1 - FperM * Fth) + (FperM / dinhyd) * (2 * Tube_Pitch * rsp / 3.14 - .5 *
Dout ^ 2 + 2 * Fth * Tube_Pitch / (3.14 * 1)) ' NoRows = 1
R4 = Tube_Pitch / ((Tube_Pitch - Dout) * (1 - Fth * FperM))
R51 = 3.14 * Dout * (1 - FperM * Fth) / Tube_Pitch + FperM * (2 * rsp - 3.14 * Dout ^ 2 / (2 *
Tube_Pitch) + 2 * Fth)
R6 = 4 * rsp / R51
R8 = 3.14 * Dout * (1 - FperM * Fth) / (2 * Tube_Pitch * rsp * FperM - 3.14 * Dout ^ 2 * FperM /
2 + 2 * FperM * Fth * Tube_Pitch)
R7 = 1 / (1 + R8)

```

```

ll = (Tube_Pitch - Dout) / 2
End Sub

```

```

Sub R345Parallel (Tube_high, Tube_wide, Tth, L_chanel_1, L_chanel_2, No_Chanel, Fth, F_H,
row_space, FinPitch, Acs_T, R3, R4, R51, R6, R7, R8, ll, dinhyd, Tube_Pitch, Orig_Rows)
  rad = Tube_wide / 2
  Tube_high1 = Tube_high - 2 * rad
  F_p = FinPitch / 1000
  Tube_Pitch = F_H + 2 * rad
  Acsw1 = L_chanel_2 * (2 * (rad - Tth)) ' per one rectangular channel
  Acsw10 = Acsw1 * (No_Chanel - 2) ' per four rectangular channel
  Acsw2 = 2 * 1000000 * (L_chanel_1 - (rad - Tth)) * (2 * (rad - Tth)) + 3.14 * 1000000 * (rad -
Tth) ^ 2 ' per two corner channel
  Acsw2 = Acsw2 / 1000000
  Acs_T = Acsw10 + Acsw2 ' cross sectional area per tube
  TWP1 = 2 * (L_chanel_2 + (2 * (rad - Tth))) ' per one rectangular channel
  TWP2 = 2 * 2 * ((L_chanel_1 - (rad - Tth)) + (2 * (rad - Tth))) + 3.14 * 2 * (rad - Tth) ' per two
corner channel
  TWP10 = TWP1 + (No_Chanel - 2) * TWP2 ' total wetted perimeter
  dinhyd = 4 * Acs_T / TWP10 ' ND1
  ll = F_H / 2
  ' =====
  R3 = ((2 * 3.14 * rad + Tube_high1) * Orig_Rows + 1.035 * (Orig_Rows * (Tube_high1 + 2 * rad)
+ (Orig_Rows - 1) * row_space) * ((F_H / F_p) * 2 + 1) + row_space * (Orig_Rows - 1) + (1 + (F_H /
F_p)) * Fth * 2) / (TWP10 * Orig_Rows)
  R4 = 1 / (1 - (2 * rad + Fth) / Tube_Pitch - Fth * F_H / (Tube_Pitch * F_p))
  R5 = ((2 * 3.14 * rad + Tube_high1) * Orig_Rows + 1.035 * (Orig_Rows * (Tube_high1 + 2 * rad)
+ (Orig_Rows - 1) * row_space) * ((F_H / F_p) * 2 + 1) + row_space * (Orig_Rows - 1) + (1 + (F_H /
F_p)) * Fth * 2) / Tube_Pitch
  R51 = R5 / Orig_Rows
  R6 = 4 * (Orig_Rows * (Tube_high1 + 2 * rad) + (Orig_Rows - 1) * row_space) / R5 ' based on
NR=2
  R8 = (2 * 3.14 * rad + Tube_high1) * Orig_Rows / (1.035 * (Orig_Rows * (Tube_high1 + 2 * rad)
+ (Orig_Rows - 1) * row_space) * ((F_H / F_p) * 2 + 1) + row_space * (Orig_Rows - 1) + (1 + (F_H /
F_p)) * Fth * 2)
  R7 = 1 / (1 + R8)
End Sub

```

```

Sub read_Geomtry (AirInlet, win, Vel_Air, ConfigType, dinhyd, Dout, FinPch, FperM, fs, Fth,
Tube_Pitch, rsp, R3, R4, R51, R6, R7, R8, ll, fFACTOR, ha, Acs_T, Orig_Rows)
  On Error GoTo Non_Dim_No_Error
  FperM = 1 / (FinPitch / 1000) ' FperM = f/m
  fs = FperM * .0254! ' fin per inch
  fs = CInt(fs)
  fname = frmMain.txtcboFinFile.Text
  If ConfigType <> 3 Then ' A,B,C and NEW fins
    fnum = FreeFile ' fname = frmMain.txtcboFinFile.Text
    Open fname For Input As fnum
    Input #fnum, Dout, dinhyd, Tube_Pitch, rsp, Fth, FinCond, Findensity, Tubedensity, fef, f0, f1,
f2, f3, f4, f5, f6, f7, j0, j1, j2, j3, j4, j5, j6, j7, ReMin, ReMax
    Fin_Filename = fname
  Close fnum
  If Error_Flag <> 0 Then Exit Sub
  Depth = Orig_Rows * rsp
  Tth = (1000 * Dout - 1000 * dinhyd) / (1000 * 2)
  Call r345(Dout, dinhyd, FperM, Fth, Tube_Pitch, rsp, R3, R4, R51, R6, R7, R8, ll)
  Acs_T = (3.1415927 * (dinhyd ^ 2)) / 4
  Dens_air = Air_Dens(AirInlet)

```

```

Cp_Air = Air_CP(AirInlet)
Vis_Air = Air_Vis(AirInlet)
Con_Air = Air_Con(AirInlet)
Rea = Vel_Air * Dens_air * R6 / Vis_Air      ' Air Reynolds Number
Pra = (Cp_Air + win * 1805) * Vis_Air / Con_Air      ' Air Prandtel Number
If Rea > ReMax Or Rea < ReMin Then Error_Flag = 44  'error , air velocity out of range
FinPitch = FinPitch / 1000
jFACTOR = j0 * Rea ^ j1 * (Fth / FinPitch) ^ j2 * (Tube_Pitch / FinPitch) ^ j3 * (rsp / FinPitch)
^ j4 * (Depth / FinPitch) ^ j5 * (Dout / FinPitch) ^ j6 * fef ^ j7
fFACTOR = f0 * Rea ^ f1 * (Fth / FinPitch) ^ f2 * (Tube_Pitch / FinPitch) ^ f3 * (rsp / FinPitch)
^ f4 * (Depth / FinPitch) ^ f5 * (Dout / FinPitch) ^ f6 * fef ^ f7
FinPitch = FinPitch * 1000
Depth = Depth * 1000
Else      ' PFC Track pack
fnum = FreeFile
Open fname For Input As fnum
  Input #fnum, Tube_high, Tube_wide, Tth, L_chanel_1, L_chanel_2, No_Chanel, Fth, F_H,
FinCond, Findensity, TubeWeight_P_M, row_space, fa0, fa1, fa2, fa3, ja0, ja1, ja2, ja3, ReMin,
ReMax
  Fin_Filename = fname
  Close fnum
  If Error_Flag <> 0 Then Exit Sub
  rsp = Tube_high
  Tube_Pitch = Tube_wide + F_H
  Call R345Parallel(Tube_high, Tube_wide, Tth, L_chanel_1, L_chanel_2, No_Chanel, Fth, F_H,
row_space, FinPitch, Acs_T, R3, R4, R51, R6, R7, R8, ll, dinhyd, Tube_Pitch, Orig_Rows)
  Dens_air = Air_Dens(AirInlet)
  Cp_Air = Air_CP(AirInlet)
  Vis_Air = Air_Vis(AirInlet)
  Con_Air = Air_Con(AirInlet)
  Rea = Vel_Air * Dens_air * R6 / Vis_Air      ' Air Reynolds Number
  Pra = (Cp_Air + win * 1805) * Vis_Air / Con_Air      ' Air Prandtel Number
  If Rea > ReMax Or Rea < ReMin Then Error_Flag = 44  'error , air velocity out of range
  lnfFactor = fa0 + fa1 * Log(Rea) + fa2 * Log(Rea) ^ 2 + fa3 * Log(Rea) ^ 3
  fFACTOR = Exp(lnfFactor)
  lnjFactor = ja0 + ja1 * Log(Rea) + ja2 * Log(Rea) ^ 2 + ja3 * Log(Rea) ^ 3
  jFACTOR = Exp(lnjFactor)
End If
9292
ha = jFACTOR * Vel_Air * Dens_air * R4 * (Cp_Air + win * 1805) / Pra ^ (2 / 3)
Exit Sub
Non_Dim_No_Error:
  Error_Flag = 4
  Resume Next
End Sub

Sub read_prop (Refrig$, CEqStatA(), CEqStatb(), CEqStatc(), k, u, cc, r, b, mw, Temp_Critical,
PressCritical, ffl, CSatPress(), CLiqDen(), CVapVol(), CIdeCp(), IC, CVapViscos(), CLiqViscos(),
CVapTherCon(), CLiqTherCon(), CVapCp(), CliqCp(), CLiqEnth(), CSatTemp())
  On Error GoTo Non_Dim_No_Error3
  ' TO READ REFRIGERANT CONSTANTS FROM DATA FILE
  fname = "R" & Refrig$ & "con.txt"
  fnum = FreeFile
  Open fname For Input As fnum
  Input #fnum, CEqStatA(1), CEqStatb(1), CEqStatc(1), CEqStatA(2), CEqStatb(2), CEqStatc(2),
CEqStatA(3), CEqStatb(3), CEqStatc(3), CEqStatA(4), CEqStatb(4), CEqStatc(4), CEqStatA(5),
CEqStatb(5), CEqStatc(5), k, u, cc, r, b, mw, Temp_Critical, PressCritical, ffl

```

```

    Input #fnum, CSatPress(1), CSatPress(2), CSatPress(3), CSatPress(4), CSatPress(5),
    CSatPress(6), CSatPress(7), CSatPress(8), CSatPress(9), CSatPress(10), CSatPress(11),
    CSatPress(12)
    Input #fnum, CLiqDen(1), CLiqDen(2), CLiqDen(3), CLiqDen(4), CLiqDen(5), CLiqDen(6),
    CLiqDen(7)
    Input #fnum, CVapVol(1), CVapVol(2), CVapVol(3), CVapVol(4), CVapVol(5)
    Input #fnum, CIdeCp(1), CIdeCp(2), CIdeCp(3), CIdeCp(4), CIdeCp(5), CIdeCp(6), CIdeCp(7),
    IC
    Input #fnum, CVapViscos(1), CVapViscos(2), CVapViscos(3), CVapViscos(4), CVapViscos(5),
    CVapViscos(6), CVapViscos(7)
    Input #fnum, CLiqViscos(1), CLiqViscos(2), CLiqViscos(3), CLiqViscos(4), CLiqViscos(5),
    CLiqViscos(6)
    Input #fnum, CVapTherCon(1), CVapTherCon(2), CVapTherCon(3), CVapTherCon(4),
    CVapTherCon(5), CVapTherCon(6), CVapTherCon(7)
    Input #fnum, CLiqTherCon(1), CLiqTherCon(2), CLiqTherCon(3), CLiqTherCon(4),
    CLiqTherCon(5), CLiqTherCon(6)
    Input #fnum, CVapCp(1), CVapCp(2), CVapCp(3), CVapCp(4), CVapCp(5), CVapCp(6)
    Input #fnum, CliqCp(1), CliqCp(2), CliqCp(3), CliqCp(4), CliqCp(5), CliqCp(6)
    Input #fnum, CLiqEnth(1), CLiqEnth(2), CLiqEnth(3), CLiqEnth(4), CLiqEnth(5), CLiqEnth(6)
    Input #fnum, CSatTemp(1), CSatTemp(2), CSatTemp(3), CSatTemp(4), CSatTemp(5),
    CSatTemp(6), CSatTemp(7), CSatTemp(8)
    Close fnum
    Exit Sub
Non_Dim_No_Error3:
    Error_Flag = 4
    Resume Next
End Sub

Sub Ref_Prop_Liq (Refrig$, Tri, Pi, VOLi, Inthi, TherConi, Viscoi, Cpi)
' to calculate liquid refrigerant properties
Select Case Refrig$
Case "12", "22"
    Call LiqSVol(Tri, VOLi, CLiqDen())
    Call LiqEnthASH(Tri, Inthi, CLiqEnth())
    Call LiqTherCondASH(Tri, TherConi, CLiqTherCon())
    Call LiqViscoASH(Tri, Viscoi, CLiqViscos())
    Call LiqCpASH(Tri, Cpi, CliqCp())
Case "134a"
    Call LiqSVol(Tri, VOLi, CLiqDen())
    Call LiqEnthICI(Tri, Inthi, Temp_Critical, CLiqEnth())
    Call LiqTherCondICI(Tri, TherConi, Temp_Critical, CLiqTherCon())
    Call LiqViscoICI(Tri, Viscoi, CLiqViscos())
    Call LiqCpASH(Tri, Cpi, CliqCp())
Case "407c"
    Call Polynomial(CSatTemp(1), CSatTemp(2), CSatTemp(3), CSatTemp(4), 0, 0, Log(Pi * 10),
    Temp(2))' sat vap temp
    Call Polynomial(CSatTemp(5), CSatTemp(6), CSatTemp(7), CSatTemp(8), 0, 0, Log(Pi * 10),
    Temp(3))' sat liq temp
    T_m = (Temp(3) + Temp(2)) / 2
    Call Polynomial12(CLiqDen(1), CLiqDen(2), CLiqDen(3), CLiqDen(4), CLiqDen(5),
    CLiqDen(6), CLiqDen(7), Temp_Critical, Tri, VOLi)'SatVapVol.
    VOLi = 1 / VOLi
    Call Polynomial12(CLiqEnth(1), CLiqEnth(2), 0, CLiqEnth(3), CLiqEnth(4), CLiqEnth(5), 0,
    Temp_Critical, Tri, Inthi)'SatLiqEnth.
    Call Polynomial11(CLiqTherCon(1), CLiqTherCon(2), CLiqTherCon(3), CLiqTherCon(4),
    T_m, TherConi) ' liq. Thermal.Con.
    Call Polynomial11(CLiqViscos(1), CLiqViscos(3), CLiqViscos(4), CLiqViscos(2), T_m, Viscoi)
' liq. Visco.

```



```

    Viscoi = (Exp(Viscoi)) / 1000
    Cpi = 1000 * Abs((180 - Inthi) / (323.15 - Tri))
End Select
End Sub

Sub Ref_Prop_Vap (Refrig$, Tref, Po, VOLi, Inthi, TherConi, Viscoi, Cpi, region$, n)
' to calculate vapour refrigerant properties
On Error GoTo Ref_Prop_Vap_Error
Select Case Refrig$
Case "12", "22"
    If n = 1 Then Call VapSVolASH(Tref, Po, VOLi, CEqStatA(), CEqStatb(), CEqStatc(),
Temp_Critical, k, r, b, mw)
    Call VapSVolASH(Tref, Po, VOLi, CEqStatA(), CEqStatb(), CEqStatc(), Temp_Critical, k, r, b,
mw)
    Call VapEnthMartAsh(Tref, VOLi, Inthi, mw, r, Temp_Critical, b, k, CEqStatA(), CEqStatb(),
CEqStatc(), CIdeCp(), IC)
    Call VapTherCondASH(Tref, TherConi, CVapTherCon())
    Call VapViscoASH(Tref, Viscoi, CVapViscos())
    If region$ = "TP" Then
        Call VapCpASH(Tref, Cpi, CVapCp())
    Else
        Call IdealCp(CIdeCp(), mw, Tref, Cpi) 'ideal Cp
        Cpi = Cpi * 1000
    End If
Case "134a"
    If n = 1 Then Call VapSVolDUP(Tref, Po, VOLi, CEqStatA(), CEqStatb(), CEqStatc(),
Temp_Critical, k, r, b, mw, cc, u)
    Call VapSVolDUP(Tref, Po, VOLi, CEqStatA(), CEqStatb(), CEqStatc(), Temp_Critical, k, r, b,
mw, cc, u)
    Call VapEnthMartDUP(Tref, VOLi, Inthi, mw, r, Temp_Critical, b, k, CEqStatA(), CEqStatb(),
CEqStatc(), CIdeCp(), IC)
    Call VapTherCondICI(Tref, TherConi, CVapTherCon())
    Call VapViscoICI(Tref, Viscoi, CVapViscos())
    If region$ = "TP" Then
        Call VapCpASH(Tref, Cpi, CVapCp())
    Else
        Call IdealCp(CIdeCp(), mw, Tref, Cpi) 'ideal Cp
        Cpi = Cpi * 1000
    End If
Case "407c"
    If region$ = "TP" Then
        Call Polynomial(CSatTemp(1), CSatTemp(2), CSatTemp(3), CSatTemp(4), 0, 0, Log(Po *
10), Temp(2))' sat vap temp
        Call Polynomial12(CVapVol(1), CVapVol(2), 0, CVapVol(3), CVapVol(4), CVapVol(5), 0,
Temp_Critical, Temp(2), VOLi) 'SatVapVol_
        VOLi = 1 / VOLi
        Call Polynomial11(CVapTherCon(4), CVapTherCon(5), CVapTherCon(6), CVapTherCon(7),
Temp(2), TherConi) 'Sat. Vap. Thermal Con.
        Call Polynomial11(CVapViscos(4), CVapViscos(5), CVapViscos(6), CVapViscos(7),
Temp(2), Viscoi) 'Sat. Vap. Viscos.
        Call Polynomial11(CIdeCp(1), CIdeCp(2), CIdeCp(3), CIdeCp(7), Temp(2), Cpi): Cpi = Cpi *
1000
        Call VapEnthMartDUP(Temp(2), VOLi, Inthi, mw, r, Temp_Critical, b, k, CEqStatA(),
CEqStatb(), CEqStatc(), CIdeCp(), IC)
    Else
        Call VapSVolDUP(Tref, Po, VOLi, CEqStatA(), CEqStatb(), CEqStatc(), Temp_Critical, k, r,
b, mw, cc, u)
    End If
End Select
End Sub

```

```

    Call Polynomial(CVapTherCon(1), CVapTherCon(2), CVapTherCon(3), 0, 0, 0, Tref,
TherConi) 'SH_ Vap_ Thermal Con_
    Call Polynomial(CVapViscos(1), CVapViscos(2), CVapViscos(3), 0, 0, 0, Tref, Viscoi) 'SH_
Vap_ VISCOSITY
    Call Polynomial11(CIdeCp(1), CIdeCp(2), CIdeCp(3), CIdeCp(7), Tref, Cpi): Cpi = Cpi *
1000
    Call VapEnthMartDUP(Tref, VOLi, Inthi, mw, r, Temp_Critical, b, k, CEqStatA(),
CEqStatb(), CEqStatc(), CIdeCp(), IC)
    End If
    End Select
    Exit Sub
Ref_Prop_Vap_Error:
    Error_Flag = 10
    Resume Next
End Sub

```

```

Sub Ref_Proper (Refrig$, T_Sat, DT(), Press(), vol(), Inth(), Visco(), TherCon(), HeatCap(),
CEqStatA(), CEqStatb(), CEqStatc(), k, u, cc, r, b, mw, Temp_Critical, PressCritical, ffl, CSatPress(),
CLiqDen(), CIdeCp(), CVapViscos(), CLiqViscos(), CVapTherCon(), CLiqTherCon(), CVapCp(),
CLiqCp(), CLiqEnth(), CSatTemp())
' to calculate refrig properties
    Select Case Refrig$
    Case "12"
        ' Super heated vapour
        Call SatPressure(T_Sat, Refrig$, CSatPress(), Press(1))
        If Error_Flag <> 0 Then Exit Sub
        Call VapSVolASH(Temp(1), Press(1), vol(1), CEqStatA(), CEqStatb(), CEqStatc(),
Temp_Critical, k, r, b, mw)
        Call VapEnthMartAsh(Temp(1), vol(1), Inth(1), mw, r, Temp_Critical, b, k, CEqStatA(),
CEqStatb(), CEqStatc(), CIdeCp(), IC)
        Call VapTherCondASH(Temp(1), TherCon(1), CVapTherCon())
        Call VapViscoASH(Temp(1), Visco(1), CVapViscos())
        Call IdealCp(CIdeCp(), mw, Temp(1), HeatCap(1)) 'ideal Cp
        HeatCap(1) = HeatCap(1) * 1000
        ' Saturated vapour
        Press(2) = Press(1) - (Dp(1) / 1000000)
        Call SatTemperature(Press(2), Refrig$, CSatTemp(), CSatPress(), 0, Temp(2))
        Call VapSVolASH(Temp(2), Press(2), vol(2), CEqStatA(), CEqStatb(), CEqStatc(),
Temp_Critical, k, r, b, mw)
        Call VapEnthMartAsh(Temp(2), vol(2), Inth(2), mw, r, Temp_Critical, b, k, CEqStatA(),
CEqStatb(), CEqStatc(), CIdeCp(), IC)
        Call VapTherCondASH(Temp(2), TherCon(2), CVapTherCon())
        Call VapViscoASH(Temp(2), Visco(2), CVapViscos())
        Call VapCpASH(Temp(2), HeatCap(2), CVapCp())
        ' Saturated Liquid
        If Dp(2) > 1000000 Then
            Error_Flag = 20 ' pressure drop too high error message
            Exit Sub
        End If
        Press(3) = Press(2) - (Dp(2) / 1000000)
        Call SatTemperature(Press(3), Refrig$, CSatTemp(), CSatPress(), 0, Temp(3))
        Call LiqSVol(Temp(3), vol(3), CLiqDen())
        Call LiqEnthASH(Temp(3), Inth(3), CLiqEnth())
        Call LiqTherCondASH(Temp(3), TherCon(3), CLiqTherCon())
        Call LiqViscoASH(Temp(3), Visco(3), CLiqViscos())
        Call LiqCpASH(Temp(3), HeatCap(3), CLiqCp())
        ' Subcooled Liquid
        Press(4) = Press(3) - (Dp(3) / 1000000)
    End Case
End Sub

```

```

Temp(4) = Temp(3) - DT(2)
Call LiqSVol(Temp(4), vol(4), CLiqDen())
Call LiqEnthASH(Temp(4), Inth(4), CLiqEnth())
Call LiqTherCondASH(Temp(4), TherCon(4), CLiqTherCon())
Call LiqViscoASH(Temp(4), Visco(4), CLiqViscos())
Call LiqCpASH(Temp(4), HeatCap(4), CliqCp())
Case "22"
' Super heated vapour
Call SatPressure(T_Sat, Refrig$, CSatPress(), Press(1))
  If Error_Flag <> 0 Then Exit Sub
  Call VapSVolASH(Temp(1), Press(1), vol(1), CEqStatA(), CEqStatb(), CEqStatc(),
Temp_Critical, k, r, b, mw)
  Call VapEnthMartAsh(Temp(1), vol(1), Inth(1), mw, r, Temp_Critical, b, k, CEqStatA(),
CEqStatb(), CEqStatc(), CIdeCp(), IC)
  Call VapTherCondASH(Temp(1), TherCon(1), CVapTherCon())
  Call VapViscoASH(Temp(1), Visco(1), CVapViscos())
  Call IdealCp(CIdeCp(), mw, Temp(1), HeatCap(1))    'ideal Cp
  HeatCap(1) = HeatCap(1) * 1000
' Saturated vapour
  Press(2) = Press(1) - (Dp(1) / 1000000)
  Call SatTemperature(Press(2), Refrig$, CSatTemp(), CSatPress(), 0, Temp(2))
  Call VapSVolASH(Temp(2), Press(2), vol(2), CEqStatA(), CEqStatb(), CEqStatc(),
Temp_Critical, k, r, b, mw)
  Call VapEnthMartAsh(Temp(2), vol(2), Inth(2), mw, r, Temp_Critical, b, k, CEqStatA(),
CEqStatb(), CEqStatc(), CIdeCp(), IC)
  Call VapTherCondASH(Temp(2), TherCon(2), CVapTherCon())
  Call VapViscoASH(Temp(2), Visco(2), CVapViscos())
  Call VapCpASH(Temp(2), HeatCap(2), CVapCp())
' Saturated Liquid
  If Dp(2) > 1000000 Then
    Error_Flag = 20 ' pressure drop too high error message
    Exit Sub
  End If
  Press(3) = Press(2) - (Dp(2) / 1000000)
  Call SatTemperature(Press(3), Refrig$, CSatTemp(), CSatPress(), 0, Temp(3))
  Call LiqSVol(Temp(3), vol(3), CLiqDen())
  Call LiqEnthASH(Temp(3), Inth(3), CLiqEnth())
  Call LiqTherCondASH(Temp(3), TherCon(3), CLiqTherCon())
  Call LiqViscoASH(Temp(3), Visco(3), CLiqViscos())
  Call LiqCpASH(Temp(3), HeatCap(3), CliqCp())
' Subcooled Liquid
  Press(4) = Press(3) - (Dp(3) / 1000000)
  Temp(4) = Temp(3) - DT(2)
  Call LiqSVol(Temp(4), vol(4), CLiqDen())
  Call LiqEnthASH(Temp(4), Inth(4), CLiqEnth())
  Call LiqTherCondASH(Temp(4), TherCon(4), CLiqTherCon())
  Call LiqViscoASH(Temp(4), Visco(4), CLiqViscos())
  Call LiqCpASH(Temp(4), HeatCap(4), CliqCp())
Case "134a"
' Super heated vapour
Call SatPressure(T_Sat, Refrig$, CSatPress(), Press(1))
  If Error_Flag <> 0 Then Exit Sub
  Call VapSVolDUP(Temp(1), Press(1), vol(1), CEqStatA(), CEqStatb(), CEqStatc(),
Temp_Critical, k, r, b, mw, cc, u)
  Call VapEnthMartDUP(Temp(1), vol(1), Inth(1), mw, r, Temp_Critical, b, k, CEqStatA(),
CEqStatb(), CEqStatc(), CIdeCp(), IC)
  Call VapTherCondICI(Temp(1), TherCon(1), CVapTherCon())
  Call VapViscoICI(Temp(1), Visco(1), CVapViscos())

```

```

Call IdeialCp(CIdeCp(), mw, Temp(1), HeatCap(1))    'ideal Cp
HeatCap(1) = HeatCap(1) * 1000
' Saturated vapour
Press(2) = Press(1) - (Dp(1) / 1000000)
Call SatTemperature(Press(2), Refrig$, CSatTemp(), CSatPress(), 0, Temp(2))
Call VapSVolDUP(Temp(2), Press(2), vol(2), CEqStatA(), CEqStatb(), CEqStatc(),
Temp_Critical, k, r, b, mw, cc, u)
Call VapEnthMartDUP(Temp(2), vol(2), Inth(2), mw, r, Temp_Critical, b, k, CEqStatA(),
CEqStatb(), CEqStatc(), CIdeCp(), IC)
Call VapTherConDICI(Temp(2), TherCon(2), CVapTherCon())
Call VapViscoICI(Temp(2), Visco(2), CVapViscos())
Call VapCpASH(Temp(2), HeatCap(2), CVapCp())
' Saturated Liquid
If Dp(2) > 1000000 Then
    Error_Flag = 20 ' pressure drop too high error message
    Exit Sub
End If
Press(3) = Press(2) - (Dp(2) / 1000000)
Call SatTemperature(Press(3), Refrig$, CSatTemp(), CSatPress(), 0, Temp(3))
Call LiqSVol(Temp(3), vol(3), CLiqDen())
Call LiqEnthICI(Temp(3), Inth(3), Temp_Critical, CLiqEnth())
Call LiqTherConDICI(Temp(3), TherCon(3), Temp_Critical, CLiqTherCon())
Call LiqViscoICI(Temp(3), Visco(3), CLiqViscos())
Call LiqCpASH(Temp(3), HeatCap(3), CliqCp())
' Subcooled Liquid
Press(4) = Press(3) - (Dp(3) / 1000000)
Temp(4) = Temp(3) - DT(2)
Call LiqSVol(Temp(4), vol(4), CLiqDen())
Call LiqEnthICI(Temp(4), Inth(4), Temp_Critical, CLiqEnth())
Call LiqTherConDICI(Temp(4), TherCon(4), Temp_Critical, CLiqTherCon())
Call LiqViscoICI(Temp(4), Visco(4), CLiqViscos())
Call LiqCpASH(Temp(4), HeatCap(4), CliqCp())
Case "407c" 'condensing temp. taken on saturation vapour line
' Super heated vapour
Call Polynomial(CSatPress(1), CSatPress(2), CSatPress(3), CSatPress(4), CSatPress(5),
CSatPress(6), T_Sat, Press(1)) 'Sat_Vap_Press_
Press(1) = Press(1) / 10
Temp(1) = DT(1) + T_Sat
Call VapSVolDUP(Temp(1), Press(1), vol(1), CEqStatA(), CEqStatb(), CEqStatc(),
Temp_Critical, k, r, b, mw, cc, u)
Call VapEnthMartDUP(Temp(1), vol(1), Inth(1), mw, r, Temp_Critical, b, k, CEqStatA(),
CEqStatb(), CEqStatc(), CIdeCp(), IC)
Call Polynomial(CVapTherCon(1), CVapTherCon(2), CVapTherCon(3), 0, 0, 0, Temp(1),
TherCon(1)) 'SH_Vap_ Thermal Con_
Call Polynomial(CVapViscos(1), CVapViscos(2), CVapViscos(3), 0, 0, 0, Temp(1), Visco(1))
'VAPOUR VISCOSITY
Call Polynomial1(CIdeCp(1), CIdeCp(2), CIdeCp(3), CIdeCp(7), Temp(1), HeatCap(1)):
HeatCap(1) = HeatCap(1) * 1000
' Saturated vapour
Press(2) = Press(1) - (Dp(1) / 1000000)
Call Polynomial(CSatTemp(1), CSatTemp(2), CSatTemp(3), CSatTemp(4), 0, 0, Log(Press(2) *
10), Temp(2))' sat vap temp
Call Polynomial12(CVapVol(1), CVapVol(2), 0, CVapVol(3), CVapVol(4), CVapVol(5), 0,
Temp_Critical, Temp(2), vol(2))'SatVapVol_
vol(2) = 1 / vol(2)
Call VapEnthMartDUP(Temp(2), vol(2), Inth(2), mw, r, Temp_Critical, b, k, CEqStatA(),
CEqStatb(), CEqStatc(), CIdeCp(), IC)

```

```

    Call Polynomial11(CVapTherCon(4), CVapTherCon(5), CVapTherCon(6), CVapTherCon(7),
Temp(2), TherCon(2)) 'Sat. Vap. Thermal Con.
    Call Polynomial11(CVapViscos(4), CVapViscos(5), CVapViscos(6), CVapViscos(7), Temp(2),
Visco(2)) 'Sat. Vap. Viscos.
    Call Polynomial11(CIdeCp(1), CIdeCp(2), CIdeCp(3), CIdeCp(7), Temp(2), HeatCap(2)):
HeatCap(2) = HeatCap(2) * 1000
    ' Saturated Liquid
    If Dp(2) > 1000000 Then
        Error_Flag = 20 ' pressure drop too high error message
        Exit Sub
    End If
    Press(3) = Press(2) - (Dp(2) / 1000000)
    Call Polynomial(CSatTemp(5), CSatTemp(6), CSatTemp(7), CSatTemp(8), 0, 0, Log(Press(3) *
10), Temp(3))' sat liq temp
    T_m = (Temp(3) + Temp(2)) / 2
    Call Polynomial12(CLiqDen(1), CLiqDen(2), CLiqDen(3), CLiqDen(4), CLiqDen(5),
CLiqDen(6), CLiqDen(7), Temp_Critical, Temp(3), vol(3))'SatVapVol.
    vol(3) = 1 / vol(3)
    Call Polynomial12(CLiqEnth(1), CLiqEnth(2), 0, CLiqEnth(3), CLiqEnth(4), CLiqEnth(5), 0,
Temp_Critical, Temp(3), Inth(3))'SatLiqEnth.
    Call Polynomial11(CLiqTherCon(1), CLiqTherCon(2), CLiqTherCon(3), CLiqTherCon(4),
T_m, TherCon(3)) ' liq. Thermal.Con.
    Call Polynomial11(CLiqViscos(1), CLiqViscos(3), CLiqViscos(4), CLiqViscos(2), T_m,
Visco(3)) ' liq. Visco.
    Visco(3) = (Exp(Visco(3))) / 1000
    HeatCap(3) = 1000 * Abs((180 - Inth(3)) / (323.15 - Temp(3)))
    ' Subcooled Liquid
    Press(4) = Press(3) - (Dp(3) / 1000000)
    Call Polynomial(CSatTemp(5), CSatTemp(6), CSatTemp(7), CSatTemp(8), 0, 0, Log(Press(3) *
10), Temp(3))' sat liq temp
    Temp(4) = Temp(3) - DT(2)
    Call Polynomial12(CLiqDen(1), CLiqDen(2), CLiqDen(3), CLiqDen(4), CLiqDen(5),
CLiqDen(6), CLiqDen(7), Temp_Critical, Temp(4), vol(4))'SatVapVol.
    vol(4) = 1 / vol(4)
    Call Polynomial12(CLiqEnth(1), CLiqEnth(2), 0, CLiqEnth(3), CLiqEnth(4), CLiqEnth(5), 0,
Temp_Critical, Temp(4), Inth(4))'SatLiqEnth.
    TherCon(4) = TherCon(3)
    Visco(4) = Visco(3)
    HeatCap(4) = HeatCap(3)
Case Else
End Select
End Sub

Sub SatPressure (T1, Refrig$, CSatPress(), P1)
    On Error GoTo SatPress_Error
    ' Vapour pressure equation
    lap = CSatPress(1) + CSatPress(2) / T1 + CSatPress(3) / T1 ^ 2 + (CSatPress(4) * Log(T1) /
2.3025851) + CSatPress(5) * T1 + CSatPress(6) * T1 ^ 2 + CSatPress(7) * T1 ^ 3 + (CSatPress(8) *
(CSatPress(9) - T1) / T1) * (Log((CSatPress(9) - T1) * CSatPress(10))) / 2.3025851
    P1 = 10 ^ lap
    If Refrig$ = "134a" Or Refrig$ = "123" Then
        P1 = P1 / 1000 ' In the equation from DUPONT pressure In KPa
    End If
    Exit Sub
SatPress_Error:
    Error_Flag = 3
    Resume Next
End Sub

```

```

Sub SatTemperature (P1, Refrig$, CSatTemp(), CSatPress(), x, T1)
  If Refrig$ = "12" Or Refrig$ = "22" Or Refrig$ = "134a" Then
    Call Polynomial(CSatTemp(1), CSatTemp(2), CSatTemp(3), CSatTemp(4), CSatTemp(5),
CSatTemp(6), P1, T1)
    T1 = Kelvin(T1)
    Call SatPressure(T1, Refrig$, CSatPress(), P2)
    If Error_Flag <> 0 Then Exit Sub
    If P1 > P2 Then
      Do
        T1 = T1 + .1
        Call SatPressure(T1, Refrig$, CSatPress(), P2)
        If Error_Flag <> 0 Then Exit Sub
      Loop Until P1 <= P2
    ElseIf P1 < P2 Then
      Do
        T1 = T1 - .1
        Call SatPressure(T1, Refrig$, CSatPress(), P2)
        If Error_Flag <> 0 Then Exit Sub
      Loop Until P1 >= P2
    End If
    ElseIf Refrig$ = "407c" Then
      Call Polynomial(CSatTemp(1), CSatTemp(2), CSatTemp(3), CSatTemp(4), 0, 0, Log(P1 * 10),
Temp(2))' sat vap temp
      Call Polynomial(CSatTemp(5), CSatTemp(6), CSatTemp(7), CSatTemp(8), 0, 0, Log(P1 * 10),
Temp(3))' sat liq temp
      T1 = Temp(3) * (1 - x) + Temp(2) * x
    End If
  End Sub

```

[EVAPORAT.BAS]

```
' EVAPORATOR MODEL
' BY
' MAHMOUD ABU-MADI
' UNIVERSITY OF BRIGHTON
' 1997
' Version III
```

Sub D_Press_SH_Eva ()

```
' To calculate SH vapour pressure drop in plain tube (friction only)
' { no bends are considered }
v_SH_m = (Vol(1) + Vol(2)) / 2
' friction
If Re_SH < 1187 Then
  Frec_SH = 64 / Re_SH
ElseIf Re_SH < 100000 Then
  Frec_SH = .3164 / Re_SH ^ .25
Else
  Frec_SH = .0032 + .221 / Re_SH ^ .237
End If
If Opt > 14 Then ' case II
  D_P_SH_f = Gr ^ 2 * Frec_SH * L_SH * v_SH_m / (2 * dinhyd)
Else ' case I
  D_P_SH_f = Gr ^ 2 * Frec_SH * L_SH * v_SH_m / (2 * dinhyd * Nostream)
End If
' momentum
D_P_SH_m = Gr ^ 2 * (Vol(1) - Vol(2))
Dp(1) = D_P_SH_f + D_P_SH_m
End Sub
```

Sub D_Press_TP_Eva ()

```
On Error GoTo D_Press_TP_Eva_Error
' To calculate TP evaporating pressure drop { from Paliwoda equation }
' friction and bends
' Pressure drop in plain tubes with evaporating
' friction
ReDim S(2)
No_Tube_Row = CInt(Nostream * OvFins / Tube_Pitch)
If Opt > 14 Then ' case II
  L_TP_Tubes_Cir = L_TP
Else ' case I
  L_TP_Tubes_Cir = L_TP / Nostream
End If
No_of_Tube_Cir = No_Tube_Row * NoRows / Nostream
No_of_Bends_Cir = (No_of_Tube_Cir - 1)
L_TP_Bends_Cir = No_of_Bends_Cir * 3.1415927 * Tube_Pitch / 2
L_TP_Cir = L_TP_Tubes_Cir + L_TP_Bends_Cir
Theta = (Vol(3) / Vol(2)) * (Visco(3) / Visco(2)) ^ .25
If Error_Flag <> 0 Then Exit Sub
x = Xi
si = (-3 / 4) * (1 - x) ^ (4 / 3) * (Theta + 2 * (1 - Theta) * x) + ((1 / 4) * x ^ 4) - ((9 / 14) * (1 -
Theta) * ((1 - x) ^ (7 / 3)))
x = Xo
so = (-3 / 4) * (1 - x) ^ (4 / 3) * (Theta + 2 * (1 - Theta) * x) + ((1 / 4) * x ^ 4) - ((9 / 14) * (1 -
Theta) * ((1 - x) ^ (7 / 3)))
ss = so - si
Bm = ss / (Xo - Xi)
eps = Bm / (Xo - Xi) ^ (1.75)
```

```

Dp_TP_f = .1582 * eps * Gr ^ 1.75 * Vol(2) * Visco(2) ^ .25 * dinhyd ^ (-1.25) * L_TP_Cir
' momentum
Dp_TP_m = Gr ^ 2 * (Vol(2) - Vol(3))
' Return bends pressure drop with evaporating
If No_of_Bends_Cir > 0 Then
  fay = .19712
  Theta = (Vol(3) / Vol(2))
  ' No of ( 180') bends / cir. = No of tubes per circuit - 1
  ' No of tube per circuit =[No of rows * No of tubes per row] / No of circuit
  x = Xo
  S(x) = ((3 * Theta / 2) - (9 / 4)) * (1 - x) ^ (4 / 3) + (9 / 7) * (1 - Theta) * (1 - x) ^ (7 / 3) + (x ^
(3.276)) / 3.276
  x = Xi
  S(x) = ((3 * Theta / 2) - (9 / 4)) * (1 - x) ^ (4 / 3) + (9 / 7) * (1 - Theta) * (1 - x) ^ (7 / 3) + (x ^
(3.276)) / 3.276
  ss = S(Xo) - S(Xi)
  Bm = ss / (Xo - Xi)
  Dp_TP_bend = Gr ^ 2 * Vol(2) * .5 * No_of_Bends_Cir * fay * Bm
Else
  Dp_TP_bend = 0
End If
Dp(2) = Dp_TP_f + Dp_TP_bend + Dp_TP_m
' outlet manifold
DpHv = .5 * Vol(1) * 2.8 * Gr ^ 2
Exit Sub
D_Press_TP_Eva_Error:
  Error_Flag = 17
  Exit Sub
End Sub

Sub Duties_eva (DT(), Xi, Inth(), ReqDis, HeatCap(), Acs, mr, Gr, Q_SH, Q_TP1, Q_SC,
C_Ref_SH)
' To calculate evaporator ReqDis from TP & SH
If DT(1) > 0 Then
  mr = 1000 * ReqDis / ((1000 * (Inth(2) - Inth(3)) * (1 - Xi)) + 1000 * (Inth(1) - Inth(2)))
  Q_TP1 = 1000 * (Inth(2) - Inth(3)) * mr * (1 - Xi)
  Q_SH = 1000 * (Inth(1) - Inth(2)) * mr
Else
  Q_SH = 0
  mr = ReqDis * 1000 / (1000 * (Inth(2) - Inth(3)) * (1 - Xi))
  Q_TP1 = ReqDis * 1000
End If
Gr = mr / Acs
C_Ref_SH = mr * (HeatCap(2) + HeatCap(1)) / 2
End Sub

Sub E_NTU_SH_II (Opt, NoRows_I, Taout_SH, win)
' To calculate SH vapour heat transfer area for air with max. or
' min. heat capacity CASE I for Evaporator
8 BTWHEAD_SH_ASS = BtwHead
m_air_SH = BTWHEAD_SH_ASS * OvFins * Dens_air * Vel_Air
C_Air_SH = m_air_SH * (Cp_Air + win * 1805)
C_SH = C_Ref_SH / C_Air_SH
If C_SH < 1 Then
  Call ENTU_SH_R_II(Opt, NoRows_I, Taout_SH) ' C_air_SH = C_max
Else
  C_SH = C_Air_SH / C_Ref_SH ' C_air_SH = C_min
  Call ENTU_SH_A_II(Opt, NoRows_I, Taout_SH, win)

```



```

End If
End Sub

Sub E_NTU_TP_S_L_i (win)
  On Error GoTo E_NTU_TP_S_L_i_Error
  ' To design the evaporator as row by row considering heat and mass
  ' transfer and the variation in surface temperature
  ' for a given face area and inlet air temperature
  DTS = NDTS
12  jj = 0
  Tsur = Trm + DTS
  ' assuming Surface Temp. = Refrig_Temp_ + 1
  h_s_1 = STEAM_enth(Tain2): Pwsur = STEAM_PRESS(Tsur)
  Wsur = Wsat(Pwsur): m_air = BtwHead_SH_E * OvFins * Dens_air * Vel_Air
  Vol_flo = BtwHead_SH_E * OvFins * Vel_Air: DWT = (win - Wsur) / (Tain2 - Tsur)
  DTi = .7
10  Ti = Tain2 - DTi: DW = DWT * (Tain2 - Ti)
  If Wsur >= win Then          ' heat transfer only
    Wi = win
  Else
    Wi = win - DW
    Pwall = STEAM_PRESS(Ti)
    If Error_Flag <> 0 Then Exit Sub
    Wwall = Wsat(Pwall)
    If Wi >= Wwall Then Wi = Wwall
  End If
  Cp_mix = (Cp_Air + win * 1805)
  Pw = Wi * 101.325 / (Wi + .62198)
  Pws = STEAM_PRESS(Ti)
  Wsdb = Wsat(Pws)
  meu = Wi / Wsdb
  fay1 = meu / (1 - (1 - meu) * (Pws / 101.325))
  ifg_air = STEAM_enth(Tain2) - water_enth(Tain2)
  h_w = water_enth(Tsur): h_s_i = STEAM_enth(Ti)
  Qsl = m_air * Cp_mix * (Tain2 - Ti)
  ha1 = Tain2 + win * (2501.3 + 1.86 * Tain2)
  ha2 = Ti + Wi * (2501.3 + 1.86 * Ti)
  Qsl = m_air * (ha1 - ha2) * 1000
  Taout = Ti
  W2 = Wi
  lmtD = ((Tain2 - Temp(3)) - (Taout - Temp(2))) / Log((Tain2 - Temp(3)) / (Taout - Temp(2)))
  If Wsur >= win Then
    Q_W = 0
    C = 0
    Lmwd = 0
  Else
    Q_W = m_air * (win - W2) * h_w * 1000
  End If
  Q_S_L = Qsl - Q_W
  ifg_air = STEAM_enth(Tain2) - water_enth(Tain2)
  C = DWT
  mm_sl = Sqr(2 * ha * (1 + C * ifg_air / (.9 * Cp_mix))) / (Fth * FinCond)
  Ef_sl = (Exp(mm_sl * ll) - Exp(-mm_sl * ll)) / (mm_sl * ll * (Exp(mm_sl * ll) + Exp(-mm_sl * ll)))
  R1_sl = 1 / (1 - R7 * (1 - Ef_sl))
  uu_TP_sl = (R1_sl / (ha * (1 + ifg_air * C / (.9 * Cp_mix)))) + (R3 / htpm)
  Uall_tp_sl = 1 / uu_TP_sl
  If Error_Flag <> 0 Then Exit Sub
  Atot = Q_S_L / (Uall_tp_sl * (Tain2 - Temp(2)))

```

```

NoRows_TP_Sl = Atot / (OvFins * BtwHead_SH_E * R51)
If NoRows_TP_Sl > 1.05 Or NoRows_TP_Sl < .95 Then
  DTi = DTi / NoRows_TP_Sl
  GoTo 10
End If
NDTS = Q_S_L / (htpm * Atot / R3)
If Abs(DTS - NDTS) > .2 Then
  DTS = (DTS + NDTS) / 2
End If
GoTo 11
7676
jj = jj + 1
If jj > 15 And jj <= 25 Then
  GrFac = .7
ElseIf jj > 25 Then
  GrFac = .1
Else
  GrFac = 1
End If
If NoRows_TP_Sl < .6 Or NoRows_TP_Sl > 1.4 Then
  ADD = 1 * GrFac
ElseIf NoRows_TP_Sl < .85 Or NoRows_TP_Sl > 1.15 Then
  ADD = .6 * GrFac
Else
  ADD = .1 * GrFac
End If
If NoRows_TP_Sl > 1.05 Then
  DTi = DTi - ADD
  GoTo 10
ElseIf NoRows_TP_Sl < .95 Then
  DTi = DTi + ADD
  GoTo 10
Else
  End If
'LOOP UNTIL ABS(1 - NoRows_TP_Sl) < .1
NDTS = Q_S_L / (htpm * Atot / R3)
If (NDTS / 2) > DTS Then
  DTS = NDTS * 1 / 2
  GoTo 12
ElseIf NDTS > (DTS + 3) Then
  DTS = DTS + Abs(NDTS - DTS) / 2
  GoTo 12
ElseIf NDTS > (DTS + .5) Then
  DTS = DTS + Abs(NDTS - DTS) / 2
  GoTo 12
ElseIf NDTS < (DTS - .1) Then
  DTS = DTS - Abs(NDTS - DTS) / 2
  GoTo 12
Else
  End If
11 Fay_out = Pw / Pws
Exit Sub
E_NTU_TP_S_L_i_Error:
Error_Flag = 13
Resume Next
End Sub

Sub E_NTU_TP_S_L_iii (win)

```

```

' To design the evaporator as row by row considering heat and mass
' transfer and the variation in surface temperature
' for a given face area and inlet air temperature
' Tain2 and Q_TP_E from the first row (with SH and TP)
NoRows = 0
Q_TP_E1 = Q_TP1
Trm = (Temp(3) + Temp(2)) / 2
13 Call E_NTU_TP_S_L_i(win)
Q_TP_E1 = Q_TP_E1 - Q_S_L
If Q_TP_E1 > 0 Then
  NoRows = NoRows + 1
  Tain2 = Ti
  win = Wi
  BtwHead_SH_E = BtwHead
  GoTo 13
Else
End If
' NoRows is completed number of rows
NoRows_TP = NoRows + ((Q_TP_E1 + Q_S_L) / Q_S_L)
If NoRows_SH >= 1 Then
  NoRows = NoRows_TP + Int(NoRows_SH)
Else
  NoRows = NoRows_TP
End If
Taout = Tain2 - (Tain2 - Ti) * (Q_S_L + Q_TP_E1) / Q_S_L
Waout = win - (win - Wi) * (Q_S_L + Q_TP_E1) / Q_S_L
Pws = STEAM_PRESS(Taout)
Pw = Waout * 101.325 / (Waout + .62198)
Fay_out = Pw / Pws
TL_cal_1 = R51 * (BtwHead - BtwHead_SH) * OvFins / (dinhyd * 3.1415927 * R3)
TL_cal_2 = (NoRows - 1) * R51 * OvFins * BtwHead / (dinhyd * 3.1415927 * R3)
L_TP = TL_cal_1 + TL_cal_2
End Sub

Sub E_NTU_TP_S_L_iiii (win)
' To design the evaporator as WHOLE COIL considering heat and mass
' transfer and the variation in surface temperature
' for a given face area and inlet air temperature
Trm = (Temp(3) + Temp(2)) / 2
Call air(AirInlet, Tainw1, TDP, win, Wsdb, Wswb, PwsDP)
hai = ((AirInlet - 273.15) + win * (2501.3 + 1.86 * (AirInlet - 273.15))) * 1000'nnnnnnn
Call AIR_PROP(AirInlet, Dens_air, Cp_Air)
ifg_air = STEAM_enth(AirInlet) - water_enth(AirInlet)
Cp_mix = (Cp_Air + win * 1805)
mm = Sqr(2 * hai / (Fth * FinCond))
ef = (Exp(mm * ll) - Exp(-mm * ll)) / (mm * ll * (Exp(mm * ll) + Exp(-mm * ll)))
R1 = 1 / (1 - R7 * (1 - ef))
uu_1 = (R1 / ha) + (R3 / htpm)
Uall = 1 / uu_1
' As whole coil
Aair = Q_TP1 / (Uall * (AirInlet - Temp(3)))
BtwHead_TP = Aair / (R51 * OvFins * NoRows)
Ain = Aair / R3
Ts = Q_TP1 / (Ain * htpm) + Temp(3)
Pws = STEAM_PRESS(Ts)
Ws = Wsat(Pws)
14 C1 = (win - Ws) / (AirInlet - Ts)
mm_sl = Sqr(2 * hai * (1 + C1 * ifg_air / (.9 * Cp_mix))) / (Fth * FinCond))

```

```

Ef_sl = (Exp(mm_sl * ll) - Exp(-mm_sl * ll)) / (mm_sl * ll * (Exp(mm_sl * ll) + Exp(-mm_sl * ll)))
R1_sl = 1 / (1 - R7 * (1 - Ef_sl))
uu_1 = (R1_sl / (ha * (1 + ifg_air * C1 / (.9 * Cp_mix)))) + (R3 / htpm)
Uall = 1 / uu_1
Aair = Q_TP1 / (Uall * (AirInlet - Temp(3)))
BtwHead_TP = Aair / (R51 * OvFins * NoRows)
Ain = Aair / R3
Ts = Q_TP1 / (Ain * htpm) + Temp(3)
Pws = STEAM_PRESS(Ts)
Wss = Wsat(Pws)
If Abs(Wss - Ws) > .0001 Then
    Ws = Wss
    GoTo 14
End If
Ws = Wss
hs = ((Ts - 273.15) + Ws * (2501.3 + 1.86 * (Ts - 273.15))) * 1000
C2 = (hai - hs) / (AirInlet - Ts)
m_air = Vel_Air * OvFins * BtwHead_TP
h_w = water_enth(Tsur) * 1000
If Ws >= win Then
    Dhaio = Q_TP1 / m_air
Else
    Dhaio = Q_TP1 / (m_air * (1 + h_w * C1 / C2))
End If
dTao = Dhaio / C2
Taout = AirInlet - dTaio
DWio = C1 * dTaio
Waout = win - DWio
Pws = STEAM_PRESS(Taout)
Pw = Waout * 101.325 / (Waout + .62198)
Fay_out = Pw / Pws
L_TP = Ain / (Nostream * 3.14 * dinhyd)
End Sub

```

Sub EVAPORATOR_A ()

```

' Programme for evaporator design Case I & Case II
' Input face area and refrigerant flux
Orig_Rows = NoRows
Fay_out = 0
L_SH_P = 0
L_TP_P = 0
Call read_prop(Refrig$, CEqStatA(), CEqStatb(), CEqStatc(), k, u, cc, r, b, mw, Temp_Critical,
PressCritical, ffl, CSatPress(), CLiqDen(), CVapVol(), CIdeCp(), IC, CVapViscos(), CLiqViscos(),
CVapTherCon(), CLiqTherCon(), CVapCp(), CliqCp(), CLiqEnth(), CSatTemp())
Call Ref_Proper_eva(Refrig$, T_Sat, DT(), PRESS(), Vol(), Inth(), Visco(), TherCon(), HeatCap(),
CEqStatA(), CEqStatb(), CEqStatc(), k, u, cc, r, b, mw, Temp_Critical, PressCritical, ffl, CSatPress(),
CLiqDen(), CIdeCp(), CVapViscos(), CLiqViscos(), CVapTherCon(), CLiqTherCon(), CVapCp(),
CliqCp(), CLiqEnth(), CSatTemp())
If Opt = 11 Or Opt = 12 Or Opt = 15 Or Opt = 16 Or Opt = 19 Or Opt = 31 Or Opt = 32 Or Opt =
35 Or Opt = 36 Or Opt = 39 Then
    NoRows_ass = 1
Else
    NoRows_ass = NoRows
    BtwHead = .2' assumption
End If
NoRows = NoRows_ass
If Opt < 30 Then ' round tube coil
    Call AIR_PROP(AirInlet, Dens_air, Cp_Air)

```

```

TL = 5
NDTS = 10
Call read_Geomtry(AirInlet, win, Vel_Air, ConfigType, dinhyd, dout, FinPtch, FperM, fs, Fth,
Tube_Pitch, Rsp, R3, R4, R51, R6, R7, R8, ll, fFactor, ha, Acs_T, Orig_Rows)
If Error_Flag <> 0 Then Exit Sub
If Opt > 14 Then 'Opt = 15 Or Opt = 16 Or Opt = 17 Or Opt = 18 Then ' case II
    OvFins = OvFins / Nostream ' per circuits
    Acs = Acs_T
    ReqDis = ReqDis / Nostream ' per circuits
Else ' case I
    Acs = Acs_T * Nostream
End If
If Opt = 19 Then
    ReqDis = .05 ' KW rating assumed as case II
End If
Call Duties_eva(DT(), Xi, Inth(), ReqDis, HeatCap(), Acs, mr, Gr, Q_SH, Q_TP1, Q_SC,
C_Ref_SH) ' even numbers for ReqDis
Else
    For I = 1 To 100 'for parallel flow evaporator and not for develop
        NC(I) = Nostream
    Next I
    Call R345Parallel(Tube_high, Tube_wide, Tth, L_chanel_1, L_chanel_2, No_Chanel, Fth, F_h,
row_space, FinPitch, Acs_T, R3, R4, R51, R6, R7, R8, ll, dinhyd, Tube_Pitch, Orig_Rows)
    Acs = Acs_T * Nostream ' assuming Nostreams to be constant
    If Opt = 39 Then ReqDis = .05 ' KW rating
    Call Duties_eva(DT(), Xi, Inth(), ReqDis, HeatCap(), Acs, mr, Gr, Q_SH, Q_TP1, Q_SC,
C_Ref_SH) ' even numbers for ReqDis
End If
If Opt < 30 Then Call Non_Dim_No_Eva(win)' round tube coil
16 If Opt > 14 Then ' case II
    Call fin_length_IIII
Else ' case I
    Call fin_length_IIII
End If
DTL = Abs(L_TP - TL)
If Abs(DTL_old - DTL) < .05 Then GoTo 15
If DTL > .01 Then
    DTL_old = DTL
    TL = Abs(TL + L_TP) / 2
    GoTo 16
End If
15 If Opt = 13 Or Opt = 14 Or Opt = 17 Then 'or Opt = 18 Then
    BtwHead = BtwHead_CAL
ElseIf Opt = 19 Then
    NoRow_calc_New = NoRows
    If Orig_Rows > NoRow_calc_New Then 'Orig_Rows = NoRows
        ReqDis_New = ReqDis * Orig_Rows / NoRows
        Delta_ReqDis = ReqDis_New - ReqDis
        ReqDis = ReqDis_New
        NoRow_calc_old = NoRows
        Call Duties_eva(DT(), Xi, Inth(), ReqDis, HeatCap(), Acs, mr, Gr, Q_SH, Q_TP1, Q_SC,
C_Ref_SH)
        Call Non_Dim_No_Eva(win)
        GoTo 16
    End If
    ReqDis = ReqDis - Delta_ReqDis * (NoRow_calc_New - Orig_Rows) / (NoRow_calc_New -
NoRow_calc_old)
ElseIf Opt > 30 Then 'PFE

```

```

GoTo 17
ElseIf Opt = 18 Then ' calculate No. of Rows
  DNR = Abs(Orig_Rows - NoRows)
  If DNR > .1 Then
    BtwHead = BtwHead * NoRows / Orig_Rows
    GoTo 16
  End If
End If
If Opt < 15 Then ' case I
  AF_tot = AF_TP1 + AF_SH + AF_SC
  R5 = R51 * NoRows
  L_SH = (AF_SH * R5) / (3.1415927 * dinhyd * R3)
  L_TP = (AF_TP1 * R5) / (3.1415927 * dinhyd * R3)
Else ' case II
  If DT(1) > 0 Then L_SH = (BtwHead * OvFins * R51 * NoRows_SH) / (3.1415927 * dinhyd *
R3) ' caseII
  End If
  If Opt < 30 Then ' Round tube coil
    Call D_Press_TP_Eva
    If DT(1) > 0 Then Call D_Press_SH_Eva
    DL_SH = Abs(L_SH - L_SH_P)
    DL_TP = Abs(L_TP - L_TP_P)
    If DL_TP > .05 Or DL_SH > .01 Then
      L_SH_P = L_SH
      L_TP_P = L_TP
      Call Ref_Proper_eva(Refrig$, T_Sat, DT(), PRESS(), Vol(), Inth(), Visco(), TherCon(),
HeatCap(), CEqStatA(), CEqStatb(), CEqStatc(), k, u, cc, r, b, mw, Temp_Critical, PressCritical, ffl,
CSatPress(), CLiqDen(), CIdeCp(), CVapViscos(), CLiqViscos(), CVapTherCon(), CLiqTherCon(),
CVapCp(), CliqCp(), CLiqEnth(), CSatTemp())
      If Opt = 11 Or Opt = 13 Or Opt = 15 Or Opt = 17 Then
        Call fluxses_Eva(Gr, Acs, Inth(), HeatCap(), Xi, mr, ReqDis, Q_SH, Q_TP1, C_Ref_SH,
C_Ref_SC)
      Else
        Call Duties_eva(DT(), Xi, Inth(), ReqDis, HeatCap(), Acs, mr, Gr, Q_SH, Q_TP1, Q_SC,
C_Ref_SH) ' even numbers for ReqDis
      End If
      Call Non_Dim_No_Eva(win)
      GoTo 16
    Else
      DP_tot = Dp(1) + Dp(2)
    End If
  End If
  If Opt > 14 Then 'Opt = 15 Or Opt = 16 Or Opt = 17 Or Opt = 18 Then ' case II
    OvFins = OvFins * Nostream
    ReqDis = ReqDis * Nostream
    mr = mr * Nostream
  End If
17 ' to calculate Twb from Tdb, W and Fay
  Twbout = Taout
18 Pswb = STEAM_PRESS(Twbout)
  Wswb = Wsat(Pswb)
  Wcal = WAIR(Taout, Twbout, Wswb)
  If Wcal > Waout Then
    Twbout = Twbout - .1
    GoTo 18
  End If
  Call D_Press_Air(AirInlet, Taout, fFactor, Vel_Air, R4, R51, NoRows, Dpa)
  kk = Fay_out

```

End Sub

Sub fin_length_IIII ()

```
' Evaporator design model CASE II as row-by-row *
' to calculate dew point Temp. and check if condensing
' will occur
Call air(AirInlet, Tainw1, TDP, win, Wsdb, Wswb, PwsDP)
BtwHead_SH = BtwHead
If DT(1) > 0 Then
  Call E_NTU_SH_I(Opt, Taout_SH, R51, NoRows_ass, Uall_SH, DTM_SH, Temp(), AirInlet,
Q_SH, Cp_Air, Dens_air, win, Vel_Air, OvFins, BtwHead_SH, C_Ref_SH)
  NoRows_SH = BtwHead_SH / BtwHead
  Tain2 = AirInlet
  If NoRows_SH > 1 Then
    Call E_NTU_SH_II(Opt, NoRows_SH, Taout_SH, win)
    BtwHead_SH = BtwHead * (NoRows_SH - Int(NoRows_SH))
    Tain2 = Taout_SH
  End If
Else
  BtwHead_SH = 0
  Tain2 = AirInlet
End If
BtwHead_SH_E = BtwHead - BtwHead_SH
Call E_NTU_TP_S_L_iii(win)
End Sub
```

Sub fin_length_IIIII ()

```
' Evaporator design model CASE I as whole *
' to calculate dew point Temp. and check if condensing
' will occur
Call air(AirInlet, Tainw1, TDP, win, Wsdb, Wswb, PwsDP)
Call E_NTU_TP_S_L_iiii(win)
BtwHead_SH = 0
BtwHead_CAL = BtwHead_TP + BtwHead_SH
End Sub
```

Sub fluxes_Eva (Gr, Acs, Inth(), HeatCap(), Xi, mr, ReqDis, Q_SH, Q_TP, C_Ref_SH, C_Ref_SC)

```
' To calculate evaporator ReqDis from TP & SH and refrigerant flux
mr = Gr * Acs
Q_TP = 1000 * (Inth(2) - Inth(3)) * mr * (1 - Xi)
If DT(1) > 0 Then
  Q_SH = 1000 * (Inth(1) - Inth(2)) * mr
Else
  Q_SH = 0
End If
ReqDis = (Q_SH + Q_TP) / 1000
C_Ref_SH = mr * (HeatCap(2) + HeatCap(1)) / 2
C_Ref_SC = mr * (HeatCap(4) + HeatCap(3)) / 2
End Sub
```

Sub Non_Dim_No_Eva (win)

```
On Error GoTo Non_Dim_No_Eva_Error
Call air(AirInlet, Tainw1, TDP, win, Wsdb, Wswb, PwsDP)
ifg_air = STEAM_enth(AirInlet) - water_enth(AirInlet)
Pii = STEAM_PRESS(Temp(3))
Wii = Wsat(Pii)
Cp_mix = Cp_Air + win * 1805
C = (win - Wii) / (AirInlet - Temp(3))
```

```

mm = Sqr(2 * ha / (Fth * FinCond))
mm_sl = Sqr(2 * ha * (1 + C * ifg_air / Cp_mix) / (Fth * FinCond))
ef = (Exp(mm * ll) - Exp(-mm * ll)) / (mm * ll * (Exp(mm * ll) + Exp(-mm * ll)))
Ef_sl = (Exp(mm_sl * ll) - Exp(-mm_sl * ll)) / (mm_sl * ll * (Exp(mm_sl * ll) + Exp(-mm_sl * ll)))
R1 = 1 / (1 - R7 * (1 - ef))
R1_sl = 1 / (1 - R7 * (1 - Ef_sl))
m_SH_m = (Visco(1) + Visco(2)) / 2
k_SH_m = (TherCon(1) + TherCon(2)) / 2
v_SH_m = (Vol(1) + Vol(2)) / 2
Cp_SH_m = (HeatCap(1) + HeatCap(2)) / 2
Re_SH = Gr * dinhyd / m_SH_m
Re_v = Gr * dinhyd / Visco(2)
Re_L = Gr * dinhyd / Visco(3)
Pr_SH = m_SH_m * Cp_SH_m / k_SH_m
Pr_V = Visco(2) * HeatCap(2) / TherCon(2)
Pr_L = Visco(3) * HeatCap(3) / TherCon(3)
PressRatio = PRESS(2) / PressCritical
' Heat transfer coefficient for refrigerant
hSH = .023 * Re_SH ^ .8 * Pr_SH ^ .3 * TherCon(1) / dinhyd
Q = Q_TP1 / (3.14 * dinhyd * TL)
Bo = Q / (Gr * ifg_ref)
hl = .023 * Re_L ^ .8 * Pr_L ^ .3 * TherCon(3) / dinhyd
' Kandlikar integrated correlation
C1 = .6683 * (Vol(3) / Vol(2)) ^ (-.1) * hl
C2 = 1058 * Bo ^ .7 * ffl * hl
c3 = 1.136 * (Vol(3) / Vol(2)) ^ (-.45) * hl
c4 = 667.2 * Bo ^ .7 * ffl * hl
ReDim A1(10), B1(10), A2(10)
x = Xo
A1(x) = .86 * x ^ 1.16 - .296 * x ^ 2.16 - .036 * x ^ 3.16 - .012 * x ^ 4.16
B1(x) = -.55 * (1 - x) ^ 1.8
A2(x) = .58 * x ^ 1.72 - .029 * x ^ 2.72 - dinhyd * x ^ 3.72
x = Xi
A1(x) = .86 * x ^ 1.16 - .296 * x ^ 2.16 - .036 * x ^ 3.16 - .012 * x ^ 4.16
B1(x) = -.55 * (1 - x) ^ 1.8
A2(x) = .58 * x ^ 1.72 - .029 * x ^ 2.72 - dinhyd * x ^ 3.72
aa1 = A1(Xo) - A1(Xi)
bb = B1(Xo) - B1(Xi)
aa2 = A2(Xo) - A2(Xi)
hitp1 = (C1 * aa1 + C2 * bb) / (1 - Xi)
hitp2 = (c3 * aa2 + c4 * bb) / (1 - Xi)
If hitp1 > hitp2 Then
    hitpm = hitp1
Else
    hitpm = hitp2
End If
' superheat
If DT(1) > 0 Then
    uu_SH = (R1 / ha) + (R3 / hSH)
    Uall_SH = 1 / uu_SH
End If
' two-phase
uu_TP = (R1 / ha) + (R3 / hitpm)
Uall_tp = 1 / uu_TP
uu_TP_sl = (R1_sl / (ha * (1 + ifg_air * C / Cp_mix))) + (R3 / hitpm)
Uall_tp_sl = 1 / uu_TP_sl
ha_m = ha / Cp_mix
DTM_SH = AirInlet - Temp(2)

```



```

If Refrig$ = "407c" Then
  DTM_TP = AirInlet - (Temp(2) + Temp(3)) / 2
Else
  DTM_TP = AirInlet - Temp(2)
End If
Exit Sub
Non_Dim_No_Eva_Error:
  Error_Flag = 12
  Resume Next
End Sub

Sub Ref_Proper_eva (Refrig$, T_Sat, DT(), PRESS(), Vol(), Inth(), Visco(), TherCon(), HeatCap(),
CEqStatA(), CEqStatb(), CEqStatc(), k, u, cc, r, b, mw, Temp_Critical, PressCritical, ffl, CSatPress(),
CLiqDen(), CIdeCp(), CVapViscos(), CLiqViscos(), CVapTherCon(), CLiqTherCon(), CVapCp(),
CliquCp(), CLiqEnth(), CSatTemp())
  Select Case Refrig$
  Case "12"
    ' Two-Phase at the inlet SATURATION LIQUID
    Call SatPressure(T_Sat, Refrig$, CSatPress(), PRESS(3))
    If Error_Flag <> 0 Then Exit Sub
    Call LiqEnthASH(Temp(3), Inth(3), CLiqEnth())
    Call LiqSVol(Temp(3), Vol(3), CLiqDen())
    Call LiqTherCondASH(Temp(3), TherCon(3), CLiqTherCon())
    Call LiqViscoASH(Temp(3), Visco(3), CLiqViscos())
    Call LiqCpASH(Temp(3), HeatCap(3), CliquCp())
    ' Saturated vapour
    If Dp(2) > 1000000 Then
      Error_Flag = 20
      Exit Sub
    End If
    PRESS(2) = PRESS(3) - (Dp(2) / 1000000)
    Call SatTemperature(PRESS(2), Refrig$, CSatTemp(), CSatPress(), x, Temp(2))
    Call VapSVolASH(Temp(2), PRESS(2), Vol(2), CEqStatA(), CEqStatb(), CEqStatc(),
Temp_Critical, k, r, b, mw)
    Call VapEnthMartAsh(Temp(2), Vol(2), Inth(2), mw, r, Temp_Critical, b, k, CEqStatA(),
CEqStatb(), CEqStatc(), CIdeCp(), IC)
    Call VapTherCondASH(Temp(2), TherCon(2), CVapTherCon())
    Call VapViscoASH(Temp(2), Visco(2), CVapViscos())
    Call VapCpASH(Temp(2), HeatCap(2), CVapCp())
    ifg_ref = (Inth(2) - Inth(3)) * 1000
    ' Super heated vapour
    PRESS(1) = PRESS(2) - (Dp(1) / 1000000)
    Temp(1) = Temp(2) + DT(1)
    Call VapSVolASH(Temp(1), PRESS(1), Vol(1), CEqStatA(), CEqStatb(), CEqStatc(),
Temp_Critical, k, r, b, mw)
    Call VapEnthMartAsh(Temp(1), Vol(1), Inth(1), mw, r, Temp_Critical, b, k, CEqStatA(),
CEqStatb(), CEqStatc(), CIdeCp(), IC)
    Call VapTherCondASH(Temp(1), TherCon(1), CVapTherCon())
    Call VapViscoASH(Temp(1), Visco(1), CVapViscos())
    Call IdeialCp(CIdeCp(), mw, Temp(1), HeatCap(1)) 'ideal Cp
    HeatCap(1) = HeatCap(1) * 1000
  Case "22"
    ' Saturated Liquid
    Call SatPressure(T_Sat, Refrig$, CSatPress(), PRESS(3))
    If Error_Flag <> 0 Then Exit Sub
    Call LiqEnthASH(Temp(3), Inth(3), CLiqEnth())
    Call LiqSVol(Temp(3), Vol(3), CLiqDen())
    Call LiqEnthASH(Temp(3), Inth(3), CLiqEnth())
  
```



```

Call VapEnthMartDUP(Temp(1), Vol(2), Inth(1), mw, r, Temp_Critical, b, k, CEqStatA(),
CEqStatb(), CEqStatc(), CIdeCp(), IC)
Call VapTherConICI(Temp(1), TherCon(1), CVapTherCon())
Call VapViscoICI(Temp(1), Visco(1), CVapViscos())
Call IdeialCp(CIdeCp(), mw, Temp(1), HeatCap(1))    'ideal Cp
HeatCap(1) = HeatCap(1) * 1000
Case "407c"
' Tow-Phase at the inlet Saturated Liquid
Temp(2) = T_Sat
Call Polynomial(CSatPress(1), CSatPress(2), CSatPress(3), CSatPress(4), CSatPress(5),
CSatPress(6), T_Sat, PRESS(2)) 'Sat_Vap_Press_
PRESS(2) = PRESS(2) / 10
If Dp(2) > 1000000 Then
    Error_Flag = 20
    Exit Sub
End If
PRESS(3) = PRESS(2) + (Dp(2) / 1000000) ' DPtp is added to the sat. vap. pressure to
determined the sat. liq. press.
Call Polynomial(CSatTemp(5), CSatTemp(6), CSatTemp(7), CSatTemp(8), 0, 0, Log(PRESS(3)
* 10), Temp(3)) ' sat liq. temp
T_m = (Temp(3) + Temp(2)) / 2
Call Polynomial12(CLiqDen(1), CLiqDen(2), CLiqDen(3), CLiqDen(4), CLiqDen(5),
CLiqDen(6), CLiqDen(7), Temp_Critical, Temp(3), Vol(3)) 'SatLiqVol.
Vol(3) = 1 / Vol(3)
Call Polynomial12(CLiqEnth(1), CLiqEnth(2), 0, CLiqEnth(3), CLiqEnth(4), CLiqEnth(5), 0,
Temp_Critical, Temp(3), Inth(3)) 'SatLiqEnth.
Call Polynomial11(CLiqTherCon(1), CLiqTherCon(2), CLiqTherCon(3), CLiqTherCon(4),
T_m, TherCon(3)) ' liq. Thermal.Con.
Call Polynomial11(CLiqViscos(1), CLiqViscos(3), CLiqViscos(4), CLiqViscos(2), T_m,
Visco(3)) ' liq. Visco.
Visco(3) = (Exp(Visco(3))) / 1000
HeatCap(3) = 1000 * Abs((180 - Inth(3)) / (323! - Temp(3)))
' Saturated vapour
Call Polynomial12(CVapVol(1), CVapVol(2), 0, CVapVol(3), CVapVol(4), CVapVol(5), 0,
Temp_Critical, Temp(2), Vol(2)) 'Sat VapVol.
Vol(2) = 1 / Vol(2)
Call VapEnthMartDUP(Temp(2), Vol(2), Inth(2), mw, r, Temp_Critical, b, k, CEqStatA(),
CEqStatb(), CEqStatc(), CIdeCp(), IC)
Call Polynomial11(CVapTherCon(4), CVapTherCon(5), CVapTherCon(6), CVapTherCon(7),
Temp(2), TherCon(2)) 'Sat. Vap. Thermal Con.
Call Polynomial11(CVapViscos(4), CVapViscos(5), CVapViscos(6), CVapViscos(7), Temp(2),
Visco(2)) 'Sat. Vap. Viscous.
Call Polynomial11(CIdeCp(1), CIdeCp(2), CIdeCp(3), CIdeCp(7), Temp(2), HeatCap(2)):
HeatCap(2) = HeatCap(2) * 1000
ifg_ref = (Inth(2) - Inth(3)) * 1000
' Super heated vapour
PRESS(1) = PRESS(2) - (Dp(1) / 1000000)
Temp(1) = Temp(2) + DT(1)
Call VapSVolDUP(Temp(1), PRESS(1), Vol(1), CEqStatA(), CEqStatb(), CEqStatc(),
Temp_Critical, k, r, b, mw, cc, u)
Call VapEnthMartDUP(Temp(1), Vol(1), Inth(1), mw, r, Temp_Critical, b, k, CEqStatA(),
CEqStatb(), CEqStatc(), CIdeCp(), IC)
Call Polynomial(CVapTherCon(1), CVapTherCon(2), CVapTherCon(3), 0, 0, 0, Temp(1),
TherCon(1)) 'SH. Vap. Thermal Con.
Call Polynomial(CVapViscos(1), CVapViscos(2), CVapViscos(3), 0, 0, 0, Temp(1), Visco(1))
'VAPOUR VISCOSITY
Call Polynomial11(CIdeCp(1), CIdeCp(2), CIdeCp(3), CIdeCp(7), Temp(1), HeatCap(1)):
HeatCap(1) = HeatCap(1) * 1000

```

Case Else
End Select
End Sub

[FORMULA.BAS]

```
' AIR AND REFRIG PROP
' BY
' MAHMOUD ABU-MADI
' UNIVERSITY OF BRIGHTON
' 1997
' Version III
```

Sub air (Tdb, Twb, TDP, Win, Wsdb, Wswb, PwsDP)

```
' To calculate air properties from dry and wet bulb temperature.
Patm = 101.325 ' kPa
' CASE 1 GIVEN [ Tdb , Twb ]
Pwsdb = STEAM_PRESS(Tdb)
Pwswb = STEAM_PRESS(Twb)
Wsdb = Wsat(Pwsdb)
Wswb = Wsat(Pwswb)
Win = WAIR(Tdb, Twb, Wswb)
m = funm(Win, Wsdb)
fay = funfay(m, Pwsdb, Patm)
PwsDP = STEAM_PRESS_DP(Patm, Win)
TDP1 = dewPoint(PwsDP)
TDP = Kelvin(TDP1)
```

End Sub

Sub AIR_PROP (T, Dens_air, Cp_Air)

```
' To calculate air density and air specific heat capacity
' for 1 atm pressure
Dens_air = Air_Dens(T)
Cp_Air = Air_CP(T)
```

End Sub

Sub D_Press_Air (Tin, Tout, fFactor, Vel_Air, R4, R51, NoRows, Dpa)

```
' to calculate air side pressure drop from f Factor
pin = Air_Dens(Tin)
pout = Air_Dens(Tout)
pave = 2 * pin * pout / (pin + pout)
Dpa = pin * Vel_Air ^ 2 * R4 ^ 2 * (fFactor * R51 * R4 * NoRows * pin / pave + (1 + 1 / R4 ^ 2) *
((pin / pout) - 1)) / 2
airarea = BtwHead * OvFins * R51 * CInt(NoRows)
```

End Sub

Sub LiqCpASH (T, Cp, CLiqCp())

```
' Liquid specific heat capacity from ASHRAE Table
oo = celsius(T)
Cp = CLiqCp(1) + CLiqCp(2) * oo + CLiqCp(3) * oo ^ 2 + CLiqCp(4) * oo ^ 3 + CLiqCp(5) * oo
^ 4 + CLiqCp(6) * oo ^ 5
```

End Sub

Sub LiqEnthASH (T, h, CLiqEnth())

```
' Liquid enthalpy from ASHRAE Table
oo = celsius(T)
h = CLiqEnth(1) + CLiqEnth(2) * oo + CLiqEnth(3) * oo ^ 2 + CLiqEnth(4) * oo ^ 3 +
CLiqEnth(5) * oo ^ 4 + CLiqEnth(6) * oo ^ 5
```

End Sub

Sub LiqEnthICI (T, h, Temp_Critical, CLiqEnth())

```
' Liquid enthalpy from ICI equation
```

```

oo = (1 - (T / Temp_Critical)) ^ (1 / 3)
h = CLiqEnth(1) + CLiqEnth(2) * oo + CLiqEnth(3) * oo ^ 2 + CLiqEnth(4) * oo ^ 3 +
CLiqEnth(5) * oo ^ 4 + CLiqEnth(6) * oo ^ 5
End Sub

```

```

Sub LiqSVol (T, v, CLiqDen())
' Saturated liquid density equation
Tr = T / Temp_Critical
LiqDen = CLiqDen(1) + CLiqDen(2) * (1 - Tr) ^ (1 / 3) + CLiqDen(3) * (1 - Tr) ^ .5 + CLiqDen(4)
* (1 - Tr) ^ (2 / 3) + CLiqDen(5) * (1 - Tr) + CLiqDen(6) * (1 - Tr) ^ (4 / 3) + CLiqDen(7) * (1 - Tr) ^
2
v = 1 / LiqDen
End Sub

```

```

Sub LiqTherCondASH (T, kk, CLiqTherCon())
' Liquid Thermal Conductivity from ASHRAE Table
oo = celsius(T)
kk = CLiqTherCon(1) + CLiqTherCon(2) * oo + CLiqTherCon(3) * oo ^ 2 + CLiqTherCon(4) * oo
^ 3 + CLiqTherCon(5) * oo ^ 4 + CLiqTherCon(6) * oo ^ 5
End Sub

```

```

Sub LiqTherCondICI (T, kk, Temp_Critical, CLiqTherCon())
' Liquid thermal conductivity from ICI
oo = (1 - (T / Temp_Critical)) ^ (1 / 3)
kk = CLiqTherCon(1) + CLiqTherCon(2) * oo + CLiqTherCon(3) * oo ^ 2 + CLiqTherCon(4) * oo
^ 3 + CLiqTherCon(5) * oo ^ 4 + CLiqTherCon(6) * oo ^ 5
End Sub

```

```

Sub LiqViscoASH (T, m, CLiqViscos())
' Liquid viscosity from ASHRAE Table
oo = celsius(T)
m = CLiqViscos(1) + CLiqViscos(2) * oo + CLiqViscos(3) * oo ^ 2 + CLiqViscos(4) * oo ^ 3 +
CLiqViscos(5) * oo ^ 4 + CLiqViscos(6) * oo ^ 5
End Sub

```

```

Sub LiqViscoICI (T, m, CLiqViscos())
' Liquid Viscosity from ICI
oo = 1 / T
ViscosL = CLiqViscos(1) + CLiqViscos(2) * oo + CLiqViscos(3) * oo ^ 2 + CLiqViscos(4) * oo ^
3 + CLiqViscos(5) * oo ^ 4 + CLiqViscos(6) * oo ^ 5
ViscosL = Exp(ViscosL)
ViscosL = ViscosL * 1000 ' to be in micro Pa.s as ASHRAE
m = ViscosL / 1000000
End Sub

```

```

Sub Polynomial (A0, A1, A2, A3, A4, A5, X, Y)
Y = A0 + A1 * X + A2 * X ^ 2 + A3 * X ^ 3 + A4 * X ^ 4 + A5 * X ^ 5
End Sub

```

```

Sub Polynomial11 (A0, A1, A2, A3, X, Y)
Y = A0 + A1 * X + A2 * X ^ 2 + A3 / X
End Sub

```

```

Sub Polynomial12 (A0, A1, A2, A3, A4, A5, A6, Temp_Critical, X, Y)
Tr = X / Temp_Critical
Y = A0 + A1 * (1 - Tr) ^ (1 / 3) + A2 * (1 - Tr) ^ (1 / 2) + A3 * (1 - Tr) ^ (2 / 3) + A4 * (1 - Tr) +
A5 * (1 - Tr) ^ (4 / 3) + A6 * (1 - Tr) ^ 2
End Sub

```

```

Sub VapCpASH (T, Cp, CVapCp())
  ' Vapour Specific heat capacity from ASHRAE Table
  oo = celsius(T)
  Cp = CVapCp(1) + CVapCp(2) * oo + CVapCp(3) * oo ^ 2 + CVapCp(4) * oo ^ 3 + CVapCp(5) *
oo ^ 4 + CVapCp(6) * oo ^ 5
End Sub

```

```

Sub VapEnthMartAsh (T, v, h, mw, R, Temp_Critical, B, k, CEqStatA(), CEqStatb(), CEqStatc(),
CIdeCp(), IC)
  On Error GoTo VapEnthMartAsh_Error
  ' Integrated from MARTEN-HOU (ASHRAE)
  ' Enthalpy routine from MH'S ( V in m3/kg )
  VV1 = v * mw
  Tr = T / Temp_Critical
  w1 = (VV1 - B): Z = (k / Temp_Critical) * Exp(-k * T / Temp_Critical)
  L1 = R / mw
  L2 = (CEqStatb(1) - CEqStatc(1) * Z)
  L3 = (CEqStatb(2) - CEqStatc(2) * Z)
  L4 = (CEqStatb(3) - CEqStatc(3) * Z)
  L5 = (CEqStatb(4) - CEqStatc(4) * Z)
  HP1 = T * (L1 * Log(w1) - L2 / w1 - L3 / (2 * w1 ^ 2) - L4 / (3 * w1 ^ 3) - L5 / (4 * w1 ^ 4))
  M1 = R * T / mw
  m2 = CEqStatA(1) + CEqStatb(1) * T + CEqStatc(1) * Exp(-k * Tr)
  m3 = CEqStatA(2) + CEqStatb(2) * T + CEqStatc(2) * Exp(-k * Tr)
  M4 = CEqStatA(3) + CEqStatb(3) * T + CEqStatc(3) * Exp(-k * Tr)
  M5 = CEqStatA(4) + CEqStatb(4) * T + CEqStatc(4) * Exp(-k * Tr)
  HP2 = (-M1 * Log(w1) + (M1 * B + 2 * m2) / w1 + (2 * m2 * B + 3 * m3) / (2 * w1 ^ 2) + (3 * m3
* B + 4 * M4) / (3 * w1 ^ 3) + (4 * M4 * B + 5 * M5) / (4 * w1 ^ 4) + (5 * M5 * B) / (5 * w1 ^ 5))
  HPV3 = CIdeCp(1) * T + (CIdeCp(2) * T ^ 2) / 2 + (CIdeCp(3) * T ^ 3) / 3 + (CIdeCp(4) * T ^ 4) /
4 - CIdeCp(5) / T + (CIdeCp(6) * T ^ 5) / 5 + CIdeCp(7) * Log(T)
  h = HP1 + HP2 + HPV3 + IC / mw
  Exit Sub
VapEnthMartAsh_Error:
  Error_Flag = 16
  Resume Next
End Sub

```

```

Sub VapEnthMartDUP (T, v, h, mw, R, Temp_Critical, B, k, CEqStatA(), CEqStatb(), CEqStatc(),
CIdeCp(), IC)
  ' Integrated from MARTEN-HOU DUPONT for R-134a , R-123
  ' and converted constant for KLEIA - 60 , 61 , 66 ICI
  ' Enthalpy routine from MH'S ( V in m3/kg )
  Tr = T / Temp_Critical
  w1 = (v - B): Z = (k / Temp_Critical) * Exp(-k * Tr)
  L1 = R * 1000 / mw
  L2 = (CEqStatb(1) - CEqStatc(1) * Z)
  L3 = (CEqStatb(2) - CEqStatc(2) * Z)
  L4 = (CEqStatb(3) - CEqStatc(3) * Z)
  L5 = (CEqStatb(4) - CEqStatc(4) * Z)
  HP1 = T * (L1 * Log(w1) - L2 / w1 - L3 / (2 * w1 ^ 2) - L4 / (3 * w1 ^ 3) - L5 / (4 * w1 ^ 4))
  M1 = R * 1000 * T / mw
  m2 = CEqStatA(1) + CEqStatb(1) * T + CEqStatc(1) * Exp(-k * Tr)
  m3 = CEqStatA(2) + CEqStatb(2) * T + CEqStatc(2) * Exp(-k * Tr)
  M4 = CEqStatA(3) + CEqStatb(3) * T + CEqStatc(3) * Exp(-k * Tr)
  M5 = CEqStatA(4) + CEqStatb(4) * T + CEqStatc(4) * Exp(-k * Tr)
  HP2 = (-M1 * Log(w1) + (M1 * B + 2 * m2) / w1 + (2 * m2 * B + 3 * m3) / (2 * w1 ^ 2) + (3 * m3
* B + 4 * M4) / (3 * w1 ^ 3) + (4 * M4 * B + 5 * M5) / (4 * w1 ^ 4) + (5 * M5 * B) / (5 * w1 ^ 5))

```

```

HPV3 = CIdeCp(1) * T + (CIdeCp(2) * T ^ 2) / 2 + (CIdeCp(3) * T ^ 3) / 3 + (CIdeCp(4) * T ^ 4) /
4 - CIdeCp(5) / T + (CIdeCp(6) * T ^ 5) / 5 + CIdeCp(7) * Log(T)
h = HP1 + HP2 + HPV3 + IC
End Sub

```

```

Sub VapSVolASH (T, P, vv, CEqStatA(), CEqStatb(), CEqStatc(), Temp_Critical, k, R, B, mw)
  On Error GoTo VapsVolASH_Error
  ' Integrated from MARTEN-HOU ASHRAE
  ' specific volume for super heated vapour
  v1 = .0083125649389 * T / P
  v = v1
  E = .0001
  Tr = T / Temp_Critical
  GMA = k * Tr      ' V in L/mol , P in MPa
  Do
    F = P - R * T / (v - B) - ((CEqStatA(1) + CEqStatb(1) * T + CEqStatc(1) * Exp(-GMA)) / (v - B)
    ^ 2 + (CEqStatA(2) + CEqStatb(2) * T + CEqStatc(2) * Exp(-GMA)) / (v - B) ^ 3 + (CEqStatA(3) +
    CEqStatb(3) * T + CEqStatc(3) * Exp(-GMA)) / (v - B) ^ 4 + (CEqStatA(4) + CEqStatb(4) * T +
    CEqStatc(4) * Exp(-GMA)) / (v - B) ^ 5) + (CEqStatA(5) + CEqStatb(5) * T + CEqStatc(5) * Exp(-
    GMA)) / (Exp(U * v) + CC * Exp(2 * U * v)))
    DF = R * T / (v - B) ^ 2 + 2 * (CEqStatA(1) + CEqStatb(1) * T + CEqStatc(1) * Exp(-GMA)) /
    (v - B) ^ 3 + 3 * (CEqStatA(2) + CEqStatb(2) * T + CEqStatc(2) * Exp(-GMA)) / (v - B) ^ 4 + 4 *
    (CEqStatA(3) + CEqStatb(3) * T + CEqStatc(3) * Exp(-GMA)) / (v - B) ^ 5 + 5 * (CEqStatA(4) +
    CEqStatb(4) * T + CEqStatc(4) * Exp(-GMA)) / (v - B) ^ 6 + ((CEqStatA(5) + CEqStatb(5) * T +
    CEqStatc(5) * Exp(-GMA)) * (U * v * Exp(U * v) + 2 * U * v * CC * Exp(2 * U * v)) / (Exp(U *
    v) + CC * Exp(2 * U * v)) ^ 2)
    If Error_Flag <> 0 Then Exit Sub
    vn = v1 - F / DF
    DIFF = Sqr((vn - v1) ^ 2)
    v1 = vn: v = v1
  Loop Until DIFF < E
  vv = v / mw
  Exit Sub
VapsVolASH_Error:
  Error_Flag = 11
  Resume Next
End Sub

```

```

Sub VapSVolDUP (T, P, v, CEqStatA(), CEqStatb(), CEqStatc(), Temp_Critical, k, R, B, mw, cc, u)
  ' Integrated from MARTEN-HOU DUPONT for R-134a , R-123
  ' and converted for KLEIA - 60 , 61 , 66 ICI
  ' To calculate specific volume for super heated vapour
  P1 = P * 1000
  v1 = (R * 1000 / mw) * T / P1
  v = v1
  E = .0001
  Tr = T / Temp_Critical
  GMA = k * Tr      ' V in m3/kg , P in kPa
  Do
    F = P1 - (R * 1000 / mw) * T / (v - B) - ((CEqStatA(1) + CEqStatb(1) * T + CEqStatc(1) * Exp(-
    GMA)) / (v - B) ^ 2 + (CEqStatA(2) + CEqStatb(2) * T + CEqStatc(2) * Exp(-GMA)) / (v - B) ^ 3 +
    (CEqStatA(3) + CEqStatb(3) * T + CEqStatc(3) * Exp(-GMA)) / (v - B) ^ 4 + (CEqStatA(4) +
    CEqStatb(4) * T + CEqStatc(4) * Exp(-GMA)) / (v - B) ^ 5)
    DF = (R * 1000 / mw) * T / (v - B) ^ 2 + 2 * (CEqStatA(1) + CEqStatb(1) * T + CEqStatc(1) *
    Exp(-GMA)) / (v - B) ^ 3 + 3 * (CEqStatA(2) + CEqStatb(2) * T + CEqStatc(2) * Exp(-GMA)) / (v -
    B) ^ 4 + 4 * (CEqStatA(3) + CEqStatb(3) * T + CEqStatc(3) * Exp(-GMA)) / (v - B) ^ 5 + 5 *
    (CEqStatA(4) + CEqStatb(4) * T + CEqStatc(4) * Exp(-GMA)) / (v - B) ^ 6 + ((CEqStatA(5) +

```



```
CEqStatb(5) * T + CEqStatc(5) * Exp(-GMA)) * (u * v * Exp(u * v) + 2 * u * v * cc * Exp(2 * u * v))
/ (Exp(u * v) + cc * Exp(2 * u * v)) ^ 2)
```

```
vn = v1 - F / DF
```

```
If vn < 0 Then vn = (R * 1000 / mw) * T / P1 + .01
```

```
DIFF = Sqr((vn - v1) ^ 2)
```

```
v1 = vn: v = v1
```

```
Loop Until DIFF < E
```

```
End Sub
```

```
Sub VapTherCondASH (T, kk, CVapTherCon())
```

```
' Vapour thermal conductivity from ASHRAE Table
```

```
oo = celsius(T)
```

```
kk = CVapTherCon(1) + CVapTherCon(2) * oo + CVapTherCon(3) * oo ^ 2 + CVapTherCon(4) *
oo ^ 3 + CVapTherCon(5) * oo ^ 4 + CVapTherCon(6) * oo ^ 5
```

```
End Sub
```

```
Sub VapTherCondICI (T, kk, CVapTherCon())
```

```
' Vapour thermal conductivity from ICI equation
```

```
oo = T
```

```
kk = CVapTherCon(1) + CVapTherCon(2) * oo + CVapTherCon(3) * oo ^ 2 + CVapTherCon(4) *
oo ^ 3 + CVapTherCon(5) * oo ^ 4 + CVapTherCon(6) * oo ^ 5
```

```
End Sub
```

```
Sub VapViscoASH (T, m, CVapViscos())
```

```
' Vapour viscosity from ASHRAE Table
```

```
oo = celsius(T)
```

```
m = CVapViscos(1) + CVapViscos(2) * oo + CVapViscos(3) * oo ^ 2 + CVapViscos(4) * oo ^ 3 +
CVapViscos(5) * oo ^ 4 + CVapViscos(6) * oo ^ 5
```

```
End Sub
```

```
Sub VapViscoICI (T, m, CVapViscos())
```

```
' Vapour viscosity from ICI
```

```
oo = T
```

```
ViscosV = CVapViscos(1) + CVapViscos(2) * oo + CVapViscos(3) * oo ^ 2 + CVapViscos(4) *
oo ^ 3 + CVapViscos(5) * oo ^ 4 + CVapViscos(6) * oo ^ 5
```

```
ViscosV = ViscosV * 1000 'to be in micro Pa.s as ASHRAE
```

```
m = ViscosV / 1000000
```

```
End Sub
```

[FUNCTION.BAS]

```
'      AIR AND WATER PROP
'      BY
'      MAHMOUD ABU-MADI
'      UNIVERSITY OF BRIGHTON
'      1997
'      Version III
```

Function Air_Con (T)

' to calculate air thermal conductivity

Air_Con = .00229 + .00008 * T

End Function

Function Air_CP (T)

' To calculate air specific heat capacity in J/kg K from TK in C

TK = Celsius(T)

Air_CP = (1.00401 + .0000147071 * TK + .0000005247691 * TK ^ 2 - .000000000396964 * TK ^ 3 - 5.42824E-15 * TK ^ 4) * 1000

End Function

Function Air_Dens (T)

' To calculate air density

Air_Dens = .4642 * 760 / T

End Function

Function Air_Vis (T)

' FUNCTION TO CALCULATE THE AIR VISCOSITY

TK = Celsius(T)

Air_Vis = (1.71621 + .00493372 * TK - .00000390801 * TK ^ 2 + .000000003552622 * TK ^ 3 - 1.62902E-12 * TK ^ 4) * 10 ^ (-5)

End Function

Function Celsius (T)

' To convert temperature to Celsius

Celsius = T - 273.15!

End Function

Function dewPoint (Pw)

' To calculate air dew point temperature from pressure (ASHRAE)

Pw = Abs(Pw)

A = Log(Pw)

If Pw > .6112 Then

dewPoint = 6.54 + 14.526 * A + .7389 * A ^ 2 + .09486 * A ^ 3 + .4569 * Pw ^ .1984

Else

dewPoint = 6.09 + 12.608 * A + .4959 * A ^ 2

End If

End Function

Function funfay (m, Pws, Patm)

' To calculate the Air relative humidity from T in 'C range 0 to 200 'C

' ASHRAE HANDBOOK (1993)

funfay = m / (1 - (1 - m) * (Pwsdb / Patm))

End Function

Function funm (W, Wsdb)

' To calculate the degree of saturation from T in 'C range 0 to 200 'C

' ASHRAE HANDBOOK (1993)

```

    funm = W / Wsdb
End Function

```

```

Function Kelvin (T)
    ' To convert temperature to Kelvin
    Kelvin = 273.15! + T
End Function

```

```

Function STEAM_enth (T)
    ' To calculate the steam enthalpy In kJ/kg from T in 'C range 0 to 100 'C
    ' data from Rogers and Mayhew (1982)
    STEAM_enth = 2502.0604 + 1.7663 * (T - 273.15)
End Function

```

```

Function STEAM_PRESS (T)
    ' To calculate the steam pressure in N/m2 from T in 'K range 273 to 473 'K
    ' equation from ASHRAE (1993)
    If T > 273 Then
        STEAM_PRESS = Exp((-5800.2206 / T) + (-5.516256) + (-.048640239 * T) + (.000041764768
* T ^ 2) + (-.000000014452093 * T ^ 3) + (6.5459673 * Log(T)))
    Else
        STEAM_PRESS = Exp((-5674.5359 / T) + (-.51523058) + (-.009677843 * T) +
(.00000062215701 * T ^ 2) + (2.0747825E-09 * T ^ 3) + (-9.484024E-13 * T ^ 4) + (4.1635019 *
Log(T)))
    End If
End Function

```

```

Function STEAM_PRESS_DP (Patm, W)
    STEAM_PRESS_DP = Patm * W / (.62198 + W)
End Function

```

```

Function WAIR (Tdb, Twb, Wswb)
    ' To calculate the Air moisture content in kg/kg from Tdb('C), Twb ('C)
    ' and Wswb range 0 to 200 'C
    ' ASHRAE HANDBOOK (1993)
    Twb = Celsius(Twb)
    Tdb = Celsius(Tdb)
    WAIR = ((2501 - 2.381 * Twb) * Wswb - (Tdb - Twb)) / (2501 + 1.805 * Tdb - 4.186 * Twb)
    Twb = Kelvin(Twb)
    Tdb = Kelvin(Tdb)
End Function

```

```

Function water_enth (T)
    ' To calculate the saturated water enthalpy in kJ/kg from T in 'C
    ' range 0 to 100 'C
    ' data from Rogers and Mayhew (1982)
    water_enth = .0836 + 4.1861 * (T - 273.15)
End Function

```

```

Function Wsat (Ps)
    ' To calculate the Air moisture content in kg/kg from P.steam
    ' range 0 to 200 'C
    ' ASHRAE HANDBOOK (1993)
    Wsat = .62198 * (Ps / (101.325 - Ps))
End Function

```

Appendix C

REFERENCES

Achaichia, A., The performance of louvred tube-and-plate fin heat transfer surfaces. PhD Thesis, *University of Brighton*, 1987.

Akers, W.W. and Rossan, H.F. Condensation inside a horizontal tube. *Chemical Engineering progressive symposium series*, Vol. 56, Part 145, No. 30, pp. 145-149, 1960.

Anderson, S.W.; Rich, D.G. and Geary, D.F. Evaporation of R22 in a horizontal 3/4 in. OD tube. *ASHRAE Transactions*, Vol. 72, pp. 28-41, 1966.

ASHRAE Handbook, Fundamentals, American Society of Heating, Refrigeration and Air Conditioning Engineers, Atlanta, 1993.

Bennett, D.L. and Chen, J.C. Forced convective boiling in vertical tubes for saturated pure components and binary mixtures. *AIChE Journal*, Vol. 26, pp. 454-461, 1980.

Bergles, A.E. and Rohsenow, W.M. The determination of forced convection surface boiling heat transfer. *ASME Journal of Heat Transfer*, Vol. 86, pp. 365-372, 1964.

Briggs, D.E. and Young, E.H., Convective heat transfer and pressure drop of air flowing across triangular pitch banks of finned tube. 5th *AIChE/ASME National Heat Transfer Conference*, Houston, Texas, 1962.

Briggs, D.E. and Young, E.H., Convective heat transfer and pressure drop of air flowing across triangular pitch banks of finned tube. *Chem. Eng. Prog. Symp. Ser.*, Vol. 59, No. 41, pp. 1-10, 1963.

Brooks, P.J. New ASHRAE local loss coefficients for HVAC fittings. ASHRAE Transaction, Vol. 99, Part 2, pp. 169-193, 1993.

Butterworth, D. A comparison of some void fraction relationships for co-current gas-liquid flow. Int. J. of Multiphase flow, Vol. 1, pp. 845-850, 1975.

Carpenter, N.E. Retrofitting HFC134a into existing CFC12 systems. Int. J. Refrigeration, Vol. 15, No. 6, pp. 332-339, 1992.

Castro, F.; Tnaut, F.V. and Ali, A.A. Automotive evaporator and condenser modelling. SAE Paper No 931121, 1993.

Cavallini, A. and Zecchin, R. A dimensionless correlation for heat transfer in forced convection condensation. In: Heat Transfer, Proceedings of the fifth International Heat Transfer Conference, Tokyo, 3-7 September, Vol. III, pp. 309-313. Tokyo; Japan Society of Mechanical Engineers, 1974.

Chaddock, J.B. and Noerager, J.A. Evaporation of R-12 in horizontal tube with constant heat flux. ASHRAE Transactions, Vol. 72, Part I, pp. 99-103, 1966.

Chato, J.C. Laminar condensation inside horizontal tubes. ASHRAE Journal, 4, 2, pp. 52-60, 1962.

Chen, J.C. A correlation for boiling heat transfer to saturated fluids in convective flow. Industrial and Engineering Chemistry, Process Design and Development, Vol. 5, No. 3, pp. 322-329, 1966.

Cooper, M.G. Saturation nucleate pool boiling. 1st U.K. National conference on heat transfer, (Industrial and Chemical Engineering Symposium Series No. 89), Vol. 2, pp. 785-793, 1984.

Dabiri, A.E. A steady state computer simulation model for air-to-air heat pumps. *ASHRAE Transaction*, Vol. 88, Part 2, pp. 973-987, 1982.

Domanski, P. and Didion, D. Computer modeling of the vapour compression cycle with constant flow area expansion device. NSB Building Science Series Report 155, National Bureau of Standard, Washington, DC, 1983.

Eckels, S.J. and Pate, M.B. A comparison of R-134a and R-12 in-tube heat transfer coefficients based on existing correlations. *ASHRAE Transaction*, Vol. 96, Part 1, pp. 256-265, 1990.

Eckels, S.J. and Pate, M.B. Evaporation and condensation of HFC-134a and CFC-12 in a smooth tube and micro-fin tube. *ASHRAE Transaction*, Vol. 97, Part 2, pp. 71-81, 1991.

Ellison, R.D. and Creswick, F.A. A computer simulation of air-to-air heat pumps. ORNL/CON-16, Oak Ridge National Laboratory, 1978.

El-Bourini, R.; Hayashi, K. and Adachi, T. Automotive air conditioning systems performance with HFC-134a refrigerant. SAE Technical Paper Series 900214.

El-Bourini, R.; Adachi, T and Tajima, K. Performance evaluation of an automotive air conditioner with expansion valve control using CFC-12 & HFC-134a refrigerants. SAE Technical Paper Series 910218.

El-Mahdy, A.H. and Biggs, R.C. Finned tube heat exchanger: correlation of dry surface heat transfer data. *ASHRAE Transaction*, Vol. 85, Part 2, pp. 262-273, 1979.

Fischer S.K. and Rice, C.K. The Oak Ridge heat pump models: I. A steady-state computer design model for air-to-air heat pumps. ORNL/CON-80/R1, Oak Ridge National Laboratory, 1983.

Gnielinski, V. New equations for heat and mass transfer in turbulent pipe and channel flow. *Int. Chem. Engineering*, Vol. 16, pp. 359-368, 1976.

Gray, D.L. and Webb, R.L., Heat transfer and friction correlations for plate finned-tube heat exchangers having plain fins. *Proceedings of the Eighth International Heat Transfer Conference*, Vol. 6. San Francisco, pp. 2745-2750, 1986.

Gungor, K.E. and Winterton, R.H.S. A general correlation for flow boiling in tubes and annuli. *Int. J. Heat and Mass Transfer*, Vol. 29, No. 3, pp. 351-358, 1986.

Gungor, K.E. and Winterton, R.H.S. Simplified general correlation for saturated flow boiling and comparisons of correlations with data. *The Canadian Journal of Chemical Engineering*, Vol. 65, No. 1, pp. 148-156, 1987.

Heikal, M.R. Thermodynamic properties of R134a. Internal Report, University of Brighton, 1991.

Hiller C.C. and Glicksman, L.R. Improving heat pump performance via compressor capacity control- Analysis and test, Report No. 24525-96, Heat Transfer Laboratory, Massachusetts Institute of Technology, Cambridge, Massachusetts, 1976.

Jallouk, P.A. Two-phase flow pressure drop and heat transfer characteristics of refrigerants in vertical tubes. Ph.D. Thesis, University of Tennessee, Knoxville, TN, 1974.

Jung, D.S.; McLinden M.; Radermacher, R. and Didio, D. Horizontal flow boiling heat transfer experiments with a mixture of R22/R114. *Int. J. Heat Mass Transfer*, Vol. 32, No. 1, pp. 131-145, 1989a.

Jung, D.S.; McLinden M.; Radermacher, R. and Didio, D. A study of flow boiling heat transfer with refrigerant mixtures. *Int. J. Heat Mass Transfer*, Vol. 32, No. 9, pp. 1751-1764, 1989b.

Jung, D.S. and Radermacher, R. Prediction of pressure drop during horizontal annular flow boiling of pure and mixed refrigerants. *Int. J. Heat Mass Transfer*, Vol. 32, No. 12, pp. 2435-2446, 1989c.

Jung, D.S and Radermacher, R. Prediction of evaporation heat transfer coefficient and pressure drop of refrigerant mixtures in horizontal tubes. *Int. J. Refrigeration*, Vol. 16, No. 3, pp. 201-209, 1993a.

Jung, D.S and Radermacher, R. Prediction of evaporation heat transfer coefficient and pressure drop of refrigerant mixtures. *Int. J. Refrigeration*, Vol. 16, No. 5, pp. 330-338, 1993b.

Kandlikar, S.G. and Thakur B.K. A new correlation for heat transfer during flow boiling. *Proceedings, 16th Southeastern Seminar on Thermal Sciences, Miami, FL., 1982.*

Kandlikar, S.G. An improved correlation for predicting two-phase flow boiling heat transfer coefficient in horizontal and vertical tubes. in *Heat Exchangers for Two-Phase Flow Applications*. ASME, New York, 1983.

Kandlikar, S.G. A general correlation for saturated two-phase flow boiling heat transfer inside horizontal and vertical tubes. *ASME Journal of Heat Transfer*, Vol. 112, pp. 219-228, 1990.

Kandlikar, S.G. A model for correlating flow boiling heat transfer in augmented tubes and compact evaporators. *ASME Journal of Heat Transfer*, Vol. 113, pp. 966-972, 1991.

Kays, W.M. and London A.L. *Compact heat exchangers*. McGraw-Hill Book Company, Third edition, 1984.

Kempiak, M.K. and Crawford, R.R. Three zone steady state modelling of a mobile air conditioning condenser. ASHRAE Transaction, Vol. 98, Part 1, pp. 475-488, 1992.

Khanpara, J.C.; Bergles A.E. and Pate, M.B. Augmentation of R-113 in-tube evaporation with micro-fin tubes. ASHRAE Paper No. PO-86-11, No. 3, 1986.

Kirkbride, C.G. Heat transfer by condensing vapour on vertical tubes. Ind. Eng. Chem., 26, 4, pp. 425-428, 1934.

KLEA 134a Physical property data sheet, ICI Klea, Runcorn, 1994.

KLEA 407C Physical property data sheet, ICI Klea, Runcorn, 1994.

Klimenko, V.V. A generalized correlation for two-phase forced flow heat transfer. Int. J. Heat Mass Transfer, Vol. 31, Part 3, pp. 541-552, 1988.

Kyle, D.M.; Mei, V.C. and Chen F.C. An automobile air conditioning design model. SAE conference proceeding, Issue 263, pp. 571-576, 1993.

Lckhart, R.W. and Martinelli, R.C. Proposed correlation of data for isothermal two-phase, two-component flow in pipe. Chem. Eng. Progress, Vol. 45, Part 1, pp. 39-48, 1949

McAdams, W.H. Heat transmission. 3rd ed., McGraw-Hill, New York, 1954.

McQuiston, F.C. and Tree, D.R. Heat transfer and flow friction data for two fin-tube surfaces. ASME, Journal of Heat Transfer, Vol. 93 , pp. 249-250, 1971.

McQuiston, F.C. Fin efficiency with combined heat and mass transfer. ASHRAE Transaction, Vol. 81, Part 1, pp. 350-355, 1975.

McQuiston, F.C. Heat, mass and momentum transfer data for five plate-fin-tube heat transfer surfaces. *ASHRAE Transaction*, Vol. 84 , Part. 1, pp. 266-293, 1978a.

McQuiston, F.C. Correlation of heat, mass and momentum transport coefficients for plate-fin-tube heat transfer surfaces with staggered tubes. *ASHRAE Transaction*, Vol. 84 , Part. 1, pp. 294-308, 1978b.

Mignot, C. and Henon, E. New R134a refrigerant fluid and parallel flow condensers technology: Development of simulation tools for new products engineering, Int. Cong. and Expos. Detroit, Michigan, SAE 950112, pp. 57-63, 1995.

Mohr, V. and Runge, R. Forced convection boiling of neon in horizontal tubes. *Heat Transfer in Boiling*, Hahne, E. and Grigull U., eds., Hemisphere Publishing Corporation, New York, 1977.

Muller-Steinhagen, H. and Heck, K. A simple friction pressure drop correlation for two-phase flow in pipes, *Chem. Eng. Process.*, Vol. 20, pp. 297-308, 1986.

Nir, A. Heat transfer and friction factor correlations for crossflow over staggered finned tube banks. *Heat Transfer Engineering*, Vol. 12, No. 1, pp. 43-58, 1991.

O'Neill, P.J. and Crawford, R.R. Modeling and optimization of a finned tube evaporator. *ASHRAE Transaction*, Vol. 95, Part 1, pp. 1256-1262, 1989.

Paliwoda, A. Generalized method of pressure drop and tube length calculation with boiling and condensing refrigerants within the entire zone of saturation. *Int. J. of Refrigeration*, Vol. 12, November, pp. 314-322, 1989.

Paliwoda, A. Generalized method of pressure drop calculation across pipe components containing two-phase flow of refrigerants. *Int. J. of Refrigeration*, Vol. 15, No. 2, pp. 119-125, 1992.

Pankhurst, R.C. Wind tunnel technique. Pitman, 1952.

Peirre, B. Flow resistance with boiling refrigerants-Part I. *ASHRAE Journal*, Vol. 6, No. 9, pp. 58-65, September, 1964.

Petukhov, B.S. Heat transfer and friction in turbulent pipe flow with variable physical properties. In: *advances in heat transfer*, Vol. 6, edited by J.P. Hartnett and T.F. Irvin, pp. 503-664, New York: Academic Press, 1970.

Prince, S.A. A theoretical and experimental investigation into the heat and mass transfer phenomena involved in air cooling and dehumidification, M.Eng. Thesis, University of Sheffield, 1994.

Raymond, D.E.; Creswick, F.A.; Fischer, S.K. and Jackson, W.L. A computer model for air-cooled refrigerant condensers with specified refrigerant circuiting. *ASHRAE Transaction*, Vol. 97, Part 1, pp. 1106-1124, 1981.

Rich, D.G. The effect of the number of tube rows on heat transfer performance of smooth plate fin-and-tube heat exchangers. *ASHRAE Transaction*, Vol. 81, Part 1, pp. 307-317, 1975.

Rich, D.G. The effect of fin spacing on the heat transfer and friction performance of multi row, smooth plate fin-and-tube heat exchangers. *ASHRAE Transaction*, Vol. 79, Part 2, pp. 137-145, 1973.

Ross, H.D. An Investigation of horizontal flow boiling of pure and mixed refrigerants. Ph.D. Thesis, University of Maryland, 1985.

Schmidt, T.E. Heat transfer calculations for extended surfaces. *Refrigerating engineering*, Vol. 57, pp. 351, Apr. 1949.

Shah, M.M. A new correlation for heat transfer during boiling flow through pipes. ASHRAE Transactions, Vol. 82, Part 2, pp. 66-86, 1976.

Shah, M.M. A general correlation for heat transfer during film condensation inside pipes. Int. J. Heat Mass Transfer, Vol. 22, pp. 547-556, 1979.

Shah, M.M. Heat transfer during film condensation in tubes and annuli: A review of the literature. ASHRAE Transactions, Vol. 87, Part 1, pp. 1086-1105, 1981.

Shah, M.M. Chart correlation for saturated boiling heat transfer: equations and further study. ASHRAE Transactions, Vol. 88, Part 1, pp. 185-196, 1982.

Souza, A.L.; Chato, J.C.; Wattlelet J.P. and Christoffersen, B.R. Pressure drop during two-phase flow of pure refrigerants and refrigerant-oil mixtures in horizontal smooth tubes. HTD-Vol. 243, Heat transfer with alternative refrigerants, ASME, pp. 35-41, 1993.

Stewart, R.B.; Jacobsen, R.T. and Penonello, S.G. ASHRAE Thermo Dynamic Properties of Refrigerant. ISBN 0-910110-47-6, ASHRAE, Atlanta, 1986.

Stroud, K.A. Engineering mathematics. Fourth edition, Macmillan Press Ltd, 1995

Struss, R.A.; Henkes, J.P. and Gabbey L.W. Performance comparison of HFC-134a and CFC-12 with various heat exchangers in automotive air conditioning systems. SAE Technical Paper Series 900598.

Sur, B. and Azer, N.Z. An analytical pressure drop prediction model for condensation inside longitudinally finned tubes. ASHRAE Transaction, Vol. 97, Part 2, pp. 54-61, 1991.

SUVA 134a Physical property data sheet, DU PONT SUVA, Runcorn, 1993.

Tandon, T.N.; Varma, H.K. and Gupta, C.P. Heat transfer during forced convection condensation inside horizontal tube. *Int. J of Refrig.*, Vol. 18, No. 3, pp. 210-214, 1995.

Traviss, D.P.; Rohsenow, W.M.; and Baron, A.B. Forced convection condensation inside tubes: a heat transfer equation for condenser design. *ASHRAE Transactions*, Vol. 79, Part 1, pp. 157-165, 1972.

Wang, C.C.; Chang Y.J.; Hsieh, Y.C. and Lin, Y.T. Sensible heat and friction characteristics of plate fin-and-tube heat exchangers having plane fins. *International journal of Refrigeration*, Vol. 19, No. 4, pp. 223-230, 1996.

Webb, R.L. and Gupte N.S. A critical review of correlations for convective vaporization in tube and tube banks. *Heat Transfer Engineering*, Vol. 13, No. 3, pp. 58-81, 1992.

Yu, L. C. A., Performance characteristics of round tube and plate fin heat transfer surfaces. PhD Thesis, *University of Brighton*, 1992.

Zukauskas, A. *Heat transfer from tubes in cross flow*, Academic Press , pp. 93-160, 1972.

Appendix D

LIST OF PUBLICATIONS

- 1- Abu-Madi, M., Johns, R. A. and Heikal, M. R., The effect of refrigerant properties on the design of automotive air conditioning systems. *Proceeding of the IMechE VTMS 2 Conference*, London, 1995, pp. 307-315.
- 2- Johns, R. A., Abu-Madi, M. and Heikal, M. R., The performance of non-ozone depleting refrigerants in condensers and evaporators. *Proceeding of the IMarE Conference on Marine Refrigeration*, Vol. 107. No. 3. London, 1995, pp. 31-48.
- 3- Abu-Madi, M., Johns, R. A. and Heikal, M. R., The performance of compact finned tube evaporators in automotive air conditioning systems using non-ozone depleting refrigerants. *Proceeding of the 4th IMechE UK National Heat Transfer Conference*, Manchester, 1995, pp. 369-373.
- 4- Abu-Madi, M., Johns, R. A. and Heikal, M. R., The performance of air conditioning evaporators in hot, humid environments with non-ozone depleting refrigerants. *Proceeding of the 1st UAE Conference on Air Conditioning in the Gulf*, Al-Ain, UAE , 1996, pp. 74-84.
- 5- Abu-Madi, M., Johns, R. A. and Heikal, M. R., Performance characteristics correlation for round tube and plate finned heat exchangers. Accepted for publication in the Int. J. of Refrig.